R-09-34

Feasibility study of a concrete plug made of low pH concrete

Lars-Olof Dahlström, Jonas Magnusson
NCC Engineering

Ginko Gueorguiev, Morgan Johansson
Reinertsen Sverige AB

September 2009

Svensk Kärnbränslehantering AB
Swedish Nuclear Fuel
and Waste Management Co

Box 250, SE-101 24 Stockholm
Phone +46 8 459 84 00

ISSN 1402-3091
SKB Rapport R-09-34

Feasibility study of a concrete plug made of low pH concrete

Lars-Olof Dahlström, Jonas Magnusson
NCC Engineering

Ginko Gueorguiev, Morgan Johansson
Reinertsen Sverige AB

September 2009

Summary

In this report a concrete plug, used as a barrier between the deposition tunnels and the access tunnel, is investigated. The objectives of the work is to see whether it is possible to use low pH concrete for the plug and whether it can be designed without using reinforcement. The requirements set on the plug are that the water leakage through it should be small enough and that the concrete stresses are limited to a value valid for the concrete used.

A modified geometry of the plug is proposed, which makes it possible to use it as a general solution in all deposition tunnels. Material properties of a low pH concrete (B200) determined by CBI have been used. Loads considered in the study is the pressure from water and swelling, the temperature change in the rock and plug due to heat development from nuclear fuel stored in nearby copper canisters, pre-stressing in the plug due to cooling during construction and the shrinkage of concrete in the plug.

Two-dimensional, axis-symmetric finite element analyses, assuming linear elastic material behaviour in rock and concrete where contact friction between concrete and rock is taken into consideration, have been used to study the structural response of the plug. A total of 48 main load combinations, consisting of 8 different load scenarios and 6 material combinations, have been used.

It is found that the concrete plug will not remain uncracked when subjected to the loads studied but that it, nevertheless, is possible to achieve an unreinforced concrete plug that satisfies the requirements set up. The minimum size of the concrete compressed zone will be 0.5 m, resulting in a water leakage through the plug determined to be lower than the requirement of 0.01 l/min set up in this study. Further, the maximum compressive stresses of interest are 33 MPa and the maximum displacement in the plug is about 3 mm, which are deemed to be satisfactorily. Consequently, it is concluded that it seems possible to use low pH concrete for the plug and design it without using reinforcement.

Finally, it can be concluded that there remains some unclearness of the plug requirements and uncertainties in material parameters used. It can especially be mentioned that this report presuppose a continued study of the material parameters of low-pH concrete. Further, a follow up using a more detailed analysis should be made to comprise the uncertainties and approximations in loads and load combinations that has been used in this report.

Sammanfattning

I den här rapporten undersöks en betongplugg, vilken utgör en barriär mellan deponeringstunnel och transporttunnel. Målen med arbetet är att klargöra om det är möjligt att använda betong med lågt pH i pluggen samt om den kan utformas utan armering. Krav som ställs på pluggen är att vattenläckaget genom denna ska vara tillräckligt små samt att uppkomna betongpåkänningar ska ligga inom de intervall som är tillåtna för den aktuella betongen.

En modifierad pluggeometri föreslås vilket gör det möjligt att använda den som en allmän lösning i samtliga deponeringstunnlar. Materialparametrar för betong med låg pH, framtagna av CBI, har använts. Laster som beaktas i studien är trycket från vatten och bentonitens svällning, temperaturökningen i berg och plugg på grund av den värmeutveckling som fås av kärnbränsle förvarat i närliggande kopparbehållare, förspänningen av plugg från kylning av denna under konstruktionsskedet samt betongens krympning i pluggen.

Tvådimensionella, axialsymmetriska finita elementanalyser, med antagande om linjärelastiskt material för berg och betong samt kontaktfriktion dem emellan, har utförts för att studera den strukturella responsen hos pluggen. Totalt 48 lastkombinationer, innefattande 8 olika lastscenarion och 6 materialkombinationer har använts.

Det visas att betongpluggen inte kommer förbli osprucken av de laster den utsätts för men att det trots detta är möjligt att uppnå en oarmerad betongplugg som uppfyller de krav som ställts upp. Den minsta storleken på betongens tryckzonshöjd är 0.5 m, vilket resulterar i ett vattenläckage genom pluggen som beräknas vara mindre än det krav på 0.01 l/min som använts för pluggen i den här studien. Vidare uppgår de maximala betongtryckspänningarna av intresse till 33 MPa och den maximala deformationen i pluggen till omkring 3 mm, vilket bedöms vara tillfredsställande. Således kan det konstateras att det synes vara möjligt att använda betong med låg pH i pluggen samt att den kan utformas utan armering.

Slutligen konstateras att det kvarstår en del oklarheter vad gäller pluggens krav samt osäkerheter i använda materialparametrar. Det kan särskilt nämnas att denna rapport förutsätter en fortsatt studie av använda materialparametrar för betong med låg pH. Vidare bör en uppföljande, mer detaljerad analys, göras för att täcka in de osäkerheter och approximationer i laster och lastkombinationer som gjorts i denna rapport.

Contents

1 Introduction

1.1 General

SKB is continuously developing and scrutinising the preferential KBS-3 method for the final deposition of the used nuclear fuel. The KBS-3 is based on a three barrier system, Figure 1-1: a) the high level radioactive waste is enclosed in a canister of steel encased in copper; b) the canisters are deposited in the bedrock at about 500 meters depth; c) imbedded in high compacted bentonite clay. Finally, when all the canisters are in place and all deposition tunnels are backfilled, access tunnels and rock caverns are backfilled and sealed.

The fuel will be taken from the interim storage Clab and placed in the copper canisters with a cast iron insert. The canisters will then be transported through the tunnel down to the "deep repository" that consists of a system of horizontal tunnels at a depth of about 500 meters. These deposition tunnels are planned to be about 250 meter long, and spaced with a distance of about 40 meters. Deposition holes will be excavated from the floor of the tunnel with an interval of about 6 meters, depending on the thermo physical properties of the rock. Parallel to the continuous deposition of canisters, the deposition tunnels are be backfilled with bentonite.

At the end of the deposition tunnels a concrete plug, will separate the deposition tunnels from the access- and transportation tunnels. The function of these plugs is to close the deposition tunnels in order to keep the backfill in place and prevent axial water flow until the access- and transportation tunnels are backfilled and saturated. These tunnels, opposite to the deposition tunnels, will be at atmospheric pressure until all canisters are deposited and the tunnels sealed. Finally when the access- and transportation tunnels are backfilled and saturated the required function of the temporary plugs are no longer required other than a volume mass to prevent density loss of the bentonite backfill. However, the deposition will prolong for a long time and therefore the plug should be designed to function for at least 100 years.

1.2 Objectives

The outer barrier at the end of the deposition tunnels is designed as a concrete plug with a spherical front side and a flat pressurised side. The function of a prototype plug has earlier been constructed and tested in the Prototype Repository at Äspö HRL, see Figure 1-2. However, the repository has continuously been developed and assumptions changed during the process. This requires an updating of the design and at the same time more detailed calculations that consider the altering conditions from the time of casting to 100 years.

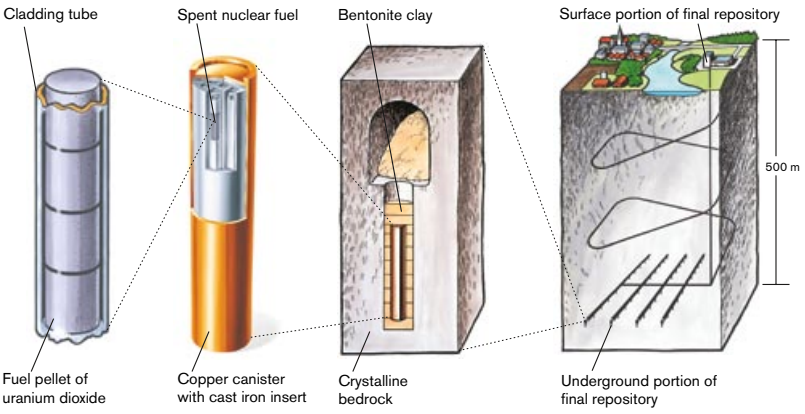

Figure 1-1. *Multiple barriers prevent the radionuclide's from escaping into the environment.*

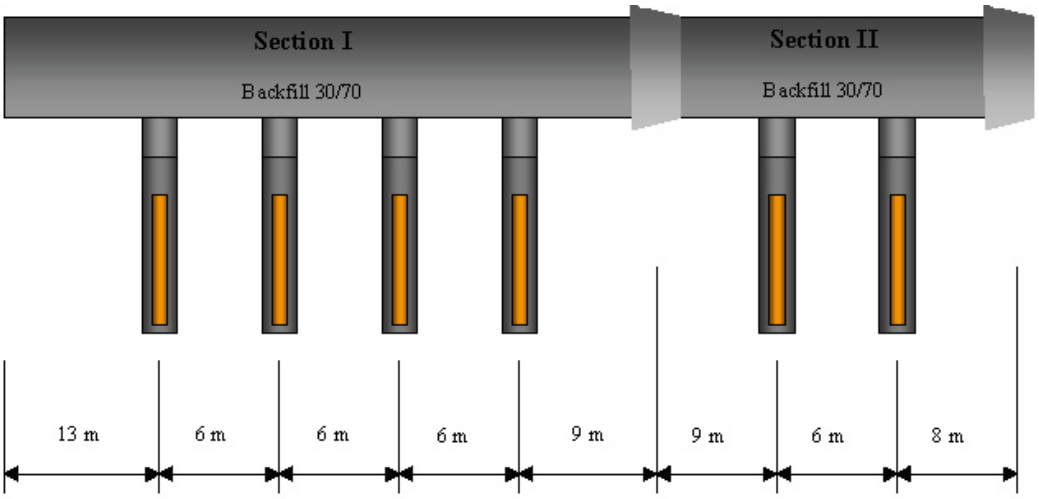

Figure 1-2. *Longitudinal section of the Prototype Repository test drift at the Äspö URL illustrating six deposition holes with canisters embedded in buffer clay.*

The two most essential changes of the plug design that should be tested are:

- Is it possible to use low pH concrete, considering its mechanical- and hydraulic properties?
- Does the plug require reinforcement, or what geometrical changes are required to exclude the reinforcement?

The low pH concrete has been developed by the Swedish Cement and Concrete Research Institute (CBI), see [1], at the request of SKB, and has a pH of about 11. That should be compared with leach water from common concrete that is about pH 14.

The reason to exclude the reinforcement is twofold. The low pH concrete is believed[1] to have less corrosion protection ability, and hence, normal steel reinforcement may be needed to be exchanged to stainless steel or some other inorganic material that can be accepted by the risk assessment group. Secondly, there will be a noticeable cost reduction since there is a positive effect on the production complexity to consider.

The study of the concrete plug reported here considers the altering load conditions (load history) that may be expected from 90 days to 100 years. According to [1] the concrete is assumed to have reached its required strength after about 90 days of curing and the plug is at this stage assumed to be stress free.

[1] There is no reference for this assumption, which is based on the idea that a concrete of lower pH probably provide less protection against corrosion of the reinforcement.

2 Design of temporary plugs

2.1 Required function of the plugs

The purpose of the concrete plug is twofold:

- to prevent outflow of axial water in the backfilled deposition tunnels during construction and before the transportation tunnels are backfilled and full water pressure has been developed,
- to hold the bentonite filling in the deposition tunnel in place.

The life span of the concrete plug is set to 100 years. After this time span the loads studied in this report is not acting anymore and the demands on the plug material is just that it shall remain in its place in the final repository and not significantly decrease in volume. Accordingly, if the cement, due to degradation of the concrete, is removed by water passing through, the plug volume shall not significantly decrease and the density of the backfill be reduced to such an extent that the latter's barrier functions are not upheld.

2.2 Prerequisite

2.2.1 Geometry of plug

The geometry of the plug and the deposition tunnel section is shown in Figure 2-1. The U-shaped cross section of the deposition tunnel is marked, both the theoretical section and a modified section widened with an assumed offset of 0.3 m. To make sure that the plug geometry determined here can be generally used in all deposition tunnels the plug shall surround the offset tunnel section as shown. Accordingly, the deposition tunnel will have to be widened from a U-shaped section to a circular one over a certain length as schematically shown in Figure 2-2.

2.2.2 The use of an unreinforced concrete plug

As stated in Section 1.2 there is a desire to construct the concrete plug completely without any reinforcement. It is believed that it is possible to design this type of structure without reinforcement since the shape of the plug and the loads acting on it will result in the appearance of large compressive forces in the plug cross sections. Hence, force equilibrium is attained even without the presence of any reinforcement and the effect of reinforcement in such a structure would mainly be to limit the crack widths and increase the size of the compressive zone. The presence of reinforcement would also help distribute uneven stresses within the plug, although this is believed to be of limited use in the case studied.

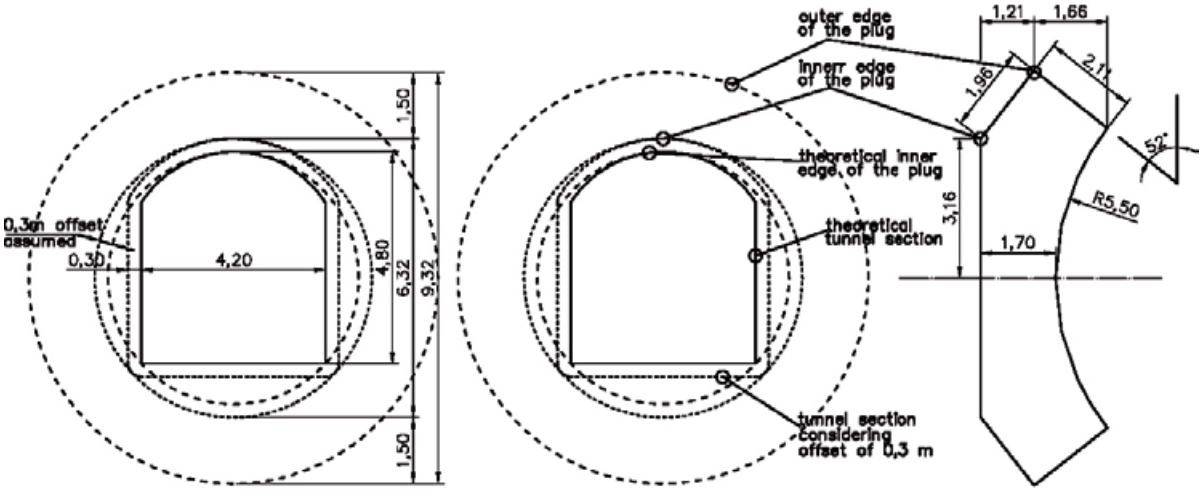

Figure 2-1. *Geometry of concrete plug.*

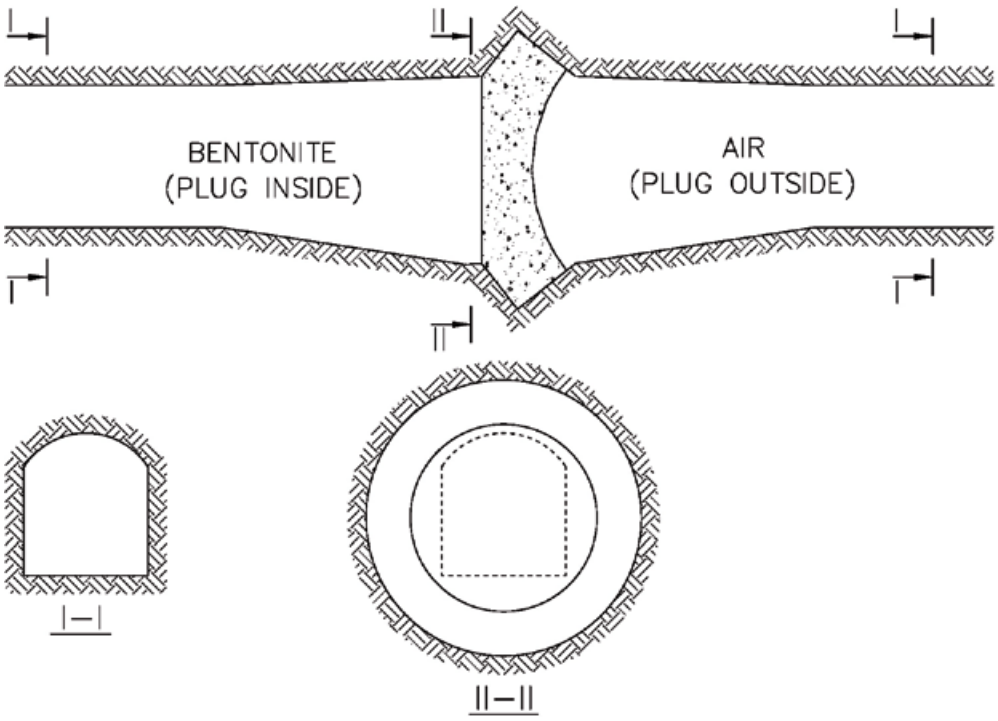

Figure 2-2. *Schematic illustration of widening of the cross section of the deposition tunnel.*

In an unreinforced concrete structure there is no reinforcement to protect, and hence, no structural limitation on what size the crack widths may obtain. Concrete cracking will affect the leakage through the plug, though. However, as long as there are no cracks extending through the whole concrete cross section, the leakage through the plug will not depend on the size of the cracks but on the size of the uncracked concrete zone and the permeability of the concrete. If it can be shown that the compressive zone is large enough to meet the leakage requirements set and the compressive stresses attained in the structure do not exceed the limited concrete value the design requirements are met. Consequently, in such a case there is no need to use reinforcement in the plug.

Consequently, if the concrete cracks there is no demand on the crack widths themselves but only on the size of the compressed concrete zone. Hence, as long as the thickness and stress requirements set on this is fulfilled there is no need to put in any reinforcing steel in the plug.

2.3 Materials and material properties

2.3.1 Concrete material properties

The type of concrete used in the plug is in many ways different from that of ordinary concrete. One such difference is the rate of hardening, where the concrete used show slower strength growth than ordinary concrete, [1]. Hence, the concrete is considered fully hardened after 90 days instead of the 28 days usually used for ordinary concrete.

The material properties are based on laboratory testing of specimens about 90 days old reported in chapter 6 in [1]. The material properties used as characteristic values are listed in Table 2-1 and are based on the use of a concrete consisting of 200 kg binder, denoted B200 in [1].

2.3.2 Rock material properties

The material properties for rock are listed in Table 2-2. Minimum and maximum values of the friction between rock and concrete have been assumed based on recommendations in BBK 04, [2]; the minimum value according to minimum friction stated between concrete and concrete in Section 6.8.3 and the maximum value based on a recess contact surface according to Section 3.11.3.

Table 2-1. Material properties for concrete, based on [1].

Material property	Denotation	90 d	1 y	10 y	100 y	Unit
Concrete compressive strength	f_{cck}	51	67	80	85	MPa
Concrete tensile strength [1)]	f_{ctk}	2.9	2.9	2.9	2.9	MPa
Concrete Young's modulus	E_c	34,0	36,5	38,5	39,0	GPa
Poisson's ratio [1)]	v	0.27	0.27	0.27	0.27	–
Concrete creep [2)]	φ	0.22/ 0.27	0.27/ 0.34	0.36/ 0.46	0.46/ 0.57	–
Permeability coefficient [1)]	K	$5{\cdot}10^{-12}$	$5{\cdot}10^{-12}$	$5{\cdot}10^{-12}$	$5{\cdot}10^{-12}$	m/s
Coeff. of thermal expansion	α	10^{-5}	10^{-5}	10^{-5}	10^{-5}	$°C^{-1}$

[1)] No valid values for concrete older than 90 days, the same value is assumed for concrete of older age.

[2)] Creep values are given with a lower and upper bound with the assumption that the loads start acting on the plug after 90 days.

Table 2-2. Material properties for rock, based on [2] and [3].

Material property	Denotation	Value	Unit
Rock compressive strength	f_{crk}	200	MPa
Rock Young's modulus [1)]	E_r	25–75	GPa
Poisson's ratio	v	0.20	–
Rock creep	φ	0.0	–
Friction rock/concrete	μ_{min}	0.3	–
	μ_{max}	2.0	–
Coeff. of thermal expansion	α	$0.7{\cdot}10^{-5}$	$°C^{-1}$

[1)] E_r = 75 GPa corresponds to intact rock with no cracks while E_r = 25 GPa corresponds to damaged rock.

2.4 Loads

2.4.1 Load summary

Loads according to Table 2-3 are used in the analyses carried out here. Each load is individually treated in the following sections and is assumed to start acting on the concrete plug 90 days after casting. When defining the loads, notions such as vertical part, diagonal slits and inside- and outside of the plug are used and are therefore defined in Figure 2-3.

There are some load cases not taken into account in this report and they are briefly treated in Section 2.4.7. There are some uncertainties in the load values used for the water and swelling pressure and the values listed below are those believed realistic, based on previous experience within the work group. The effect of possible discrepancies from the load values listed in Table 2-3 are further discussed in Chapter 6.

Table 2-3. Summary of load properties used in the analyses.

Load type	Value
Water pressure	4 MPa
Swelling pressure of bentonite	2 MPa
Temperature difference in concrete plug	+10°C
Temperature difference in rock	Max = +25°C Min = +7°C
Shrinkage of concrete plug [1)]	Max = –0.29‰ Min = –0.07‰

[1)] When expressed as temperature, based on coefficient of thermal expansion $\alpha = 10^{-5}°C^{-1}$.

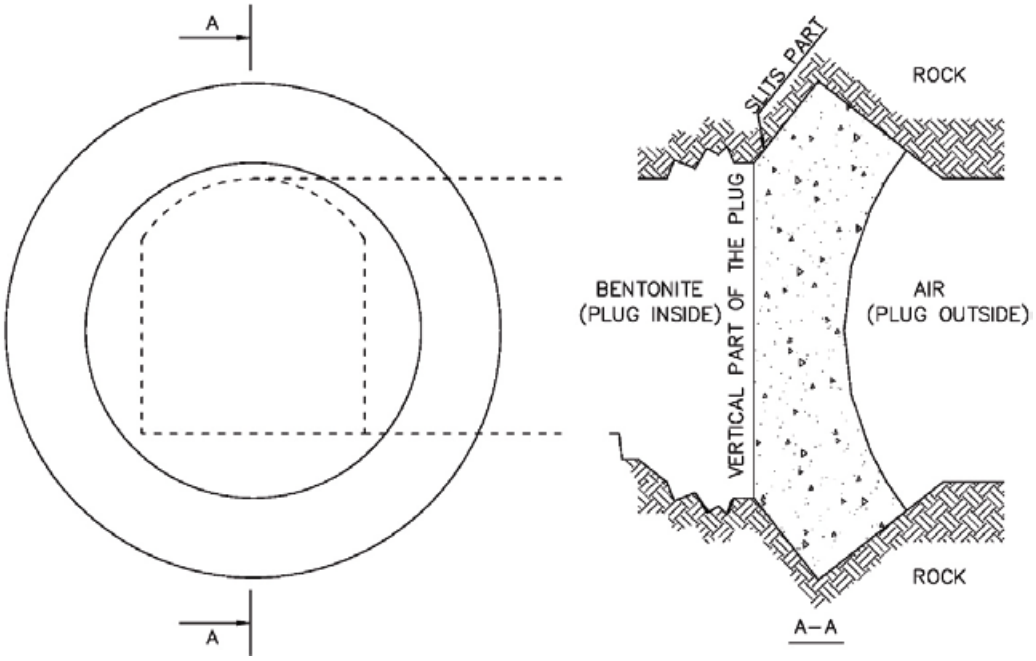

Figure 2-3. *Definition of notions used in Section 2.4.2 to 2.4.6 when defining the loads acting on the concrete plug.*

2.4.2 Water pressure

In the water pressure is set to an evenly distributed value of q_w = 4 MPa and may affect just the vertical part of the plug or both the vertical part and the diagonal slit between plug and rock as schematically shown in Figure 2-4.

2.4.3 Swelling pressure of bentonite

The swelling pressure of bentonite depends on the design of the tunnel and the type of bentonite finally used but is here set to an evenly distributed value of q_s = 2 MPa that affects just the vertical part of the plug, compare Figure 2-4a.

2.4.4 Temperature difference in concrete plug

When tightening the concrete plug after an age of about 90 days, the plug is planned to be cooled down from T_0 = +15°C to +5°C, i.e. ΔT = –10°C, and kept at this temperature until the grouting has hardened. Later, when the temperature in the plug is allowed to normalise again this will result in a pre-stressing of the plug corresponding to a temperature increase of ΔT_{plug} = +10°C.

This value is also used in the analyses of the plug. The tolerances used in this report for the temperature and shrinkage loads should cover the possibility of a somewhat lower or higher temperature difference $\Delta T_{plug.}$ In the final design, though, there will be a need to state what tolerance of the temperature difference may be accepted when cooling the plug at this construction stage.

2.4.5 Temperature difference in rock foundation

2.4.5.1 Temperature

The spent nuclear fuel will be stored in copper canisters positioned in bentonite filled holes in the disposition tunnels, see Section 1.1. Over time there will be a heat development from the fuel into the surrounding rock, increasing the temperature above the normal +15 ºC acting in the tunnel. This temperature increase will also affect the resulting stresses in the concrete plug.

An estimation of the rock temperature at the site of the concrete plug has been made based on the iso-plot results given in [5] and is presented in Appendix A. Two series of extreme values have been determined for a range of points in time, see Table 2-4.

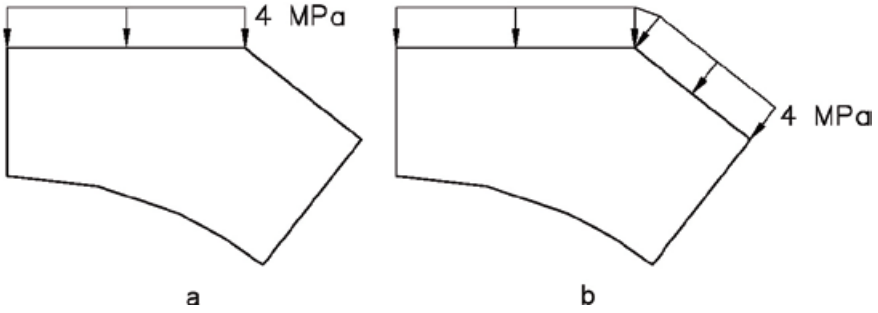

Figure 2-4. *Water pressure on concrete plug: (a) pressure on vertical part and (b) pressure on vertical and diagonal parts.*

Table 2-4. Extreme temperature differences ΔT_r in the rock foundation during a range of 0–100 years, see Appendix A. The normal temperature in the tunnel is T_0 = +15ºC.

Temperature differences, ΔT_r		
Time [years]	**Min [°C]**	**Max [°C]**
0	+0	+0
1	+0	+1
10	+2	+10
100	+7	+25

2.4.5.2 Even temperature difference

An even temperature change in the plug presupposes that the temperature on either side of the plug is the same; i.e. the free air on the outside of the plug is assumed to reach the same temperature as the rock and the bentonite at the inside of the plug. When this condition is assumed the temperature change ΔT_r, see Table 2-4, is set to be constant in the whole plug.

2.4.5.3 Temperature gradient

A temperature gradient over the plug presupposes that there is a difference in temperature between the bentonite and the air on either side of the plug; i.e. different temperature on the inside and outside, respectively. In an extreme case the bentonite is assumed to obtain the same temperature as the surrounding rock while the air maintain the original temperature of T_0 = +15°C. Hence, the temperature boundary conditions are set to ΔT = 0°C on the outside and $\Delta T = \Delta T_r$ (according to Table 2-4) on the inside of the plug, see Figure 2-5.

2.4.6 Shrinkage in concrete plug

The shrinkage of the concrete plug is assumed to be evenly distributed according to Table 2-5. An even shrinkage is assumed due to the expected high relative humidity on the outside of the plug while there will be water present on the inside (RH = 100%). The shrinkage values in Table 2-5 are based on zero shrinkage after 90 days of curing, at which time the concrete plug is assumed to be free of stresses due to shrinkage, see Appendix B.

2.4.7 Loads not taken into account

2.4.7.1 Uneven pressure

No uneven pressure is taken into account in the analyses since it is not possible with the boundary conditions applied (axial symmetry) in the finite element model used. However, this approximation is believed to be acceptable in the current stage of the work but has to be considered in a forth-coming, more detailed analysis, see Chapter 6.

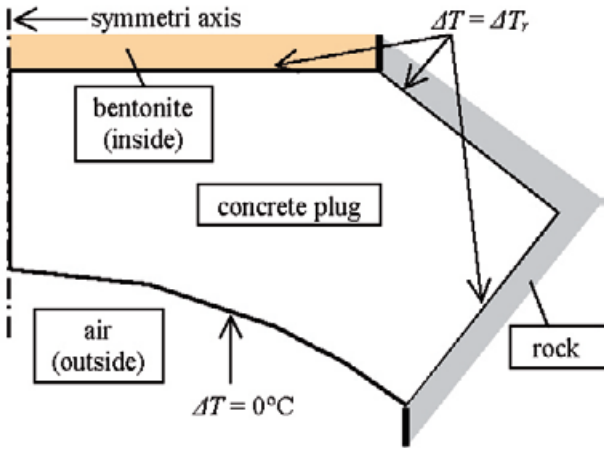

Figure 2-5. *Temperature boundary conditions used when taking in accordance the temperature gradient over the concrete plug thickness.*

2.4.7.2 Self weight

The self weight of the concrete plug is not taken into account in the analyses since it is not possible with the boundary conditions applied (axial symmetry) in the finite element model used. This approximation is believed to have negligible influence on the results presented herein but may be further considered in a forthcoming, more detailed analysis, see Chapter 6.

2.4.7.3 Seismic load

A seismic load of realistic magnitude is believed to have negligible contribution to the stress state of the plug. The load was disregarded at this stage of the work but may remain as a point for further control in a forthcoming study, see Chapter 6.

2.5 Design criteria

2.5.1 Orientation

In Section 2.1 the required functions of the plug are stated as

- to make sure that the water flow through the bentonite is below critical inflow,
- to hold the bentonite in place.

The first function is a tightness demand; i.e. the amount of water that is allowed to leak through the plug, while the second one is a structural demand on the stresses that will arise in the concrete material. The following sections deal with the requirements set up for the water leakage and concrete strengths used when evaluating the results from the analyses presented in Chapter 4.

Table 2-5. Shrinkage ε_{cs} in concrete plug during a range from 0–100 years, see [1] and Appendix B.

	Shrinkage, ε_{cs}		Temperature, ΔT_{cs} [1)]	
Time [years]	Min [‰]	Max [‰]	Min [°C]	Max [°C]
0	0.00	0.00	–0	–0
1	0.02	0.07	–2	–7
10	0.04	0.18	–4	–19
100	0.07	0.29	–7	–29

[1)] Based on coefficient of thermal expansion $\alpha = 10^{-5}°C^{-1}$.

2.5.2 Water tightness of concrete plug

The allowed water leakage through the concrete plug is in this work set to 0.01 l/min, i.e. 14.4 l/day. This value is a rough estimation based on the maximum amount of bentonite that is allowed to be transported away in the deposition tunnel and assumes that the water leakage through the interface between the plug and rock is the same as that through the plug itself. However, it can be concluded that the weak points due to water leakage will not be through the plug itself but through the rock close to the plug or in the plug/rock-interface. The value given here can hence be regarded as an allowable limit defined in order to find a relevant criterion for a minimum height of uncracked concrete in the plug.

In order to meet the above requirement the concrete plug needs a compressive zone of at least 0.4 m in any given cross section, see Appendix C. If this requirement is fulfilled the tightness of the concrete plug is deemed to be satisfactory.

2.5.3 Displacement of plug

The displacement of the plug shall be in a reasonable range in order to retain the function of the bentonite backfill. Further, such displacements in the interface between plug and rock that may cause problem with water leakage shall be prevented. What resulting displacement that thus may be allowed is not clear but a permissible average plug displacement of 10 mm is regarded as a reasonable approximation.

2.5.4 Bearing capacity of concrete plug

The bearing capacity of the concrete plug is satisfied if force equilibrium is reached in such a way that the stresses in the structure are within the required limits. Hence, as long as this condition is fulfilled there is no demand that the plug should remain uncracked.

The load acting on the plug may all be considered as long term loads and all results are based on linear elastic analyses in which the concrete Young's modulus is set to an effective modulus $E_{c,ef}$, affected by the concrete creep φ as

$$E_{c,ef} = \frac{E_c}{1+\varphi} \qquad \text{(Eq. 2-1)}$$

This creep factor, though, is based on linear creep, which presumes that the concrete still acts linearly, i.e. that the stresses obtained in the concrete is low enough. In BBK 04, [2], the limit for elastic behaviour of concrete in compression is set to

$$\sigma_c \leq 0.6 f_{cc} \qquad \text{(Eq. 2-2)}$$

while Eurocode 2, [4], use

$$\sigma_c \leq 0.45 f_{cc} \qquad \text{(Eq. 2-3)}$$

However, tests on the low-pH concrete used in the plug show a somewhat different behaviour with a larger elastic portion than is the case for normal concrete. Hence, based on the investigation presented in Appendix D it is found that it is safe to follow the recommendation made in [2]. However, it is also shown in Appendix D that it is reasonable to increase the elastic limit to

$$\sigma_c \leq 0.65 f_{cc} \qquad \text{(Eq. 2-4)}$$

and hence this relation is used herein to determine the elastic limit of concrete in compression.

3 Modelling of plug

3.1 General

The analyses of the concrete plug and its behaviour under certain loading conditions are performed in a 2D axis symmetric finite element model using the general finite element programme ADINA, [6] and [7].

The model represents the rotated surface of the concrete plug as well as a limited part of the surrounding rock. In the performed analysis are included not only the expected loads, but also a variation of the rock material parameters Young's modulus and coefficient of friction between rock and concrete.

Linear elastic materials are assumed for both the concrete and the surrounding rock. Nevertheless, a non-linear effect is included through considering a combination of contact and friction between the plug and the rock. Both steady-state thermal and structural analyses are used. The characteristics of the model as well as the assumptions made in the modelling process are presented in the following sections.

3.2 Geometry

The geometry of the plug follows the geometry outlines as presented in Section 2.2.1. The surrounding rock is modelled as a half-spherical space with a radius of 5 m where the rotational axis goes through the middle of the plug as shown in Figure 3-1 and Figure 3-2.

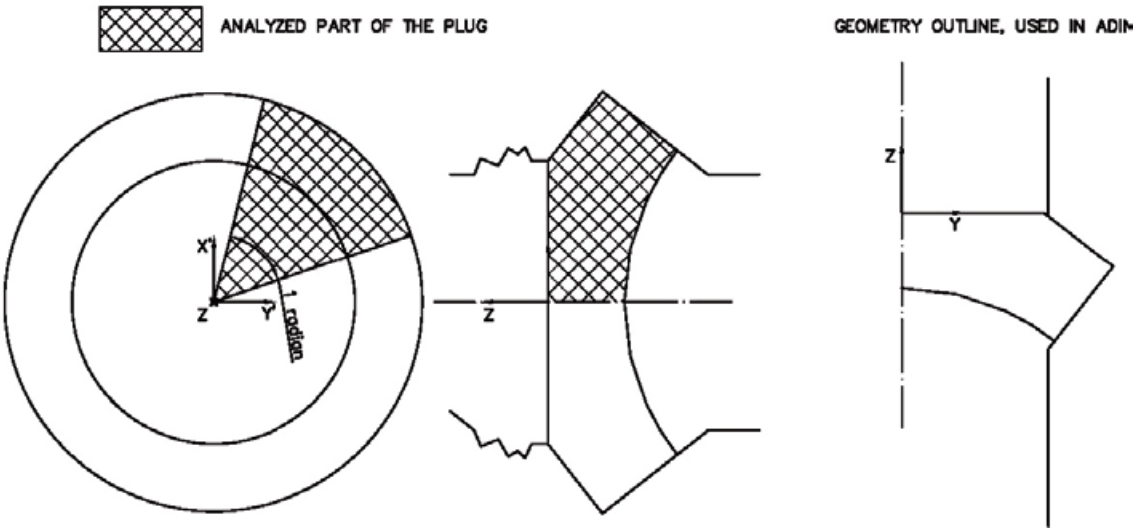

Figure 3-1. *Analysed part of concrete plug.*

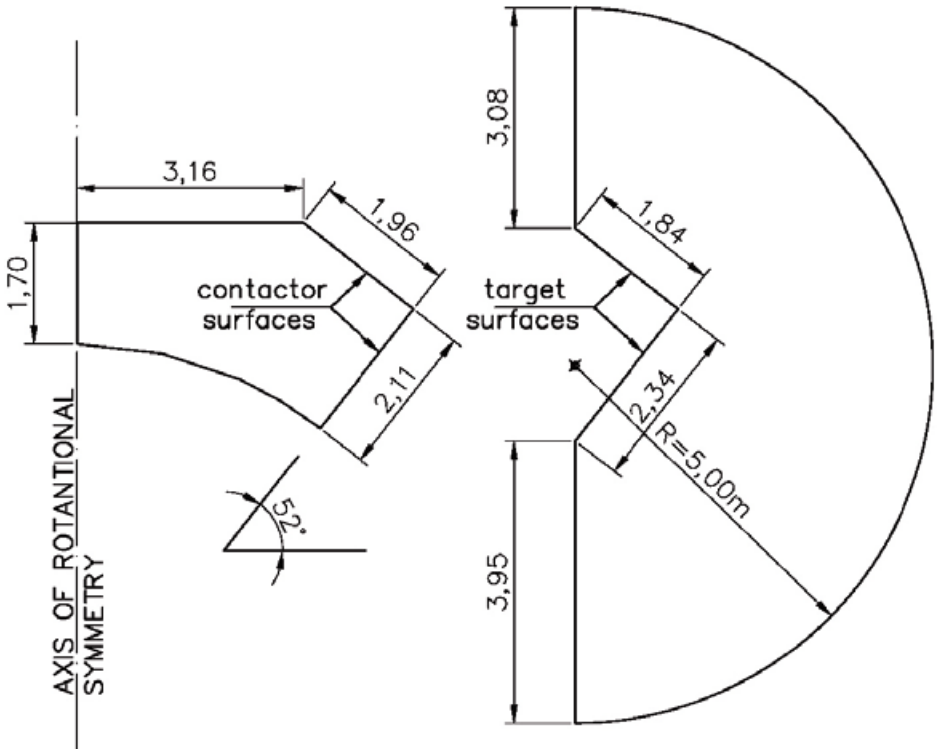

Figure 3-2. *Assumed geometry of the plug and the surrounding rock.*

3.3 Finite element model

3.3.1 Finite element mesh

The two-dimensional finite element mesh of the plug and the surrounding rock is shown in Figure 3-3 and the two element groups used in Figure 3-4. A three-dimensional projection of the plug and the surrounding concrete, i.e. the two-dimensional model revolved around the symmetry axis, is shown in Figure 3-5. A similar 3D projection of the concrete plug only is shown in Figure 3-6.

Two-dimensional, 4-node, axis-symmetric elements, using 2 x 2 Gaus integration, are used for modelling both the concrete plug and the rock. This element type has both a structural elastic and thermal formulation, which makes it possible to use identical meshes for the structural and thermal analyses. The local co-ordinate system and the related output are presented with the results.

3.3.2 Boundary conditions

The interaction between the plug and the surrounding rock is modelled with contact surfaces, the plug being the contactor and the rock the target surface. The conditions for the contact are further described in Section 3.6.

3.4 Material properties

3.4.1 Concrete properties

Both structural and thermal properties of the concrete material are considered in the model, see Table 3-1. In both cases the material is linear isotropic. Values for Young's modulus and concrete creep are based on Table 2-1 where the values used have been determined in order to get a high as possible effective Young's modulus $E_{c,ef}$ according to Equation 2-1. The thermal properties are of no importance since the thermal analyses used herein are used to find a stage of steady-state flow only.

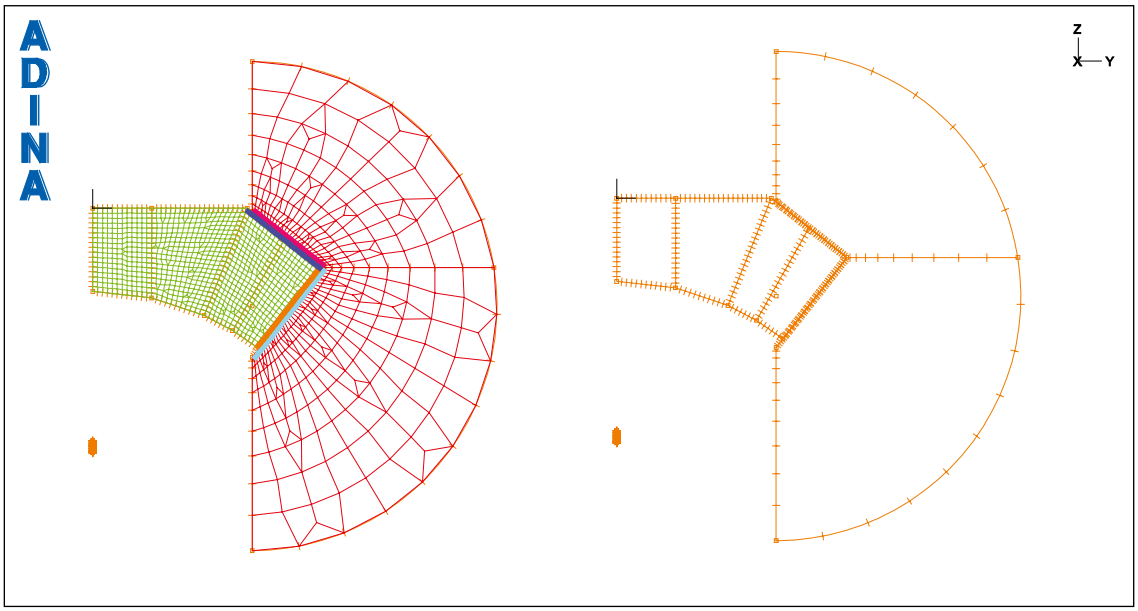

Figure 3-3. *FE model of the plug, element mesh and geometry. The different colours represent different element group as shown in Figure 3-4.*

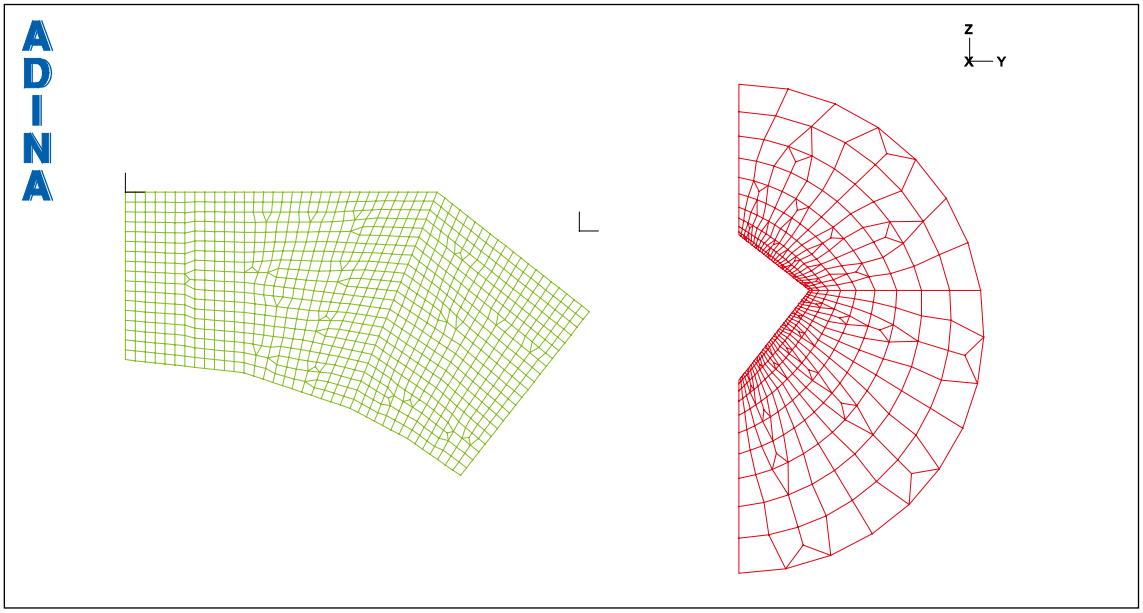

Figure 3-4. *Element groups used in the model: concrete plug (left) and rock (right).*

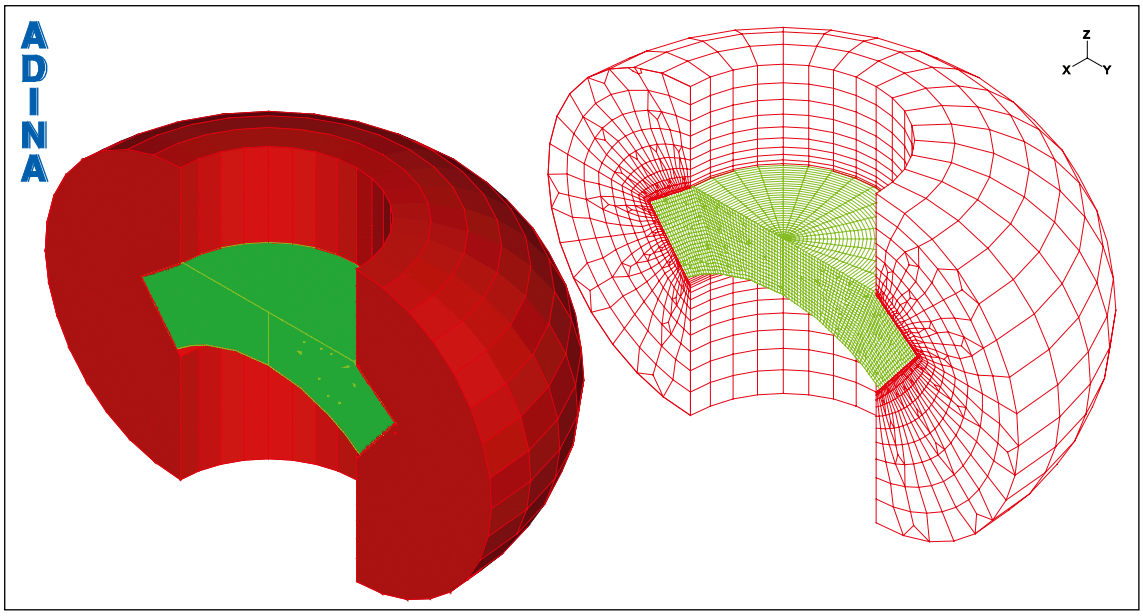

Figure 3-5. *Three-dimensional projection of the plug (green part) and the surrounding rock (red part).*

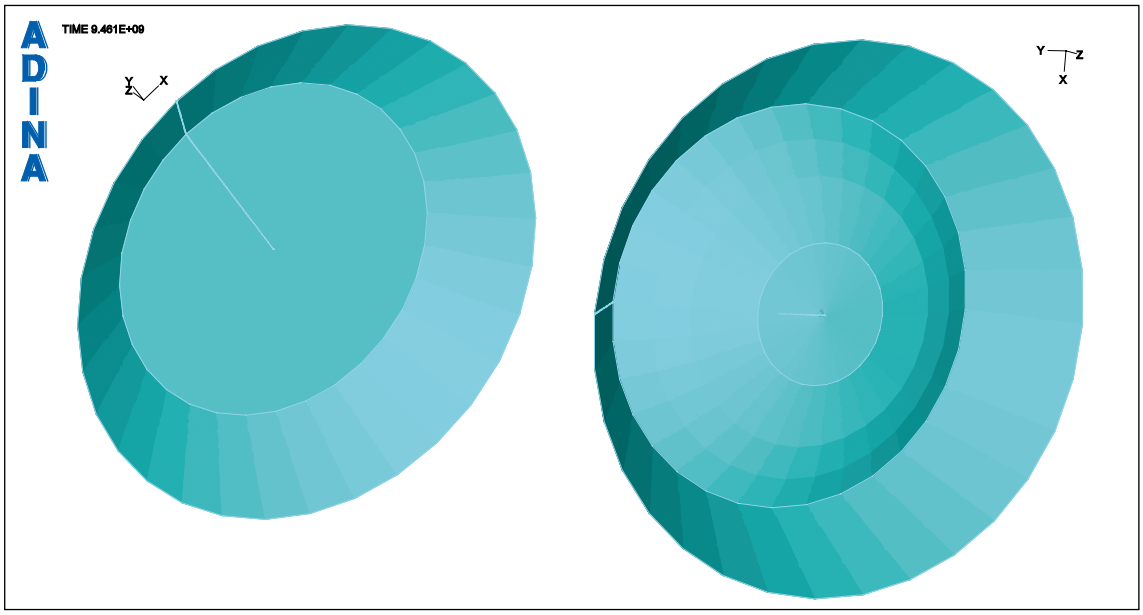

Figure 3-6. *Three-dimensional projection of the concrete plug, seen from the inside (left) and the outside (right), respectively.*

Table 3-1. Material properties for concrete used in the analyses.

Material property	Denotation	Value	Unit
Young's modulus [1)]	$E_{c,ef}$	26.7	GPa
Poisson's ratio	ν	0.27	–
Coeff. of thermal expansion	α	$1.0 \cdot 10^{-5}$	$°C^{-1}$

[1)] Young's modulus determined according to Equation 2-1 where E_c = 39,0 GPa and φ = 0.46 according to Table 2-1 when t = 100 years.

3.4.2 Rock properties

The properties of the rock are shown in Table 3-2 and are considered with some variation in order to cover the uncertainties and the irregularity of the material.

3.5 Loads

3.5.1 Orientation

The loads applied on the plug are those described in Section 2.4 and are divided into separate load cases. The loads used can be separated into pressure loads and temperature loads.

The loading from the combined effects of temperature changes and shrinkage is presented through the temperature difference at all points of the model. In all load cases the load definition is determined in separate thermal analyses. All loads are related to those expected after 100 years.

3.5.2 Load cases

3.5.2.1 Pressure loads

The pressure loads, water pressure and swelling, are described in Section 2.4.2 and Section 2.4.3, respectively, and are divided into two general cases as listed below and shown in Figure 3-7.

Table 3-2. Material properties for rock used in the analyses.

Material property	Denotation	Value	Unit
Rock Young's modulus [1)]	E_r	25, 50, 75	GPa
Poisson's ratio	v	0.20	–
Friction rock/concrete	μ	0.3, 2.0	–
Coeff. of thermal expansion	α	$0.7 \cdot 10^{-5}$	$^{o}C^{-1}$

[1)] Young's modulus determined according to Equation 2-1 where E_c = 39,0 GPa and φ = 0.46 according to Table 2-1 when t = 100 years.

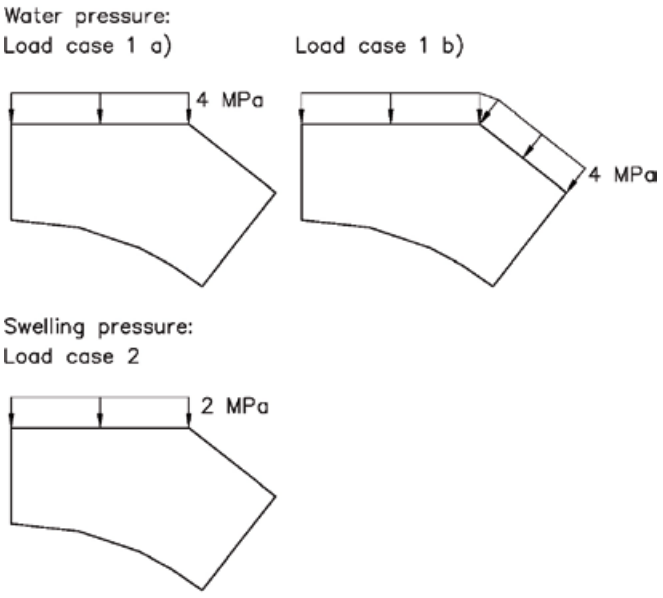

Figure 3-7. *Pressure loads, load cases 1a, 1b and 2.*

Load case 1: Water pressure

- 1a) water pressure on vertical part – 4 MPa
- 1b) water pressure on vertical part and diagonal slit – 4 MPa

Load case 2: Swelling pressure of bentonite

- 2) swelling pressure on vertical part – 2 MPa

3.5.2.2 Temperature loads

The temperature loads are described in Section 2.4.4 to Section 2.4.6. In its physical meaning they represent not only temperature changes in the plug and the surrounding environment but also the concrete shrinkage as dealt with in Appendix A. All loads refer to the situation expected after 100 years and are listed below.

Load case 3: Temperature (considering shrinkage)

- 3a) Temperature difference in plug – pre-stressing of plug,
  $\Delta T_{plug} = +10°C$
- 3b) Temperature difference in rock and plug – maximum rock temperature and minimum shrinkage assuming even distribution,
  $\Delta T_r = +25°C$, $\Delta T_{plug} = +18$ ºC
- 3c) Temperature difference in rock and plug – minimum rock temperature and maximum shrinkage assuming even distribution,
  $\Delta T_r = +7°C$, $\Delta T_{plug} = -22$ ºC
- 3d) Temperature gradient in the plug – maximum rock temperature and minimum shrinkage assuming temperature gradient of $\Delta T_{grad} = 25°C$
  $\Delta T_r = +0°C$, $\Delta T_{plug,out} = +0°C$, $\Delta T_{plug,in} = -25°C$
- 3e) Temperature gradient in the plug – minimum rock temperature and maximum shrinkage assuming temperature gradient of $\Delta T_{grad} = 7°C$
  $\Delta T_r = +0°C$, $\Delta T_{plug,out} = +0°C$, $\Delta T_{plug,in} = -7°C$

The temperature values given for the plug in load cases 3b–3e, ΔT_{plug}, are fictitious temperatures since they are a combination of rock temperature and concrete shrinkage while the temperatures in load case 3a and the rock, ΔT_r, are pure temperature values. Further, the temperature load cases are related to each other. Hence, case 3b and 3d, or case 3c and 3e, are connected in a sense that they may act together. Further, the temperature gradient, i.e. case 3d and 3e, is only considered in combination with case 3b and 3c, respectively. The possible temperature load combinations are illustrated in Figure 3-8 and are determined as

$$\Delta T = \Delta T_{3a} + \Delta T_{3b/3c} + \Delta T_{-/3d/3e} \qquad \text{(Eq. 3-1)}$$

where the index indicate which load case is considered.

3.5.3 Load combinations

Several different load combinations are considered in the analyses and are summarised in Table 3-3. The load case combinations are further expanded with the variation of the rock material properties shown in Table 3-2. Hence, a total of 8 general loading scenarios with 6 additional variations for material and friction give a total of 48 load combinations.

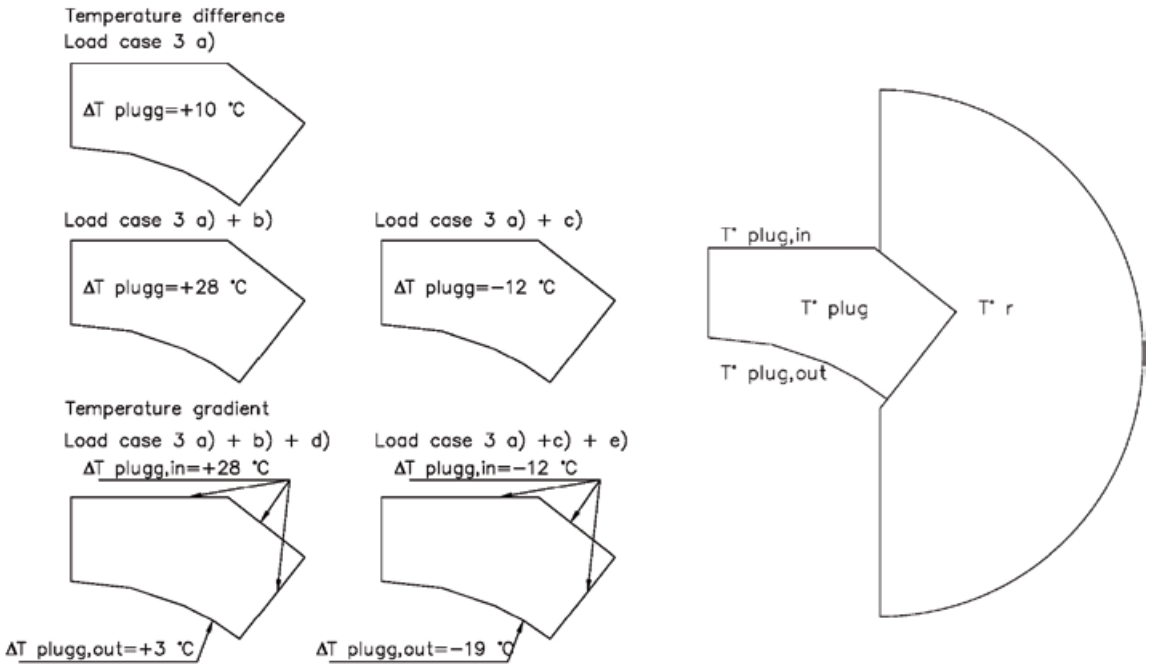

Figure 3-8. *Temperature loads, load cases 3a–3e.*

Table 3-3. Load cases and load scenarios used in the analyses.

		Load cases							
		1a	**1b**	**2**	**3a**	**3b**	**3c**	**3d**	**3e**
Load scenarios	1	x		x	x	x			
	2	x		x	x	x		x	
	3	x		x	x		x		
	4	x		x	x		x		x
	5		x	x	x	x			
	6		x	x	x	x		x	
	7		x	x	x		x		
	8		x	x	x		x		x

The difference between load combinations 1–4 and 5–8 is the water pressure acting on the diagonal slit as shown in Figure 2-4. Load combinations 1, 3, 5 and 7 consider the load cases where the rock temperature is high and the concrete shrinkage is low. Hence, these combinations will result in large compressive stresses in the plug. Correspondingly, load combinations 2, 4, 6 and 8 consider the load cases where the rock temperature is low and the concrete shrinkage high, resulting in large tensile stresses in the plug.

Table 3-4. Load combinations obtained when combining the 8 load scenarios listed in Table 3-3 and the 6 possible material variations for the surrounding rock.

Load scenario X, X=1–8		
Load combination	**E_r [GPa]**	**μ**
X.1	25	0.3
X.2	25	2.0
X.3	50	0.3
X.4	50	2.0
X.5	75	0.3
X.6	75	2.0

3.6 Boundary conditions

3.6.1 General

The boundary conditions in the model are trivial full restrain, applied to the rock boundaries, and contact between the plug and the rock, see Figure 3-9.

Since the model is axis-symmetric, there is no need to further apply symmetry boundary conditions. ADINA does that automatically, assuming the Z-axis at Y = 0 as the axis of rotation.

3.6.2 Contact between concrete plug and rock

The contact conditions between the plug and the surrounding rock is described in ADINA using the segmental contact formulation using a Coulomb friction with a friction coefficient μ defined as a constant value in each analysis. In order to represent the frictional influence, two cases are considered according to Table 2-2; i.e. $\mu = 0.3$ and $\mu = 2.0$ for the low and high boundary, respectively.

Two contact pairs, representing the contact surfaces between the plug and the rock, are defined in the model. As the two contact surfaces overlap in the corner point, it was chosen to include the corner node included in contact pair 2, see Figure 3-10. Since contact is modelled between plug and rock this means that a possible crack between them both will be simulated, hence transforming this to a partly non-linear model.

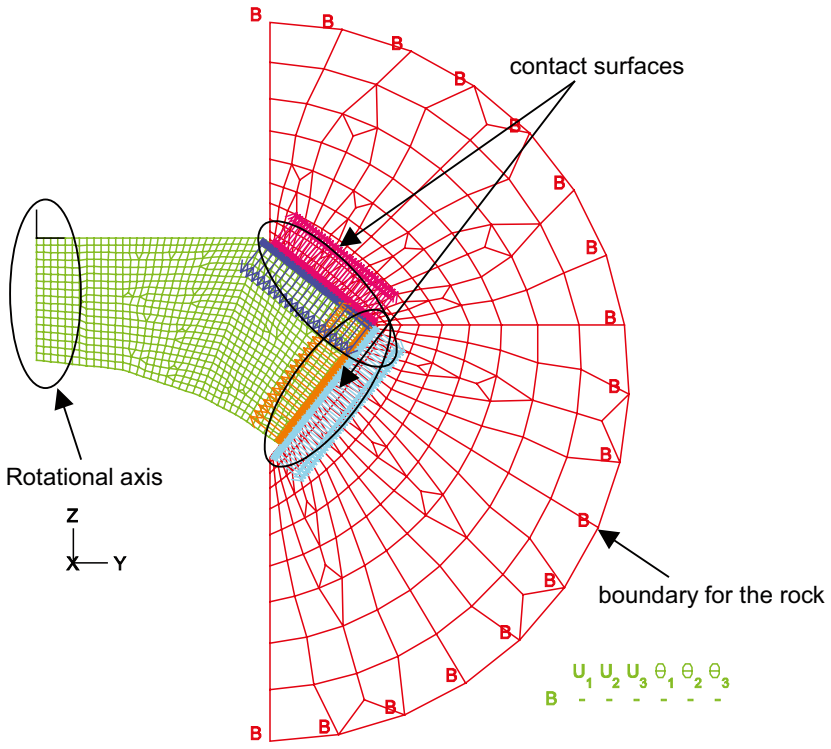

Figure 3-9. *Boundary conditions, general overview.*

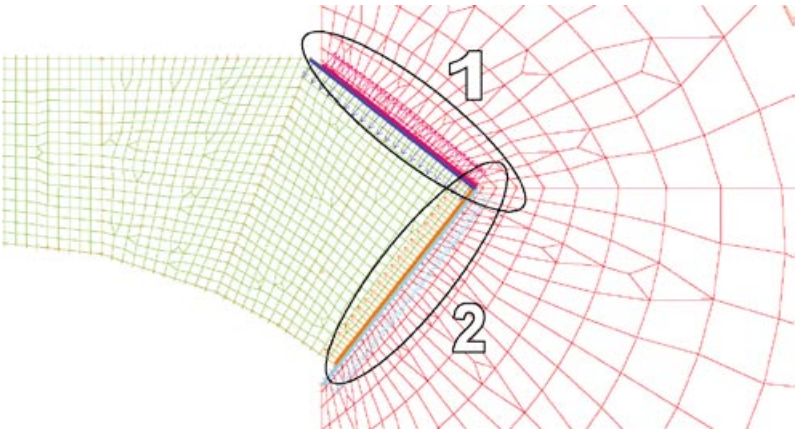

Figure 3-10. *Contact between the plug and the rock.*

3.7 Analyses

3.7.1 Thermal analyses

Thermal analyses are done for all load scenarios and are performed as steady state analyses using the temperature boundary conditions defined in Figure 3-8. The resulting temperature distribution is then used as load input in the structural analyses. Since the meshes in the structural and thermal analyses are identical, no extrapolation for the temperature in non-coincide nodes is necessary.

3.7.2 Structural analyses

The structural analysis is performed as a linear elastic static analysis considering large deformations. The loads in each respective load combination are applied at the same time without regard to the real load history and the contact between the plug and the rock is calculated using Full Newton-Raphson iteration and an energy tolerance to find force equilibrium in the structure.

4 Results of the analysis

4.1 Thermal analyses

The temperature boundary conditions used in the analyses are shown in Figure 3-8. The resulting temperature distribution after reaching steady state, in load scenarios 1–4 and 5–8 are presented in Figure 4-1 to Figure 4-4 and are used as loads (mapped to the respective load-step) in the structural analyses.

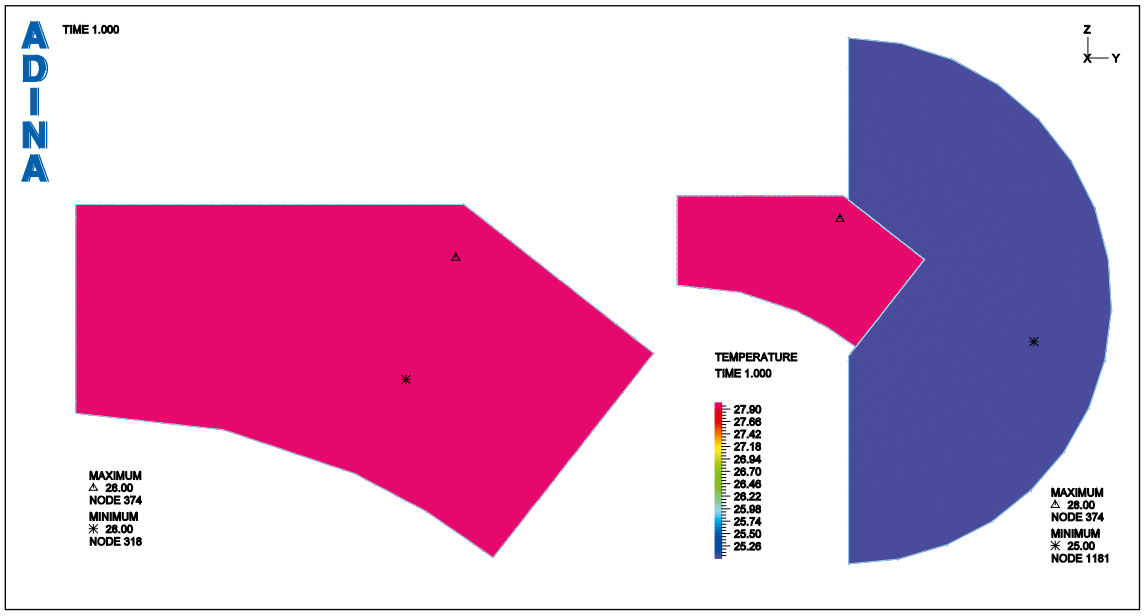

Figure 4-1. *Temperature difference in concrete plug of +28°C and temperature difference in the rock of +25°C. These temperatures correspond to load scenarios 1 and 5, compare Figure 3-8 and Table 3-3.*

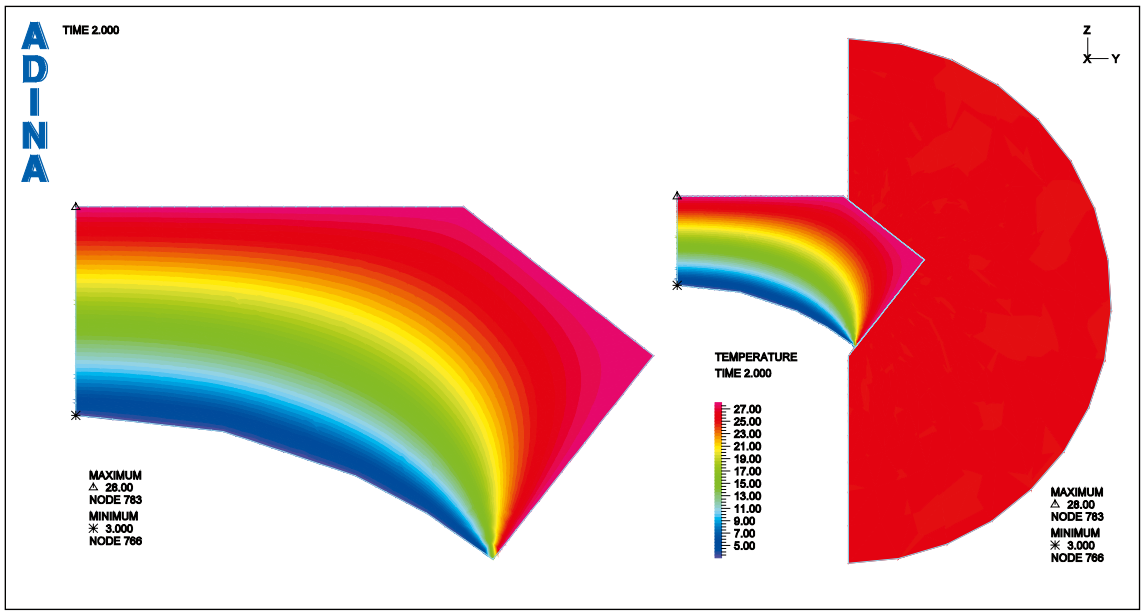

Figure 4-2. *Temperature difference in concrete plug describing a temperature gradient from +28°C to +3°C and a temperature difference in the rock of +25°C. These temperatures correspond to load scenarios 2 and 6, compare Figure 3-8 and Table 3-3.*

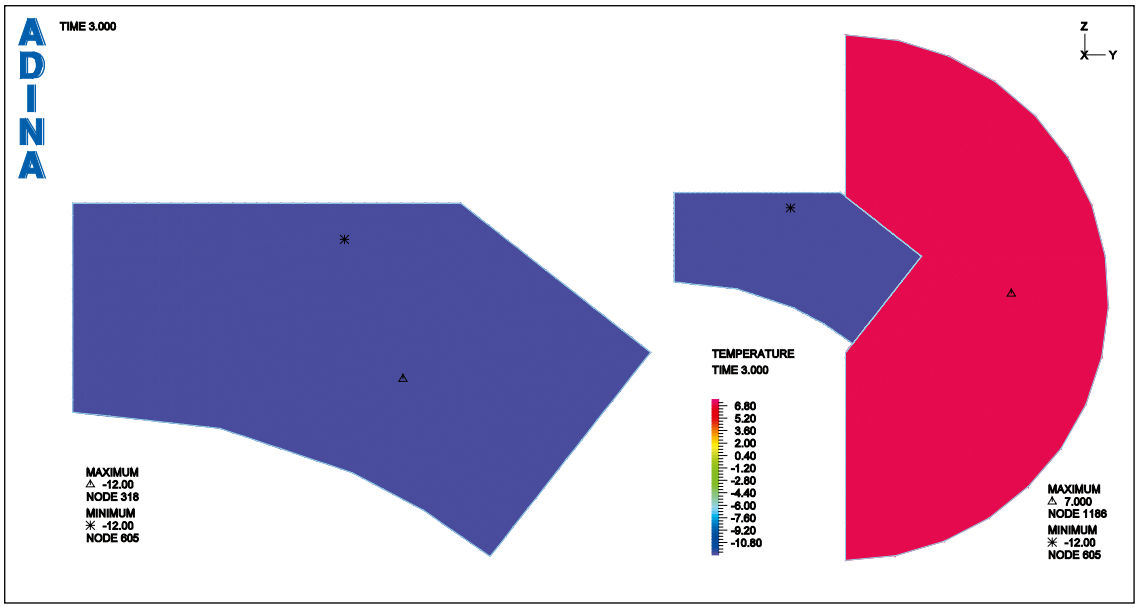

Figure 4-3. *Temperature difference in concrete plug of –12°C and temperature difference in the rock of +7°C. These temperatures correspond to load scenarios 3 and 7, compare Figure 3-8 and Table 3-3.*

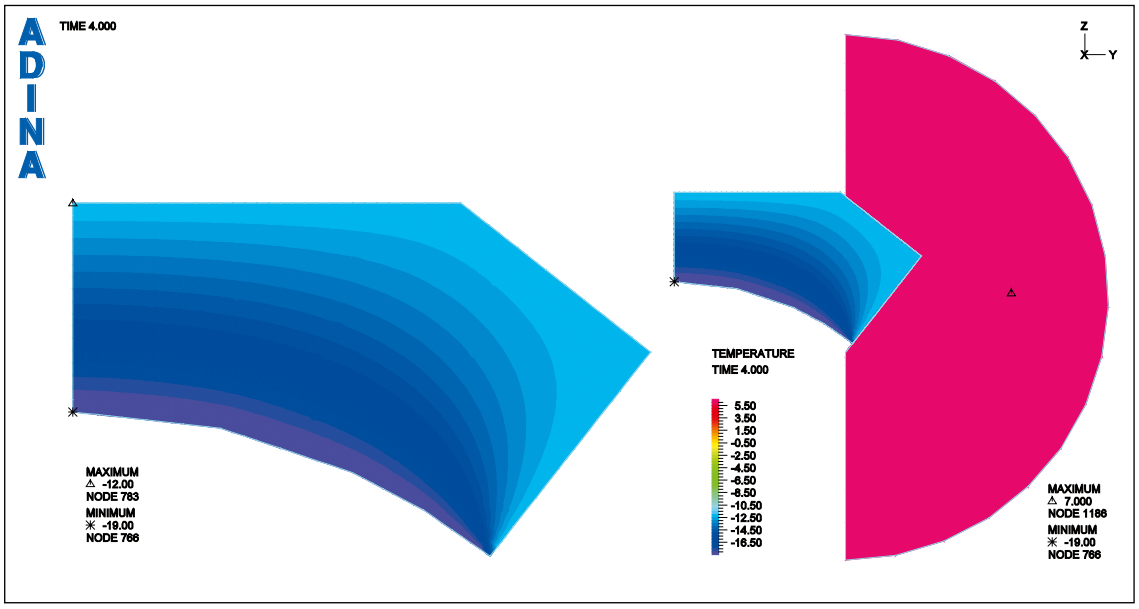

Figure 4-4. *Temperature difference in concrete plug describing a temperature gradient from –12°C to –29°C and a temperature difference in the rock of +7°C. These temperatures correspond to load scenarios 4 and 8, compare Figure 3-8 and Table 3-3.*

4.2 Structural analyses

4.2.1 Resulting stresses

The resulting stresses from the structural analysis are summarised in Table 4-1 and Table 4-2. The stresses σ_1 and σ_3 presented in the tables are the maximal and minimal principal stresses and represent the absolute peak values obtained in the analyses, often related to singular points. The stress σ_y represents the stresses acting perpendicular (y-direction, see e.g. Figure 4-1) to the rotational axis along the mid plug mid section, i.e. the rotational axis shown in Figure 3-9, and is considered to represent reliable stress values acting in the structure.

The resulting stresses and integrated section forces for all load combinations are presented in Appendix E and F, respectively. Some extra complementing analyses are also carried out and presented in Appendix G.

Table 4-1. Resulting maximum and minimum principal stresses (σ_1 and σ_2), and stresses σ_y perpendicular to the rotational axis for load scenarios 1–4. Deviations may occur from those values shown in the stress plots presented in Appendix E.

Load scenarios	Load combination	E_r [GPa]	μ [–]	σ_1 [MPa] min	max	σ_3 [MPa] min	max	σ_y [MPa] [1] top	bot.	Cracked Section [2]
1	1.1	25	0.3	–12.9	5.2	–39.5	–5.6	–17.2	–16.1	N
	1.2	25	2.0	–13.8	4.9	–45.7	–4.9	–18.1	–15.7	N
	1.3	50	0.3	–18.7	5.1	–40.1	–7.1	–18.4	–22.8	N
	1.4	50	2.0	–19.2	5.1	–50.6	–6.8	–19.3	–22.0	N
	1.5	75	0.3	–21.7	4.3	–40.4	–8.8	–19.1	–25.8	N
	1.6	75	2.0	–21.9	4.3	–53.4	–8.1	–19.9	–24.8	N
2	2.1	25	0.3	–10.2	5.0	–21.2	–3.4	–19.8	–4.2	N
	2.2	25	2.0	–10.9	4.4	–27.7	–2.6	–21.0	–3.3	N
	2.3	50	0.3	–15.1	2.5	–21.0	–8.2	–21.0	–10.2	N
	2.4	50	2.0	–15.6	4.4	–29.6	–7.0	–22.1	–8.8	N
	2.5	75	0.3	–17.6	3.1	–23.7	–9.1	–21.6	–12.8	N
	2.6	75	2.0	–17.8	3.2	–31.0	–9.0	–22.7	–11.4	N
3	3.1	25	0.3	–6.0	7.5	–22.2	0.5	–14.9	7.0	Y
	3.2	25	2.0	–6.0	11.1	–23.6	0.9	–15.8	10.3	Y
	3.3	50	0.3	–6.0	5.9	–19.3	0.4	–14.0	5.5	Y
	3.4	50	2.0	–6.0	9.6	–21.7	1.0	–14.8	8.9	Y
	3.5	75	0.3	–6.0	5.3	–17.8	0.4	–13.6	4.9	Y
	3.6	75	2.0	–6.0	9.0	–20.7	1.1	–14.4	8.4	Y
4	4.1	25	0.3	–6.0	9.1	–18.8	0.6	–15.9	8.4	Y
	4.2	25	2.0	–6.0	13.4	–20.6	0.9	–16.7	12.4	Y
	4.3	50	0.3	–6.0	7.9	–15.9	0.6	–15.0	7.3	Y
	4.4	50	2.0	–6.3	12.1	–18.8	0.9	–15.8	11.2	Y
	4.5	75	0.3	–6.3	7.5	–14.7	0.5	–14.7	6.9	Y
	4.6	75	2.0	–6.6	11.6	–17.9	0.8	–15.5	10.8	Y

[1] Refers to cracks in the plug mid section, top and bottom, acting perpendicular to the rotational axis.

[2] Refers to cracks that are not due to the stresses in a singular point, see Section 4.2.2.2.

Table 4-2. Resulting maximum and minimum principal stresses (σ_1 and σ_2), and stresses σ_y perpendicular to the rotational axis for load scenarios 5–8. Deviations may occur from those values shown in the stress plots presented in Appendix E.

Load scenarios	Load combination	E_r [GPa]	μ [–]	σ_1 [MPa] min	max	σ_3 [MPa] min	max	σy [MPa] 1) top	bot.	Cracked Section 2)
5	5.1	25	0.3	–12.0	1.3	–35.1	–10.4	–16.1	–20.3	N
	5.2	25	2.0	–13.2	–0.1	–44.8	–9.7	–17.9	–19.0	N
	5.3	50	0.3	–17.8	–0.2	–31.9	–11.5	–17.2	–26.2	N
	5.4	50	2.0	–18.8	–0.2	–46.3	–10.6	–18.8	–25.1	N
	5.5	75	0.3	–20.7	–0.2	–31.3	–12.1	–17.8	–28.9	N
	5.6	75	2.0	–21.5	–0.2	–47.2	–11.1	–19.3	–27.8	N
6	6.1	25	0.3	–9.5	1.0	–22.2	–5.9	–19.7	–7.3	N
	6.2	25	2.0	–9.9	0.0	–27.2	–5.1	–20.8	–6.3	N
	6.3	50	0.3	–14.4	0.3	–20.6	–9.9	–20.6	–12.3	N
	6.4	50	2.0	–15.1	0.0	–25.6	–9.2	–21.7	–11.5	N
	6.5	75	0.3	–16.8	0.4	–21.1	–11.7	–21.1	–14.7	N
	6.6	75	2.0	–17.4	0.0	–24.9	–11.0	–22.1	–13.8	N
7	7.1	25	0.3	–7.0	1.8	–29.4	–0.4	–17.5	–0.5	N
	7.2	25	2.0	–7.0	5.1	–33.0	0.4	–18.5	4.7	Y
	7.3	50	0.3	–7.0	1.6	–25.3	–1.6	–16.3	–2.0	N
	7.4	50	2.0	–7.0	3.3	–28.7	0.2	–17.1	3.1	Y
	7.5	75	0.3	–7.3	1.4	–23.5	–2.1	–15.9	–2.7	N
	7.6	75	2.0	–7.0	2.7	–26.9	0.2	–16.6	2.4	Y
8	8.1	25	0.3	–7.0	1.4	–25.3	–0.3	–18.2	–0.4	N
	8.2	25	2.0	–7.0	7.0	–30.3	0.5	–19.5	6.5	Y
	8.3	50	0.3	–7.9	1.1	–21.3	–1.4	–17.2	–1.8	N
	8.4	50	2.0	–7.0	5.3	–26.6	0.4	–18.2	4.9	Y
	8.5	75	0.3	–8.4	1.0	–19.5	–1.9	–16.9	–2.3	N
	8.6	75	2.0	–7.3	4.6	–24.8	0.3	–17.7	4.3	Y

1) Refers to cracks in the plug mid section, top and bottom, acting perpendicular to the rotational axis.

2) Refers to cracks that are not due to the stresses in a singular point, see Section 4.2.2.2.

It shall be pointed out that there is a difference between the values listed in Table 4-1 and Table 4-2 compared to those values shown in the stress-plots presented in Appendix E. The reason for this is that the latter represent an approximate value based on a smoothing technique used in ADINA. Hence, the true stress results are those shown in Table 4-1 and Table 4-2 and the listed results in the stress-plots should just be regarded as approximate values.

4.2.2 Comment about tensile stresses

4.2.2.1 Tensile strength

When determining whether the tensile stresses obtained in the analyses cause cracking or not it has to be compared with the concrete tensile strength available. From Table 2-1 a characteristic tensile strength f_{ctk} = 2.9 MPa is given. However, in order to decide whether the plug is cracked or not it is reasonable to use a safety factor ζ. In [2] the use of ζ = 2.0 is recommended when the tensile strength is used to show necessary capacity in the ultimate limit state. Hence, this value is also used here for the tensile strength. Further, a material partial factor γ_m = 1.5 (from [2] and [4]) that takes into account uncertainties in the material properties, is also included giving a final value of

$$f_{ct} = \frac{f_{ctk}}{\gamma_m \cdot \xi} = \frac{2.9}{1.5 \cdot 2.0} = 0.97 \approx 1.0 \text{ MPa} \qquad \text{(Eq. 4-1)}$$

Hence, the tensile stresses obtained in the analyses are compared with f_{ct} = 1.0 MPa and if $\sigma_c \leq f_{ct}$ the plug is considered uncracked and cracked if $\sigma_c > f_{ct}$.

4.2.2.2 Comparison of tensile stresses and tensile strength

Generally, tensile stresses appear in all of the studied cases, see Table 4-1 and Table 4-2. Nevertheless, in load scenarios 1 and 2, in Table 4-1, the plug is still denoted as uncracked since the tensile stresses obtained are localised to one element only. This is also the case for many load combinations. High tensile stresses are concentrated to a few elements due to singular effects; compare stresses σ_I for load combination 1.1 in Figure 4-5 from which it is clear that the concrete plug is in compression in all but one or two single elements. Hence, such singular tensile peaks are disregarded in the evaluation and the plug and these sections are considered uncracked and denoted accordingly.

However, for load scenarios 3 and 4 there are large tensile stresses due to bending over an extensive part of the plug, compare the maximum principal stresses caused by load combination 3.1 in Figure 4-6, and hence the plug is considered being cracked.

The largest tensile stresses are obtained for load combination 4.2, see Table 4-1, where σ_c = 13.4 MPa is reached. Tensile stresses appear when the internal pressure, i.e. stresses caused by expansion due to temperature, cannot compensate for the bending tension induced from the water and swelling pressure and the concrete shrinkage. Principal stresses for all load combinations are shown in Appendix E.

The structural analyses presented in this report use a linear elastic material assumption; i.e. no cracking of the concrete is considered in the analyses. Hence, if no cracking appear the analyses carried out are fully valid. However, if this requirement is not fulfilled the concrete plug will crack and the results acquired from the analyses have to be properly modified to describe the correct structural behaviour of the plug. From the above it is clear that there will be cracking in some of the load combinations investigated. Hence, a recalculation of the results has to be done in order to determine the stresses obtained in the plug, something which is further dealt with in Appendix F and G.

4.2.3 Comment about compressive stresses

4.2.3.1 Compressive strength

When determining whether the compressive stresses obtained in the analyses may cause crushing of the concrete they have to be compared with the available concrete compressive strength. From Table 2-1 characteristic compressive strengths are given for concrete of different ages ranging from 90 days to 100 years. However, due to uncertainties in the long term strength of this type of concrete it is recommended in [1] that a conservative value is chosen and hence the effect of ageing is not initially considered. Hence, the value for a concrete 90 days old, i.e. f_{cck} = 51 MPa, is primarily used when determining allowable compressive stresses.

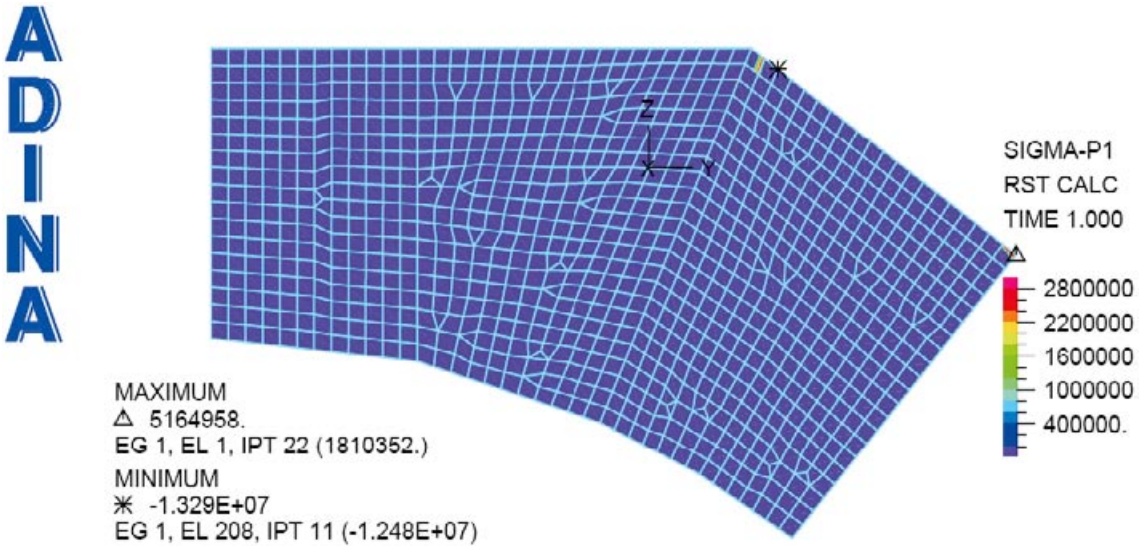

Figure 4-5. *Maximum principal stresses σ_1 in concrete plug when subjected to load combination 1.1. Tensile stresses (not blue colour) are considered to be due to singular effects.*

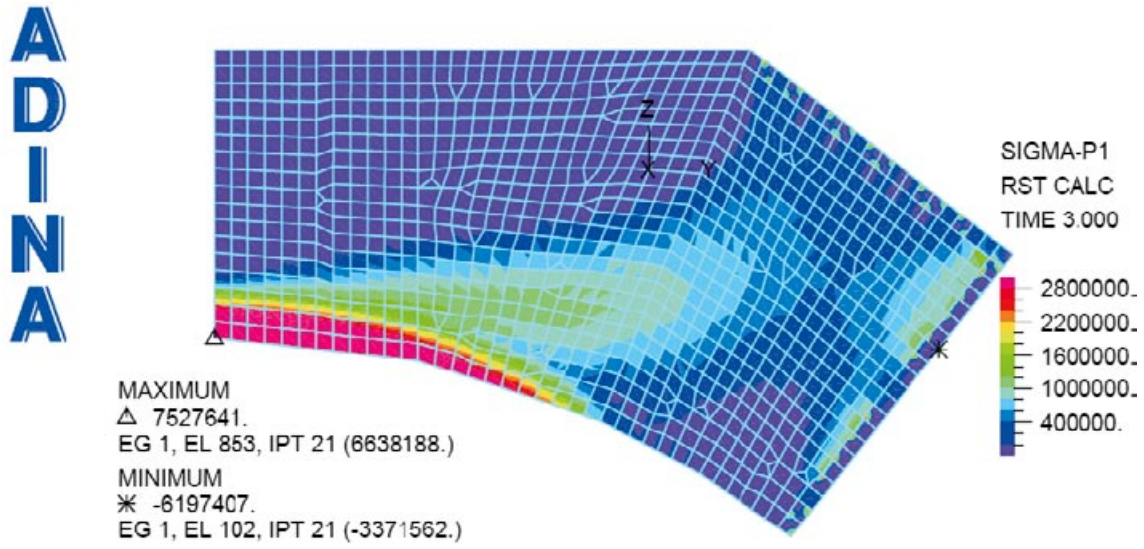

Figure 4-6. *Maximum principal stresses σ_1 in concrete plug when subjected to load combination 3.1. There are large tensile stresses (red colour) in a large area, and hence, the plug is considered to be cracked.*

As dealt with in Section 2.5.4 the analyses carried out presuppose a linear elastic behaviour of the concrete material and in order to fulfil this requirement the compressive stresses have to fulfil the requirement of

$$\sigma_c \leq 0.65 f_{cc} \qquad \text{(Eq. 4-2)}$$

Hence, if

$$\sigma_c \leq 0.65 f_{cc} = 0.65 \cdot 51 = 33.1 \text{ MPa} \qquad \text{(Eq. 4-3)}$$

is fulfilled the presumption of linear behaviour is correct and the analyses show that the plug can handle the stresses obtained. If the compressive stresses exceed the requirement in Equation 4-3 it is still possible to show that the capacity of the plug is sufficient. The difference is that the concrete in compression then reaches its non-linear behaviour and the stress distribution in the structure will become somewhat different.

The load combinations studied are assumed to take place after 100 years, see Section 3.5.1. After this time it is realistic that the concrete strength has increased due to ageing. If taking this into account an alternative allowable compressive stress may be determined. According to Table 2-1 the characteristic compressive strength after 1 year is $f_{cck,1y}$ = 67 MPa, 10 years is $f_{cck,10y}$ = 80 MPa and after 100 years is $f_{cck,100y}$ = 85 MPa. Hence, taking this into account and applying Equation 4-3 give allowable stresses of 43 MPa, 52 MPa and 55 MPa, respectively. Accordingly, even though it is recommended in [1] that a conservative value should be chosen it is fruitful to know the limits possible if the prediction of the compressive strength is fully used.

4.2.3.2 Comparison of compressive stresses and compressive strength

From Table 4-1 and Table 4-2 it is shown that the maximum compressive stress is σ_3 = –53.4 MPa. This stress is obtained for load combination 1.6; i.e. maximum water pressure combined with high even temperature increase when there is a high coefficient of friction between plug and rock and high rock stiffness. The stress peak appears at the extreme edge of the plug in its contact with the rock and from the stress plots in Appendix E it can be seen that the large stress is located to a very limited area of one element. However, such large, localised, stresses are believed to be due to numerical reasons in the analyses rather than to real stresses and are therefore not primarily regarded.

Accordingly, if the extreme stresses obtained for load scenarios 1 and 5 are disregarded the largest compressive stress is σ_3 = –33.0 MPa for load combination 7.2. However, as shown in Equation 4-3 the allowable compressive stress is σ_c = 33.1 MPa, and consequently the stresses obtained in the

analyses are within given limits. It may be argued that the difference in maximum compressive stress and allowable stress is small. However, considering the reserve capacity of the increased concrete strength due to ageing, i.e. σ_c = 43–55 MPa according to Section 4.2.3.1 it is plausible to accept this without further comments.

In Section 4.2.2.2 it is concluded that the concrete plug will not remain uncracked for some load combinations. Hence, a different stress distribution will come up in which the compressive stresses will change compared to those given in Table 4-1 and Table 4-2. Consequently, this has to be investigated and is further dealt with in Appendix F and G.

4.2.4 Resulting displacements

The resulting displacements of the plug are shown in Table 4-3 and Table 4-4 for load combinations 1–4 and 5–8, respectively. Midpoint displacements are given in the direction of the rotational axis (z-direction) and the displacement of the plug bottom edge is given as sliding along the rock interface.

Table 4-3. Resulting displacements in midpoint of plug and bottom edge of the plug at the rock interface for load combinations 1–4.

Load scenarios	Load combination	E_r [GPa]	μ [–]	Mid- point [mm]	Bot. edge [mm]
1	1.1	25	0.3	0.54	0.79
	1.2	25	2.0	0.56	0.51
	1.3	50	0.3	0.16	0.90
	1.4	50	2.0	0.20	0.54
	1.5	75	0.3	0.01	0.99
	1.6	75	2.0	0.06	0.61
2	2.1	25	0.3	0.84	1.00
	2.2	25	2.0	0.89	0.63
	2.3	50	0.3	0.50	1.15
	2.4	50	2.0	0.56	0.72
	2.5	75	0.3	0.37	1.23
	2.6	75	2.0	0.44	0.78
3	3.1	25	0.3	3.13	1.06
	3.2	25	2.0	3.10	0.61
	3.3	50	0.3	2.75	0.97
	3.4	50	2.0	2.75	0.50
	3.5	75	0.3	2.61	0.95
	3.6	75	2.0	2.62	0.49
4	4.1	25	0.3	3.27	1.27
	4.2	25	2.0	3.24	0.71
	4.3	50	0.3	2.90	1.14
	4.4	50	2.0	2.90	0.60
	4.5	75	0.3	2.77	1.10
	4.6	75	2.0	2.78	0.58

Table 4-4. Resulting displacements in midpoint of plug and bottom edge of the plug at the rock interface for load combinations 5–8.

Load scenarios	Load combination	E_r [GPa]	μ [–]	Mid point [mm]	Bot. edge [mm]
5	5.1	25	0.3	0.59	1.46
	5.2	25	2.0	0.66	0.93
	5.3	50	0.3	0.12	1.48
	5.4	50	2.0	0.19	0.94
	5.5	75	0.3	0.05	1.53
	5.6	75	2.0	0.02	0.99
6	6.1	25	0.3	0.96	1.45
	6.2	25	2.0	1.00	1.05
	6.3	50	0.3	0.53	1.48
	6.4	50	2.0	0.57	1.09
	6.5	75	0.3	0.37	1.51
	6.6	75	2.0	0.42	1.13
7	7.1	25	0.3	3.74	1.92
	7.2	25	2.0	3.71	1.24
	7.3	50	0.3	3.18	1.67
	7.4	50	2.0	3.17	1.03
	7.5	75	0.3	2.97	1.60
	7.6	75	2.0	2.98	0.99
8	8.1	25	0.3	3.90	2.29
	8.2	25	2.0	3.84	1.37
	8.3	50	0.3	3.33	2.02
	8.4	50	2.0	3.32	1.15
	8.5	75	0.3	3.13	1.93
	8.6	75	2.0	3.13	1.10

4.2.5 Comment about plug displacements

The displacements of the plug for all load combinations are presented in Table 4-3 and Table 4-4. From this it can be found that the maximum displacement in the plug midpoint is 3.3 mm and the maximum sliding in the concrete/rock interface is 2.3 mm sliding along the interface. Both displacements are caused by load combination 8.1; i.e. when the water pressure is acting on both the vertical part and the diagonal slit, and maximum concrete shrinkage with an uneven temperature is acting on the plug and the rock is stiff and the frictional coefficient is low.

The permissible displacement is set to be 10 mm, see Section 2.5.3, so hence the displacements obtained is deemed acceptable.

5 Conclusions

In this report a concrete plug, used as a barrier between the deposition tunnels and the access tunnel, is investigated. The objectives of the work is to see whether it is possible to use low pH concrete for the plug and whether it can be designed without using reinforcement. The requirements set on the plug are that the water leakage through it should be small enough and that the concrete stresses are limited to a value valid for the concrete used.

A modified geometry of the plug is proposed, which makes it possible to use it as a general solution in all deposition tunnels. It is assumed that the concrete plug will be cooled down in conjunction with grouting between plug and concrete after 90 days of hardening and it is shown that a temperature difference of $\Delta T = -10$ºC will be sufficient for obtaining the response needed to achieve this.

Loads considered in the study is the pressure from water and swelling, the temperature change in the rock and plug due to heat development from nuclear fuel stored in nearby copper canisters, pre-stressing in the plug due to cooling during construction and the shrinkage of concrete in the plug. It is found that the concrete plug will not remain uncracked when subjected to these loads but that it, nevertheless, seems possible to achieve an unreinforced concrete plug that satisfy the requirements set up.

The minimum size of the concrete compressed zone will be 0.5 m, resulting in a water leakage through the plug estimated to be lower than 0.01 l/min, which is less than required. Further, the maximum compressive stresses of interest are 33 MPa and the maximum displacement in the plug is about 3 mm, which are deemed to be satisfactorily. Consequently, it is concluded that it seems possible to use low pH concrete for the plug and design it without using reinforcement.

It shall be pointed out that there are uncertainties in the parameters used and that the conclusions drawn are due to the approximations made in this report. Hence, a follow-up study should be made in which these issues are further addressed, see Chapter 6

6 Items for further work

This report has been made using some uncertainties in the requirements set up, material properties of the plug used and the loads applied on the structure. Hence, there is a need to follow up these uncertainties and further investigate what effect they may have on the conclusions drawn herein.

Below topics are proposed to be further studied in a following, more detailed, report, where given proposals are of different dignity, some are due to lack of knowledge and some due to shortage of time when this report was made.

Requirements

- The requirement of water leakage through the plug is not clearly defined and has to be further investigated.
- Allowable displacements of the plug, especially the sliding along the rock interface, should be better defined.

Material parameters

- The concrete material parameters, including shrinkage, are based on [1] but since this is a new type of concrete and the tests carried out so far only cover a time period of less than two years there are still some uncertainties. Hence, the results in this report presume that there will be a continuous investigation of the material properties of the low pH concrete. Of special interest is to confirm whether the increase in strength, due to ageing, develops as expected and whether the concrete shrinkage predicted and used in this report is correct or not.
- The value on the Poisson's ratio used is unusually high, a more normal value for concrete is about $\nu = 0.2$, and a sensitivity analysis of this should be carried out.
- The influence of lower Young's modulus for the concrete has not been fully investigated in the analyses and will have to be further studied.

Loads and load combinations

- The load values used for the water pressure and swelling pressure of bentonite are not clearly defined and the effect of larger pressures may have to be further studied.
- The effect of uneven water pressure in the diagonal slit between plug and rock has not been taken into account in this study and will hence have to be further studied.
- In this report it has been assumed that there will be high RH on either side of the concrete plug, thus justifying the concrete shrinkage used in the analyses. However, a case where no water on the inside of the plug is taken into account, and hence, a larger and uneven shrinkage, have to be taken into account.
- A load combination, considering the effect of shrinkage only without water or swelling pressure, taking into account a possible uneven shrinkage over the plug thickness, may be of interest. An analysis should be made whether this is a load combination of interest, and if so, a complementary analysis should be made.
- The rock temperatures used in the analyses are determined based on a rather early report in which the temperatures given include some rough uncertainties. Hence, it seems realistic to get a somewhat more precise prediction of the temperatures that will be valid for the final choice of site.
- In the analyses a temperature increase in the rock has been assumed. However, a load combination wherein this temperature increase is null should also be investigated.

Results

- Expected size of concrete crack widths in the plug. The size of these cracks will not be of any consequence in relation to the demands set on the plug, but may be of importance for other reasons, e.g. too large crack widths may transmit the erroneous feeling that it the plug is not safe enough.

7 References

[1] Vogt C, Lagerblad B, Wallin K, Baldy F, Jonasson J-E, 2008. Low PH self compacting concrete for plugging of deposition tunnels in a repository for spent nuclear fuel. CBI report in press, CBI, Stockholm, Sweden.

[2] Boverket, 2004. Boverkets handbok om Betongkonstruktioner, BBK 04. Boverket, Karlskrona, Sweden.

[3] L-O Dahlström, 2008. Experiences from the design and installation of plug II in the Prototype Repository. SKB id. 1179756, Svensk Kärnbränslehantering AB.

[4] CEN, 2004. Eurocode 2: Design of concrete structures – Part 1-1: General rules and rules for buildings, CEN, Bryssel, Belgium.

[5] Ageskog L and Jansson P, 1999. Heat propagation in and around the deep repository, Thermal calculations applied to three hypothetical sites: Aberg, Beberg and Ceberg. TR-99-02, Svensk Kärnbränslehantering AB.

[6] ADINA, 2008. Command Reference Manual, Volume I: ADINA Model Definition, Report ARD 08-2, ADINA R&D, Inc. February 2008.

[7] ADINA, 2008. Command Reference Manual, Volume IV: Display Processing, Report ARD 08-5, ADINA R&D, Inc. February 2008.

[8] Ljungkrantz C, Möller G, Peterson N, 1994. Betonghandboken – Material, utgåva 2. Redigerad av Ljungkrantz C, Möller G och Peterson N, Svensk Byggtjänst, Stockholm, Sweden.

Appendix A

Load from temperature and shrinkage

A.1 Orientation

The temperature values presented in this Appendix are based on [5] in which the temperature in the rock has been determined for different rock configurations. The values used here are collected from temperature iso-plots presented with an accuracy of 5 ºC. Hence, the precision of temperatures proposed herein are limited to the same magnitude.

A.2 Cases studied

Three concepts of deep repository using rock with different material parameters were studied in [5], see Figure A-1. Temperature analyses have been carried out for each concept in the different deposition areas and are presented using iso-plots.

A.3 Temperature in rock

Based on the temperature iso-plots given in [5] the maximum and minimum temperature have been interpreted at the mouth of the deposition tunnels, see Figure A-2. For each concept different values are shown for deposition area 1 and 2, and hence, two set of temperature curves are given for each case.

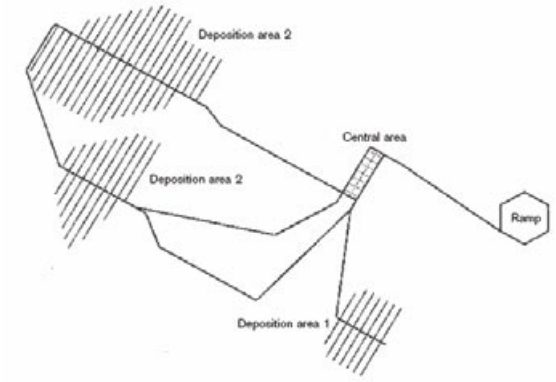

Concept 1 - Aberg

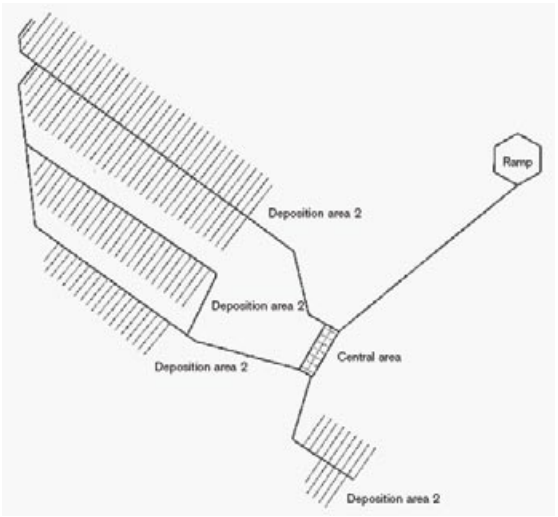

Concept 2 – Bberg

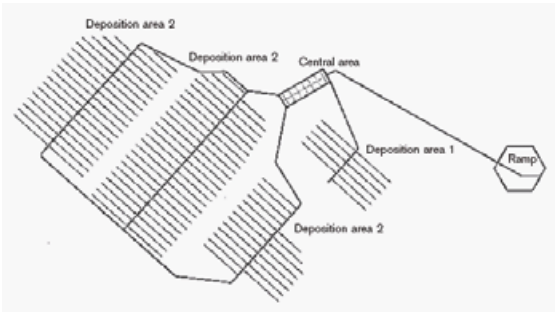

Concept 3 – Cberg

Figure A-1. *Concepts studied for deep repository.*

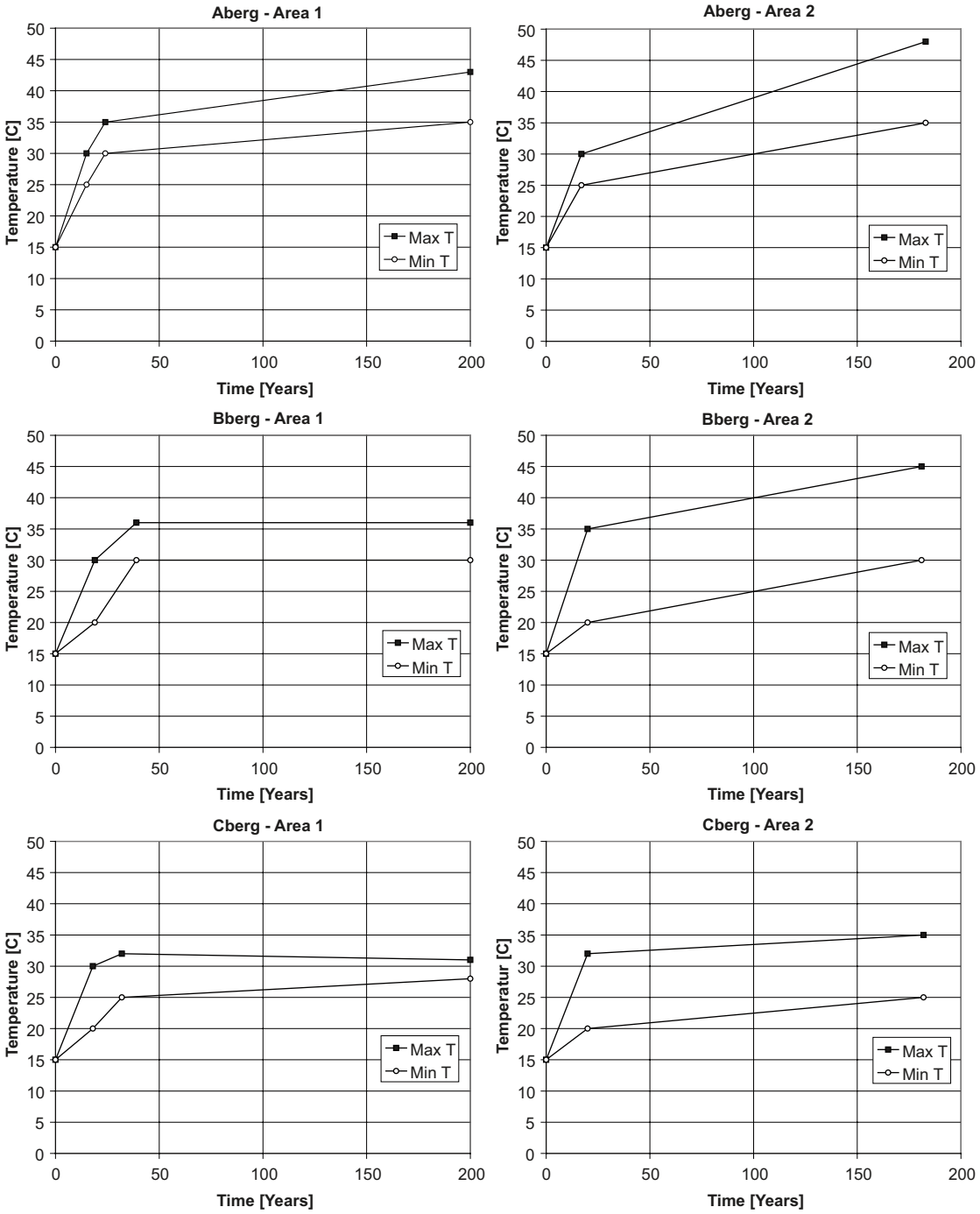

Figure A-2. *Max and min temperatures for the concepts showed in Figure A-1. An initial (normal) temperature of T_0 = +15 C was assumed for the rock in the analyses.*

From the results in Figure A-2 it is clear that the rock temperature varies rather much for the different concepts and respective areas. However, as a conservative approach all these temperatures are summarised in Figure A-3 and a maximum and minimum envelop is determined. Based on these two envelopes are the maximum and minimum temperatures determined for the following point in times: 0, 1, 10 and 100 years, se Table A-1.

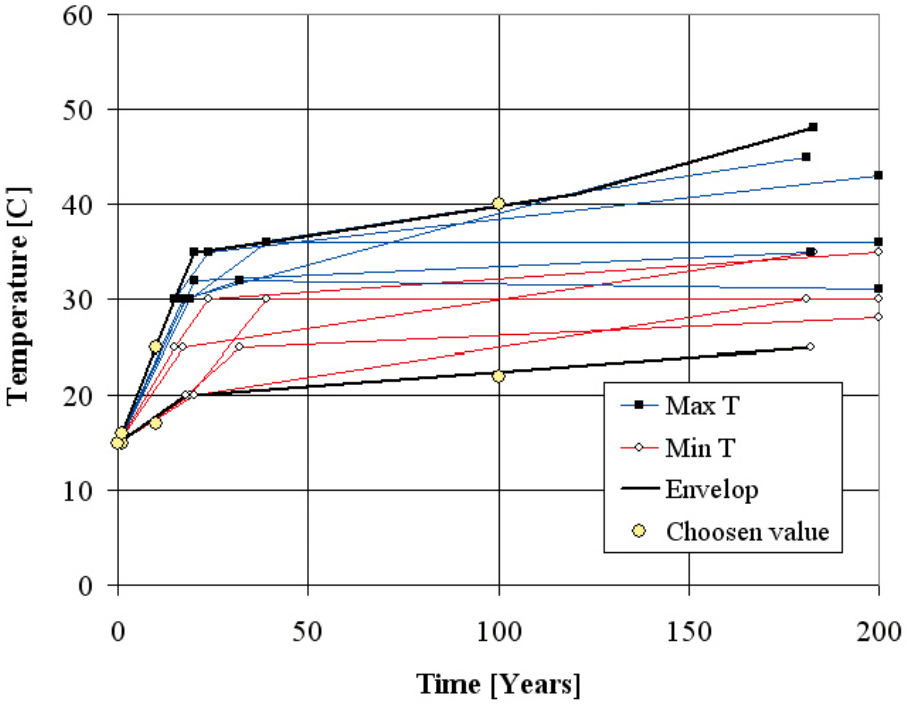

Figure A-3. *Envelopes max and min temperatures based on values shown in Figure A-2. The resulting temperatures for 0, 1, 10 and 100 years are listed in Table 7-1.*

Table A-1. Maximum and minimum temperatures in rock according to Figure A-3. An incremental temperature ΔTr is determined based on the temperature after 0 years.

Time [years]	$T_{r,min}$ [ºC]	$T_{r,max}$ [ºC]	$\Delta T_{r,min}$ [ºC]	$\Delta T_{r,max}$ [ºC]
0	15	15	+0	+0
1	15	16	+0	+1
10	17	25	+2	+10
100	22	40	+7	+25

A.4 Combination with shrinkage

The values ΔT_{min} and ΔT_{max} hence describe the minimum and maximum expected temperature change, respectively, during the next 100 years after installation of the concrete plugs.

These temperatures can then be combined with that of the shrinkage in the concrete plug, see Table 2-5, and a resulting temperature can be determined in order to see what kind of restraining movement will appear, see Table A-2 and Figure A-4.

Table A-2. Combined temperature in concrete plug based on temperature ΔTr in rock (Table A-1) and concrete shrinkage ΔTcs (Table 2-5).

Time [years]	$\Delta_{Tr,min}$ [ºC]	$\Delta_{Tr,max}$ [ºC]	$\Delta T_{cs,min}$ [ºC]	$\Delta T_{cs,max}$ [ºC]	ΔT_{min} [ºC]	ΔT_{max} [ºC]
0	+0	+0	–0	–0	±0	±0
1	+0	+1	–2	–7	–7	–1
10	+2	+10	–4	–19	–17	+6
100	+7	+25	–7	–29	–22	+18

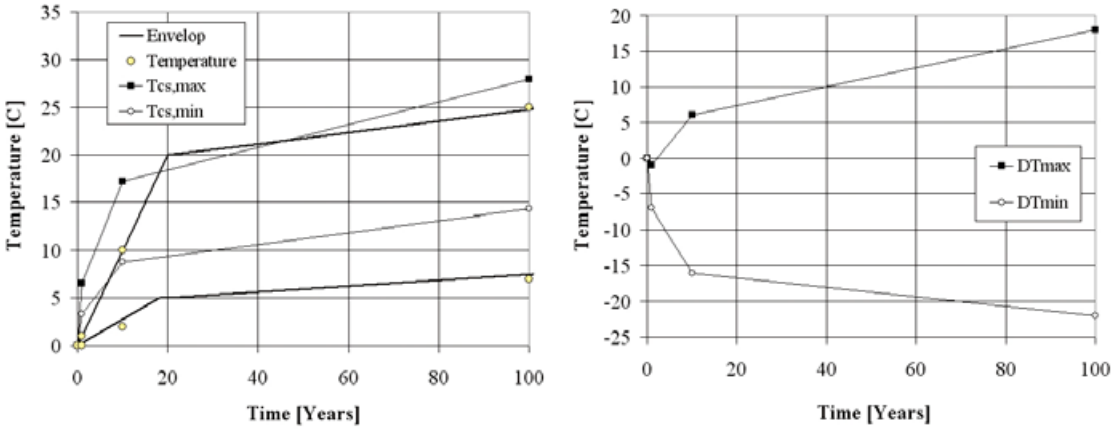

Figure A-4. *Temperature envelope with values listed in Table A-2 marked.*

The resulting values ΔT_{min} and ΔT_{max} are used to determine the movement of the concrete plug in the analyses carried out in Chapter 3.

A.5 Conclusions

The incremental temperatures $\Delta T_{r,min}$ and $\Delta T_{r,max}$ in *Table A-1* are used to describe the temperature in the rock and the incremental temperatures ΔT_{min} and ΔT_{max} in *Table A-2* are used to describe the combined effect of temperature and shrinkage in the concrete plug.

Appendix B

Shrinkage in concrete plug

B.1 Orientation

In the analyses carried out it is assumed that there are no concrete stresses due to restrained movement of even shrinkage in the plug at a time after 90 days. That is, the shrinkage movement appearing in the plug until that time is assumed to occur without causing any resulting stresses. In order to fulfil this assumption, though, it is necessary to make sure that the edges of the concrete plug have loosened from the surrounding rock and is completely free along the whole perimeter at this stage.

This appendix investigates if this is a reasonable assumption or not.

B.2 Accounting factors

B.2.1 Creep

The concrete creep will affect what stresses will occur in the plug from shrinkage. Since the shrinkage will start acting on the plug more or less immediately a creep value higher than that stated in Table 2-1 will be the case. From reference [1] the creep from concrete loaded after 2.5 days are given and listed in Table B-1.

B.2.2 Concrete Young's modulus

The Young's modulus of concrete after 90 days of hardening are used, see Table 2-1, which gives E_c = 34,0 GPa. An effective Young's modulus $E_{c,ef}$ are determined using the creep as

$$E_{c,ef} = \frac{E_c}{1+\varphi} \qquad \text{(Eq. B-1)}$$

B.2.3 Shrinkage

The mean, unreduced concrete shrinkage is according to [1] ε'_{csm} = 0,11‰ after 90 days. Using the same factors as in [1] the characteristic shrinkage can be determined as

$$\varepsilon'_{cs,min} = 0.5 \cdot \varepsilon'_{csm} = 0.5 \cdot 0.11 = 0.05‰ \qquad \text{(Eq. B-2)}$$

$$\varepsilon'_{cs,max} = 2.0 \cdot \varepsilon'_{csm} = 2.0 \cdot 0.11 = 0.22‰ \qquad \text{(Eq. B-3)}$$

where $\varepsilon'_{cs,min}$ = 0.05‰ will be used in the following calculation.

Table B-1. Concrete creep when the concrete is loaded after 2.5 and 90 days of hardening. Values for φ_{min} corresponds to the creep valid for a load of shrinkage only while φ_{max} corresponds to miscellaneous loading.

Time [years]	$\varphi_{2.5d,min}$ [–]	$\varphi_{2.5d,max}$ [–]	$\varphi 9_{0d,min}$ [–]	$\varphi 9_{0d,max}$ [–]
0	2.04	2.55	0.22	0.27
1	2.39	2.99	0.27	0.34
10	2.98	3.72	0.36	0.46
100	3.56	4.45	0.46	0.57

B.2.4 Temperature in plug

There is no temperature increase in the rock due to heat developments in the canisters at this early stage. However, the concrete plug will be cooled down with a temperature of $\Delta T_{plug} = -10$ ºC, see Section 2.4.4, which corresponds to a strain $\varepsilon_{c,plug} = 0.10$‰.

B.3 Stress calculations

B.3.1 Stress in concrete prism

The expected stress in the plug is initially checked assuming a behaviour similar to a fully restrained concrete prism. In such a case the stress can be determined as

$$\sigma_c = \varepsilon'_{cs,\min} \cdot \frac{E_c}{1+\varphi_{2.5d,\min}} + \varepsilon_{c,plug} \cdot \frac{E_c}{1+\varphi_{90d,\max}} \qquad \text{(Eq. B-4)}$$

and with values according to Section 8.2 yields

$$\sigma_c = 0.05 \cdot \frac{34.0}{1+2.04} + 0.10 \cdot \frac{34.0}{1+0.27} = 0.56 + 2.68 = 3.24 \text{ MPa} \qquad \text{(Eq. B-5)}$$

B.3.2 Stress in concrete plug

In the previous section the concrete stresses are determined assuming a concrete prism. However, the plug geometry differ quite considerably from such a case, and hence, the stresses acquired in the plug will be somewhat different. To get a better view of this, three analyses were carried out where the movement perpendicular to the contact surface between concrete and rock was fully restrained. Movement parallel to this surface was either fully restrained along the whole length or in one point only at the top or bottom of the concrete cross section.

In *Figure B-1* the stresses in the interface between concrete and rock are shown for a temperature change of $\Delta T = \pm 1$ ºC for the studied boundary conditions when $E_c = 34.0$ GPa. From this it is clear that the stresses varies along the interface; i.e. a moment is acting on the cross section, and a mean stress value, $0.40 \leq \sigma_{cm} \leq 1.0$ MPa, for the whole interface is determined. This mean value is a conservative value used to control what stress is acquired in interface.

$\sigma_m = 1{,}04$ MPa

$\sigma_m = 0{,}75$ MPa

$\sigma_m = 0{,}40$ MPa

A fully restrained concrete prism, with $E_c = 34.0$ GPa, exposed to a temperature change of $\Delta T = -1$°C yields a tensile stress of

$$\sigma_c = 0.01 \cdot 34.0 = 0.34 \text{ MPa} \qquad \text{(Eq. B-6)}$$

This value may be compared with the lowest mean stress value, $\sigma_c = 0{,}40$ MPa, found in Figure B-1. Therefore, using a very conservative point of view the concrete plug will obtain a tensile stress that is

$$\sigma_c = \frac{0.40}{0.34} = 1.18 \qquad \text{(Eq. B-7)}$$

times higher than that in a concrete prism. Accordingly the resulting tensile stress obtained in the concrete plug will be

$$\sigma_c = 1.18 \cdot 3.24 = 3.81 \text{ MPa} \qquad \text{(Eq. B-8)}$$

B.3.3 Tensile strength in concrete/rock interface

It seems realistic to expect the tensile strength of the interface between concrete and rock to be lower than that of concrete. However, a conservative value is used in this comparison and the upper characteristic concrete tensile strength, $f_{ctk,0.95}$, is used.

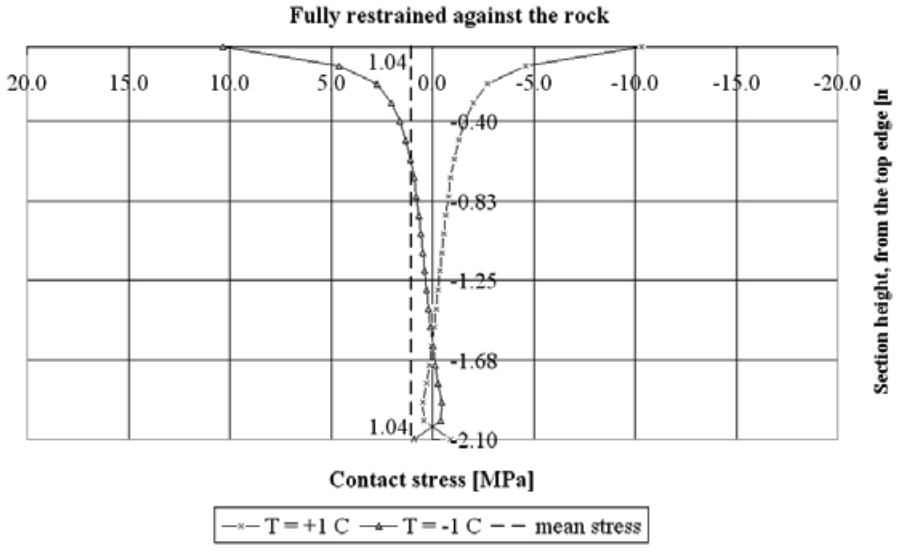

σ_m = 1,04 MPa

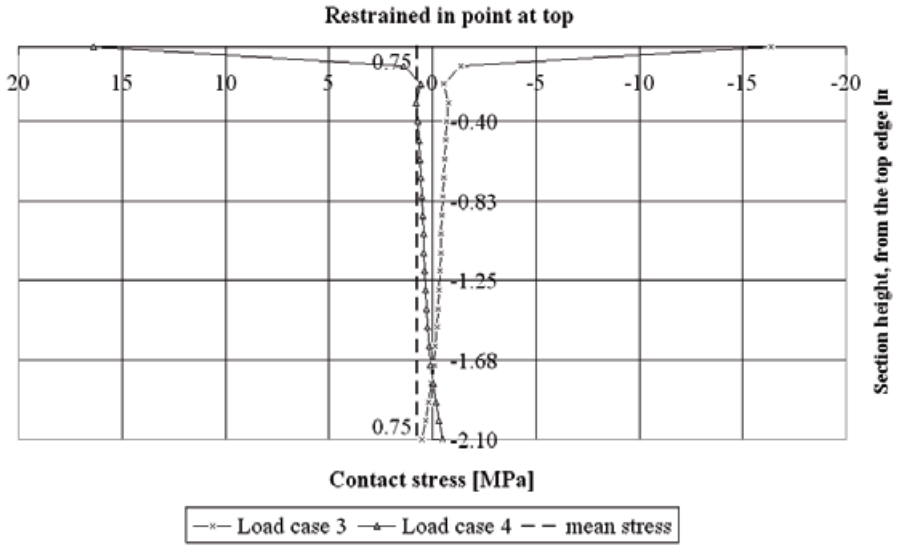

σ_m = 0,75 MPa

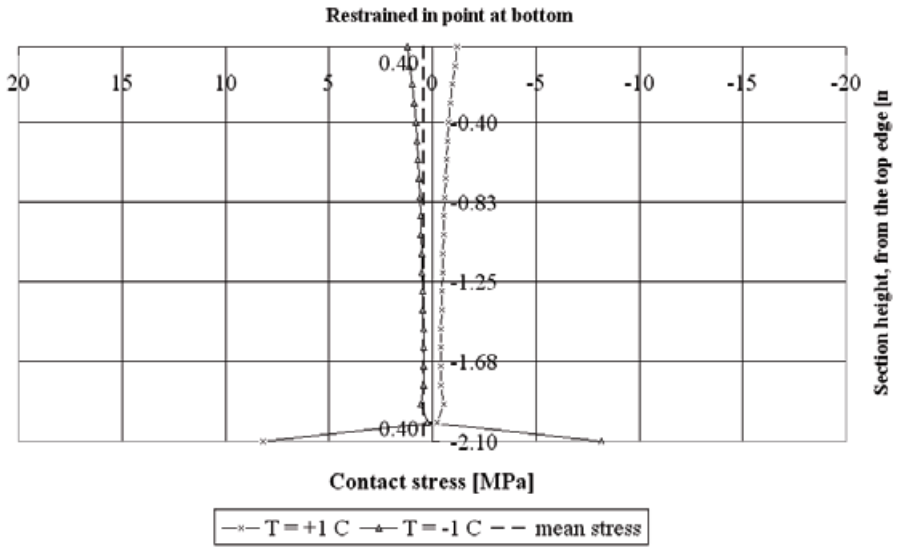

σ_m = 0,40 MPa

Figure B-1. *Stresses in interface between concrete and rock when assuming different boundary conditions and a temperature load of ΔT = ±1°C is applied.*

According to [1] the mean concrete tensile strength is f_{ctm} = 3.3 MPa and the lower characteristic tensile strength is $f_{ctk,0.05}$ = 2.9 MPa, Accordingly the upper tensile strength can be determined as

$$f_{ctk,0.95} = f_{ctm} + (f_{ctm} - f_{ctk,0.05}) = 3.3 + (3.3 - 2.9) = 3.7 \text{ MPa} \quad \text{(Eq. B-9)}$$

B.3.4 Comparison of tensile strength and obtained stresses

A conservative value on the tensile strength, $f_{ctk,0.95}$ = 3.7 MPa, is shown to be lower than an estimation of the mean tensile stress, σ_c = 3.8 MPa. Consequently, cracking will occur between concrete and rock and free movement due to shrinkage will be possible.

B.4 Conclusions

When cooling the plug with ΔT = –10 ºC after 90 days of curing, cracks will appear between concrete and rock. Hence, the movement needed is fulfilled and there will be no restrain left in the plug meaning that the stresses previously obtained due to shrinkage will disappear.

Consequently, the assumption of using a concrete shrinkage that is set to zero at an age of 90 days in the analyses is correct.

Appendix C

Water leakage through concrete plug

C.1 Calculations

The water leakage through the plug may be determined using the calculation method described in [8] using Darcy's law

$$q = K\frac{dP_w}{dx} \qquad \text{(Eq. C-1)}$$

where q is the flow per area unit, K is the permeability coefficient of concrete, dP_w is the water pressure expressed in height of water and dx is the thickness of the concrete wall. The flow q can be determined by the total flow Q and the area A of the plug as

$$q = \frac{Q}{A} \qquad \text{(Eq. C-2)}$$

where A is based on the plug diameter D = 6.3 m as

$$A = \frac{\pi D^2}{4} = \frac{\pi \cdot 6.3^2}{4} = 31.2 \text{ m}^2 \qquad \text{(Eq. C-3)}$$

Using $K = 5 \cdot 10^{-12}$ m/s (Table 2-1), $dP_w = 400$ m (Table 2-3) and an allowed leakage through the tunnel of $Q = 0.01$ l/min $= 1.67 \cdot 10^{-4}$ l/s $= 1.67 \cdot 10^{-7}$ m^3/s (Section 2.5.2) the necessary concrete thickness can be determined as

$$dx = K\frac{dP_w \cdot A}{Q} = 5 \cdot 10^{-12} \cdot \frac{400 \cdot 31.2}{1.67 \cdot 10^{-7}} = 0.38 \text{ m} \approx 0.40 \text{ m} \qquad \text{(Eq. C-4)}$$

C.2 Conclusions

If achieving a thickness of uncracked concrete of at least 0.40 m in all concrete cross sections the requirement of a maximum water leakage of 0.01 l/min through the plug is satisfied.

Appendix D

Elastic part of concrete in compression

As discussed in Section 2.5.4 it is of importance what compressive stress may be allowed in the concrete before it start to respond non-linearly. This is further compared in Figure D-1, where the compressive stress-strain relations from two tested concrete cylinders, [1], are shown. These stress-strain relations are originally from tests carried out to examine the Young's modulus and Poisson's ratio but present some useful information of what the material response look like in the initial stage.

The compressive stress $\sigma_c(\varepsilon_c)$ is compared with a linear response $E_c\varepsilon_c$ using a ratio η defined as

$$\eta = \left| \frac{E_c \varepsilon_c}{\sigma_c(\varepsilon_c)} \right| - 1 \qquad \text{(Eq. D-1)}$$

In Table D-1 the resulting ratio $E_c\varepsilon_c / f_{ccm}$ is shown for the two tests presented in Figure D-1. A ratio is given for η equal to 0.01, 0.02 and 0.05; i.e. an error of 1%, 2% and 5%, respectively. From this it can be concluded that it is safe, and even rather conservative, to a use a relation according to that used in BBK 04, [2]; i.e.

$$\sigma_c \le 0.6 f_{cc} \qquad \text{(Eq. D-2)}$$

However, these results also render it possible to use a somewhat larger elastic region if so is needed; a relation of

$$\sigma_c \le 0.65 f_{cc} \qquad \text{(Eq. D-3)}$$

being reasonable.

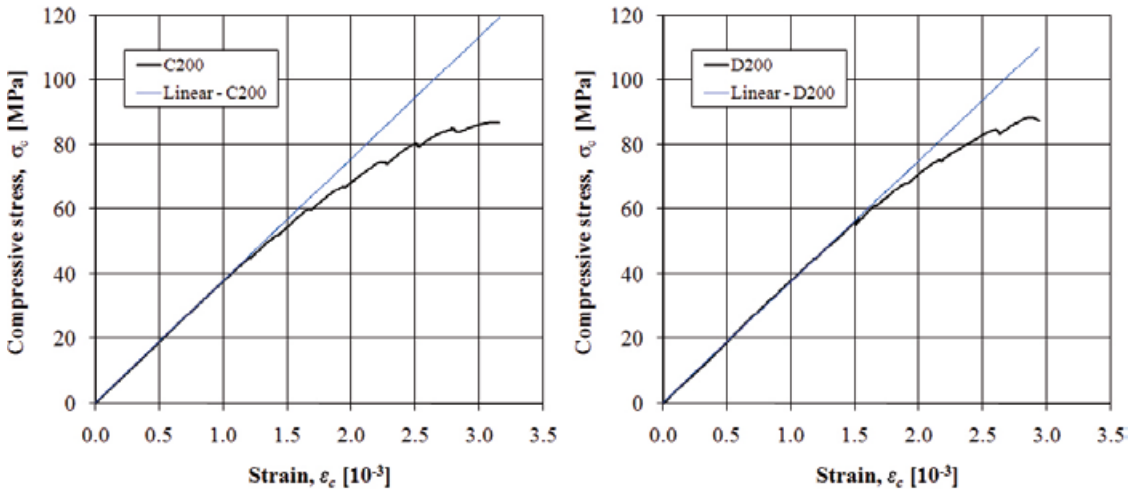

Figure D-1. *Stress-strain relations for concrete B200 in tests of the concrete Young's modulus. Based on [1].*

Table D-1. Evaluation of linearity of low-pH concrete in compression. Values based on Figure D-1.

	C200 [1]		D200 [2]		Mean value
η	$E_c\varepsilon_c$ [MPa]	$E_c\varepsilon_c / f_{ccm}$ [–]	$E_c\varepsilon_c$ [MPa]	$E_c\varepsilon_c / f_{ccm}$ [–]	$E_c\varepsilon_c / f_{ccm}$ [–]
0.99	45.5	0.52	57.4	0.65	0.59
0.98	50.0	0.58	62.3	0.70	0.64
0.95	62.5	0.72	71.6	0.81	0.76

[1] E_c = 37.9 GPa, f_{ccm} = 87.0 MPa.
[2] E_c = 37.5 GPa, f_{ccm} = 88.5 MPa.

Appendix E

Stress plots from the analyses

E.1 Orientation

In this appendix are presented the resulting stress plots for the load combinations described in Section 3.5.3.

The plots present the stress distribution in the plug through the three principal stresses and a plot depicting the contact forces against the plug surface is also included. A typical plot is presented in Figure D-1 with explanation on the information it shows.

In Figure D-1 the plots are as follow:

1. Principal stresses, σ_1 (max tension), [Pa]
2. Principal stresses, σ_2, [Pa]
3. Principal stresses, σ_3 (max compression), [Pa]
4. Contact forces, surface against the rock, [N/rad]

The title of the plot gives the information about the load scenario and the material parameters of the rock. In this particular case, the corresponding load combination is 8.6 (load scenario 8, material parameters type X.6 – according to Table 3-4).

It is important to note, that since the axis symmetrical model represent one radian of the structure, and the contact force are in N /per one radian. This means that the force at a node is actually distributed over a length equal to the radius of revolution of this node (the radius here being the distance to the centre of the plug).

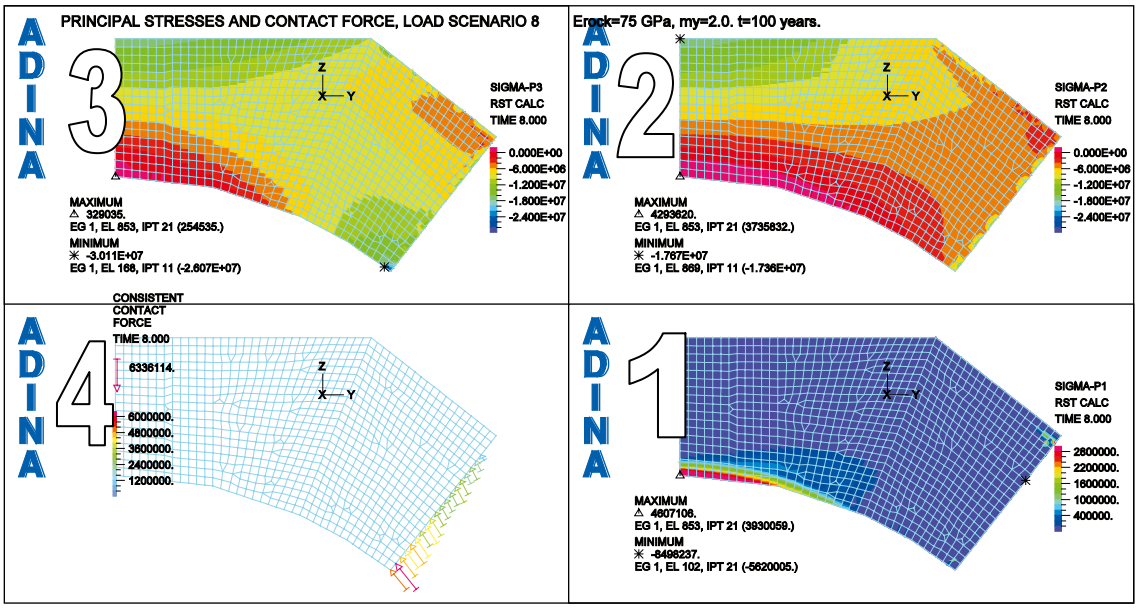

Figure E-1. *Typical stress plot (here, for load combination 8.6) shown in Sections E.2 to 0.*

E.2 Stress plots, load combinations 1.1–8.1

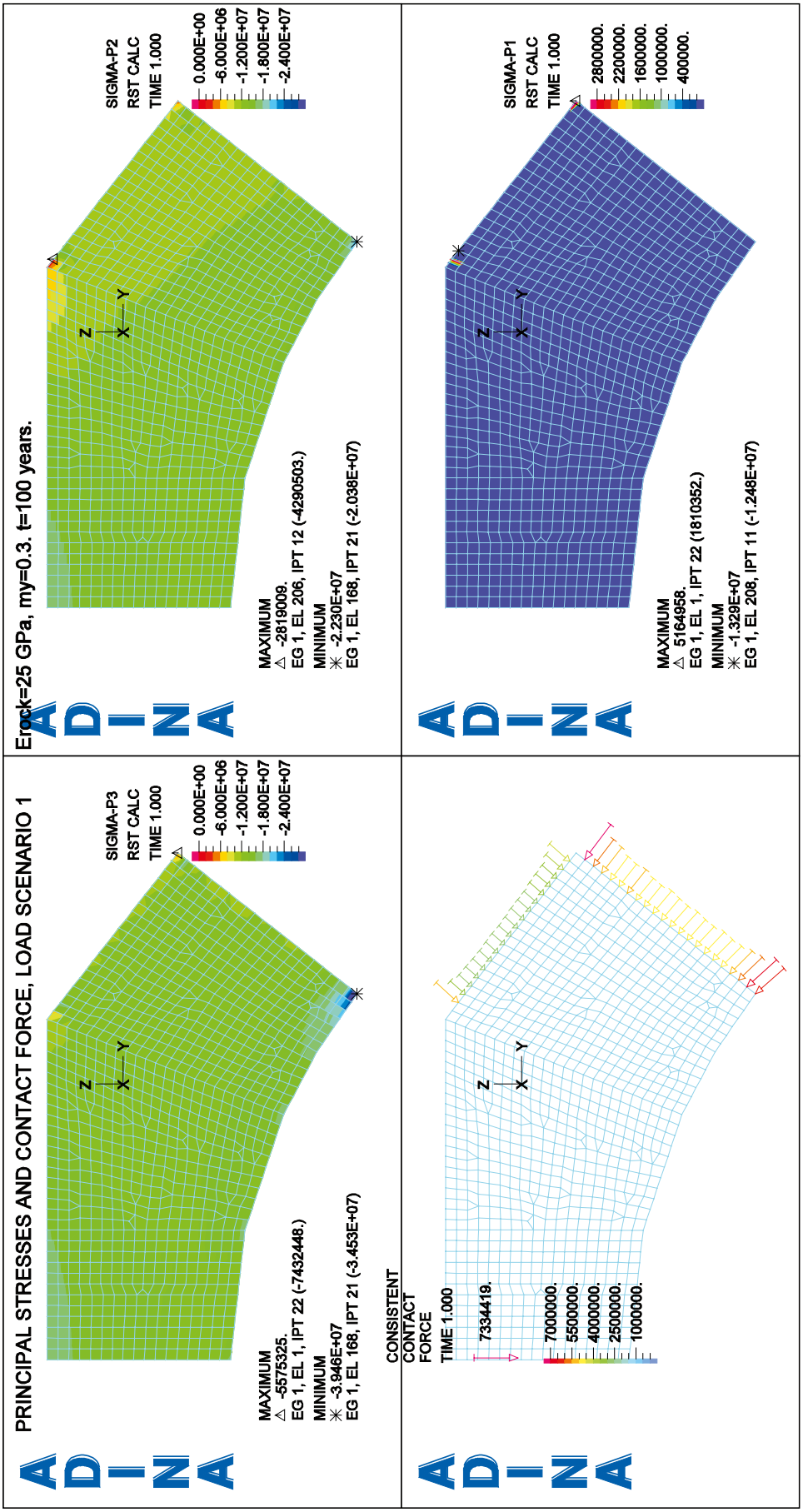

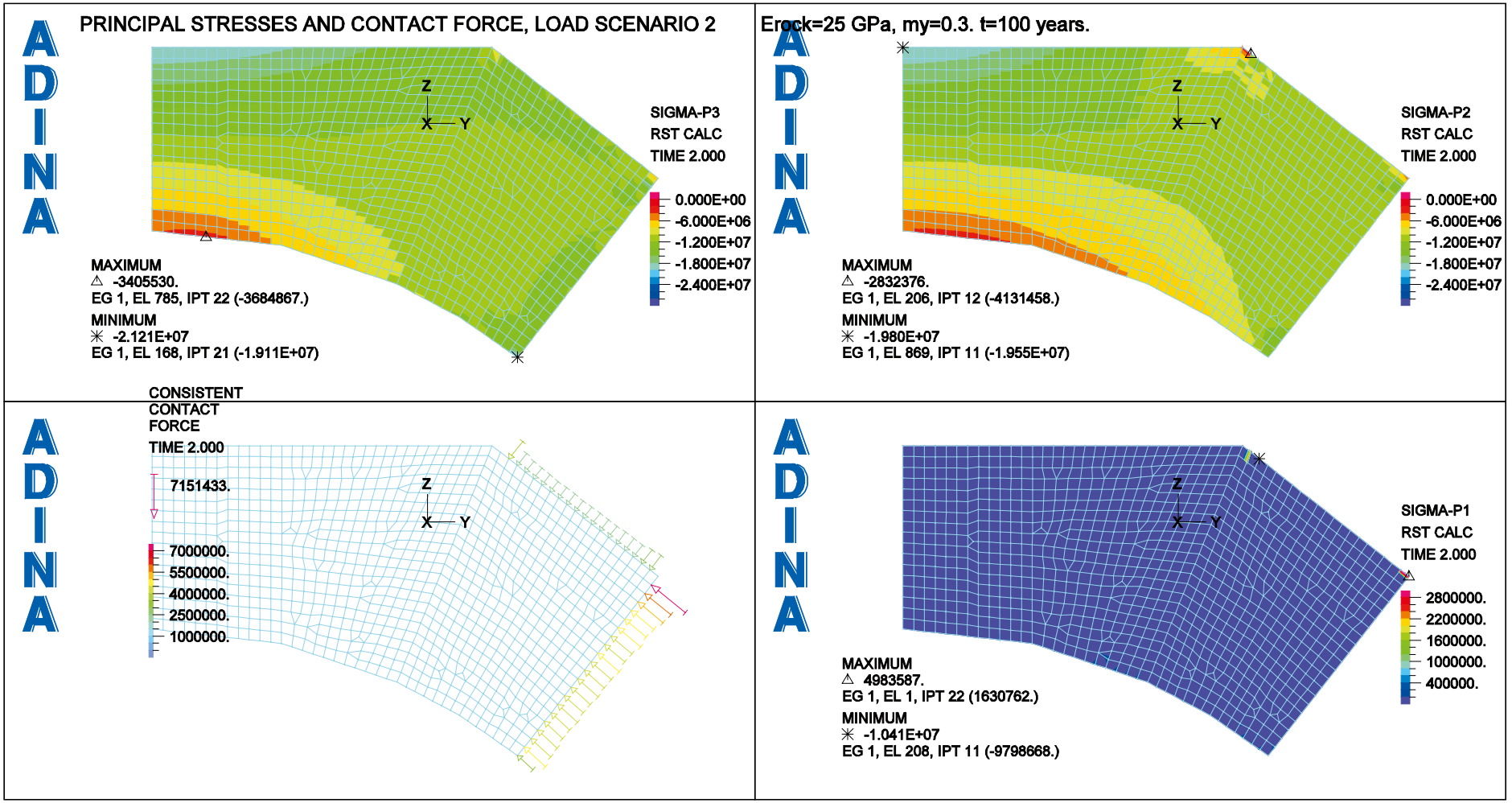
PRINCIPAL STRESSES AND CONTACT FORCE, LOAD SCENARIO 2
SIGMA-P3
RST CALC
TIME 2.000
0.000E+00
-6.000E+06
-1.200E+07
-1.800E+07
-2.400E+07
MAXIMUM
-3405530.
EG 1, EL 785, IPT 22 (-3684867.)
MINIMUM
-2.121E+07
EG 1, EL 168, IPT 21 (-1.911E+07)
Erock=25 GPa, my=0.3. t=100 years.
SIGMA-P2
RST CALC
TIME 2.000
0.000E+00
-6.000E+06
-1.200E+07
-1.800E+07
-2.400E+07
MAXIMUM
-2832376.
EG 1, EL 206, IPT 12 (-4131458.)
MINIMUM
-1.980E+07
EG 1, EL 869, IPT 11 (-1.955E+07)
CONSISTENT
CONTACT
FORCE
TIME 2.000
7151433.
7000000.
5500000.
4000000.
2500000.
1000000.
SIGMA-P1
RST CALC
TIME 2.000
2800000.
2200000.
1600000.
1000000.
400000.
MAXIMUM
4983587.
EG 1, EL 1, IPT 22 (1630762.)
MINIMUM
-1.041E+07
EG 1, EL 208, IPT 11 (-9798668.)

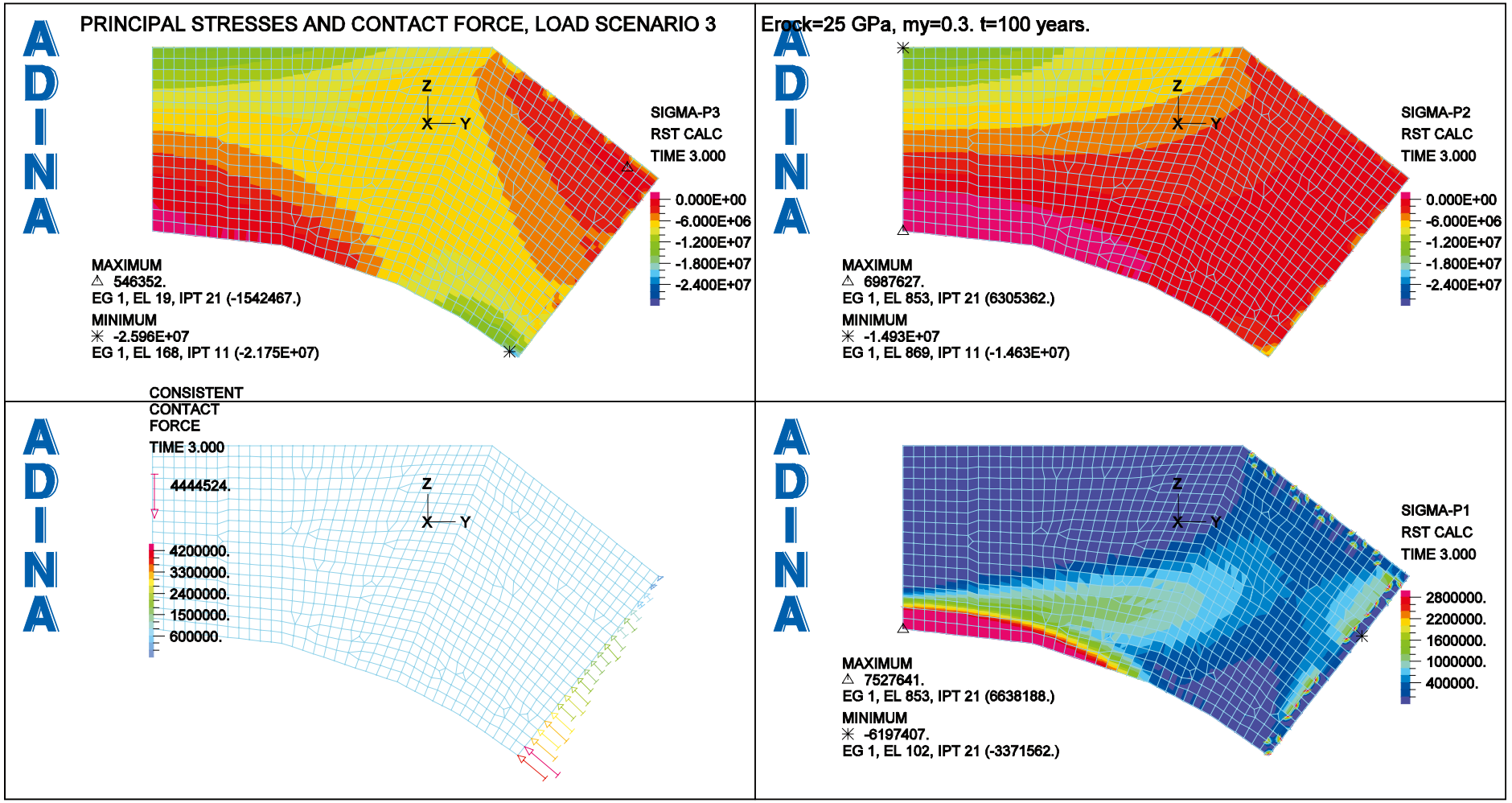
PRINCIPAL STRESSES AND CONTACT FORCE, LOAD SCENARIO 3
Erock=25 GPa, my=0.3. t=100 years.
ADINA
SIGMA-P3
RST CALC
TIME 3.000
0.000E+00
-6.000E+06
-1.200E+07
-1.800E+07
-2.400E+07
MAXIMUM
546352.
EG 1, EL 19, IPT 21 (-1542467.)
MINIMUM
-2.596E+07
EG 1, EL 168, IPT 11 (-2.175E+07)
SIGMA-P2
RST CALC
TIME 3.000
0.000E+00
-6.000E+06
-1.200E+07
-1.800E+07
-2.400E+07
MAXIMUM
6987627.
EG 1, EL 853, IPT 21 (6305362.)
MINIMUM
-1.493E+07
EG 1, EL 869, IPT 11 (-1.463E+07)
CONSISTENT
CONTACT
FORCE
TIME 3.000
4444524.
4200000.
3300000.
2400000.
1500000.
600000.
SIGMA-P1
RST CALC
TIME 3.000
2800000.
2200000.
1600000.
1000000.
400000.
MAXIMUM
7527641.
EG 1, EL 853, IPT 21 (6638188.)
MINIMUM
-6197407.
EG 1, EL 102, IPT 21 (-3371562.)
Z
X
Y

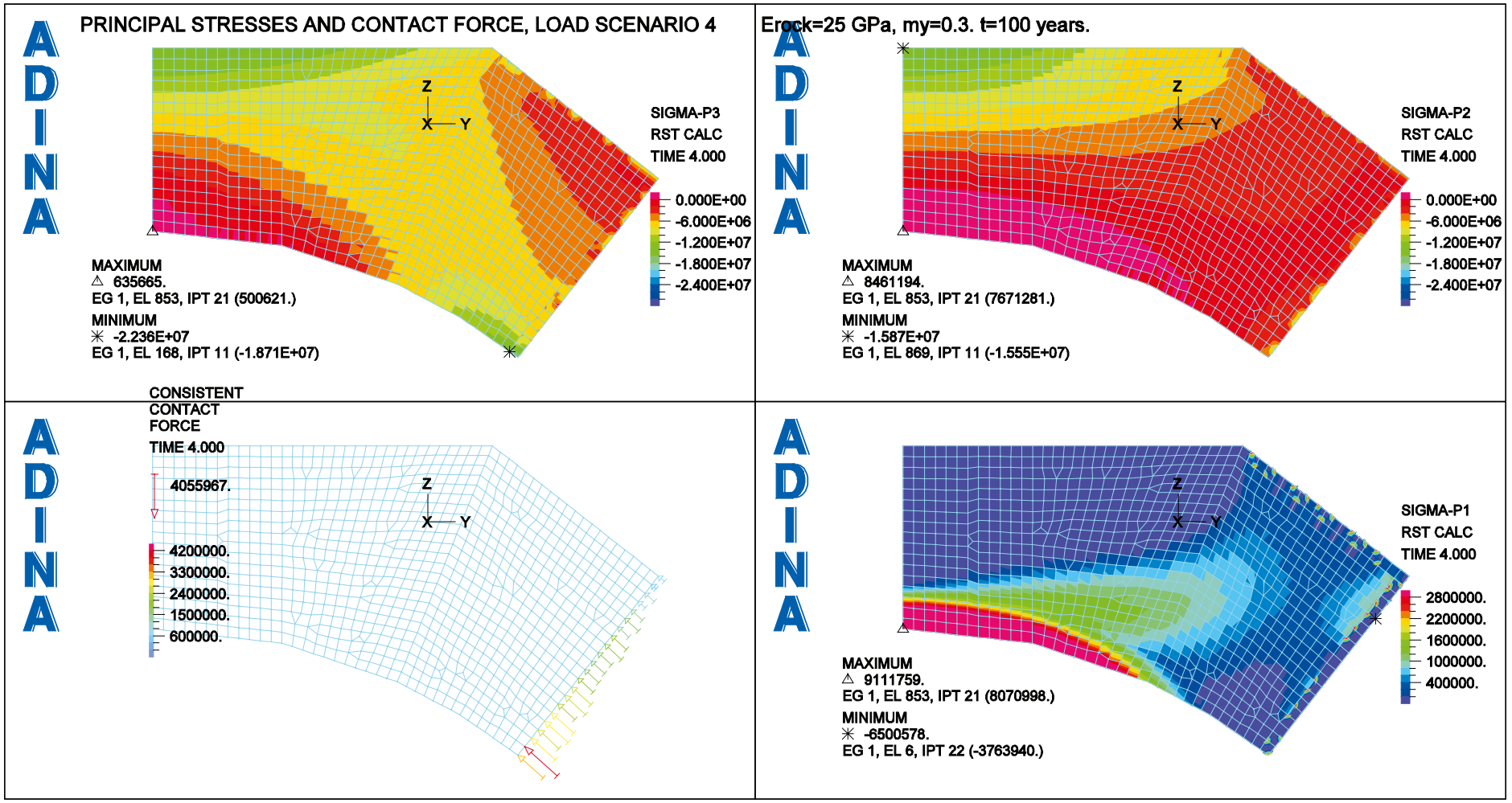
PRINCIPAL STRESSES AND CONTACT FORCE, LOAD SCENARIO 4
SIGMA-P3
RST CALC
TIME 4.000
0.000E+00
-6.000E+06
-1.200E+07
-1.800E+07
-2.400E+07
MAXIMUM
635665.
EG 1, EL 853, IPT 21 (500621.)
MINIMUM
-2.236E+07
EG 1, EL 168, IPT 11 (-1.871E+07)
Erock=25 GPa, my=0.3. t=100 years.
SIGMA-P2
RST CALC
TIME 4.000
0.000E+00
-6.000E+06
-1.200E+07
-1.800E+07
-2.400E+07
MAXIMUM
8461194.
EG 1, EL 853, IPT 21 (7671281.)
MINIMUM
-1.587E+07
EG 1, EL 869, IPT 11 (-1.555E+07)
CONSISTENT
CONTACT
FORCE
TIME 4.000
4055967.
4200000.
3300000.
2400000.
1500000.
600000.
SIGMA-P1
RST CALC
TIME 4.000
2800000.
2200000.
1600000.
1000000.
400000.
MAXIMUM
9111759.
EG 1, EL 853, IPT 21 (8070998.)
MINIMUM
-6500578.
EG 1, EL 6, IPT 22 (-3763940.)

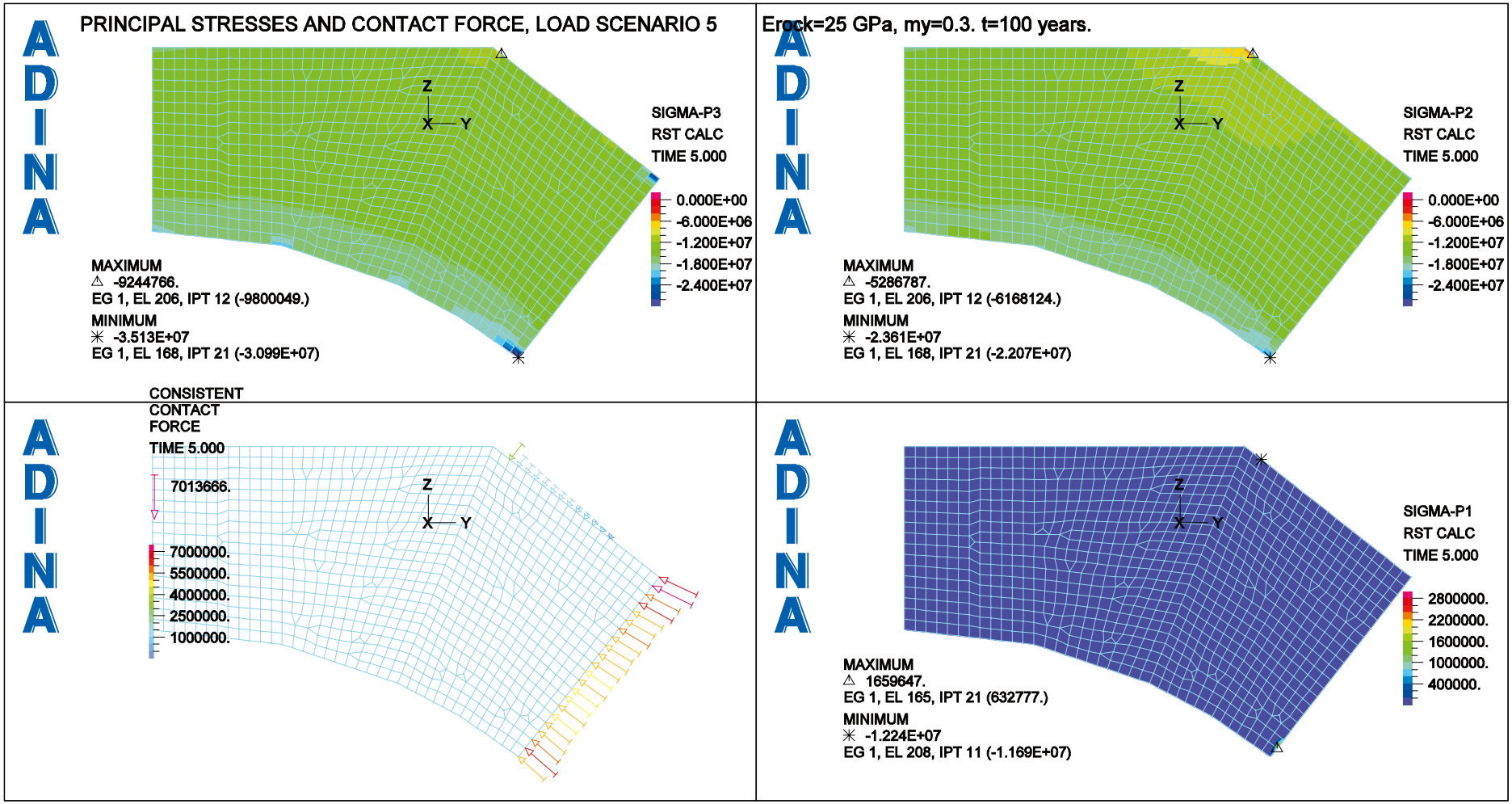
PRINCIPAL STRESSES AND CONTACT FORCE, LOAD SCENARIO 5
ADINA
Z
X
Y
SIGMA-P3
RST CALC
TIME 5.000
0.000E+00
-6.000E+06
-1.200E+07
-1.800E+07
-2.400E+07
MAXIMUM
-9244766.
EG 1, EL 206, IPT 12 (-9800049.)
MINIMUM
-3.513E+07
EG 1, EL 168, IPT 21 (-3.099E+07)
Erock=25 GPa, my=0.3. t=100 years.
ADINA
Z
X
Y
SIGMA-P2
RST CALC
TIME 5.000
0.000E+00
-6.000E+06
-1.200E+07
-1.800E+07
-2.400E+07
MAXIMUM
-5286787.
EG 1, EL 206, IPT 12 (-6168124.)
MINIMUM
-2.361E+07
EG 1, EL 168, IPT 21 (-2.207E+07)
ADINA
CONSISTENT
CONTACT
FORCE
TIME 5.000
7013666.
7000000.
5500000.
4000000.
2500000.
1000000.
Z
X
Y
ADINA
Z
X
Y
SIGMA-P1
RST CALC
TIME 5.000
2800000.
2200000.
1600000.
1000000.
400000.
MAXIMUM
1659647.
EG 1, EL 165, IPT 21 (632777.)
MINIMUM
-1.224E+07
EG 1, EL 208, IPT 11 (-1.169E+07)

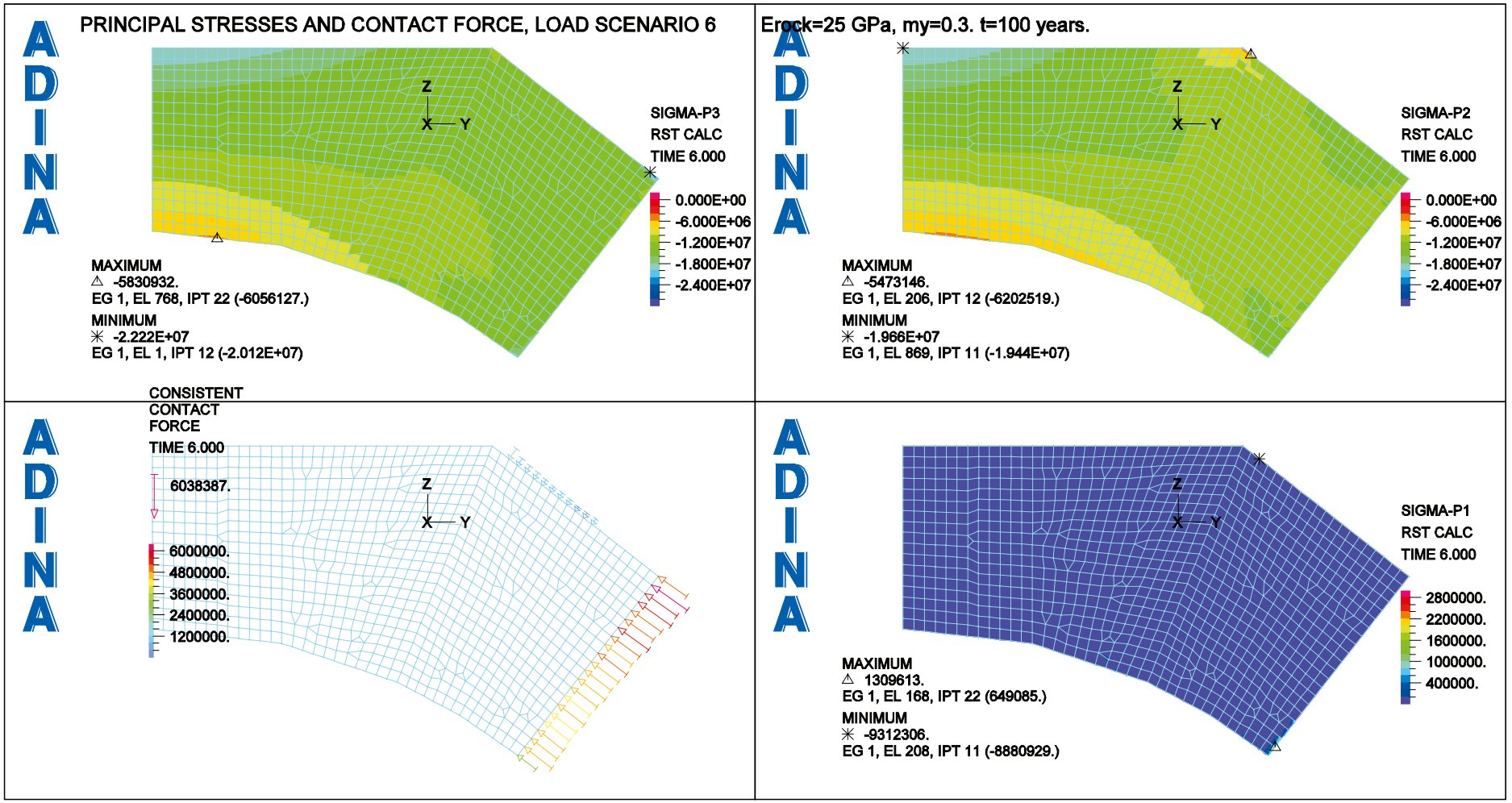
PRINCIPAL STRESSES AND CONTACT FORCE, LOAD SCENARIO 6
SIGMA-P3
RST CALC
TIME 6.000
0.000E+00
-6.000E+06
-1.200E+07
-1.800E+07
-2.400E+07
MAXIMUM
-5830932.
EG 1, EL 768, IPT 22 (-6056127.)
MINIMUM
-2.222E+07
EG 1, EL 1, IPT 12 (-2.012E+07)
Erock=25 GPa, my=0.3. t=100 years.
SIGMA-P2
RST CALC
TIME 6.000
0.000E+00
-6.000E+06
-1.200E+07
-1.800E+07
-2.400E+07
MAXIMUM
-5473146.
EG 1, EL 206, IPT 12 (-6202519.)
MINIMUM
-1.966E+07
EG 1, EL 869, IPT 11 (-1.944E+07)
CONSISTENT
CONTACT
FORCE
TIME 6.000
6038387.
6000000.
4800000.
3600000.
2400000.
1200000.
SIGMA-P1
RST CALC
TIME 6.000
2800000.
2200000.
1600000.
1000000.
400000.
MAXIMUM
1309613.
EG 1, EL 168, IPT 22 (649085.)
MINIMUM
-9312306.
EG 1, EL 208, IPT 11 (-8880929.)

PRINCIPAL STRESSES AND CONTACT FORCE, LOAD SCENARIO 7

Erock=25 GPa, my=0.3. t=100 years.

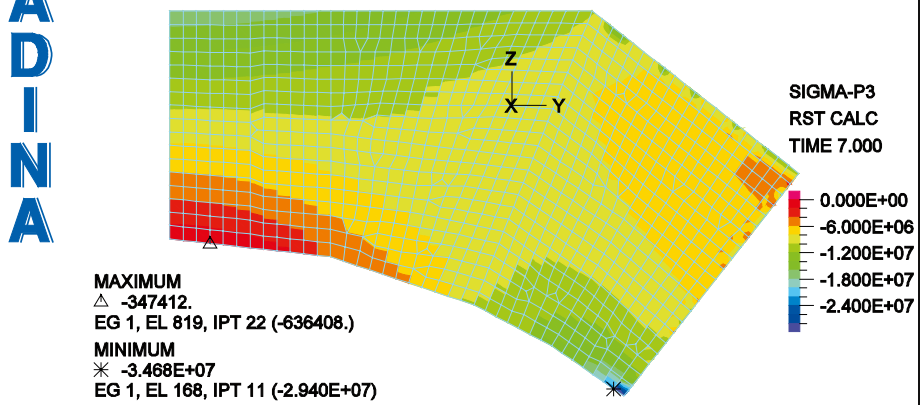

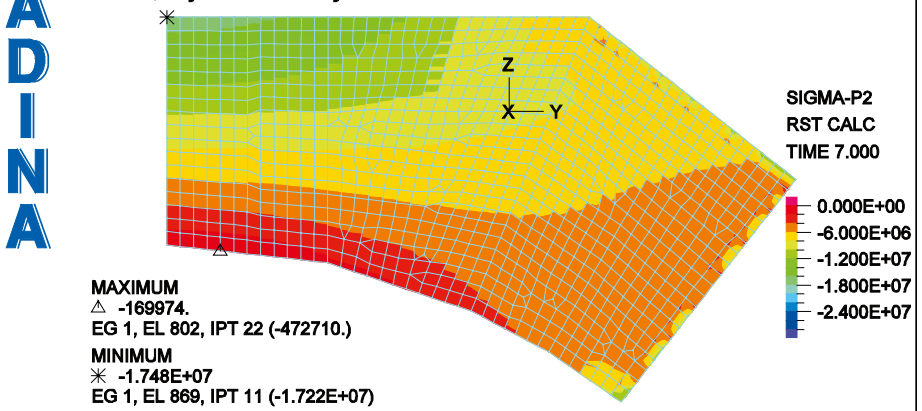

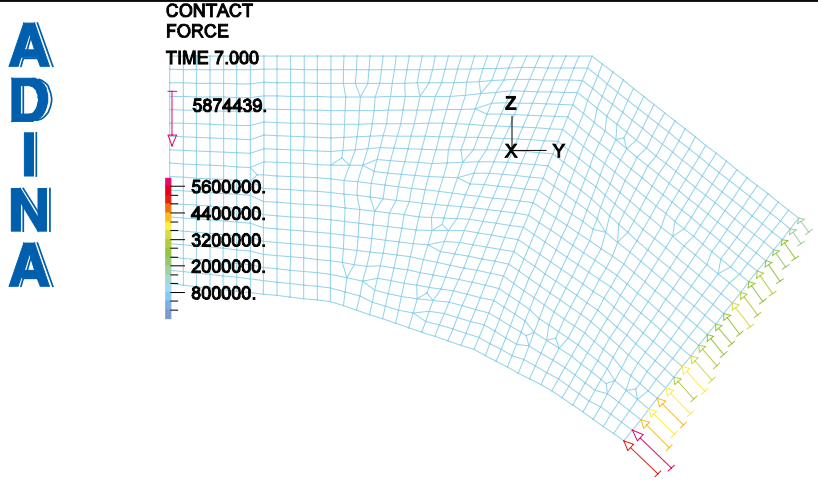

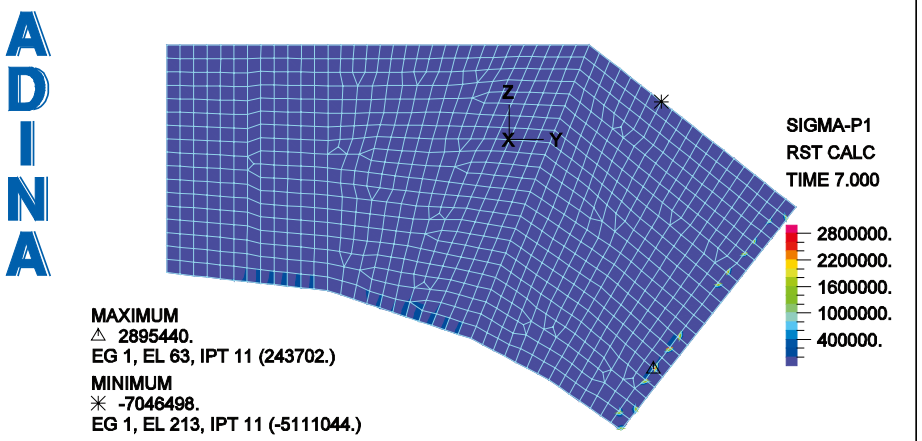

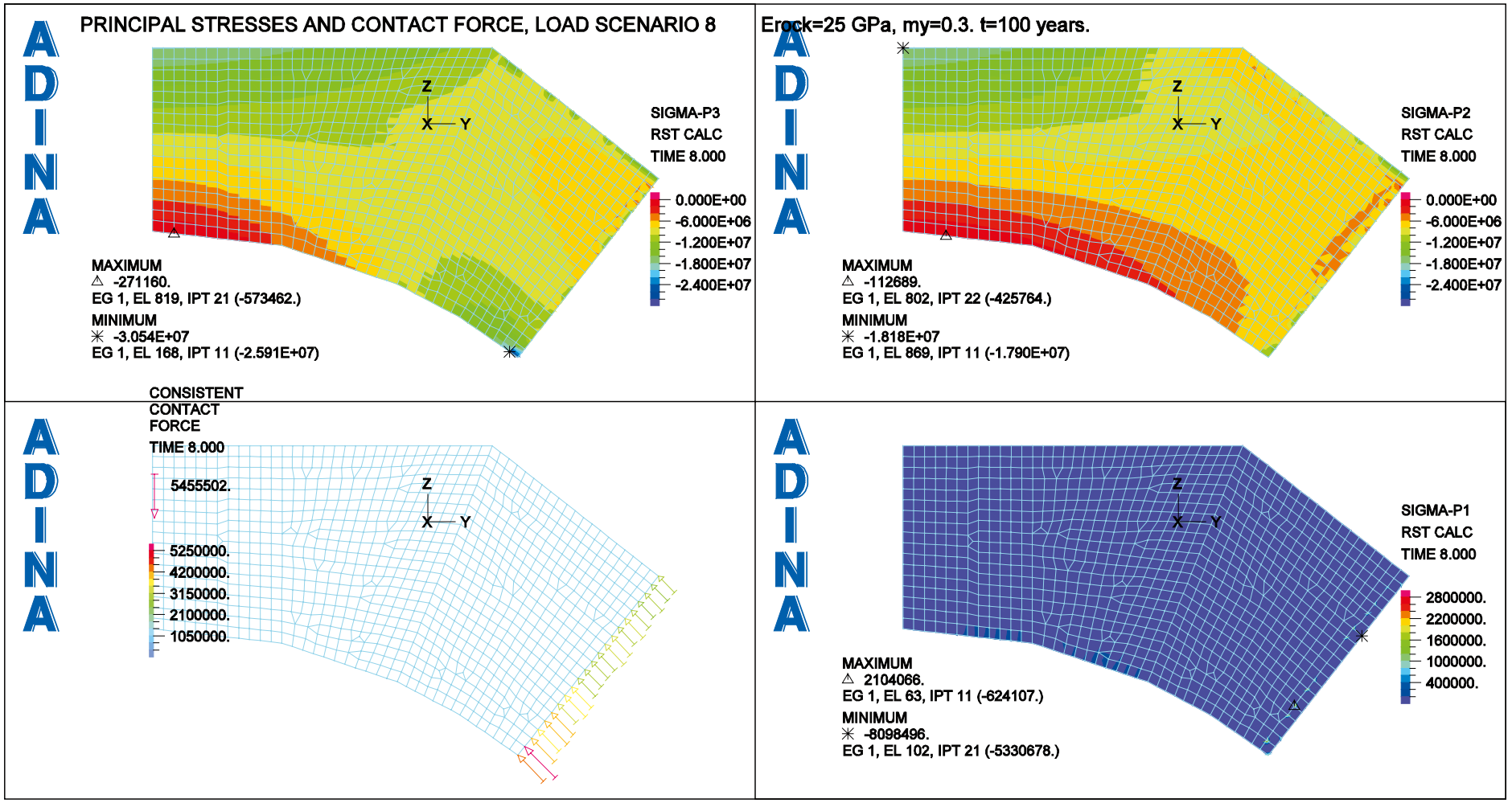
PRINCIPAL STRESSES AND CONTACT FORCE, LOAD SCENARIO 8
SIGMA-P3
RST CALC
TIME 8.000
0.000E+00
-6.000E+06
-1.200E+07
-1.800E+07
-2.400E+07
MAXIMUM
-271160.
EG 1, EL 819, IPT 21 (-573462.)
MINIMUM
-3.054E+07
EG 1, EL 168, IPT 11 (-2.591E+07)
Erock=25 GPa, my=0.3. t=100 years.
SIGMA-P2
RST CALC
TIME 8.000
0.000E+00
-6.000E+06
-1.200E+07
-1.800E+07
-2.400E+07
MAXIMUM
-112689.
EG 1, EL 802, IPT 22 (-425764.)
MINIMUM
-1.818E+07
EG 1, EL 869, IPT 11 (-1.790E+07)
CONSISTENT
CONTACT
FORCE
TIME 8.000
5455502.
5250000.
4200000.
3150000.
2100000.
1050000.
SIGMA-P1
RST CALC
TIME 8.000
2800000.
2200000.
1600000.
1000000.
400000.
MAXIMUM
2104066.
EG 1, EL 63, IPT 11 (-624107.)
MINIMUM
-8098496.
EG 1, EL 102, IPT 21 (-5330678.)

E.3 Stress plots, load combinations 1.2–8.2

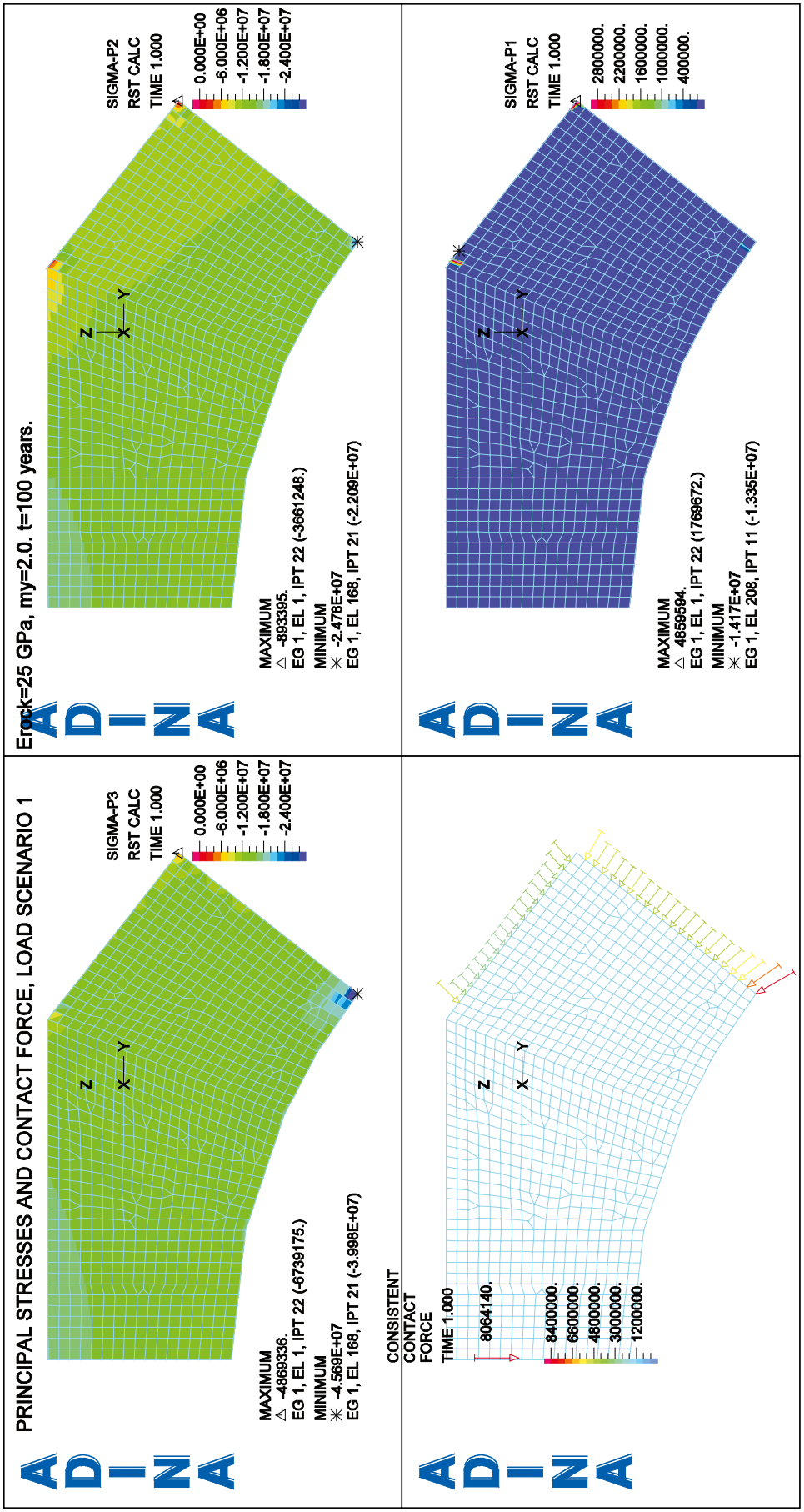

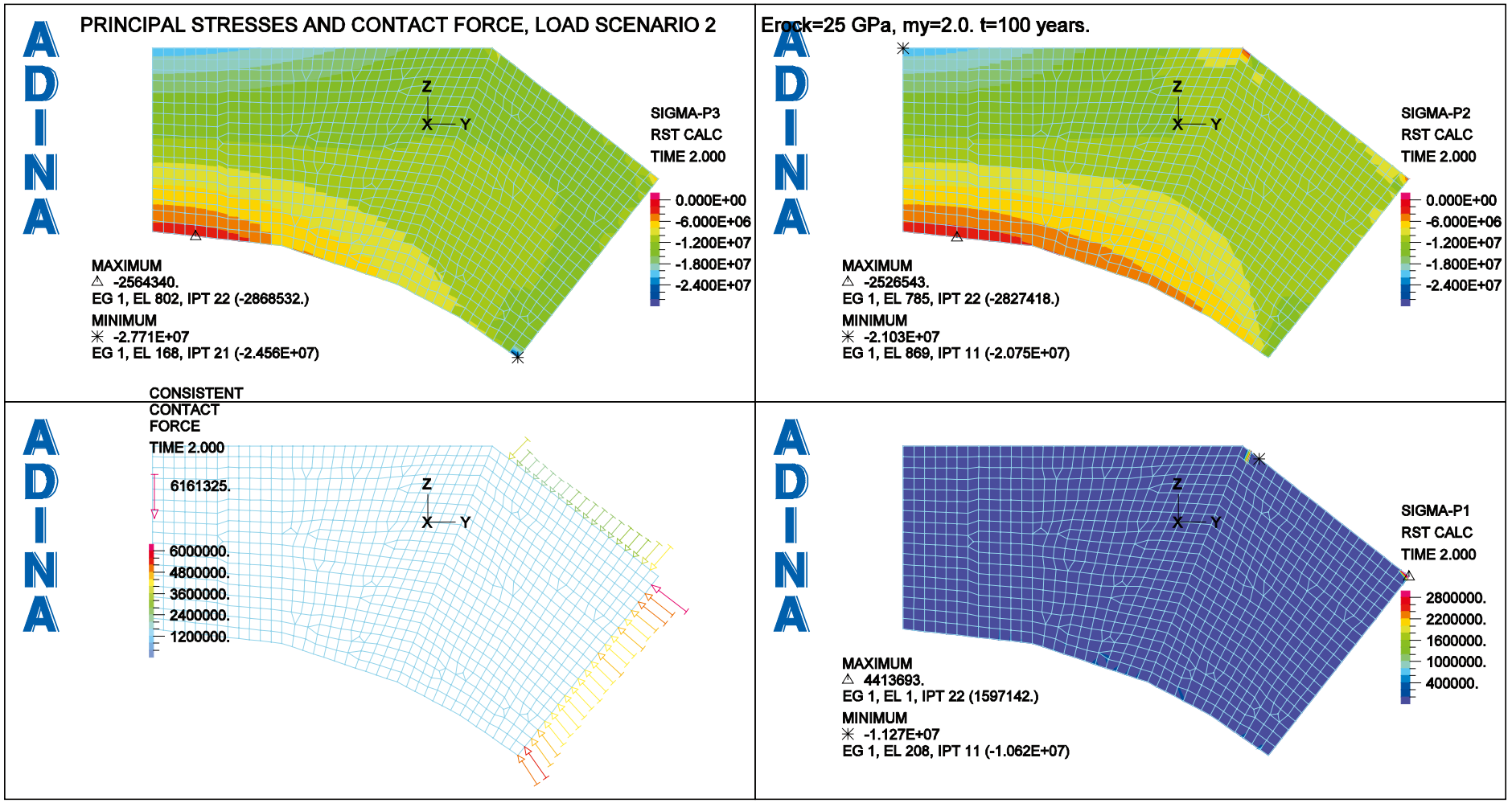
PRINCIPAL STRESSES AND CONTACT FORCE, LOAD SCENARIO 2
SIGMA-P3
RST CALC
TIME 2.000
0.000E+00
-6.000E+06
-1.200E+07
-1.800E+07
-2.400E+07
MAXIMUM
-2564340.
EG 1, EL 802, IPT 22 (-2868532.)
MINIMUM
-2.771E+07
EG 1, EL 168, IPT 21 (-2.456E+07)
Erock=25 GPa, my=2.0. t=100 years.
SIGMA-P2
RST CALC
TIME 2.000
0.000E+00
-6.000E+06
-1.200E+07
-1.800E+07
-2.400E+07
MAXIMUM
-2526543.
EG 1, EL 785, IPT 22 (-2827418.)
MINIMUM
-2.103E+07
EG 1, EL 869, IPT 11 (-2.075E+07)
CONSISTENT
CONTACT
FORCE
TIME 2.000
6161325.
6000000.
4800000.
3600000.
2400000.
1200000.
SIGMA-P1
RST CALC
TIME 2.000
2800000.
2200000.
1600000.
1000000.
400000.
MAXIMUM
4413693.
EG 1, EL 1, IPT 22 (1597142.)
MINIMUM
-1.127E+07
EG 1, EL 208, IPT 11 (-1.062E+07)

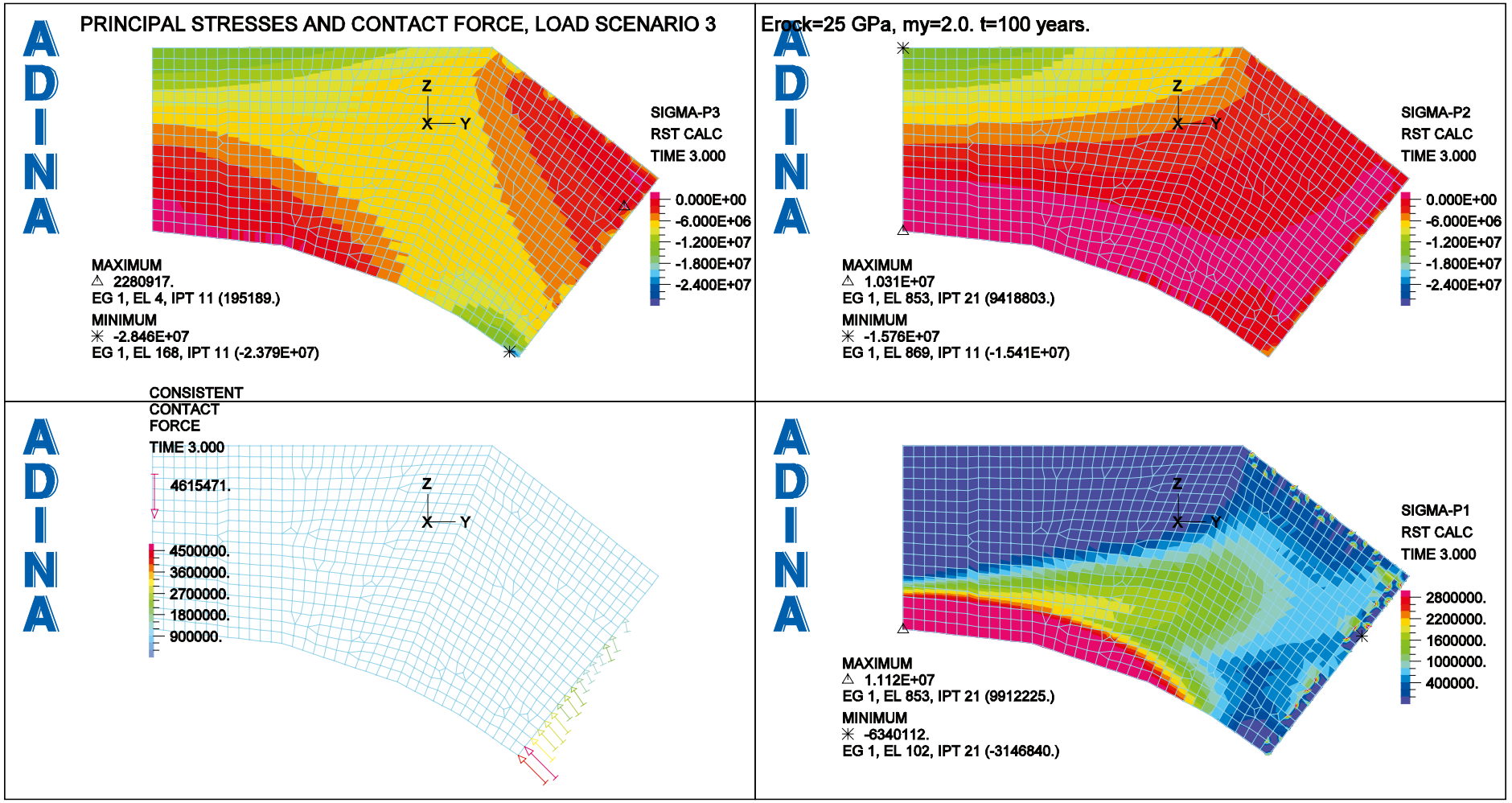
PRINCIPAL STRESSES AND CONTACT FORCE, LOAD SCENARIO 3
Erock=25 GPa, my=2.0. t=100 years.
ADINA
SIGMA-P3
RST CALC
TIME 3.000
0.000E+00
-6.000E+06
-1.200E+07
-1.800E+07
-2.400E+07
MAXIMUM
2280917.
EG 1, EL 4, IPT 11 (195189.)
MINIMUM
-2.846E+07
EG 1, EL 168, IPT 11 (-2.379E+07)
SIGMA-P2
RST CALC
TIME 3.000
0.000E+00
-6.000E+06
-1.200E+07
-1.800E+07
-2.400E+07
MAXIMUM
1.031E+07
EG 1, EL 853, IPT 21 (9418803.)
MINIMUM
-1.576E+07
EG 1, EL 869, IPT 11 (-1.541E+07)
CONSISTENT
CONTACT
FORCE
TIME 3.000
4615471.
4500000.
3600000.
2700000.
1800000.
900000.
SIGMA-P1
RST CALC
TIME 3.000
2800000.
2200000.
1600000.
1000000.
400000.
MAXIMUM
1.112E+07
EG 1, EL 853, IPT 21 (9912225.)
MINIMUM
-6340112.
EG 1, EL 102, IPT 21 (-3146840.)

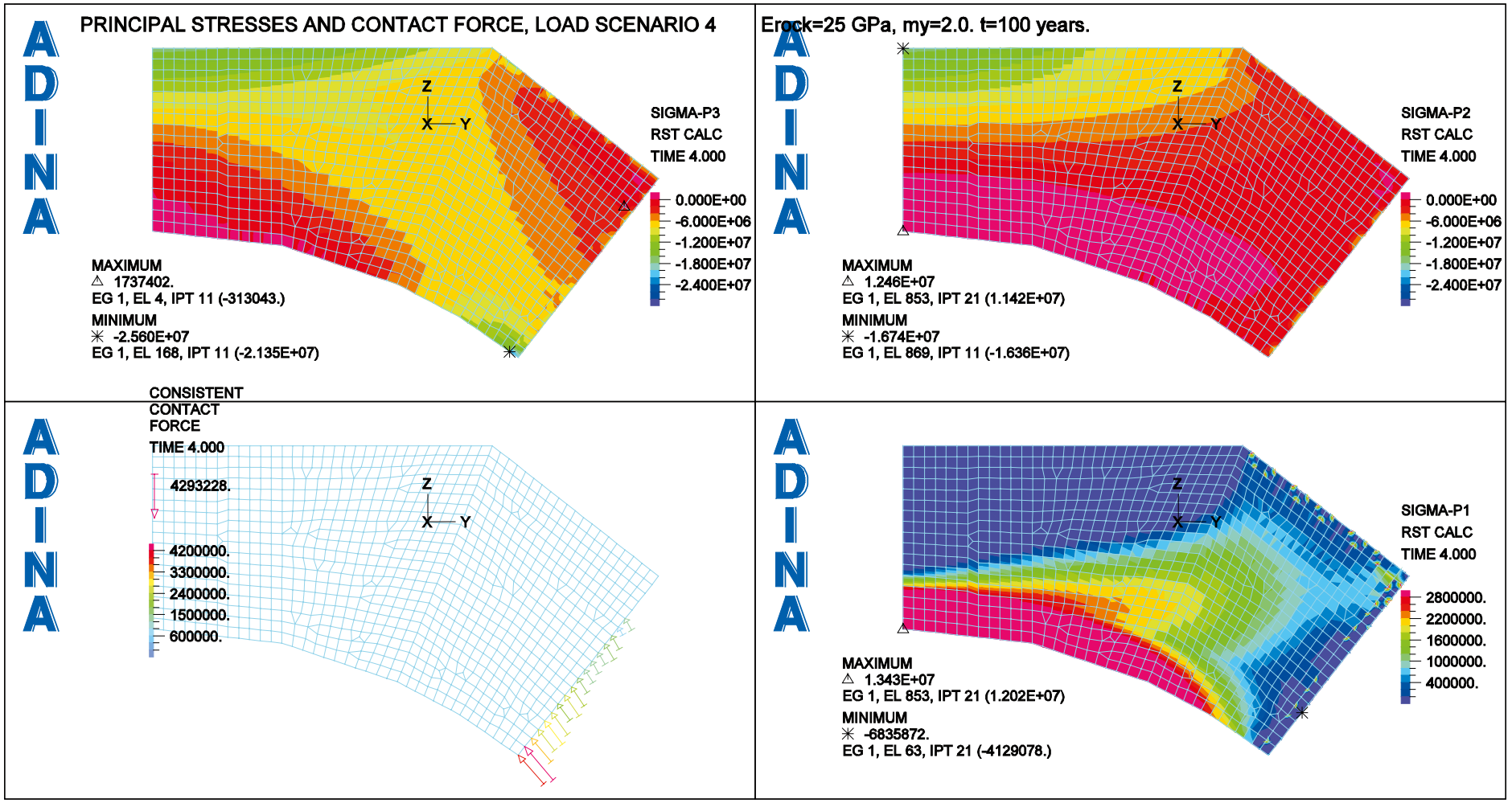
PRINCIPAL STRESSES AND CONTACT FORCE, LOAD SCENARIO 4
SIGMA-P3
RST CALC
TIME 4.000
0.000E+00
-6.000E+06
-1.200E+07
-1.800E+07
-2.400E+07
MAXIMUM
1737402.
EG 1, EL 4, IPT 11 (-313043.)
MINIMUM
-2.560E+07
EG 1, EL 168, IPT 11 (-2.135E+07)
Erock=25 GPa, my=2.0. t=100 years.
SIGMA-P2
RST CALC
TIME 4.000
0.000E+00
-6.000E+06
-1.200E+07
-1.800E+07
-2.400E+07
MAXIMUM
1.246E+07
EG 1, EL 853, IPT 21 (1.142E+07)
MINIMUM
-1.674E+07
EG 1, EL 869, IPT 11 (-1.636E+07)
CONSISTENT
CONTACT
FORCE
TIME 4.000
4293228.
4200000.
3300000.
2400000.
1500000.
600000.
SIGMA-P1
RST CALC
TIME 4.000
2800000.
2200000.
1600000.
1000000.
400000.
MAXIMUM
1.343E+07
EG 1, EL 853, IPT 21 (1.202E+07)
MINIMUM
-6835872.
EG 1, EL 63, IPT 21 (-4129078.)

PRINCIPAL STRESSES AND CONTACT FORCE, LOAD SCENARIO 5

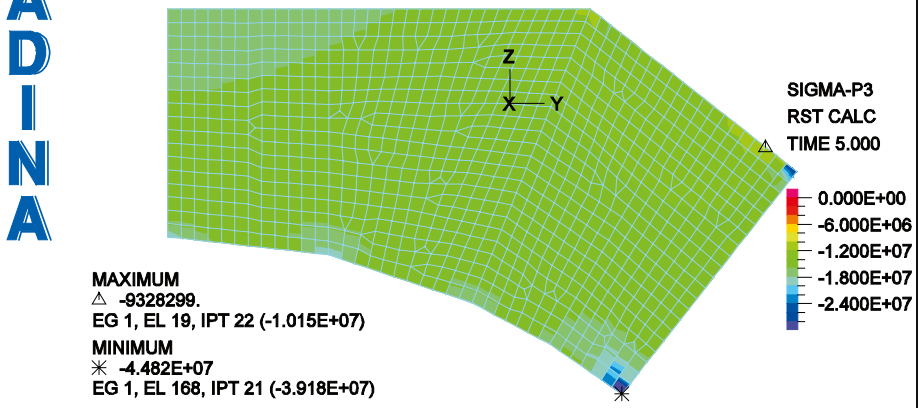

Erock=25 GPa, my=2.0. t=100 years.

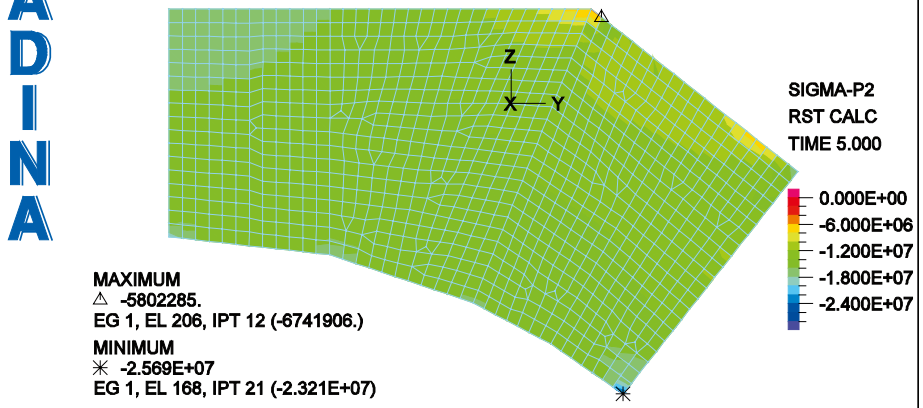

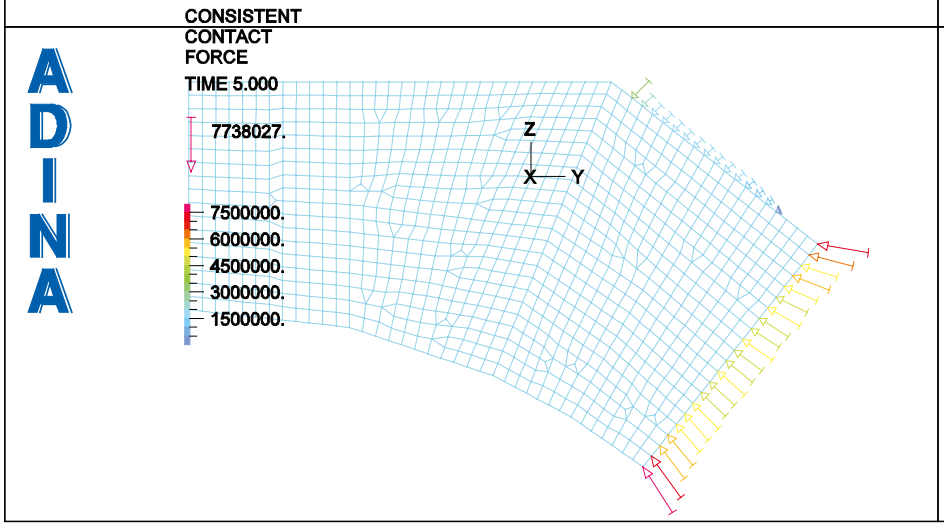

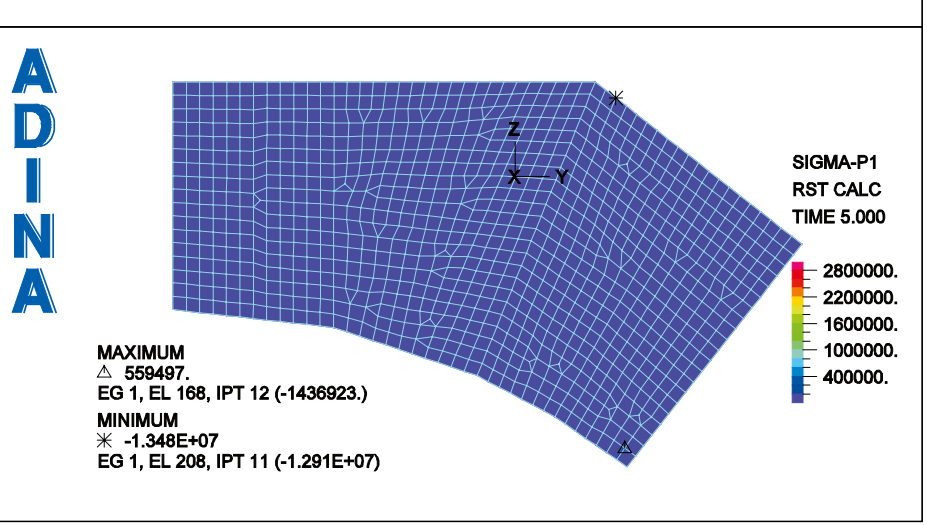

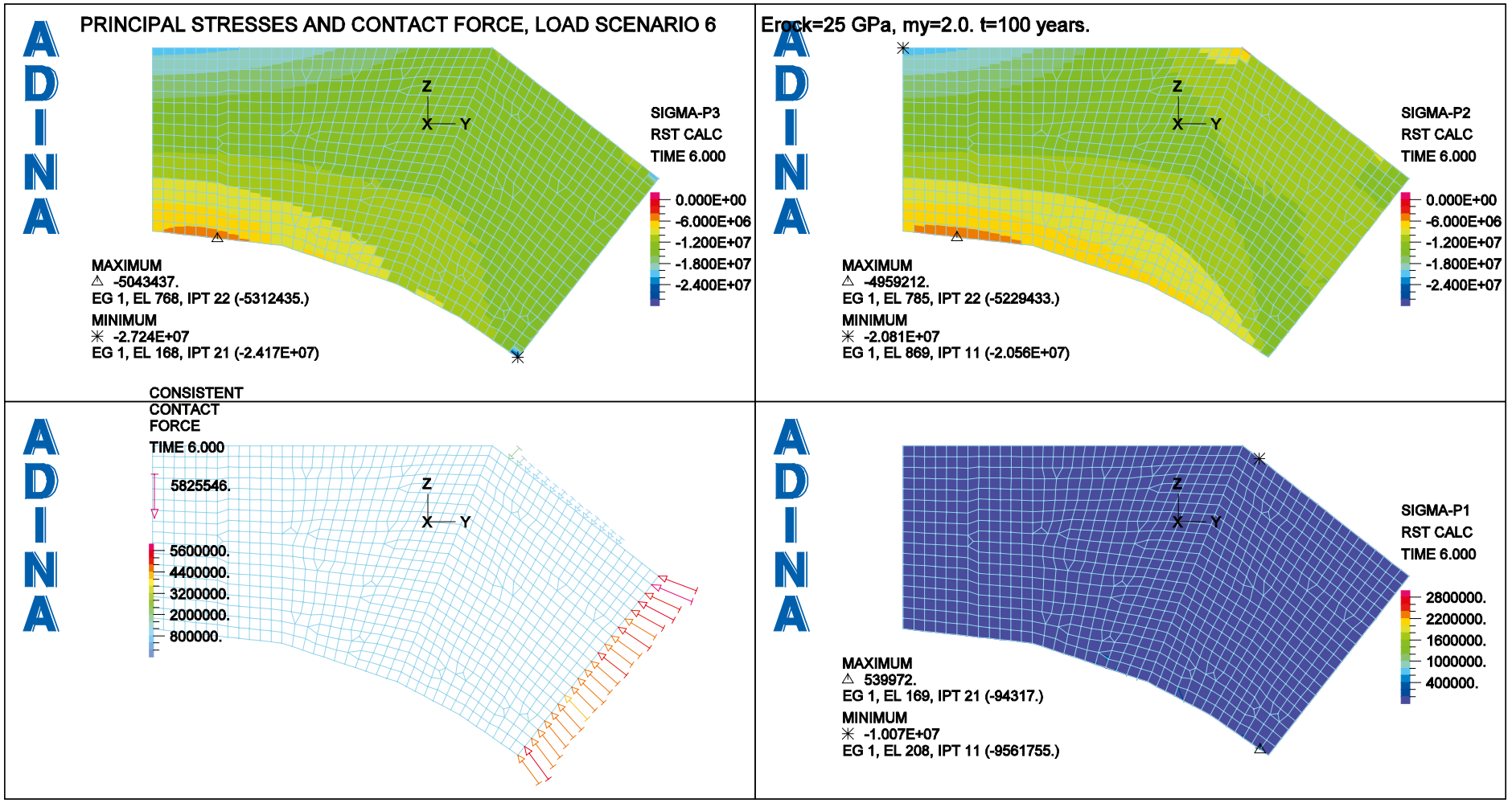
PRINCIPAL STRESSES AND CONTACT FORCE, LOAD SCENARIO 6
SIGMA-P3
RST CALC
TIME 6.000
0.000E+00
-6.000E+06
-1.200E+07
-1.800E+07
-2.400E+07
MAXIMUM
-5043437.
EG 1, EL 768, IPT 22 (-5312435.)
MINIMUM
-2.724E+07
EG 1, EL 168, IPT 21 (-2.417E+07)
Erock=25 GPa, my=2.0. t=100 years.
SIGMA-P2
RST CALC
TIME 6.000
0.000E+00
-6.000E+06
-1.200E+07
-1.800E+07
-2.400E+07
MAXIMUM
-4959212.
EG 1, EL 785, IPT 22 (-5229433.)
MINIMUM
-2.081E+07
EG 1, EL 869, IPT 11 (-2.056E+07)
CONSISTENT
CONTACT
FORCE
TIME 6.000
5825546.
5600000.
4400000.
3200000.
2000000.
800000.
SIGMA-P1
RST CALC
TIME 6.000
2800000.
2200000.
1600000.
1000000.
400000.
MAXIMUM
539972.
EG 1, EL 169, IPT 21 (-94317.)
MINIMUM
-1.007E+07
EG 1, EL 208, IPT 11 (-9561755.)

PRINCIPAL STRESSES AND CONTACT FORCE, LOAD SCENARIO 7

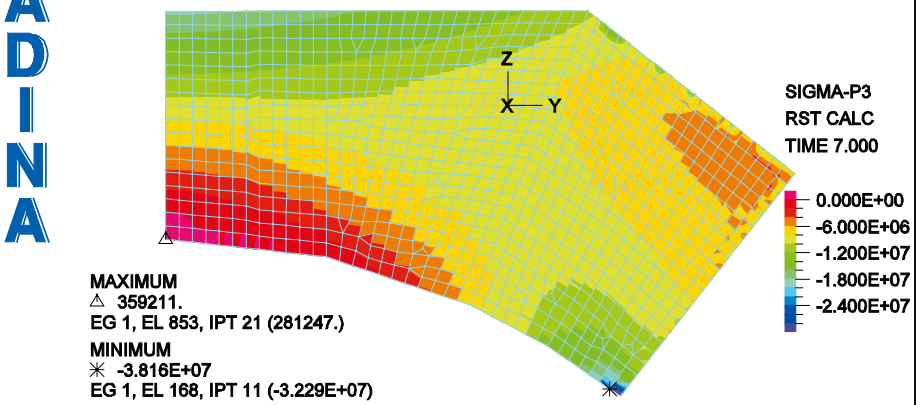

Erock=25 GPa, my=2.0. t=100 years.

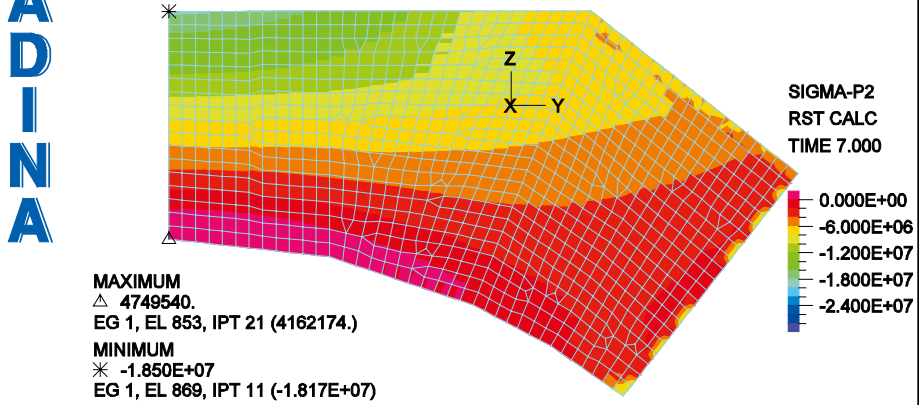

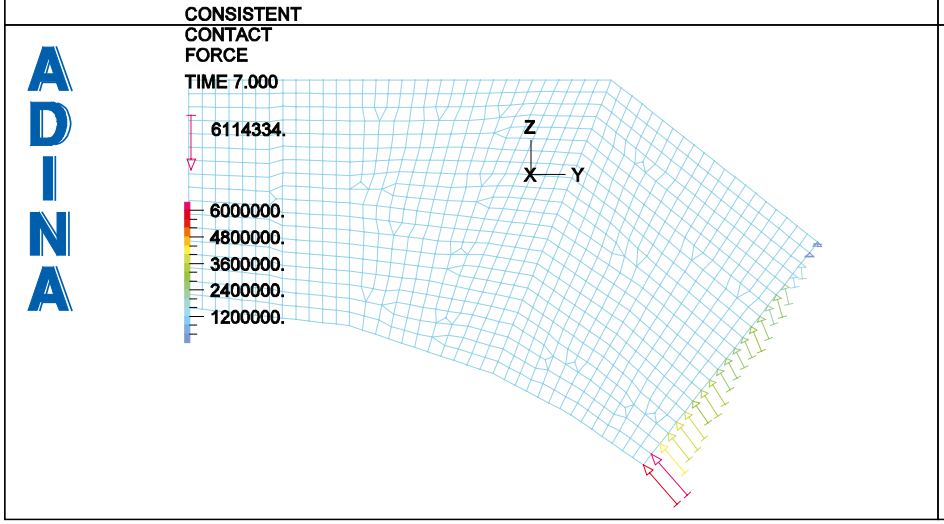

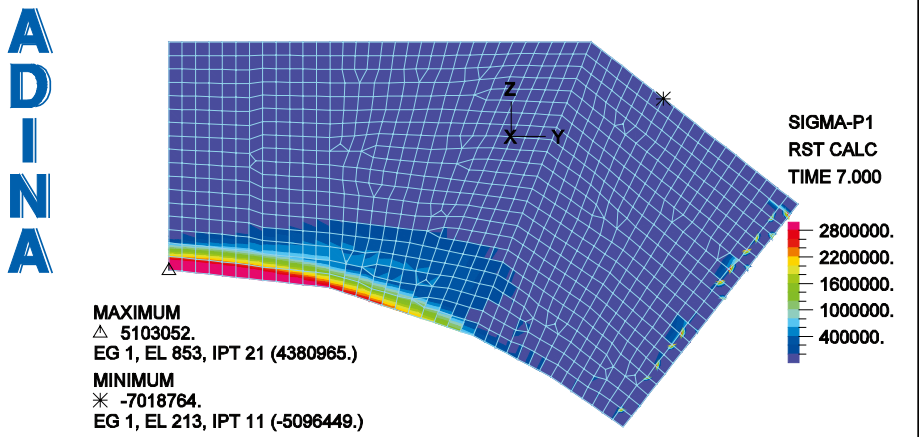

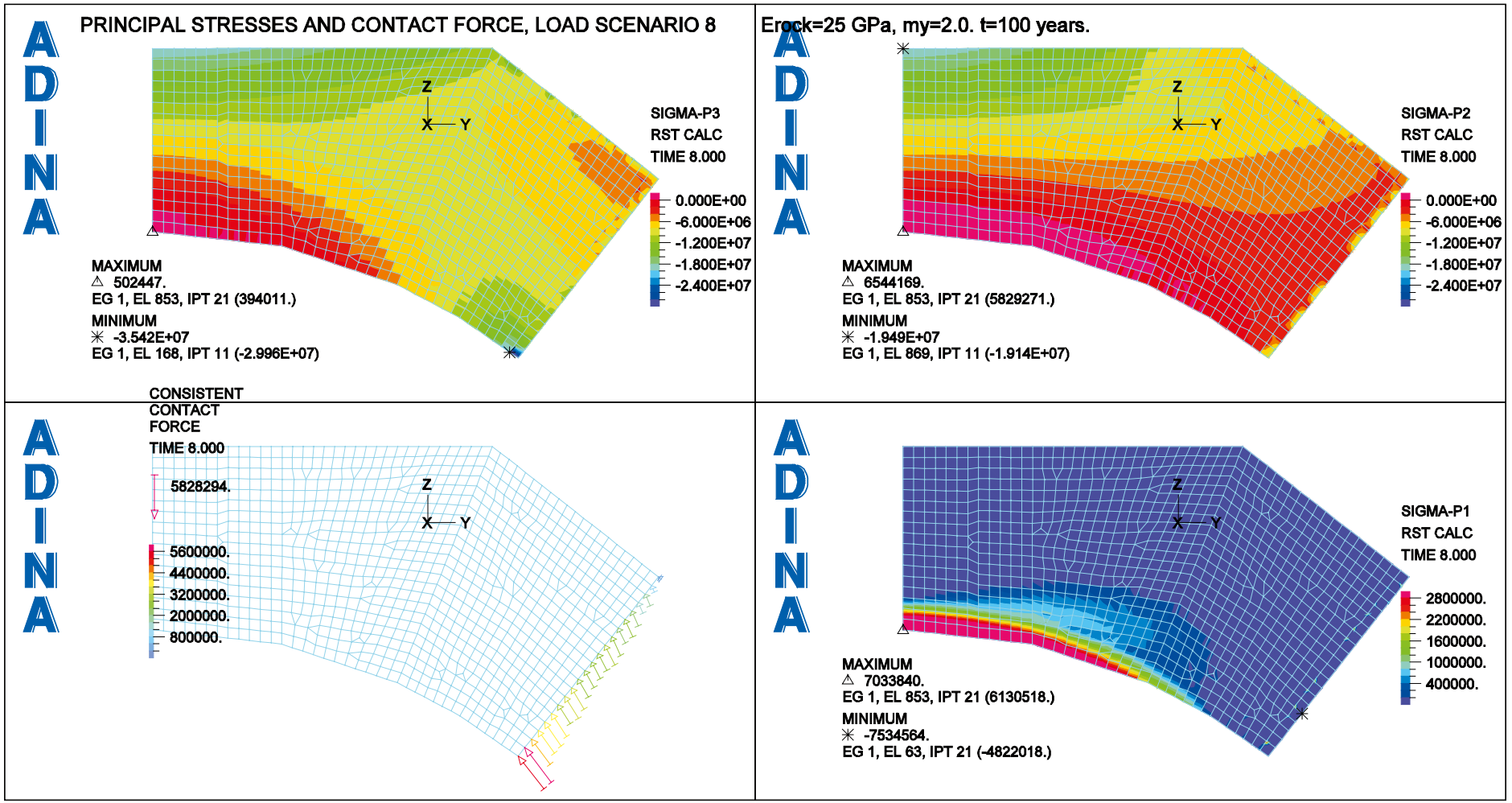
PRINCIPAL STRESSES AND CONTACT FORCE, LOAD SCENARIO 8
SIGMA-P3
RST CALC
TIME 8.000
0.000E+00
-6.000E+06
-1.200E+07
-1.800E+07
-2.400E+07
MAXIMUM
△ 502447.
EG 1, EL 853, IPT 21 (394011.)
MINIMUM
✳ -3.542E+07
EG 1, EL 168, IPT 11 (-2.996E+07)
Erock=25 GPa, my=2.0. t=100 years.
SIGMA-P2
RST CALC
TIME 8.000
0.000E+00
-6.000E+06
-1.200E+07
-1.800E+07
-2.400E+07
MAXIMUM
△ 6544169.
EG 1, EL 853, IPT 21 (5829271.)
MINIMUM
✳ -1.949E+07
EG 1, EL 869, IPT 11 (-1.914E+07)
CONSISTENT
CONTACT
FORCE
TIME 8.000
5828294.
5600000.
4400000.
3200000.
2000000.
800000.
SIGMA-P1
RST CALC
TIME 8.000
2800000.
2200000.
1600000.
1000000.
400000.
MAXIMUM
△ 7033840.
EG 1, EL 853, IPT 21 (6130518.)
MINIMUM
✳ -7534564.
EG 1, EL 63, IPT 21 (-4822018.)

E.4 Stress plots, load combinations 1.3–8.3

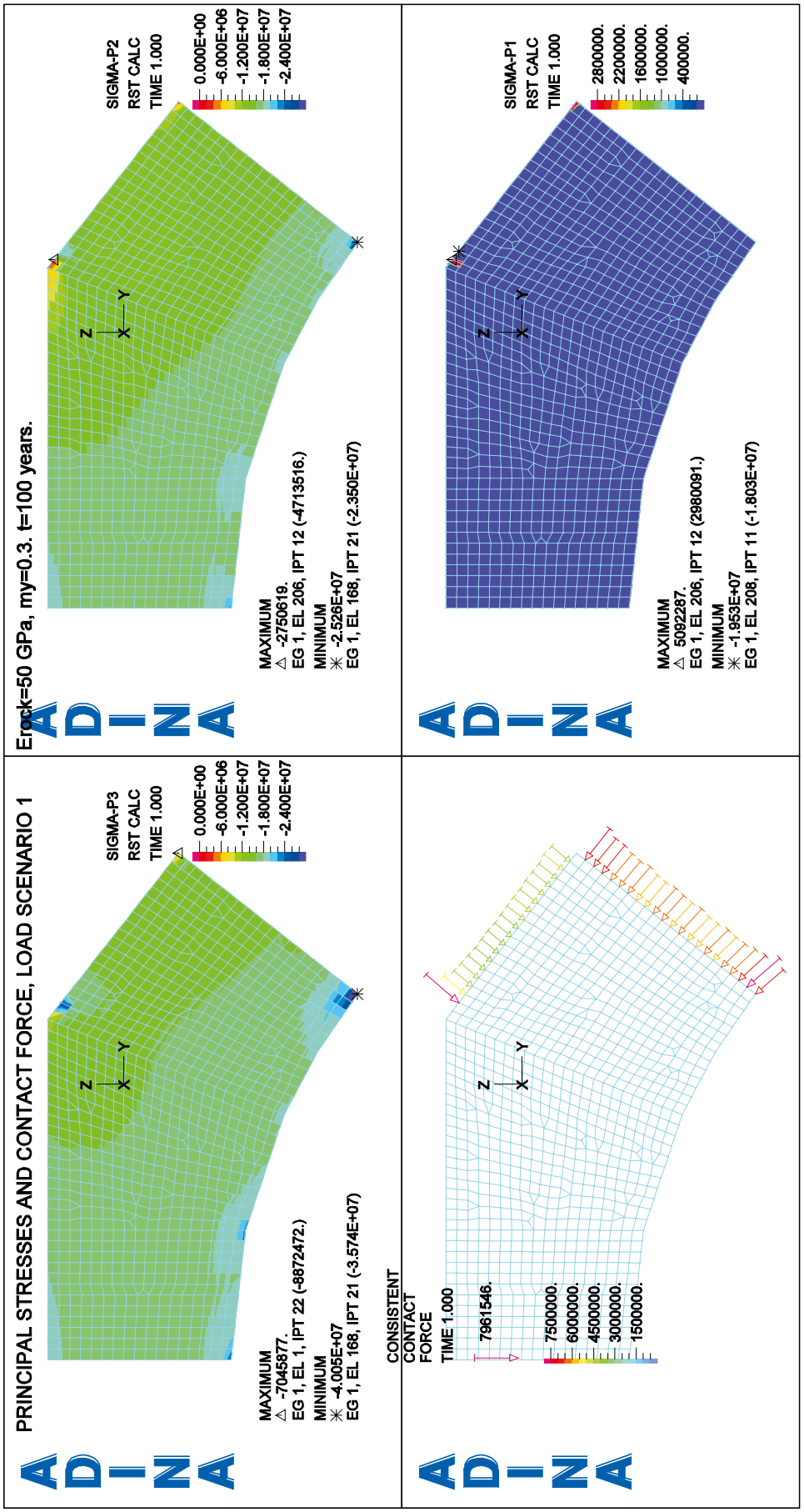

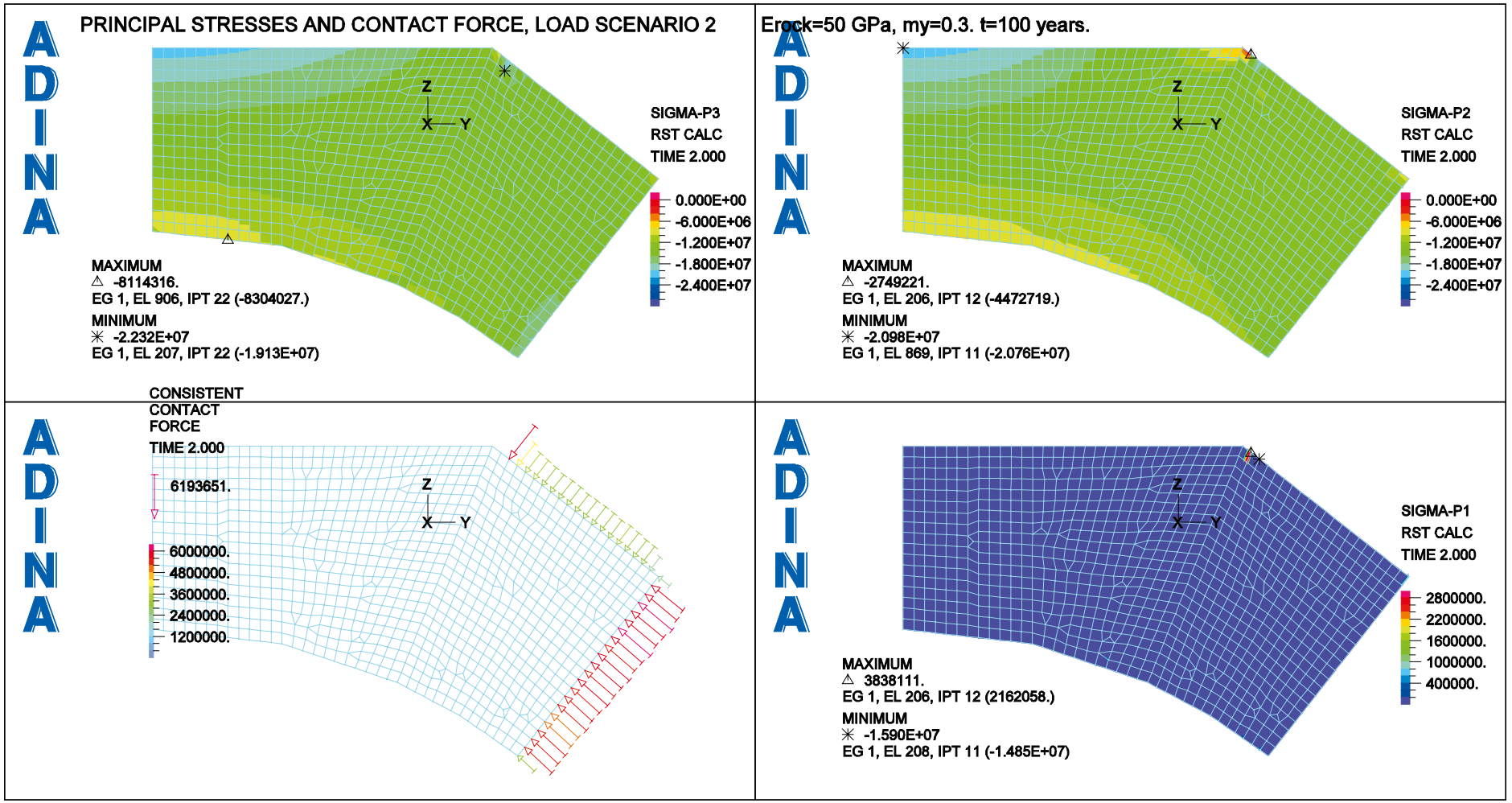
PRINCIPAL STRESSES AND CONTACT FORCE, LOAD SCENARIO 2
SIGMA-P3
RST CALC
TIME 2.000
0.000E+00
-6.000E+06
-1.200E+07
-1.800E+07
-2.400E+07
MAXIMUM
-8114316.
EG 1, EL 906, IPT 22 (-8304027.)
MINIMUM
-2.232E+07
EG 1, EL 207, IPT 22 (-1.913E+07)
Erock=50 GPa, my=0.3. t=100 years.
SIGMA-P2
RST CALC
TIME 2.000
0.000E+00
-6.000E+06
-1.200E+07
-1.800E+07
-2.400E+07
MAXIMUM
-2749221.
EG 1, EL 206, IPT 12 (-4472719.)
MINIMUM
-2.098E+07
EG 1, EL 869, IPT 11 (-2.076E+07)
CONSISTENT
CONTACT
FORCE
TIME 2.000
6193651.
6000000.
4800000.
3600000.
2400000.
1200000.
SIGMA-P1
RST CALC
TIME 2.000
2800000.
2200000.
1600000.
1000000.
400000.
MAXIMUM
3838111.
EG 1, EL 206, IPT 12 (2162058.)
MINIMUM
-1.590E+07
EG 1, EL 208, IPT 11 (-1.485E+07)

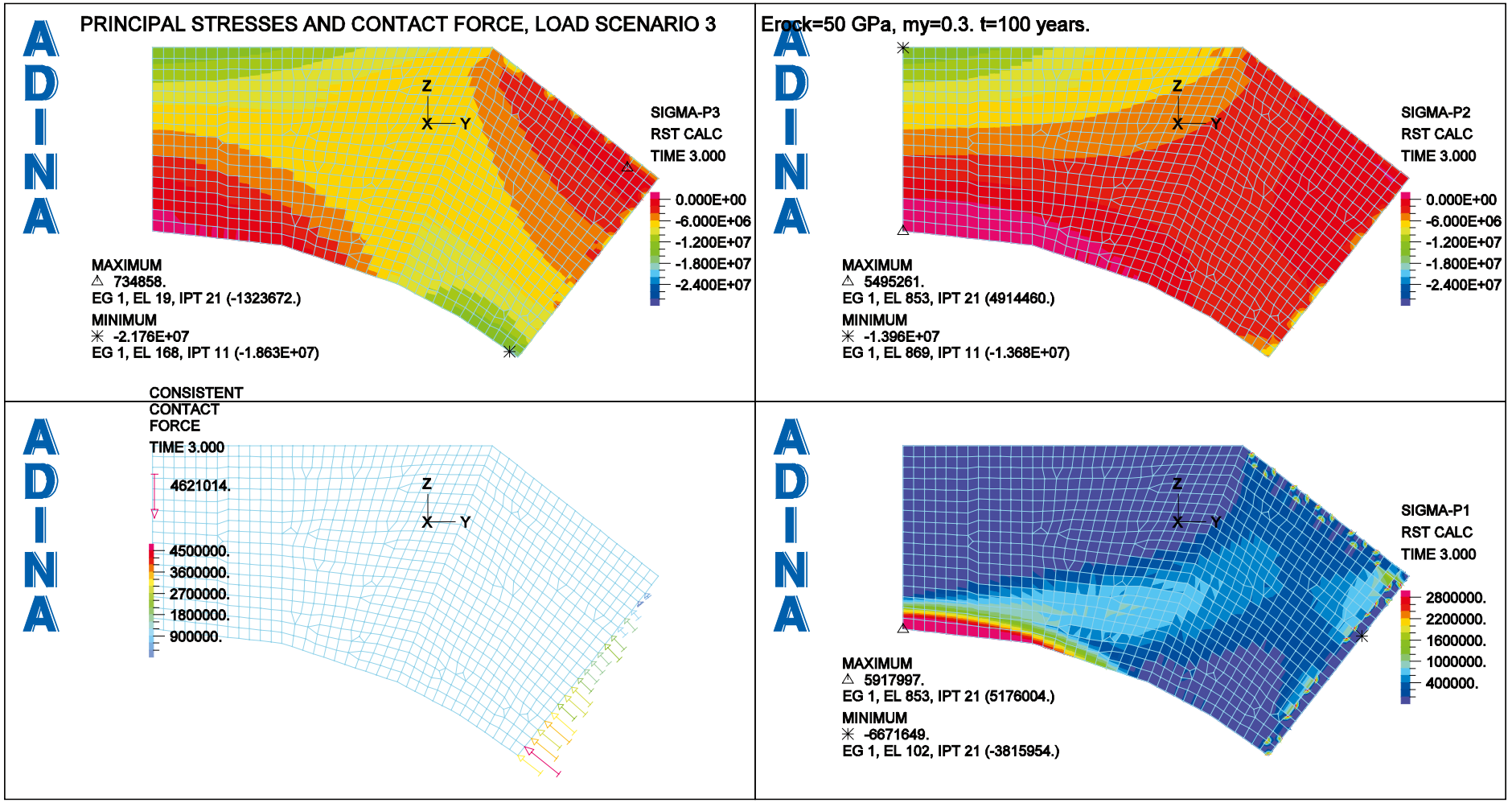
PRINCIPAL STRESSES AND CONTACT FORCE, LOAD SCENARIO 3
Erock=50 GPa, my=0.3. t=100 years.
ADINA
SIGMA-P3
RST CALC
TIME 3.000
0.000E+00
-6.000E+06
-1.200E+07
-1.800E+07
-2.400E+07
MAXIMUM
734858.
EG 1, EL 19, IPT 21 (-1323672.)
MINIMUM
-2.176E+07
EG 1, EL 168, IPT 11 (-1.863E+07)
SIGMA-P2
RST CALC
TIME 3.000
0.000E+00
-6.000E+06
-1.200E+07
-1.800E+07
-2.400E+07
MAXIMUM
5495261.
EG 1, EL 853, IPT 21 (4914460.)
MINIMUM
-1.396E+07
EG 1, EL 869, IPT 11 (-1.368E+07)
CONSISTENT
CONTACT
FORCE
TIME 3.000
4621014.
4500000.
3600000.
2700000.
1800000.
900000.
SIGMA-P1
RST CALC
TIME 3.000
2800000.
2200000.
1600000.
1000000.
400000.
MAXIMUM
5917997.
EG 1, EL 853, IPT 21 (5176004.)
MINIMUM
-6671649.
EG 1, EL 102, IPT 21 (-3815954.)
Z
X
Y

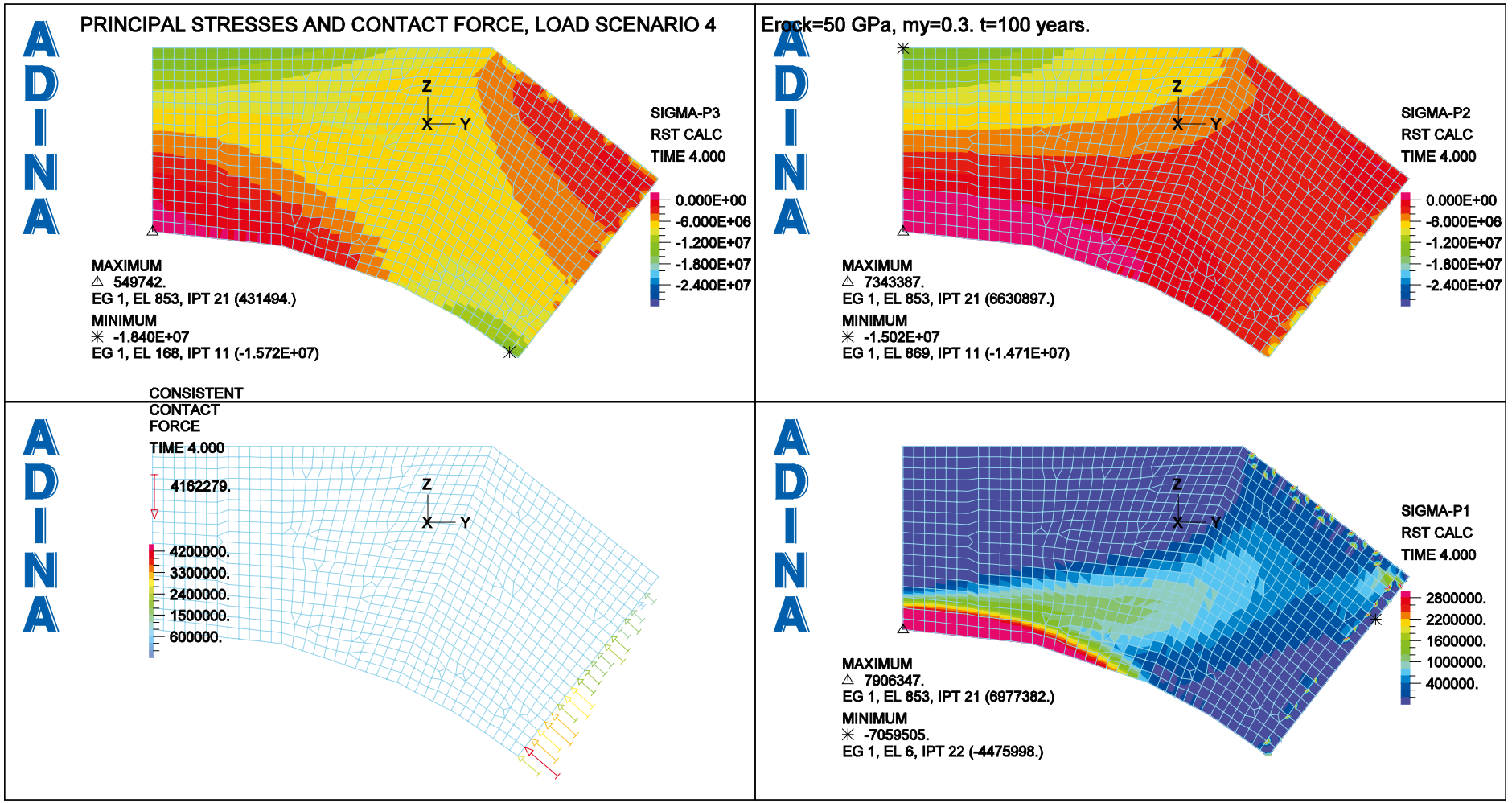
PRINCIPAL STRESSES AND CONTACT FORCE, LOAD SCENARIO 4
SIGMA-P3
RST CALC
TIME 4.000
0.000E+00
-6.000E+06
-1.200E+07
-1.800E+07
-2.400E+07
MAXIMUM
549742.
EG 1, EL 853, IPT 21 (431494.)
MINIMUM
-1.840E+07
EG 1, EL 168, IPT 11 (-1.572E+07)
Erock=50 GPa, my=0.3. t=100 years.
SIGMA-P2
RST CALC
TIME 4.000
0.000E+00
-6.000E+06
-1.200E+07
-1.800E+07
-2.400E+07
MAXIMUM
7343387.
EG 1, EL 853, IPT 21 (6630897.)
MINIMUM
-1.502E+07
EG 1, EL 869, IPT 11 (-1.471E+07)
CONSISTENT
CONTACT
FORCE
TIME 4.000
4162279.
4200000.
3300000.
2400000.
1500000.
600000.
SIGMA-P1
RST CALC
TIME 4.000
2800000.
2200000.
1600000.
1000000.
400000.
MAXIMUM
7906347.
EG 1, EL 853, IPT 21 (6977382.)
MINIMUM
-7059505.
EG 1, EL 6, IPT 22 (-4475998.)

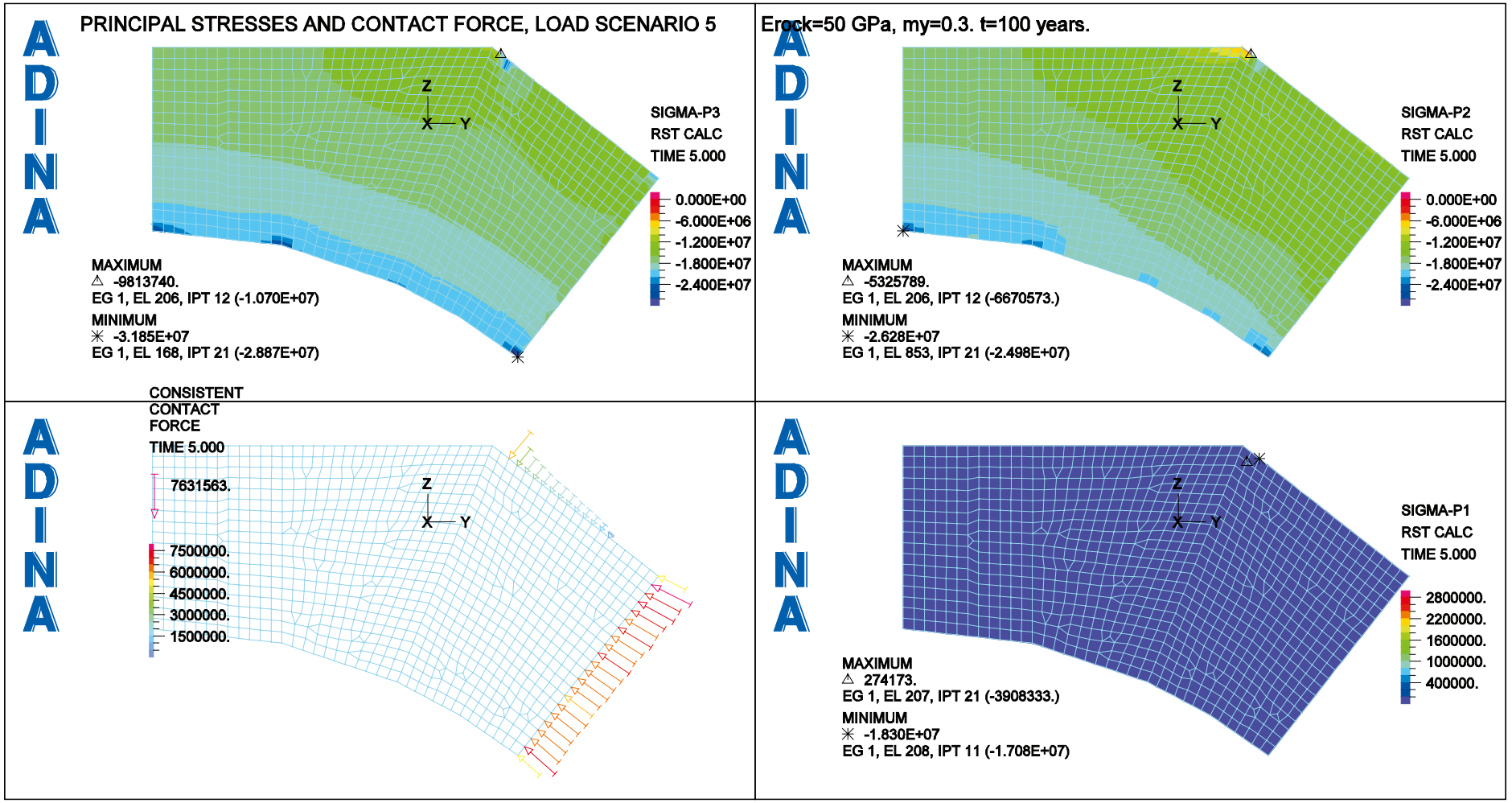
PRINCIPAL STRESSES AND CONTACT FORCE, LOAD SCENARIO 5
Erock=50 GPa, my=0.3. t=100 years.
ADINA
SIGMA-P3
RST CALC
TIME 5.000
0.000E+00
-6.000E+06
-1.200E+07
-1.800E+07
-2.400E+07
MAXIMUM
-9813740.
EG 1, EL 206, IPT 12 (-1.070E+07)
MINIMUM
-3.185E+07
EG 1, EL 168, IPT 21 (-2.887E+07)
SIGMA-P2
RST CALC
TIME 5.000
0.000E+00
-6.000E+06
-1.200E+07
-1.800E+07
-2.400E+07
MAXIMUM
-5325789.
EG 1, EL 206, IPT 12 (-6670573.)
MINIMUM
-2.628E+07
EG 1, EL 853, IPT 21 (-2.498E+07)
CONSISTENT
CONTACT
FORCE
TIME 5.000
7631563.
7500000.
6000000.
4500000.
3000000.
1500000.
SIGMA-P1
RST CALC
TIME 5.000
2800000.
2200000.
1600000.
1000000.
400000.
MAXIMUM
274173.
EG 1, EL 207, IPT 21 (-3908333.)
MINIMUM
-1.830E+07
EG 1, EL 208, IPT 11 (-1.708E+07)
Z
X
Y

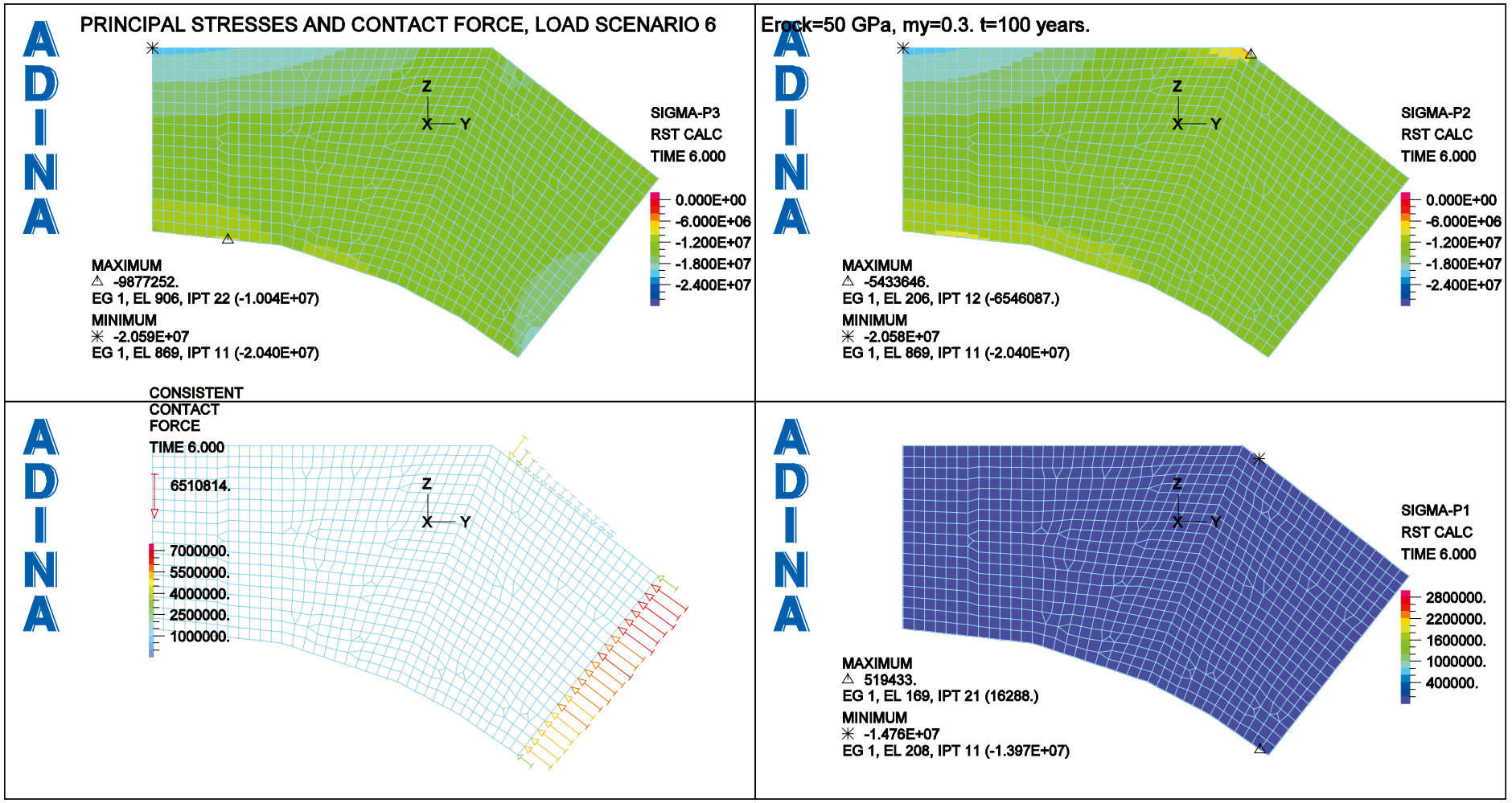
PRINCIPAL STRESSES AND CONTACT FORCE, LOAD SCENARIO 6
SIGMA-P3
RST CALC
TIME 6.000
0.000E+00
-6.000E+06
-1.200E+07
-1.800E+07
-2.400E+07
MAXIMUM
-9877252.
EG 1, EL 906, IPT 22 (-1.004E+07)
MINIMUM
-2.059E+07
EG 1, EL 869, IPT 11 (-2.040E+07)
Erock=50 GPa, my=0.3. t=100 years.
SIGMA-P2
RST CALC
TIME 6.000
0.000E+00
-6.000E+06
-1.200E+07
-1.800E+07
-2.400E+07
MAXIMUM
-5433646.
EG 1, EL 206, IPT 12 (-6546087.)
MINIMUM
-2.058E+07
EG 1, EL 869, IPT 11 (-2.040E+07)
CONSISTENT
CONTACT
FORCE
TIME 6.000
6510814.
7000000.
5500000.
4000000.
2500000.
1000000.
SIGMA-P1
RST CALC
TIME 6.000
2800000.
2200000.
1600000.
1000000.
400000.
MAXIMUM
519433.
EG 1, EL 169, IPT 21 (16288.)
MINIMUM
-1.476E+07
EG 1, EL 208, IPT 11 (-1.397E+07)

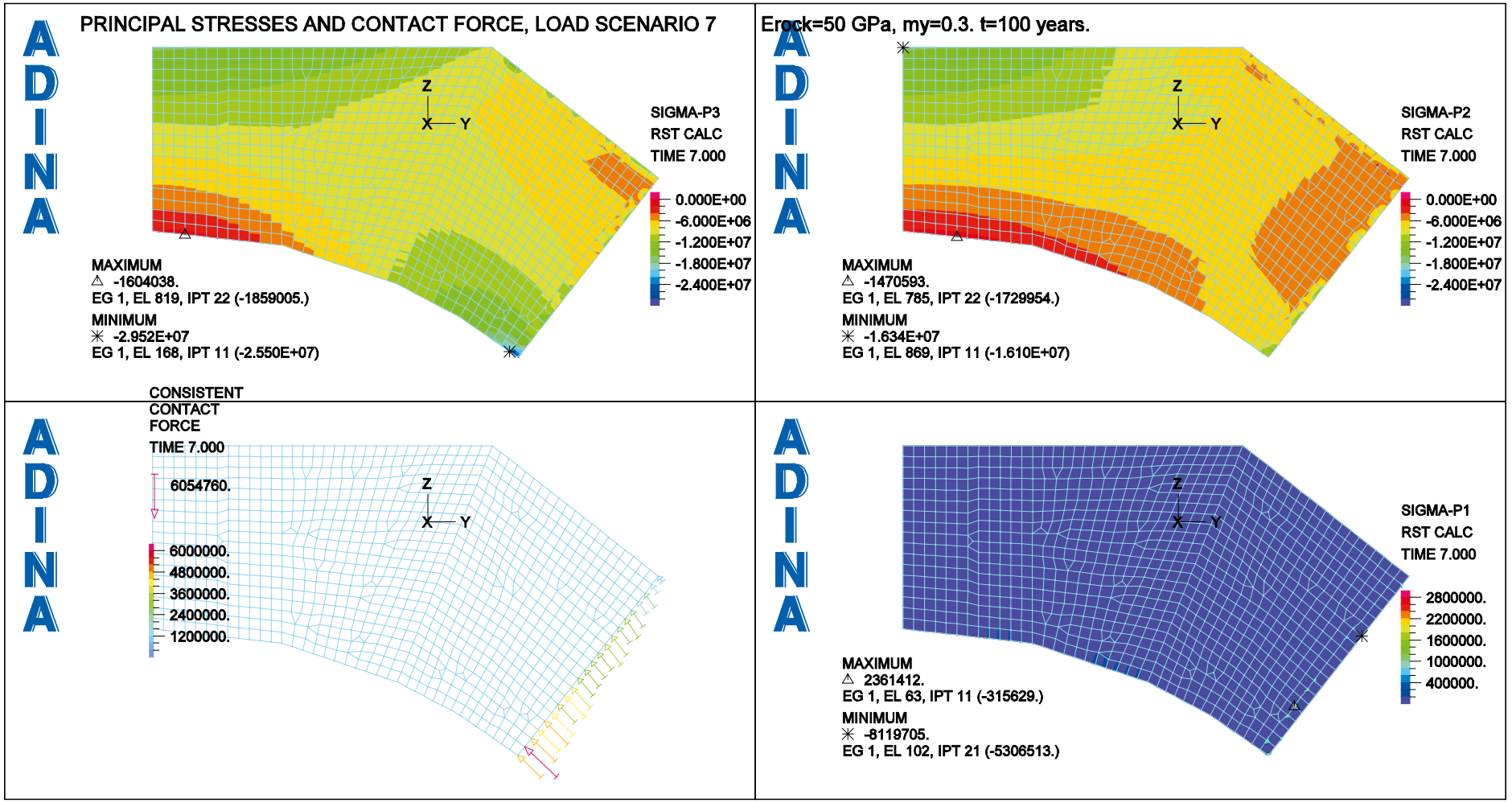
PRINCIPAL STRESSES AND CONTACT FORCE, LOAD SCENARIO 7
Erock=50 GPa, my=0.3. t=100 years.
ADINA
SIGMA-P3
RST CALC
TIME 7.000
0.000E+00
-6.000E+06
-1.200E+07
-1.800E+07
-2.400E+07
MAXIMUM
-1604038.
EG 1, EL 819, IPT 22 (-1859005.)
MINIMUM
-2.952E+07
EG 1, EL 168, IPT 11 (-2.550E+07)
SIGMA-P2
RST CALC
TIME 7.000
0.000E+00
-6.000E+06
-1.200E+07
-1.800E+07
-2.400E+07
MAXIMUM
-1470593.
EG 1, EL 785, IPT 22 (-1729954.)
MINIMUM
-1.634E+07
EG 1, EL 869, IPT 11 (-1.610E+07)
CONSISTENT
CONTACT
FORCE
TIME 7.000
6054760.
6000000.
4800000.
3600000.
2400000.
1200000.
SIGMA-P1
RST CALC
TIME 7.000
2800000.
2200000.
1600000.
1000000.
400000.
MAXIMUM
2361412.
EG 1, EL 63, IPT 11 (-315629.)
MINIMUM
-8119705.
EG 1, EL 102, IPT 21 (-5306513.)

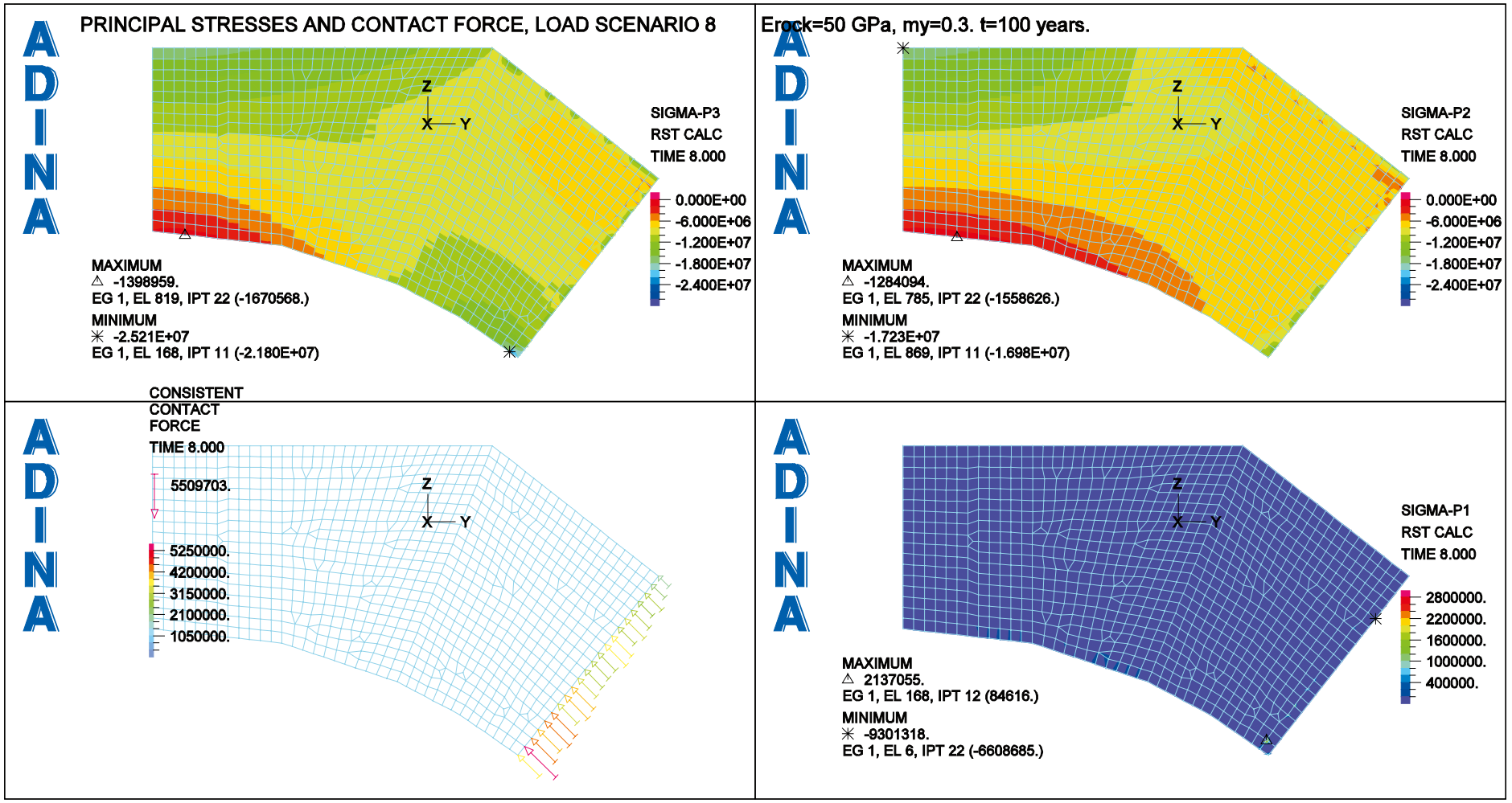
PRINCIPAL STRESSES AND CONTACT FORCE, LOAD SCENARIO 8
SIGMA-P3
RST CALC
TIME 8.000
0.000E+00
-6.000E+06
-1.200E+07
-1.800E+07
-2.400E+07
MAXIMUM
-1398959.
EG 1, EL 819, IPT 22 (-1670568.)
MINIMUM
-2.521E+07
EG 1, EL 168, IPT 11 (-2.180E+07)
Erock=50 GPa, my=0.3. t=100 years.
SIGMA-P2
RST CALC
TIME 8.000
0.000E+00
-6.000E+06
-1.200E+07
-1.800E+07
-2.400E+07
MAXIMUM
-1284094.
EG 1, EL 785, IPT 22 (-1558626.)
MINIMUM
-1.723E+07
EG 1, EL 869, IPT 11 (-1.698E+07)
CONSISTENT
CONTACT
FORCE
TIME 8.000
5509703.
5250000.
4200000.
3150000.
2100000.
1050000.
SIGMA-P1
RST CALC
TIME 8.000
2800000.
2200000.
1600000.
1000000.
400000.
MAXIMUM
2137055.
EG 1, EL 168, IPT 12 (84616.)
MINIMUM
-9301318.
EG 1, EL 6, IPT 22 (-6608685.)

E.5 Stress plots, load combinations 1.4–8.4

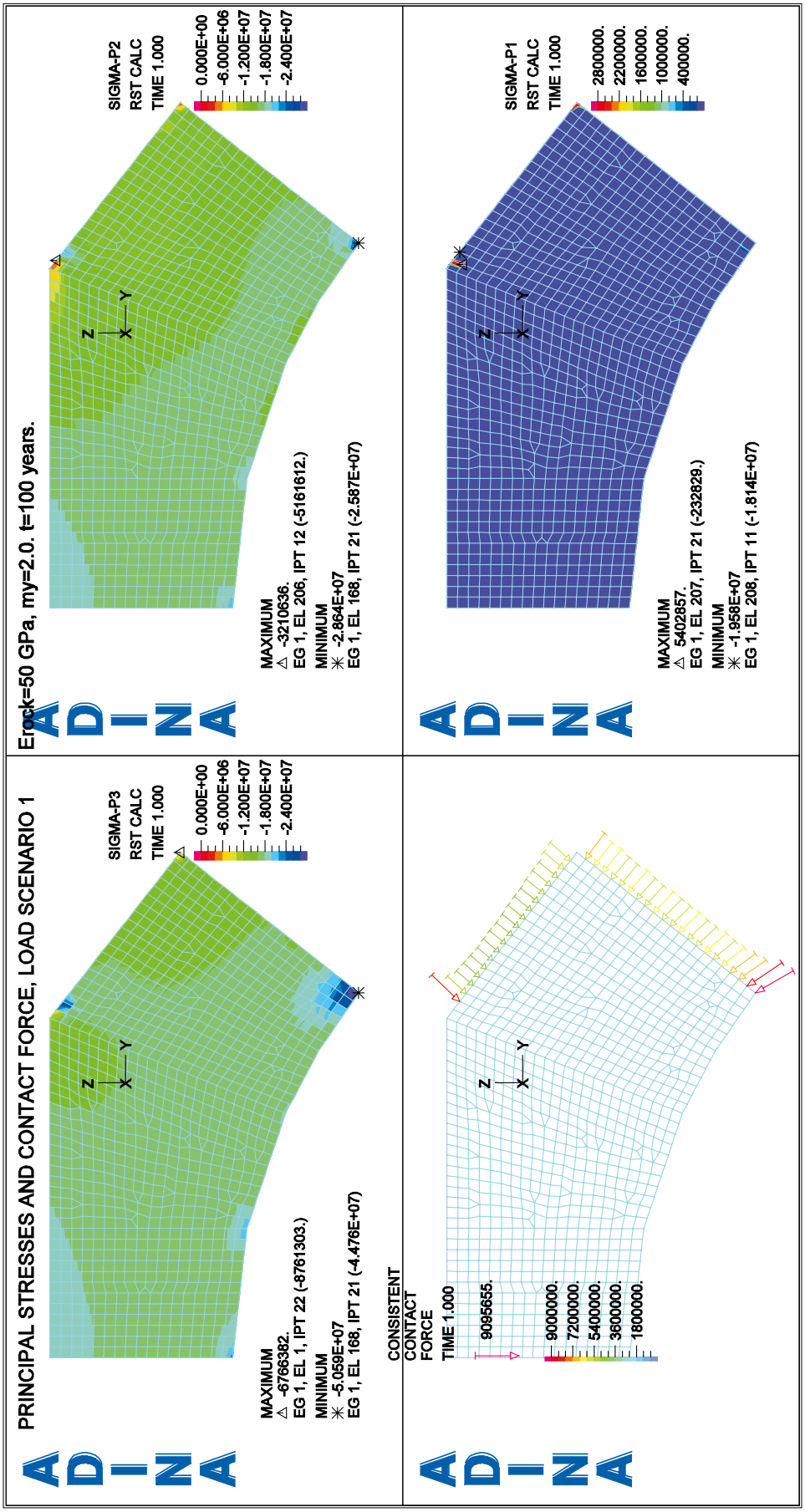

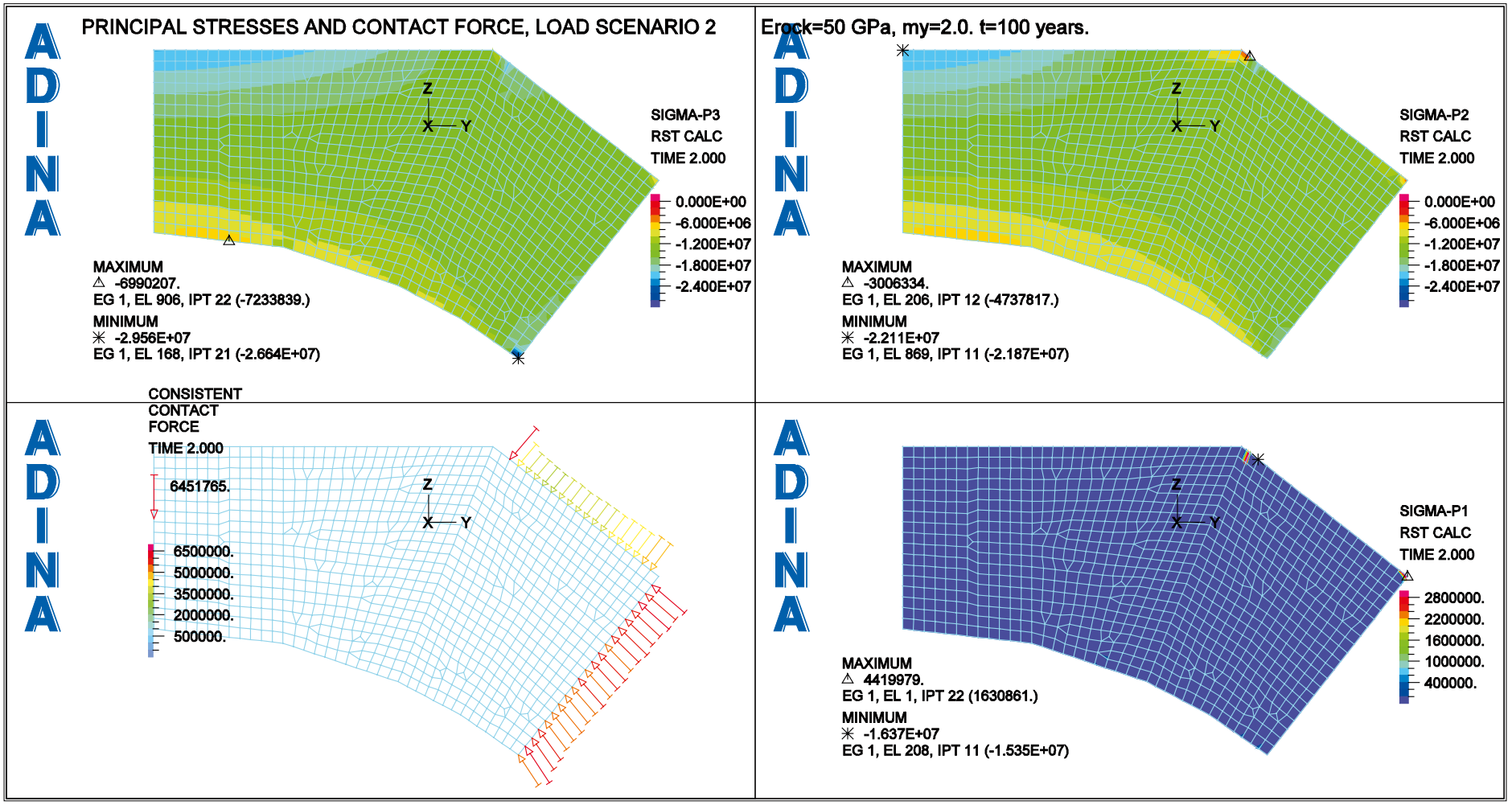
PRINCIPAL STRESSES AND CONTACT FORCE, LOAD SCENARIO 2
ADINA
Z
X
Y
SIGMA-P3
RST CALC
TIME 2.000
0.000E+00
-6.000E+06
-1.200E+07
-1.800E+07
-2.400E+07
MAXIMUM
-6990207.
EG 1, EL 906, IPT 22 (-7233839.)
MINIMUM
-2.956E+07
EG 1, EL 168, IPT 21 (-2.664E+07)
Erock=50 GPa, my=2.0. t=100 years.
ADINA
Z
X
Y
SIGMA-P2
RST CALC
TIME 2.000
0.000E+00
-6.000E+06
-1.200E+07
-1.800E+07
-2.400E+07
MAXIMUM
-3006334.
EG 1, EL 206, IPT 12 (-4737817.)
MINIMUM
-2.211E+07
EG 1, EL 869, IPT 11 (-2.187E+07)
ADINA
CONSISTENT
CONTACT
FORCE
TIME 2.000
6451765.
6500000.
5000000.
3500000.
2000000.
500000.
Z
X
Y
ADINA
Z
X
Y
SIGMA-P1
RST CALC
TIME 2.000
2800000.
2200000.
1600000.
1000000.
400000.
MAXIMUM
4419979.
EG 1, EL 1, IPT 22 (1630861.)
MINIMUM
-1.637E+07
EG 1, EL 208, IPT 11 (-1.535E+07)

PRINCIPAL STRESSES AND CONTACT FORCE, LOAD SCENARIO 3

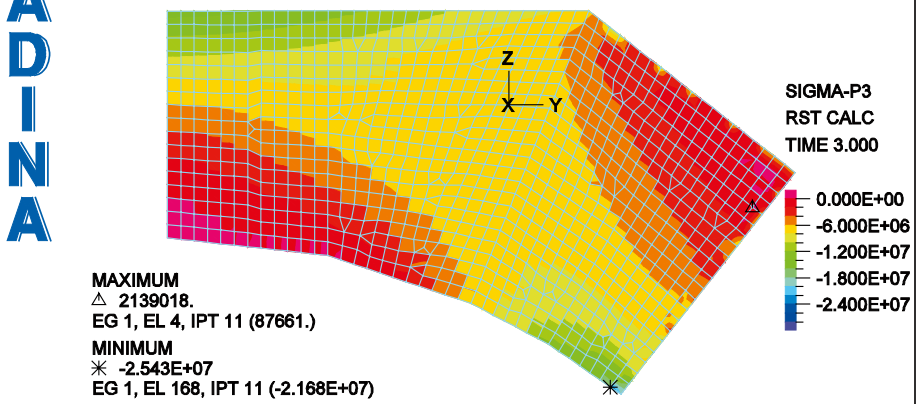

Erock=50 GPa, my=2.0. t=100 years.

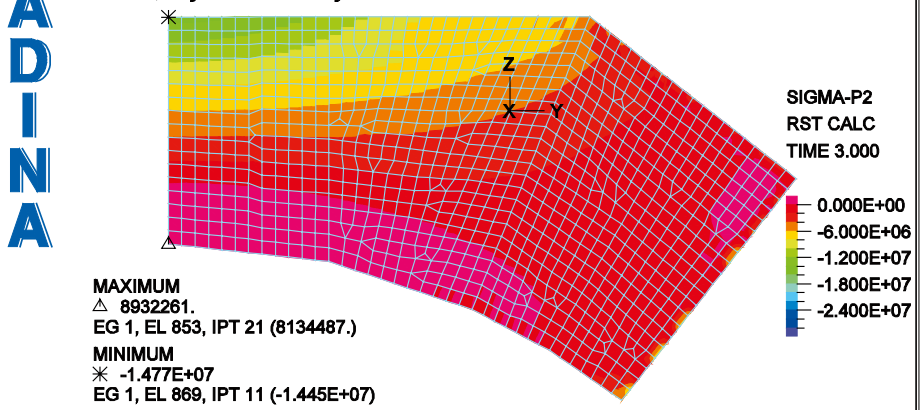

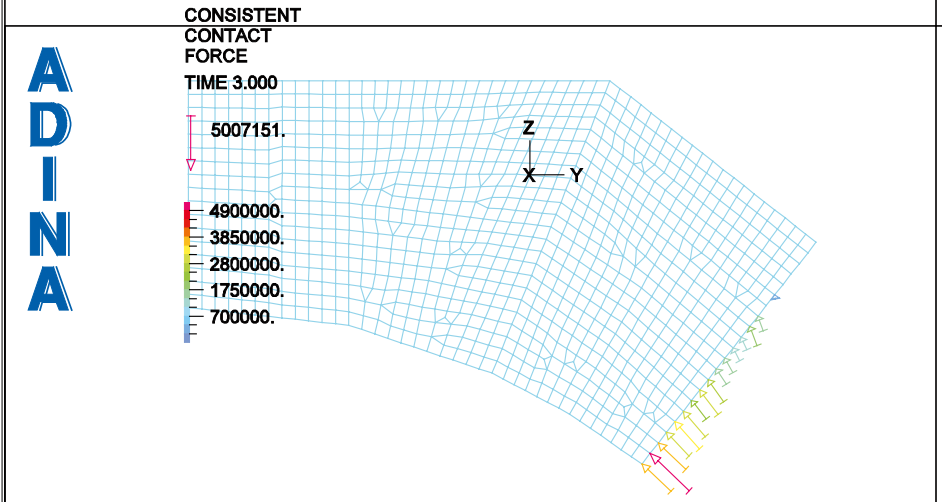

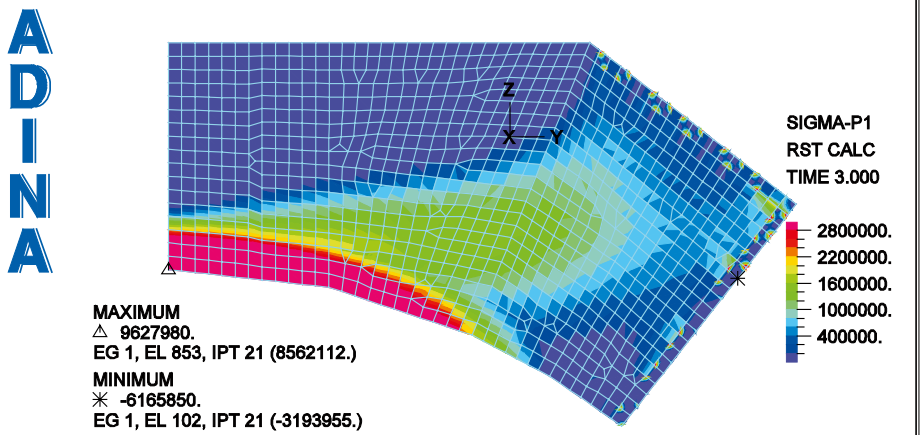

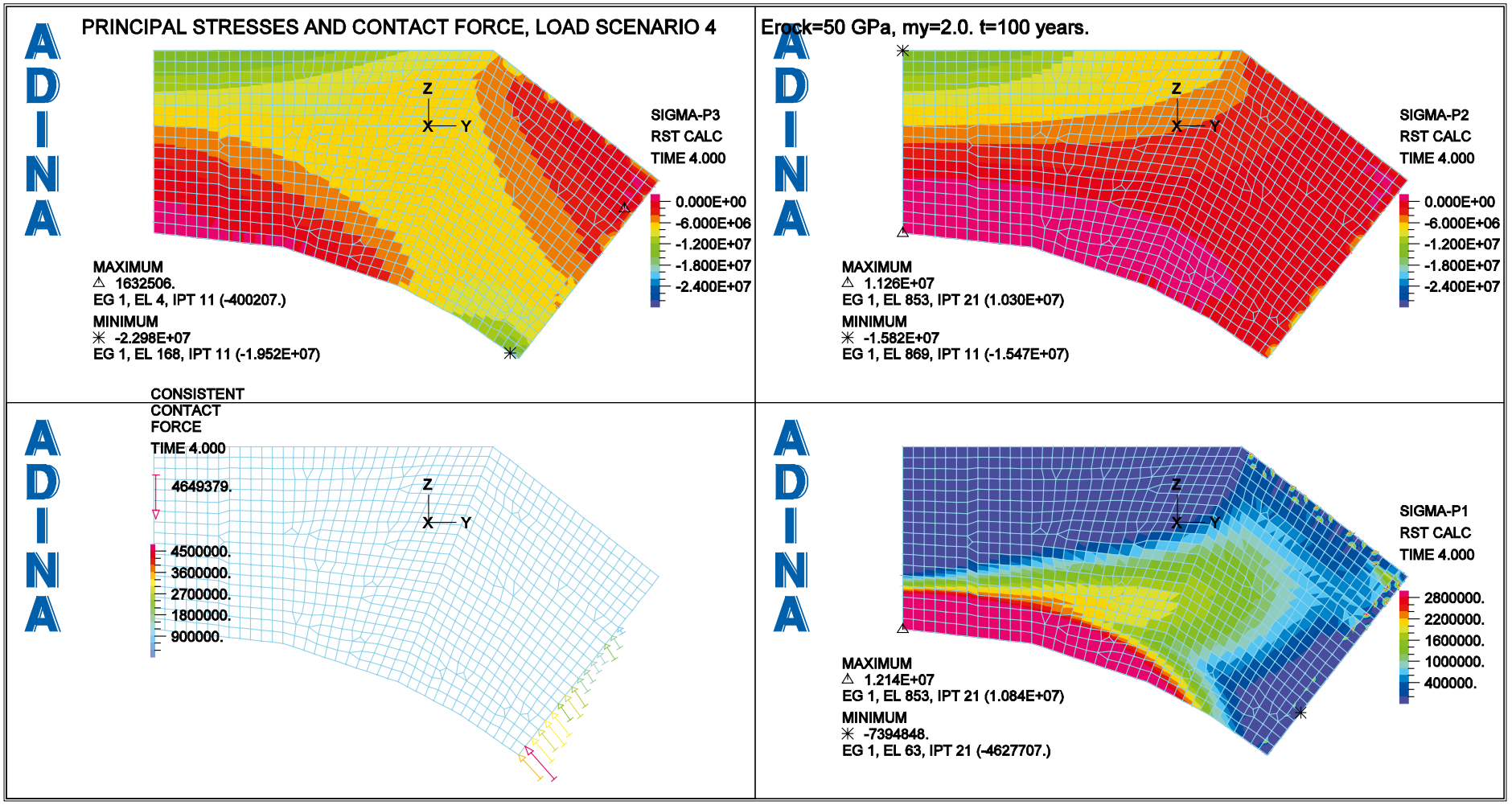
PRINCIPAL STRESSES AND CONTACT FORCE, LOAD SCENARIO 4
SIGMA-P3
RST CALC
TIME 4.000
0.000E+00
-6.000E+06
-1.200E+07
-1.800E+07
-2.400E+07
MAXIMUM
1632506.
EG 1, EL 4, IPT 11 (-400207.)
MINIMUM
-2.298E+07
EG 1, EL 168, IPT 11 (-1.952E+07)
Erock=50 GPa, my=2.0. t=100 years.
SIGMA-P2
RST CALC
TIME 4.000
0.000E+00
-6.000E+06
-1.200E+07
-1.800E+07
-2.400E+07
MAXIMUM
1.126E+07
EG 1, EL 853, IPT 21 (1.030E+07)
MINIMUM
-1.582E+07
EG 1, EL 869, IPT 11 (-1.547E+07)
CONSISTENT
CONTACT
FORCE
TIME 4.000
4649379.
4500000.
3600000.
2700000.
1800000.
900000.
SIGMA-P1
RST CALC
TIME 4.000
2800000.
2200000.
1600000.
1000000.
400000.
MAXIMUM
1.214E+07
EG 1, EL 853, IPT 21 (1.084E+07)
MINIMUM
-7394848.
EG 1, EL 63, IPT 21 (-4627707.)

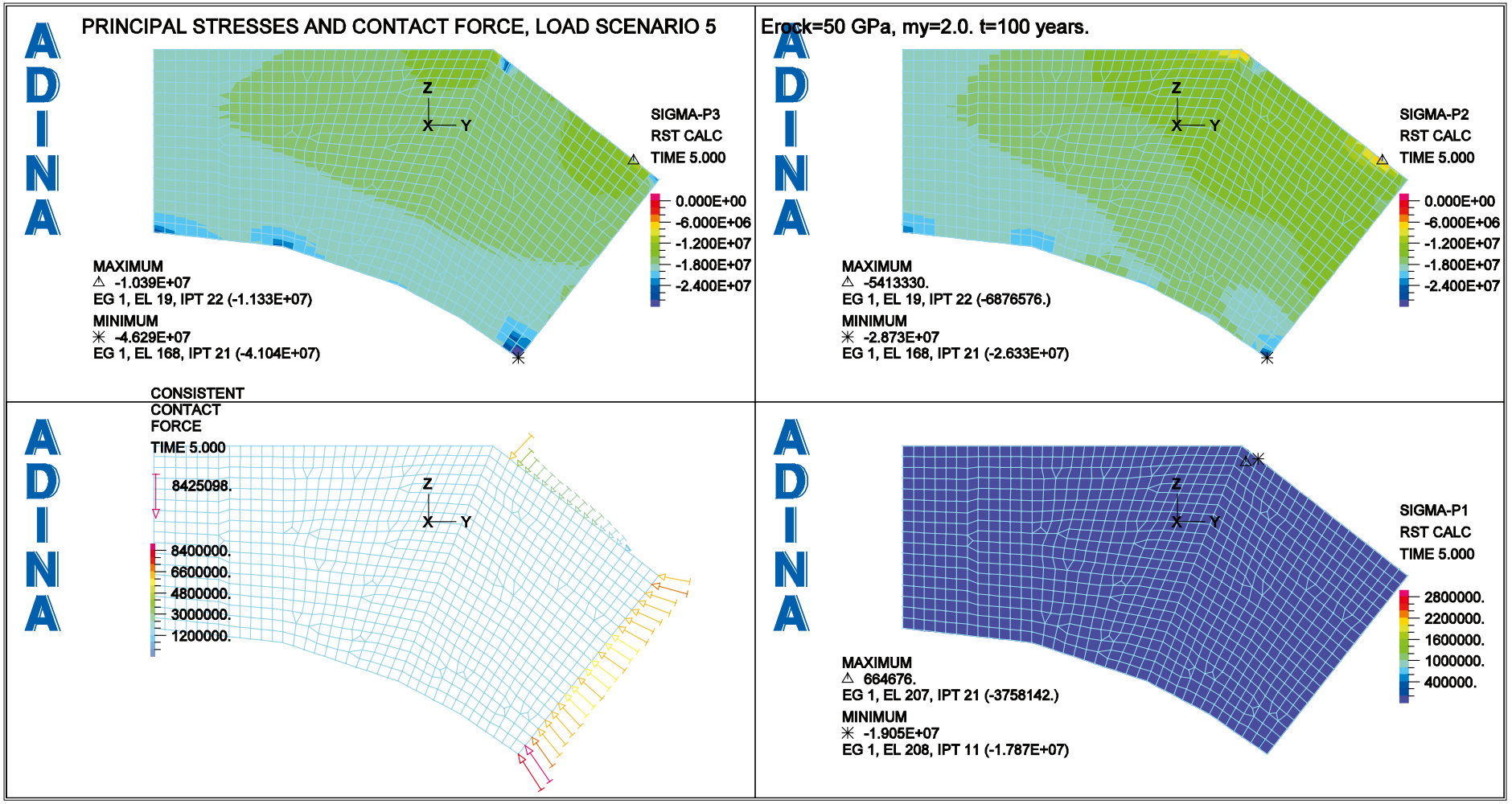
PRINCIPAL STRESSES AND CONTACT FORCE, LOAD SCENARIO 5
ADINA
Z
X
Y
SIGMA-P3
RST CALC
TIME 5.000
0.000E+00
-6.000E+06
-1.200E+07
-1.800E+07
-2.400E+07
MAXIMUM
-1.039E+07
EG 1, EL 19, IPT 22 (-1.133E+07)
MINIMUM
-4.629E+07
EG 1, EL 168, IPT 21 (-4.104E+07)
Erock=50 GPa, my=2.0. t=100 years.
ADINA
SIGMA-P2
RST CALC
TIME 5.000
0.000E+00
-6.000E+06
-1.200E+07
-1.800E+07
-2.400E+07
MAXIMUM
-5413330.
EG 1, EL 19, IPT 22 (-6876576.)
MINIMUM
-2.873E+07
EG 1, EL 168, IPT 21 (-2.633E+07)
ADINA
CONSISTENT
CONTACT
FORCE
TIME 5.000
8425098.
8400000.
6600000.
4800000.
3000000.
1200000.
ADINA
SIGMA-P1
RST CALC
TIME 5.000
2800000.
2200000.
1600000.
1000000.
400000.
MAXIMUM
664676.
EG 1, EL 207, IPT 21 (-3758142.)
MINIMUM
-1.905E+07
EG 1, EL 208, IPT 11 (-1.787E+07)

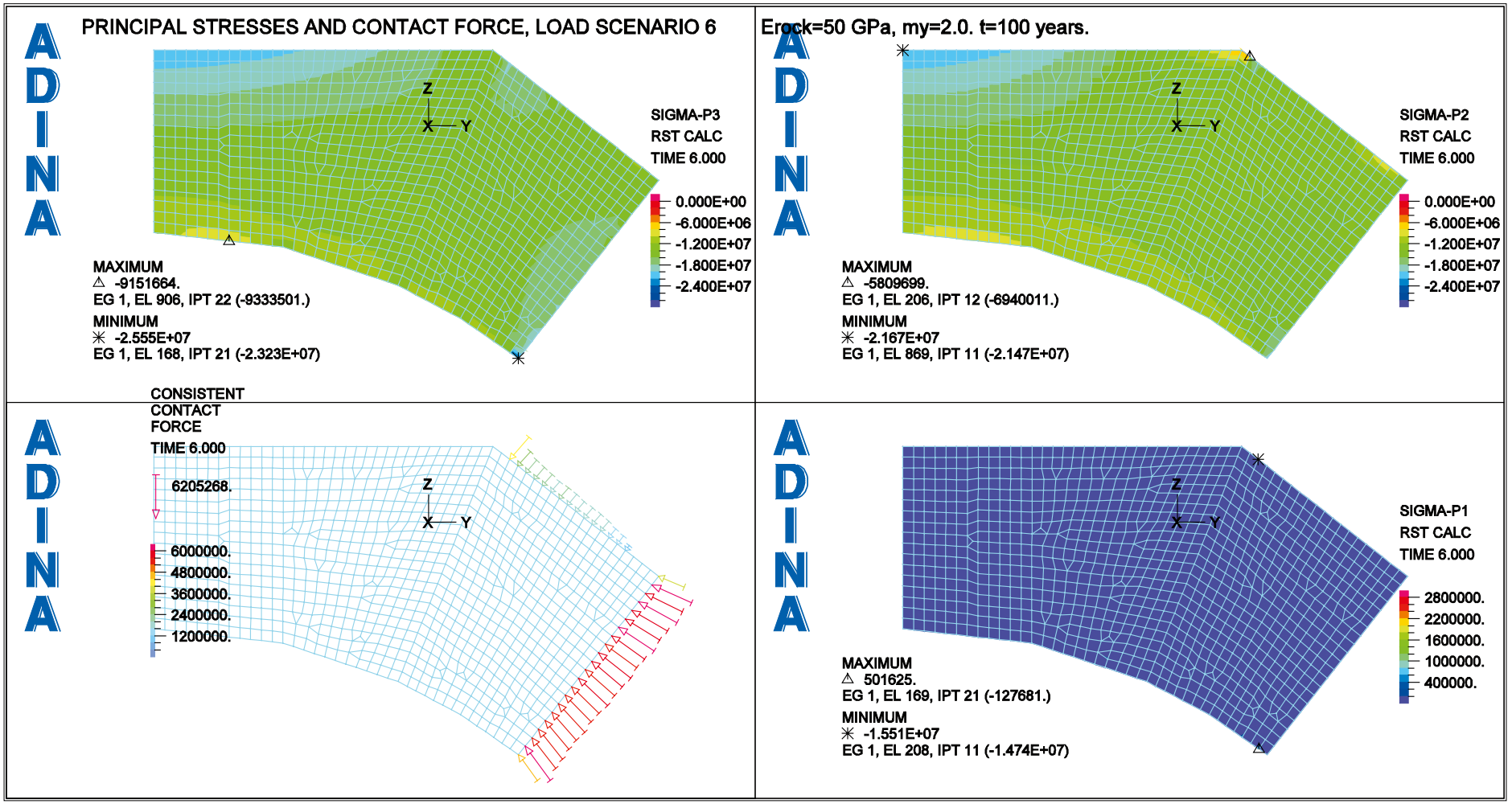
PRINCIPAL STRESSES AND CONTACT FORCE, LOAD SCENARIO 6
SIGMA-P3
RST CALC
TIME 6.000
0.000E+00
-6.000E+06
-1.200E+07
-1.800E+07
-2.400E+07
MAXIMUM
-9151664.
EG 1, EL 906, IPT 22 (-9333501.)
MINIMUM
-2.555E+07
EG 1, EL 168, IPT 21 (-2.323E+07)
Erock=50 GPa, my=2.0. t=100 years.
SIGMA-P2
RST CALC
TIME 6.000
0.000E+00
-6.000E+06
-1.200E+07
-1.800E+07
-2.400E+07
MAXIMUM
-5809699.
EG 1, EL 206, IPT 12 (-6940011.)
MINIMUM
-2.167E+07
EG 1, EL 869, IPT 11 (-2.147E+07)
CONSISTENT
CONTACT
FORCE
TIME 6.000
6205268.
6000000.
4800000.
3600000.
2400000.
1200000.
SIGMA-P1
RST CALC
TIME 6.000
2800000.
2200000.
1600000.
1000000.
400000.
MAXIMUM
501625.
EG 1, EL 169, IPT 21 (-127681.)
MINIMUM
-1.551E+07
EG 1, EL 208, IPT 11 (-1.474E+07)

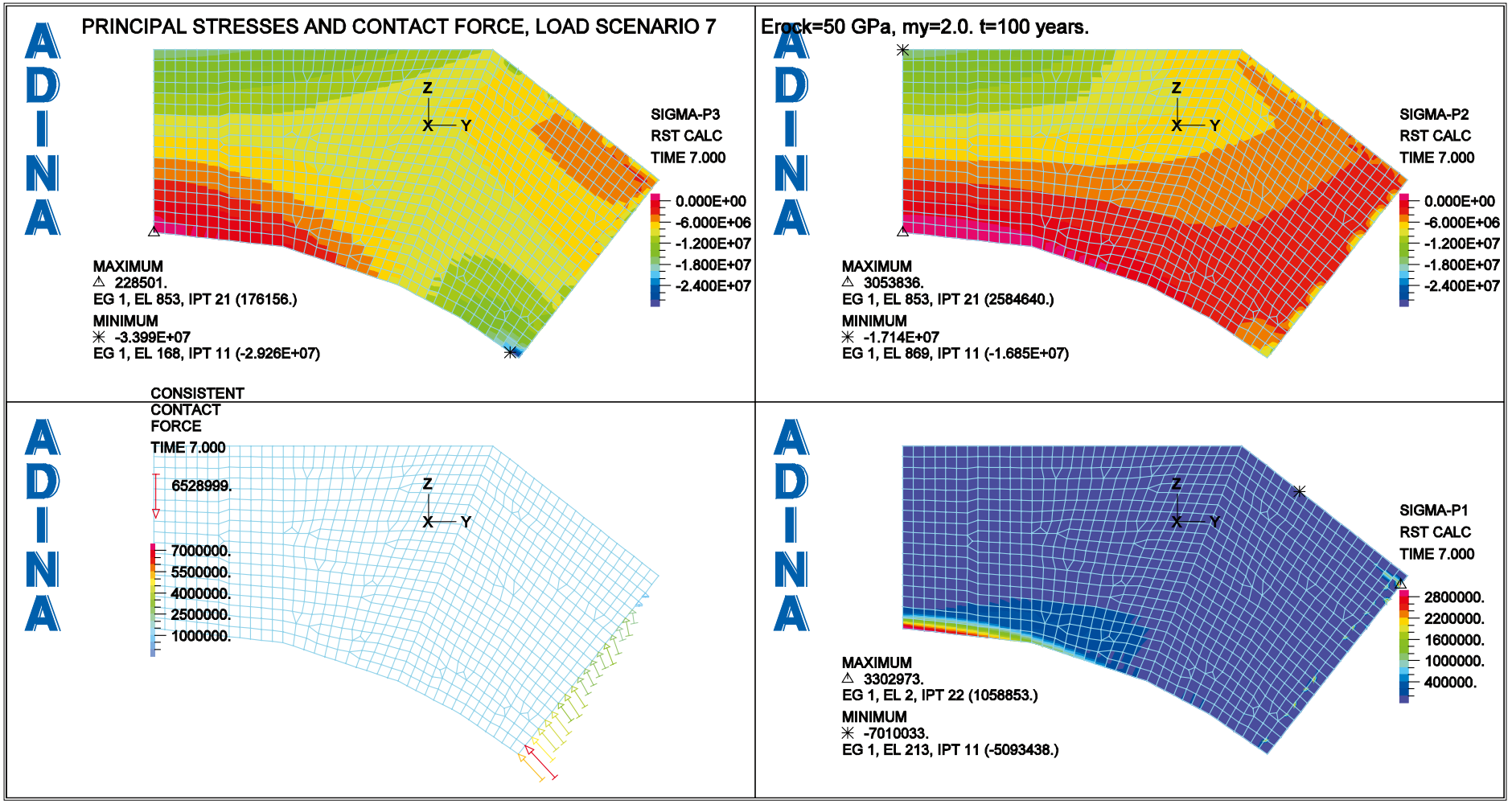
PRINCIPAL STRESSES AND CONTACT FORCE, LOAD SCENARIO 7
Erock=50 GPa, my=2.0. t=100 years.
ADINA
SIGMA-P3
RST CALC
TIME 7.000
0.000E+00
-6.000E+06
-1.200E+07
-1.800E+07
-2.400E+07
MAXIMUM
228501.
EG 1, EL 853, IPT 21 (176156.)
MINIMUM
-3.399E+07
EG 1, EL 168, IPT 11 (-2.926E+07)
SIGMA-P2
RST CALC
TIME 7.000
0.000E+00
-6.000E+06
-1.200E+07
-1.800E+07
-2.400E+07
MAXIMUM
3053836.
EG 1, EL 853, IPT 21 (2584640.)
MINIMUM
-1.714E+07
EG 1, EL 869, IPT 11 (-1.685E+07)
CONSISTENT
CONTACT
FORCE
TIME 7.000
6528999.
7000000.
5500000.
4000000.
2500000.
1000000.
SIGMA-P1
RST CALC
TIME 7.000
2800000.
2200000.
1600000.
1000000.
400000.
MAXIMUM
3302973.
EG 1, EL 2, IPT 22 (1058853.)
MINIMUM
-7010033.
EG 1, EL 213, IPT 11 (-5093438.)

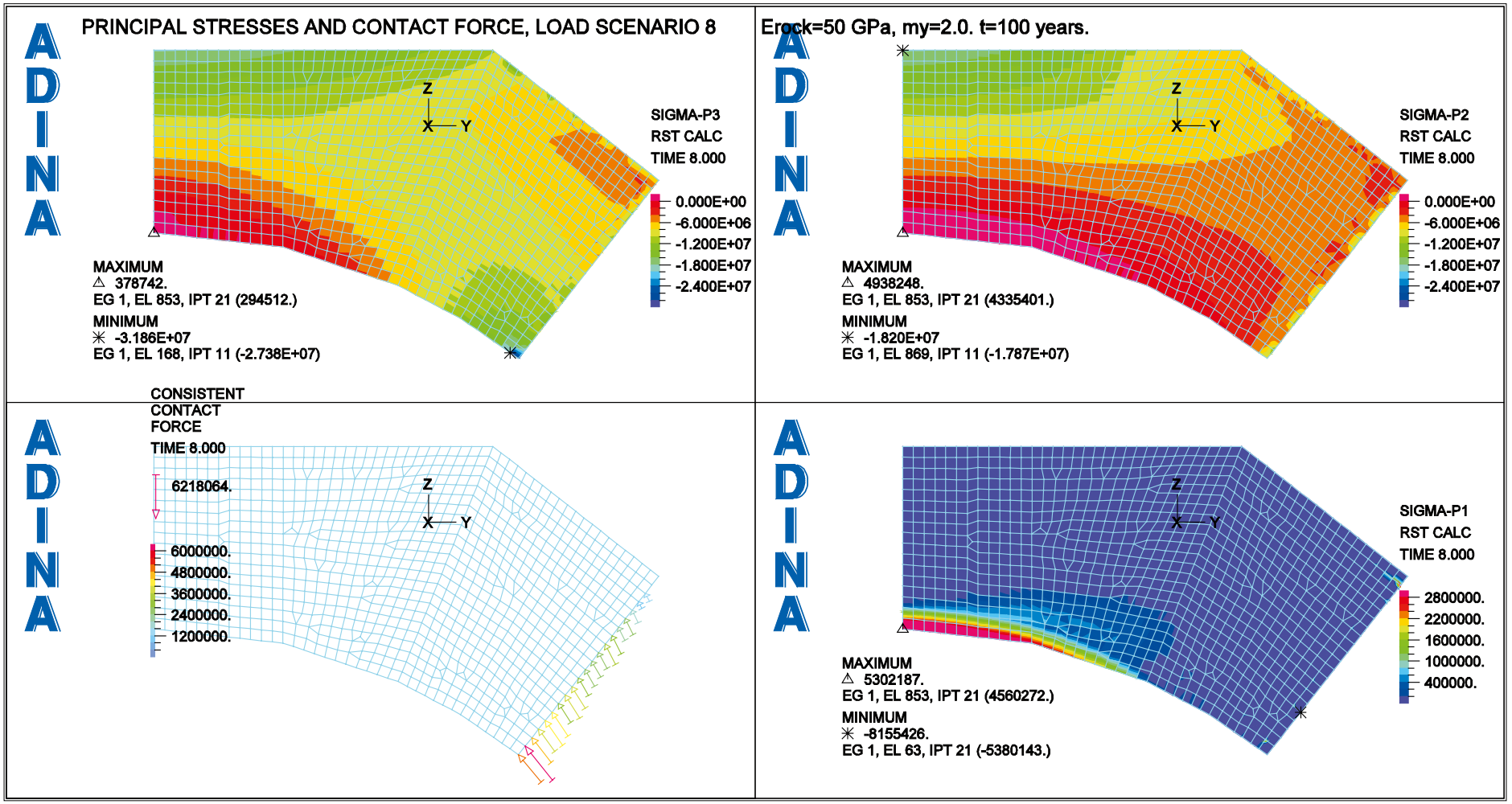
PRINCIPAL STRESSES AND CONTACT FORCE, LOAD SCENARIO 8
ADINA
Z
X
Y
SIGMA-P3
RST CALC
TIME 8.000
0.000E+00
-6.000E+06
-1.200E+07
-1.800E+07
-2.400E+07
MAXIMUM
△ 378742.
EG 1, EL 853, IPT 21 (294512.)
MINIMUM
✳ -3.186E+07
EG 1, EL 168, IPT 11 (-2.738E+07)
Erock=50 GPa, my=2.0. t=100 years.
ADINA
Z
X
Y
SIGMA-P2
RST CALC
TIME 8.000
0.000E+00
-6.000E+06
-1.200E+07
-1.800E+07
-2.400E+07
MAXIMUM
△ 4938248.
EG 1, EL 853, IPT 21 (4335401.)
MINIMUM
✳ -1.820E+07
EG 1, EL 869, IPT 11 (-1.787E+07)
ADINA
CONSISTENT
CONTACT
FORCE
TIME 8.000
6218064.
6000000.
4800000.
3600000.
2400000.
1200000.
Z
X
Y
ADINA
Z
X
Y
SIGMA-P1
RST CALC
TIME 8.000
2800000.
2200000.
1600000.
1000000.
400000.
MAXIMUM
△ 5302187.
EG 1, EL 853, IPT 21 (4560272.)
MINIMUM
✳ -8155426.
EG 1, EL 63, IPT 21 (-5380143.)

E.6 Stress plots, load combinations 1.5–8.5

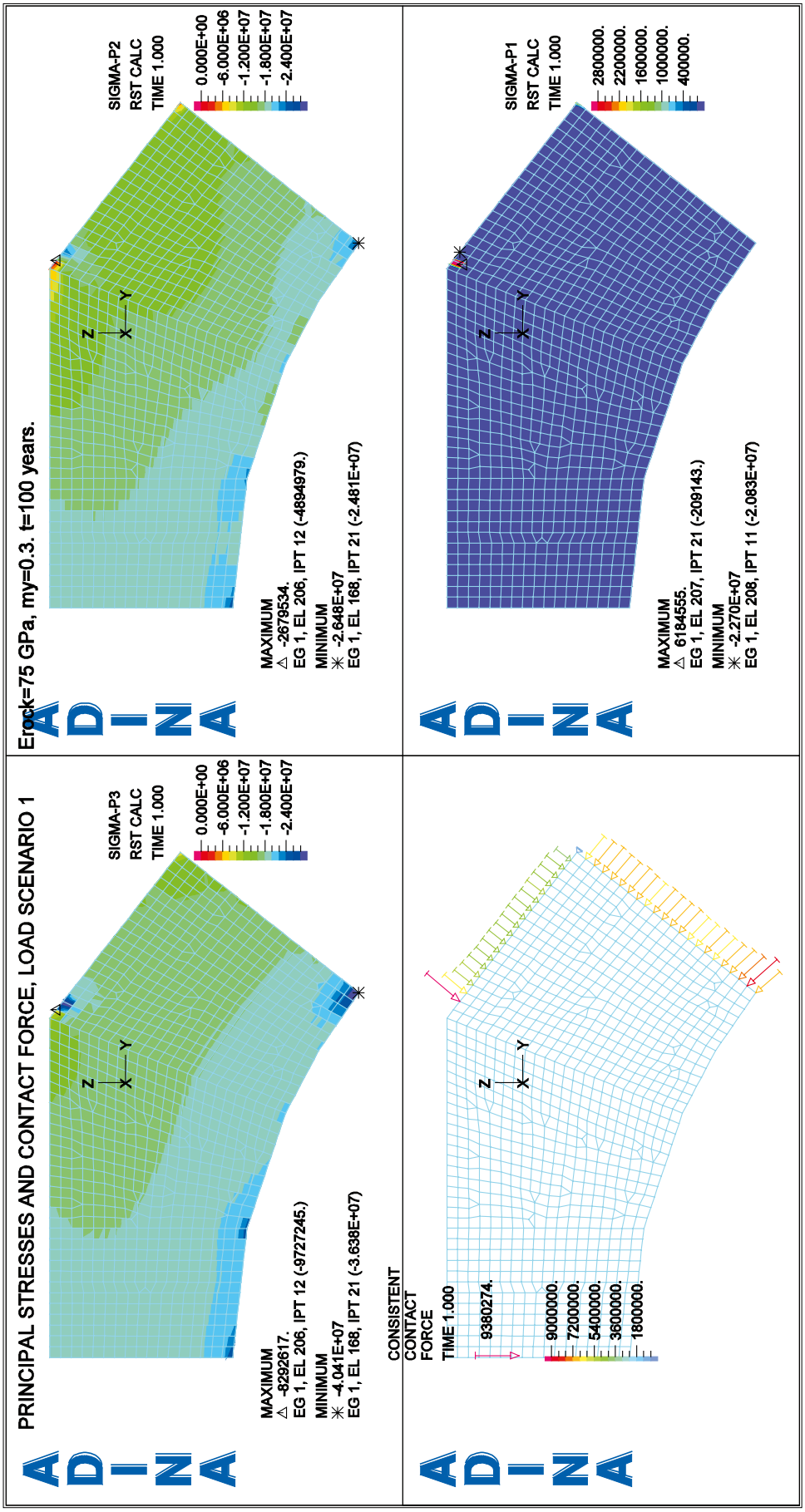

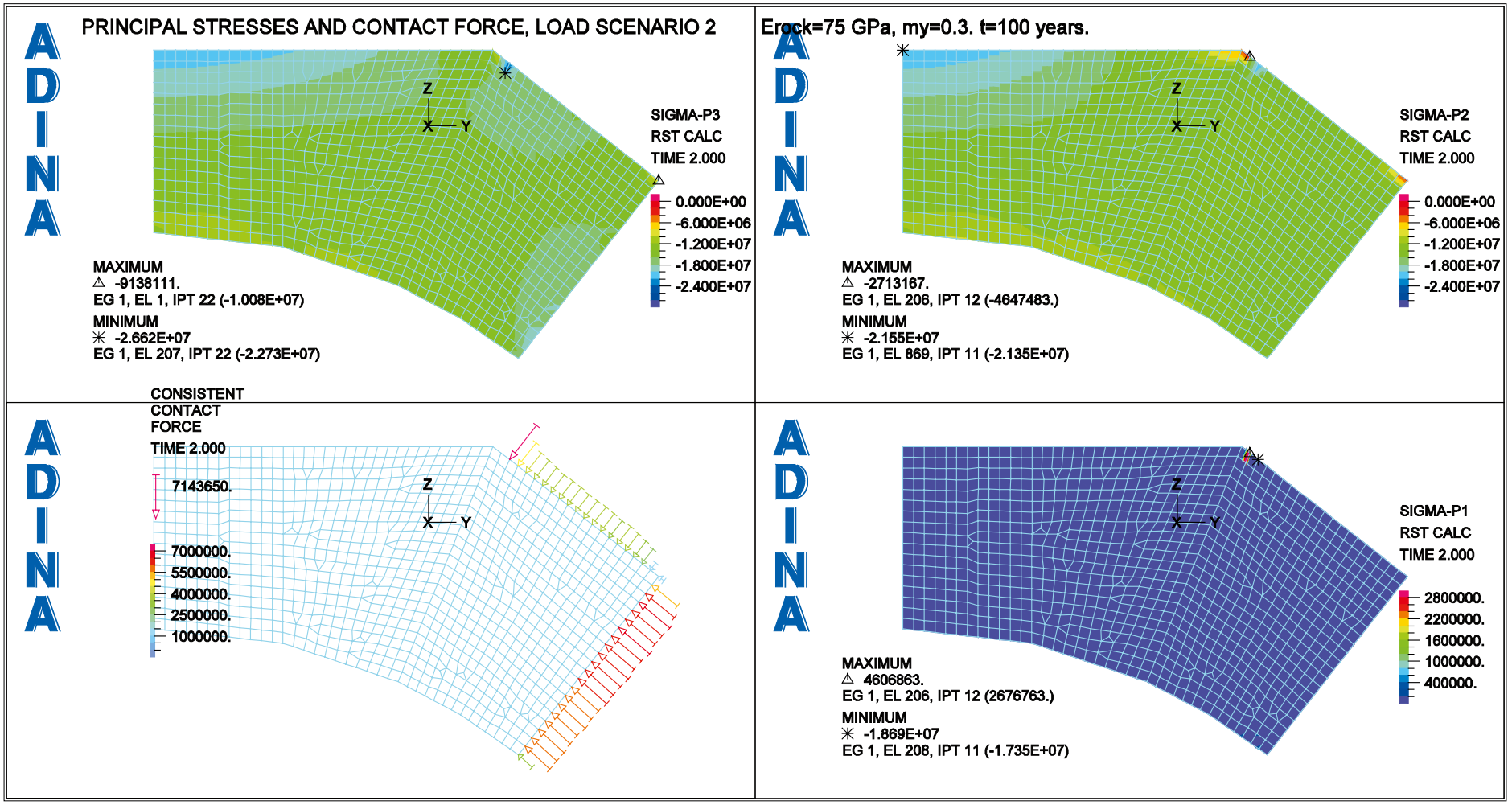
PRINCIPAL STRESSES AND CONTACT FORCE, LOAD SCENARIO 2
SIGMA-P3
RST CALC
TIME 2.000
0.000E+00
-6.000E+06
-1.200E+07
-1.800E+07
-2.400E+07
MAXIMUM
-9138111.
EG 1, EL 1, IPT 22 (-1.008E+07)
MINIMUM
-2.662E+07
EG 1, EL 207, IPT 22 (-2.273E+07)
Erock=75 GPa, my=0.3. t=100 years.
SIGMA-P2
RST CALC
TIME 2.000
0.000E+00
-6.000E+06
-1.200E+07
-1.800E+07
-2.400E+07
MAXIMUM
-2713167.
EG 1, EL 206, IPT 12 (-4647483.)
MINIMUM
-2.155E+07
EG 1, EL 869, IPT 11 (-2.135E+07)
CONSISTENT
CONTACT
FORCE
TIME 2.000
7143650.
7000000.
5500000.
4000000.
2500000.
1000000.
SIGMA-P1
RST CALC
TIME 2.000
2800000.
2200000.
1600000.
1000000.
400000.
MAXIMUM
4606863.
EG 1, EL 206, IPT 12 (2676763.)
MINIMUM
-1.869E+07
EG 1, EL 208, IPT 11 (-1.735E+07)

PRINCIPAL STRESSES AND CONTACT FORCE, LOAD SCENARIO 3

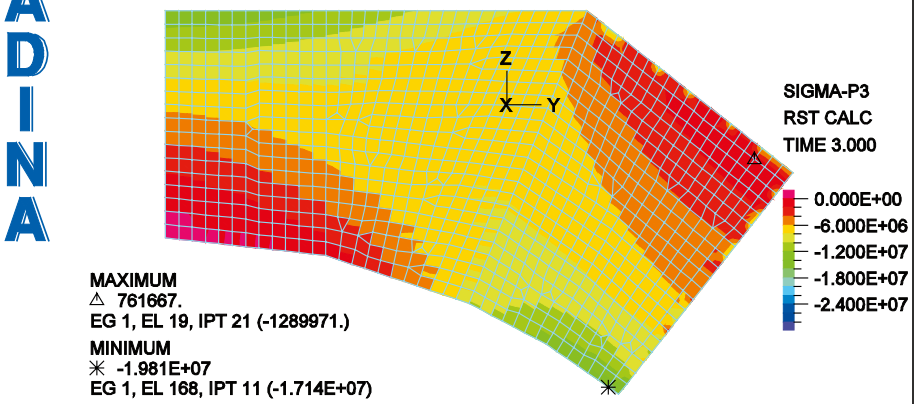

Erock=75 GPa, my=0.3. t=100 years.

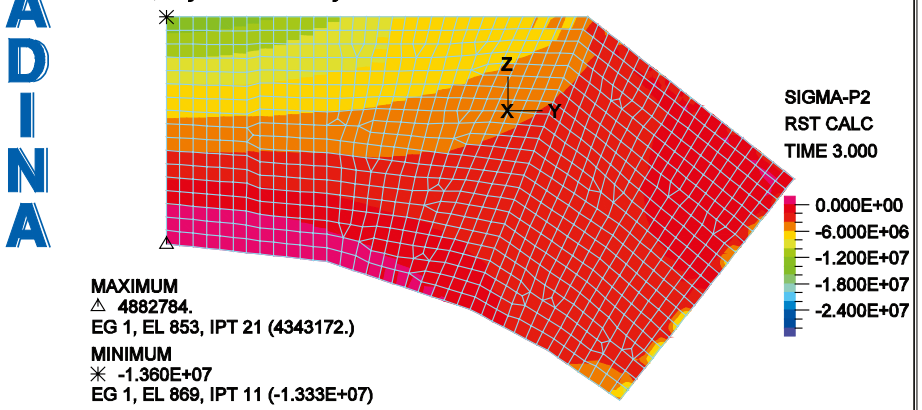

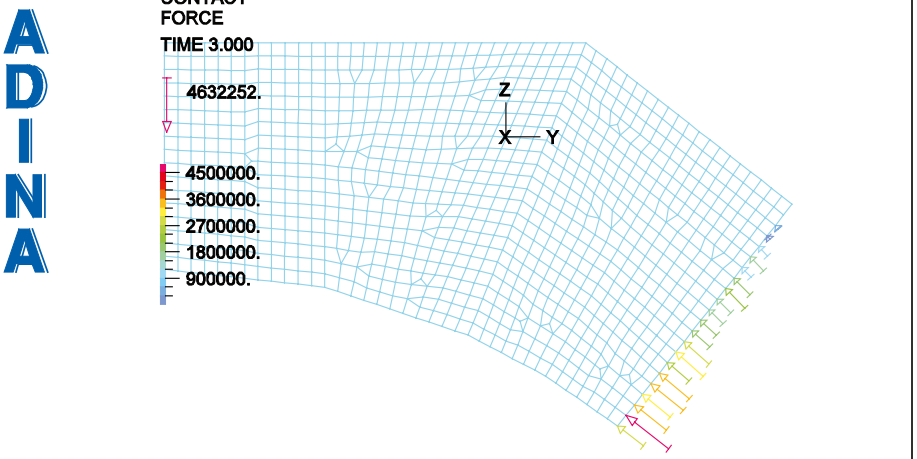

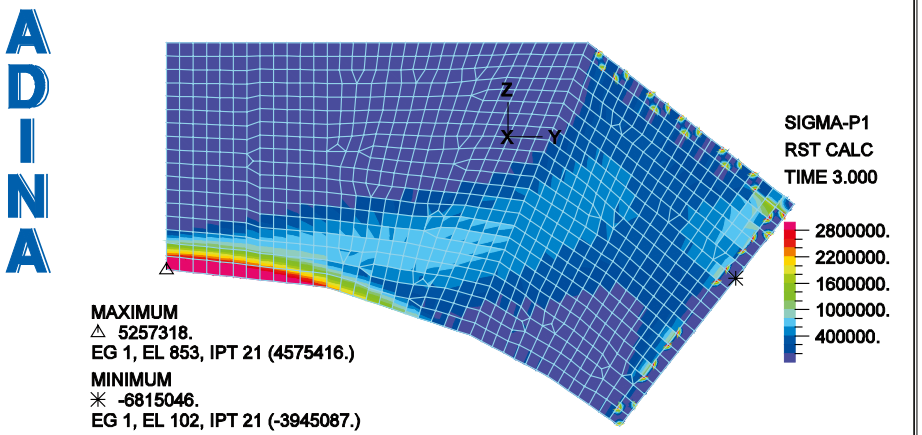

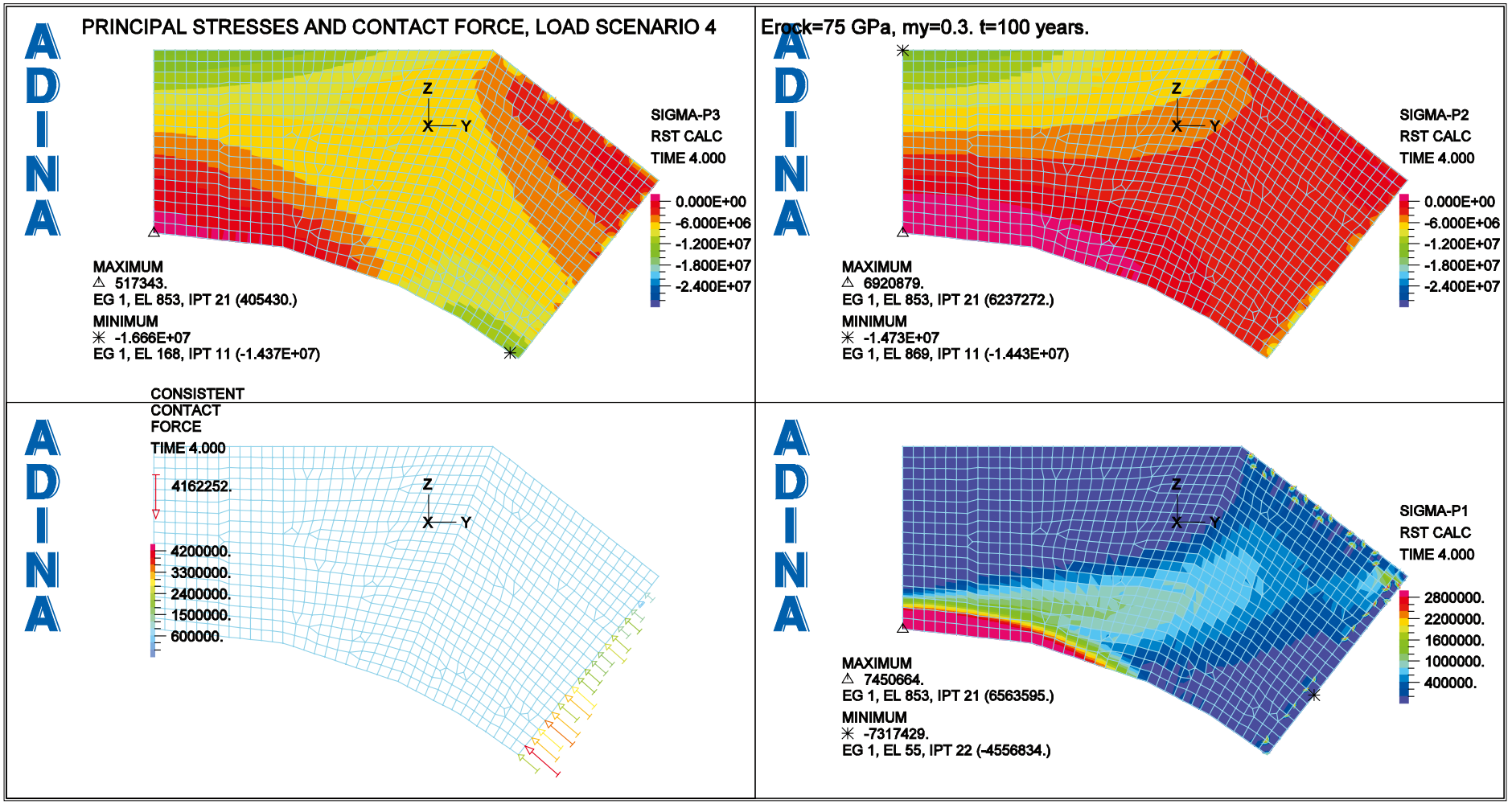
PRINCIPAL STRESSES AND CONTACT FORCE, LOAD SCENARIO 4
SIGMA-P3
RST CALC
TIME 4.000
0.000E+00
-6.000E+06
-1.200E+07
-1.800E+07
-2.400E+07
MAXIMUM
517343.
EG 1, EL 853, IPT 21 (405430.)
MINIMUM
-1.666E+07
EG 1, EL 168, IPT 11 (-1.437E+07)
Erock=75 GPa, my=0.3. t=100 years.
SIGMA-P2
RST CALC
TIME 4.000
0.000E+00
-6.000E+06
-1.200E+07
-1.800E+07
-2.400E+07
MAXIMUM
6920879.
EG 1, EL 853, IPT 21 (6237272.)
MINIMUM
-1.473E+07
EG 1, EL 869, IPT 11 (-1.443E+07)
CONSISTENT
CONTACT
FORCE
TIME 4.000
4162252.
4200000.
3300000.
2400000.
1500000.
600000.
SIGMA-P1
RST CALC
TIME 4.000
2800000.
2200000.
1600000.
1000000.
400000.
MAXIMUM
7450664.
EG 1, EL 853, IPT 21 (6563595.)
MINIMUM
-7317429.
EG 1, EL 55, IPT 22 (-4556834.)

PRINCIPAL STRESSES AND CONTACT FORCE, LOAD SCENARIO 5

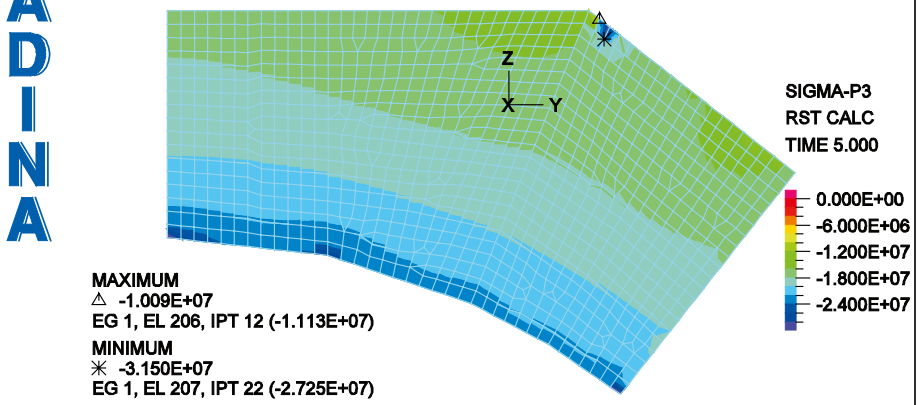

Erock=75 GPa, my=0.3. t=100 years.

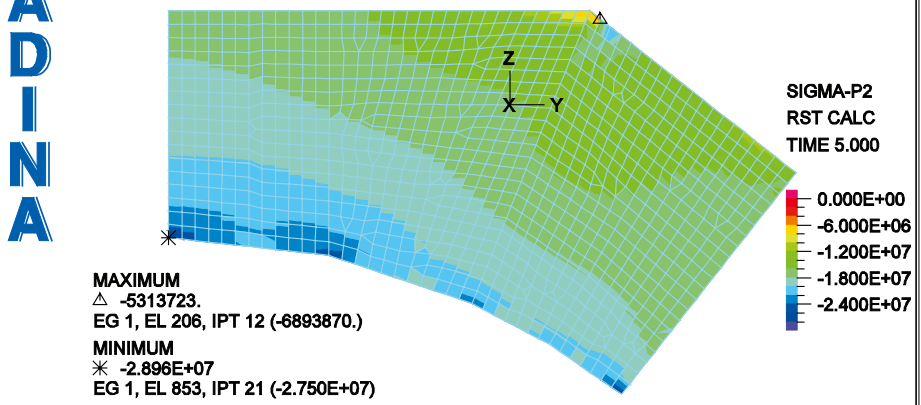

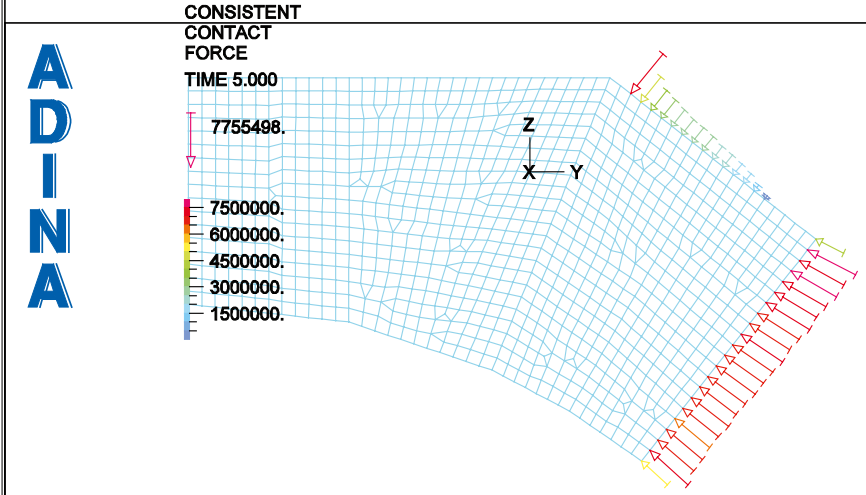

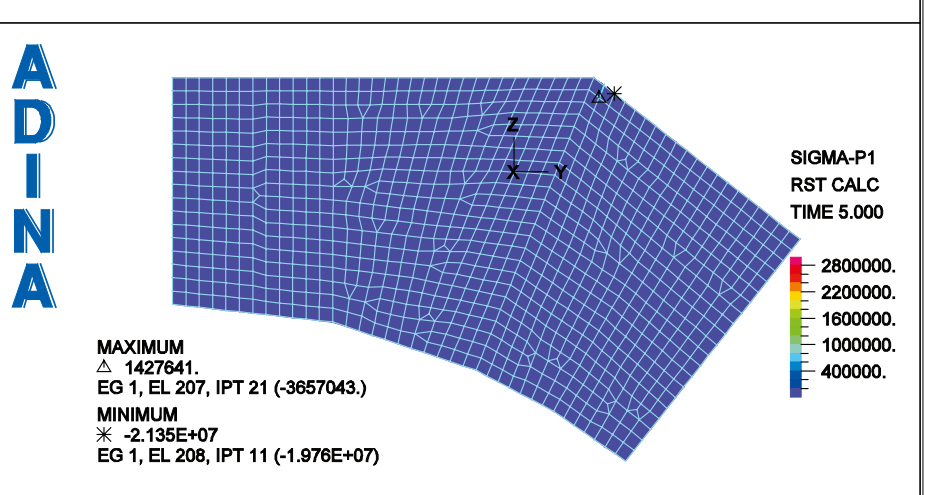

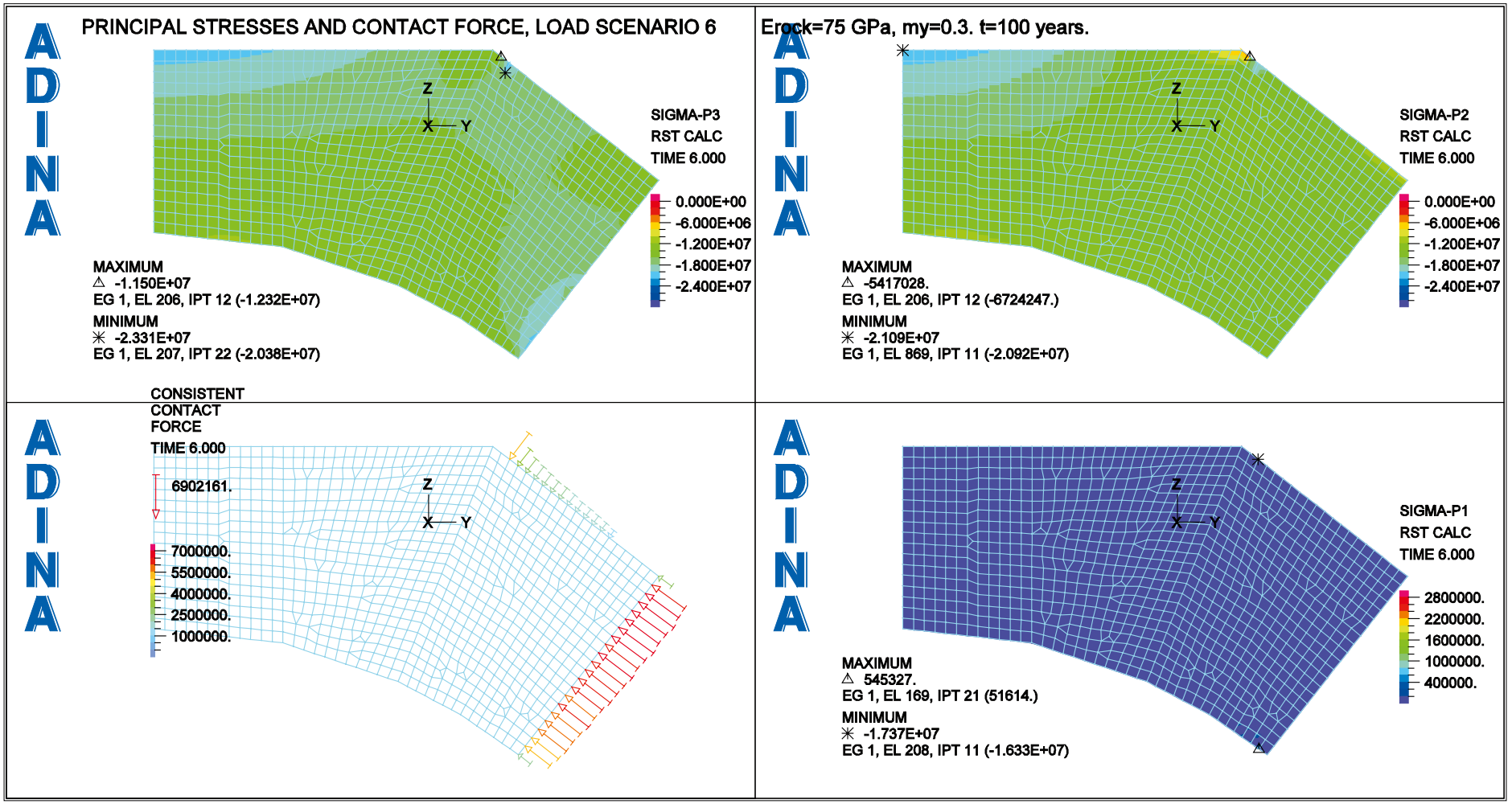
PRINCIPAL STRESSES AND CONTACT FORCE, LOAD SCENARIO 6
SIGMA-P3
RST CALC
TIME 6.000
0.000E+00
-6.000E+06
-1.200E+07
-1.800E+07
-2.400E+07
MAXIMUM
-1.150E+07
EG 1, EL 206, IPT 12 (-1.232E+07)
MINIMUM
-2.331E+07
EG 1, EL 207, IPT 22 (-2.038E+07)
Erock=75 GPa, my=0.3. t=100 years.
SIGMA-P2
RST CALC
TIME 6.000
0.000E+00
-6.000E+06
-1.200E+07
-1.800E+07
-2.400E+07
MAXIMUM
-5417028.
EG 1, EL 206, IPT 12 (-6724247.)
MINIMUM
-2.109E+07
EG 1, EL 869, IPT 11 (-2.092E+07)
CONSISTENT
CONTACT
FORCE
TIME 6.000
6902161.
7000000.
5500000.
4000000.
2500000.
1000000.
SIGMA-P1
RST CALC
TIME 6.000
2800000.
2200000.
1600000.
1000000.
400000.
MAXIMUM
545327.
EG 1, EL 169, IPT 21 (51614.)
MINIMUM
-1.737E+07
EG 1, EL 208, IPT 11 (-1.633E+07)

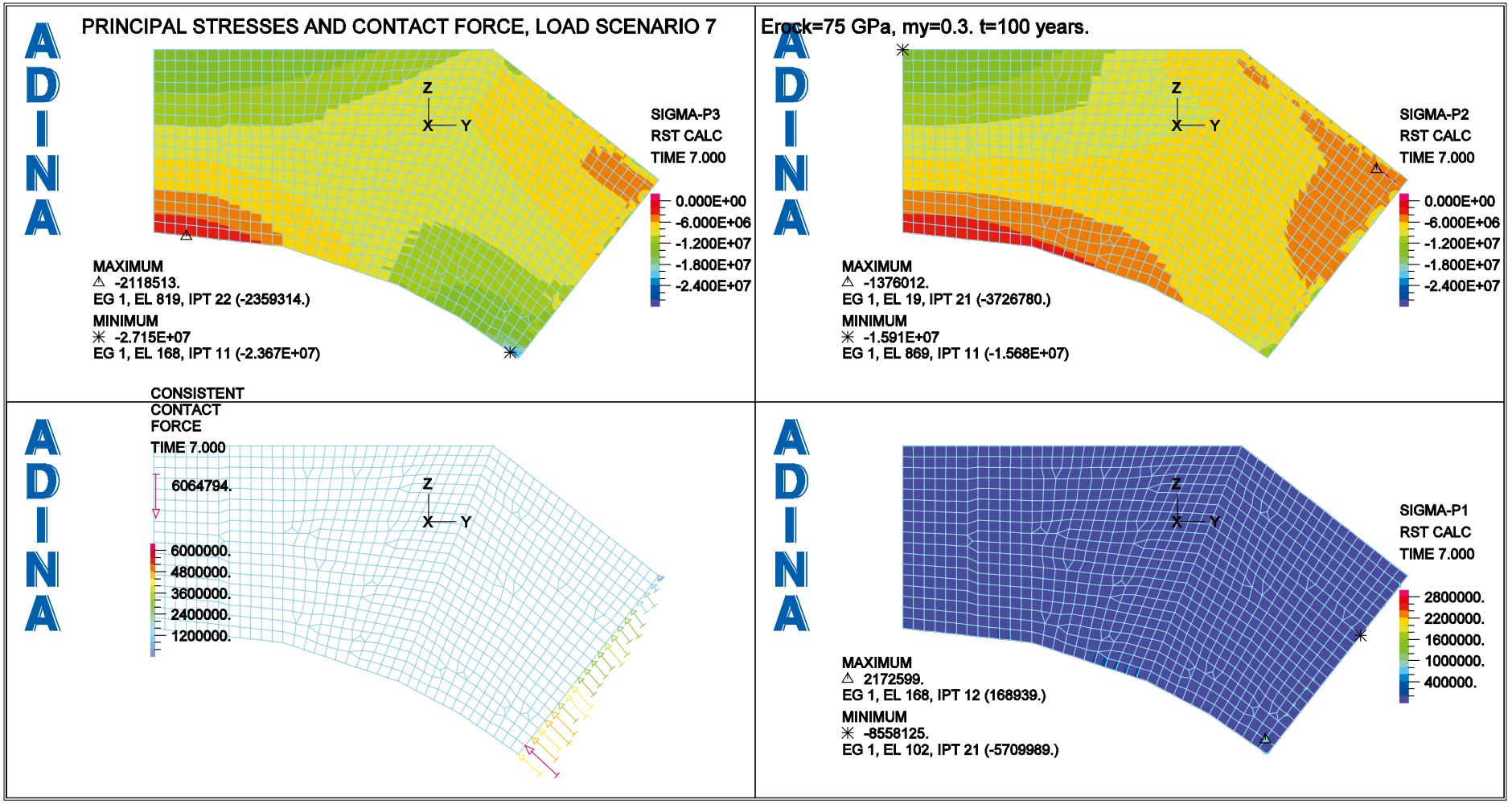
PRINCIPAL STRESSES AND CONTACT FORCE, LOAD SCENARIO 7
Erock=75 GPa, my=0.3. t=100 years.
ADINA
SIGMA-P3
RST CALC
TIME 7.000
0.000E+00
-6.000E+06
-1.200E+07
-1.800E+07
-2.400E+07
MAXIMUM
-2118513.
EG 1, EL 819, IPT 22 (-2359314.)
MINIMUM
-2.715E+07
EG 1, EL 168, IPT 11 (-2.367E+07)
SIGMA-P2
RST CALC
TIME 7.000
MAXIMUM
-1376012.
EG 1, EL 19, IPT 21 (-3726780.)
MINIMUM
-1.591E+07
EG 1, EL 869, IPT 11 (-1.568E+07)
CONSISTENT
CONTACT
FORCE
TIME 7.000
6064794.
6000000.
4800000.
3600000.
2400000.
1200000.
SIGMA-P1
RST CALC
TIME 7.000
2800000.
2200000.
1600000.
1000000.
400000.
MAXIMUM
2172599.
EG 1, EL 168, IPT 12 (168939.)
MINIMUM
-8558125.
EG 1, EL 102, IPT 21 (-5709989.)

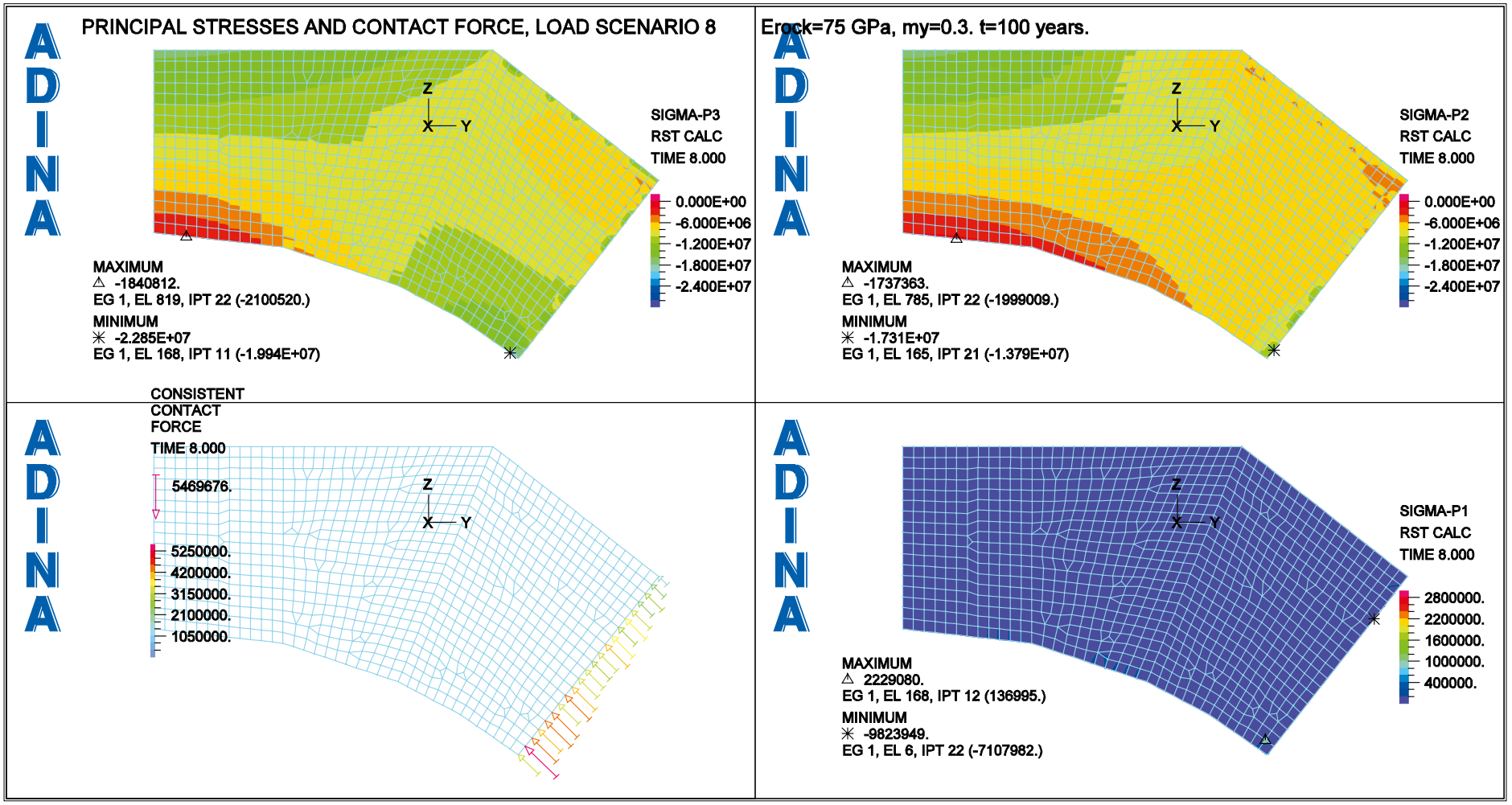
PRINCIPAL STRESSES AND CONTACT FORCE, LOAD SCENARIO 8
ADINA
Z
X
Y
SIGMA-P3
RST CALC
TIME 8.000
0.000E+00
-6.000E+06
-1.200E+07
-1.800E+07
-2.400E+07
MAXIMUM
-1840812.
EG 1, EL 819, IPT 22 (-2100520.)
MINIMUM
-2.285E+07
EG 1, EL 168, IPT 11 (-1.994E+07)
Erock=75 GPa, my=0.3. t=100 years.
ADINA
Z
X
Y
SIGMA-P2
RST CALC
TIME 8.000
0.000E+00
-6.000E+06
-1.200E+07
-1.800E+07
-2.400E+07
MAXIMUM
-1737363.
EG 1, EL 785, IPT 22 (-1999009.)
MINIMUM
-1.731E+07
EG 1, EL 165, IPT 21 (-1.379E+07)
ADINA
CONSISTENT
CONTACT
FORCE
TIME 8.000
5469676.
5250000.
4200000.
3150000.
2100000.
1050000.
Z
X
Y
ADINA
Z
X
Y
SIGMA-P1
RST CALC
TIME 8.000
2800000.
2200000.
1600000.
1000000.
400000.
MAXIMUM
2229080.
EG 1, EL 168, IPT 12 (136995.)
MINIMUM
-9823949.
EG 1, EL 6, IPT 22 (-7107982.)

E.7 Stress plots, load combinations 1.6–8.6

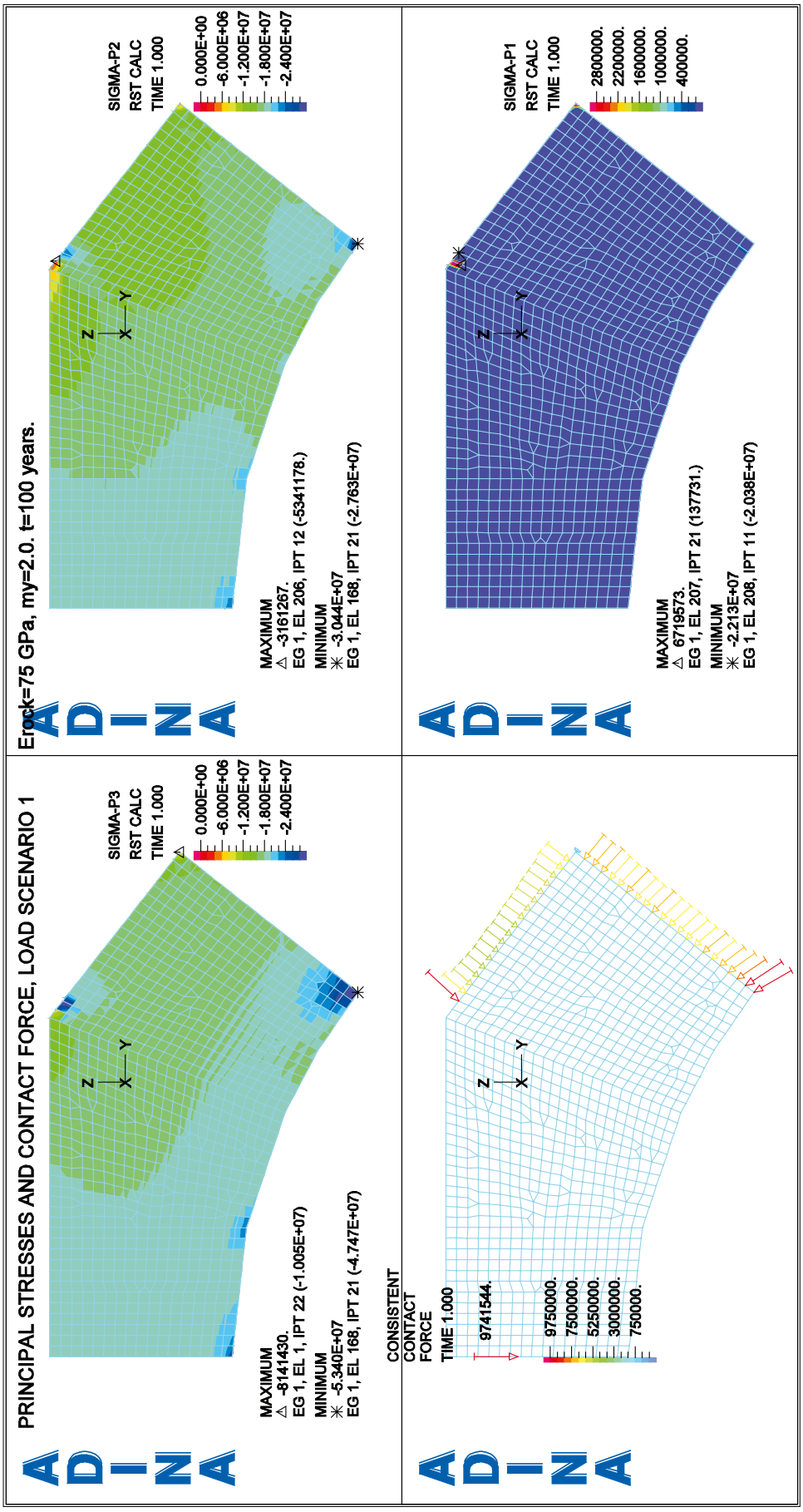

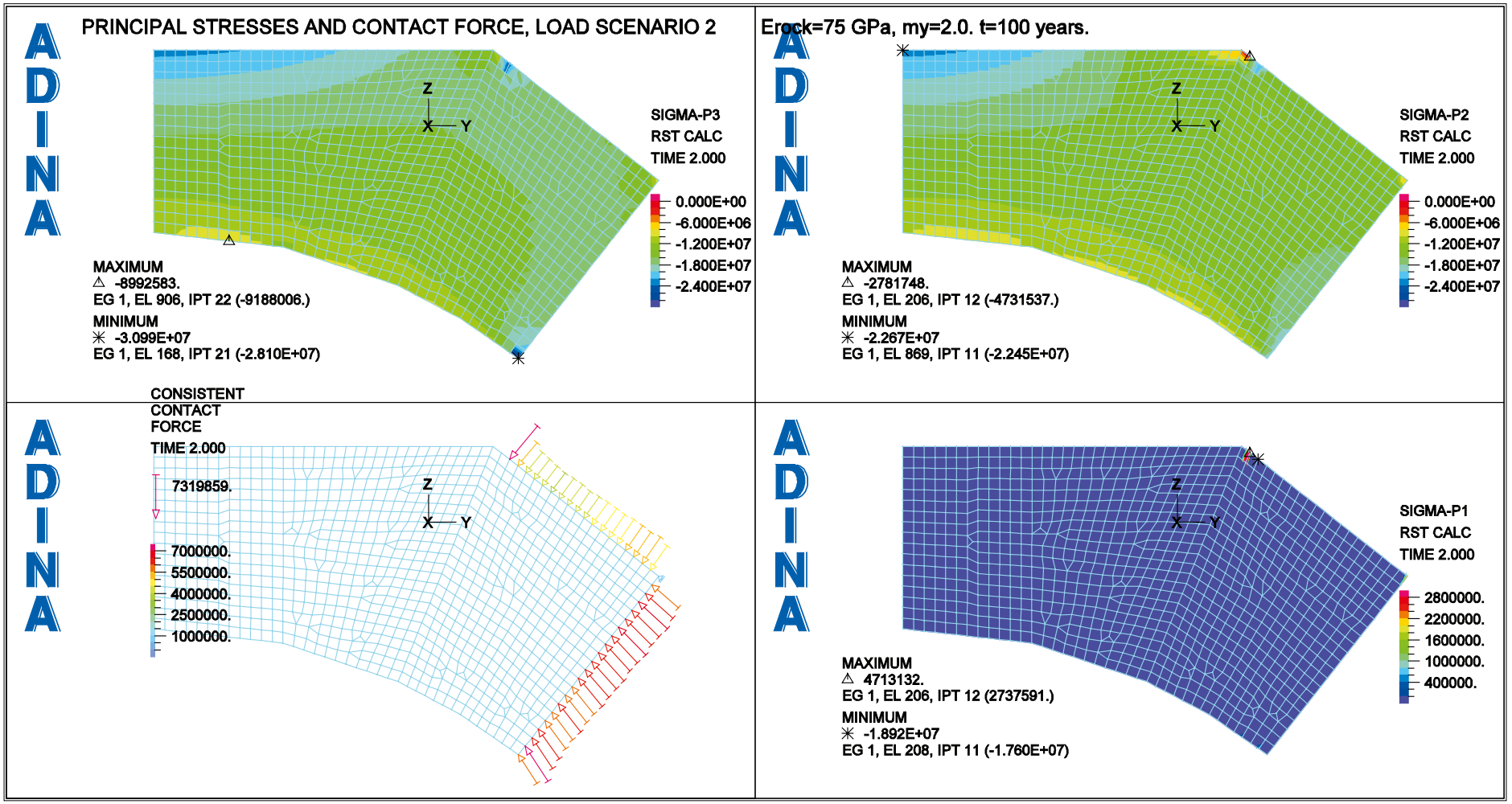
PRINCIPAL STRESSES AND CONTACT FORCE, LOAD SCENARIO 2
SIGMA-P3
RST CALC
TIME 2.000
0.000E+00
-6.000E+06
-1.200E+07
-1.800E+07
-2.400E+07
MAXIMUM
-8992583.
EG 1, EL 906, IPT 22 (-9188006.)
MINIMUM
-3.099E+07
EG 1, EL 168, IPT 21 (-2.810E+07)
Erock=75 GPa, my=2.0. t=100 years.
SIGMA-P2
RST CALC
TIME 2.000
0.000E+00
-6.000E+06
-1.200E+07
-1.800E+07
-2.400E+07
MAXIMUM
-2781748.
EG 1, EL 206, IPT 12 (-4731537.)
MINIMUM
-2.267E+07
EG 1, EL 869, IPT 11 (-2.245E+07)
CONSISTENT
CONTACT
FORCE
TIME 2.000
7319859.
7000000.
5500000.
4000000.
2500000.
1000000.
SIGMA-P1
RST CALC
TIME 2.000
2800000.
2200000.
1600000.
1000000.
400000.
MAXIMUM
4713132.
EG 1, EL 206, IPT 12 (2737591.)
MINIMUM
-1.892E+07
EG 1, EL 208, IPT 11 (-1.760E+07)

PRINCIPAL STRESSES AND CONTACT FORCE, LOAD SCENARIO 3

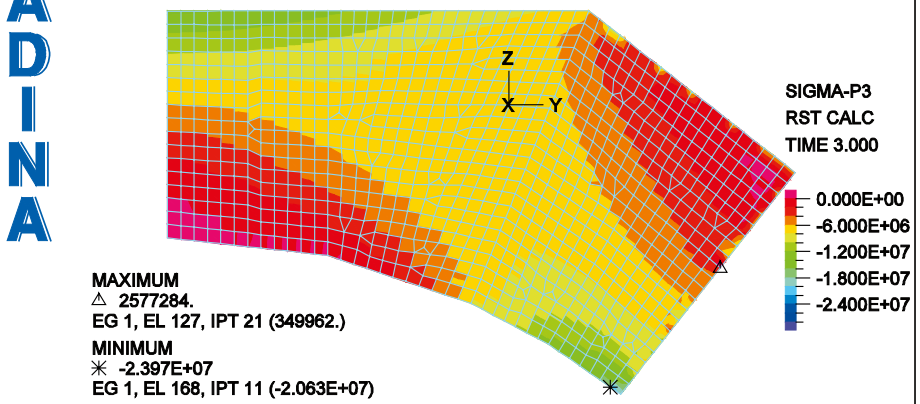

Erock=75 GPa, my=2.0. t=100 years.

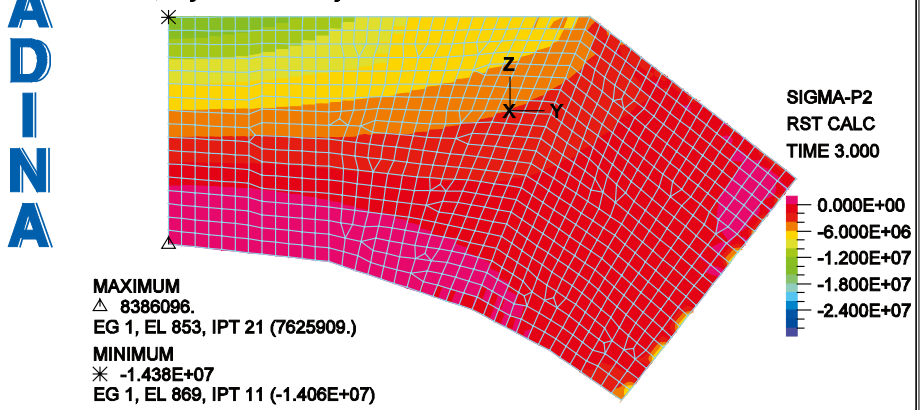

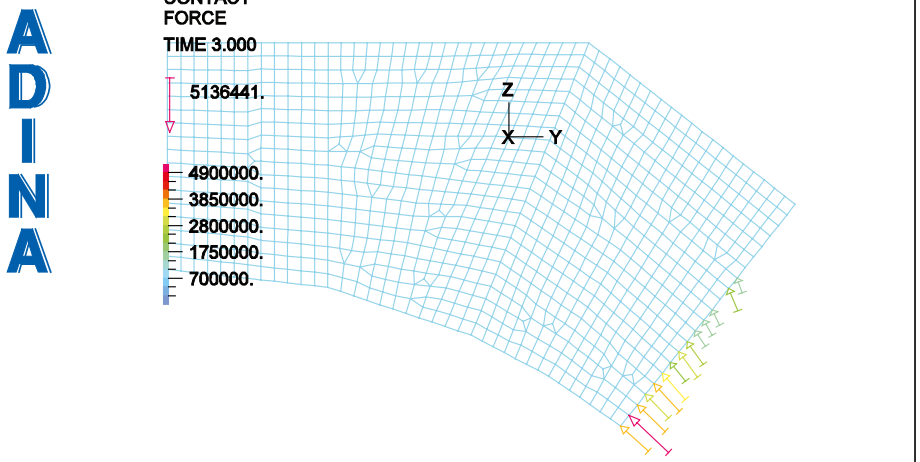

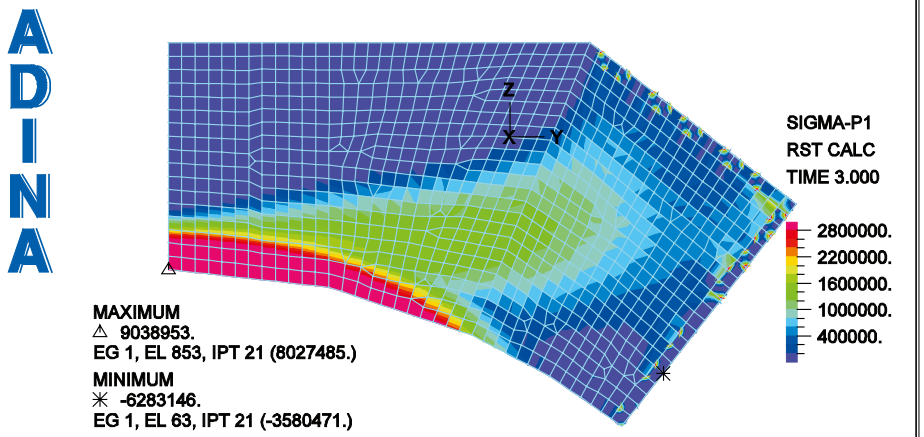

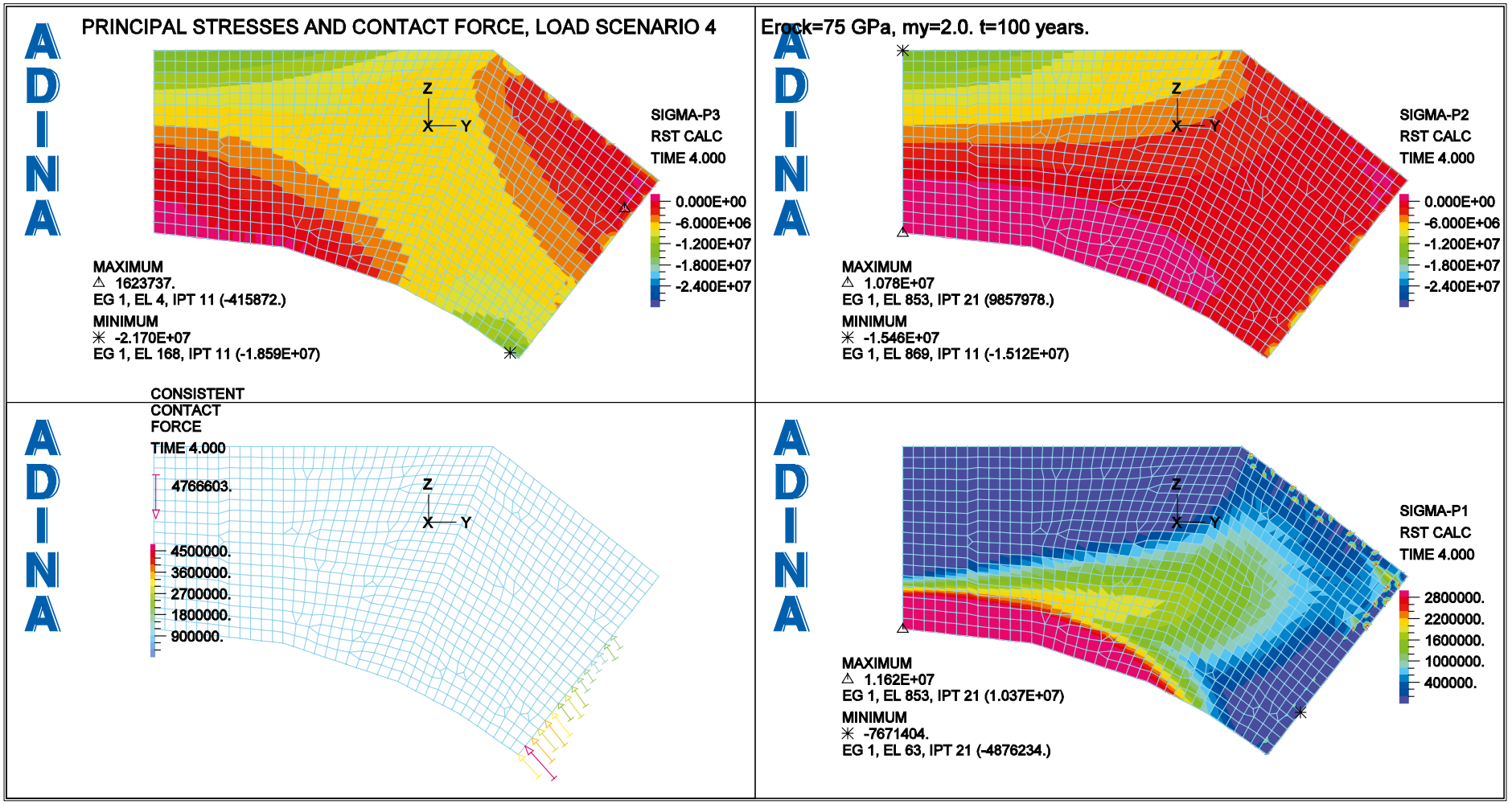
PRINCIPAL STRESSES AND CONTACT FORCE, LOAD SCENARIO 4
SIGMA-P3
RST CALC
TIME 4.000
0.000E+00
-6.000E+06
-1.200E+07
-1.800E+07
-2.400E+07
MAXIMUM
1623737.
EG 1, EL 4, IPT 11 (-415872.)
MINIMUM
-2.170E+07
EG 1, EL 168, IPT 11 (-1.859E+07)
Erock=75 GPa, my=2.0. t=100 years.
SIGMA-P2
RST CALC
TIME 4.000
0.000E+00
-6.000E+06
-1.200E+07
-1.800E+07
-2.400E+07
MAXIMUM
1.078E+07
EG 1, EL 853, IPT 21 (9857978.)
MINIMUM
-1.546E+07
EG 1, EL 869, IPT 11 (-1.512E+07)
CONSISTENT
CONTACT
FORCE
TIME 4.000
4766603.
4500000.
3600000.
2700000.
1800000.
900000.
SIGMA-P1
RST CALC
TIME 4.000
2800000.
2200000.
1600000.
1000000.
400000.
MAXIMUM
1.162E+07
EG 1, EL 853, IPT 21 (1.037E+07)
MINIMUM
-7671404.
EG 1, EL 63, IPT 21 (-4876234.)

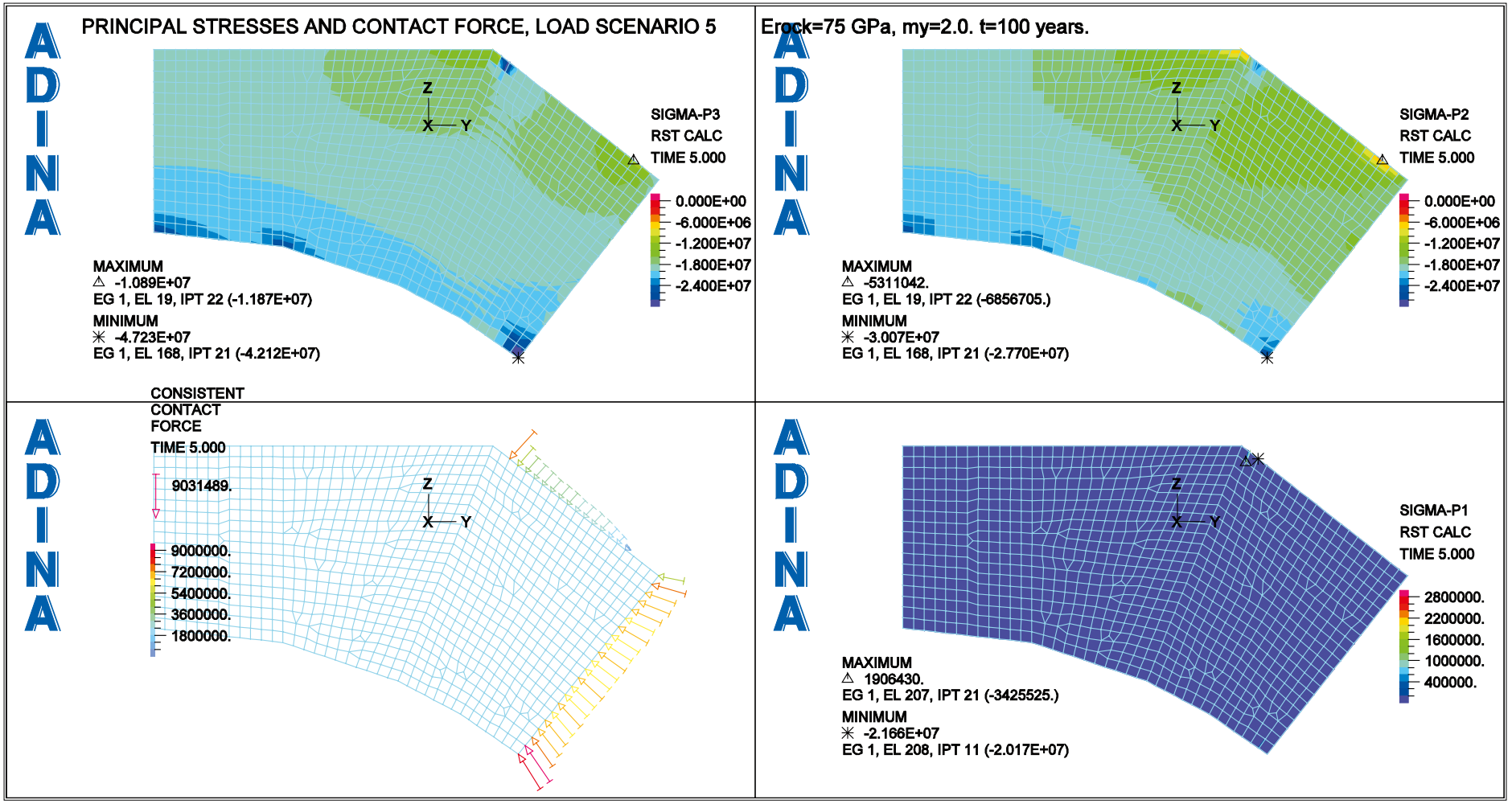
PRINCIPAL STRESSES AND CONTACT FORCE, LOAD SCENARIO 5
ADINA
Z
X
Y
SIGMA-P3
RST CALC
TIME 5.000
0.000E+00
-6.000E+06
-1.200E+07
-1.800E+07
-2.400E+07
MAXIMUM
-1.089E+07
EG 1, EL 19, IPT 22 (-1.187E+07)
MINIMUM
-4.723E+07
EG 1, EL 168, IPT 21 (-4.212E+07)
Erock=75 GPa, my=2.0. t=100 years.
SIGMA-P2
RST CALC
TIME 5.000
0.000E+00
-6.000E+06
-1.200E+07
-1.800E+07
-2.400E+07
MAXIMUM
-5311042.
EG 1, EL 19, IPT 22 (-6856705.)
MINIMUM
-3.007E+07
EG 1, EL 168, IPT 21 (-2.770E+07)
CONSISTENT
CONTACT
FORCE
TIME 5.000
9031489.
9000000.
7200000.
5400000.
3600000.
1800000.
SIGMA-P1
RST CALC
TIME 5.000
2800000.
2200000.
1600000.
1000000.
400000.
MAXIMUM
1906430.
EG 1, EL 207, IPT 21 (-3425525.)
MINIMUM
-2.166E+07
EG 1, EL 208, IPT 11 (-2.017E+07)

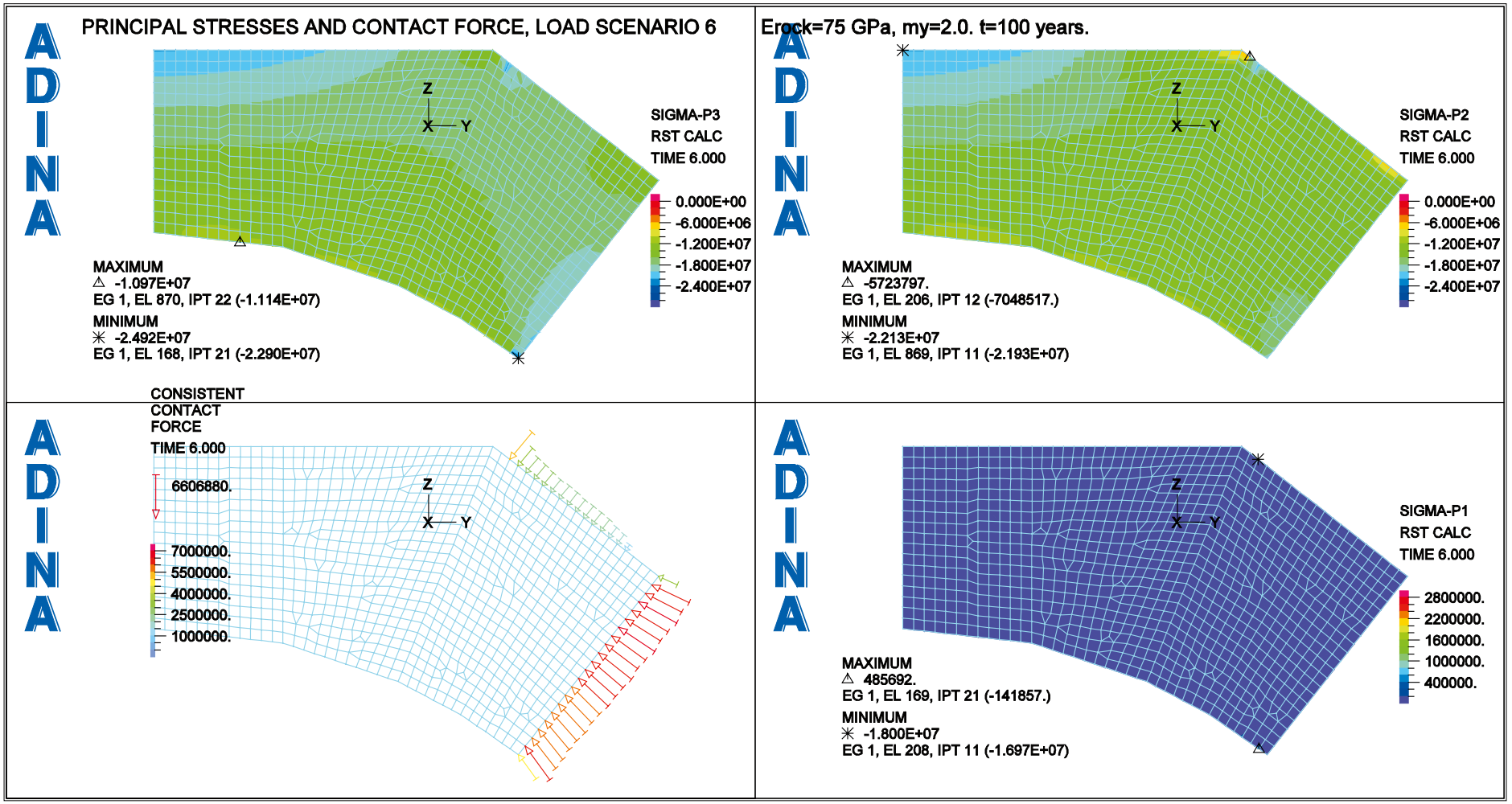
PRINCIPAL STRESSES AND CONTACT FORCE, LOAD SCENARIO 6
SIGMA-P3
RST CALC
TIME 6.000
0.000E+00
-6.000E+06
-1.200E+07
-1.800E+07
-2.400E+07
MAXIMUM
-1.097E+07
EG 1, EL 870, IPT 22 (-1.114E+07)
MINIMUM
-2.492E+07
EG 1, EL 168, IPT 21 (-2.290E+07)
Erock=75 GPa, my=2.0. t=100 years.
SIGMA-P2
RST CALC
TIME 6.000
0.000E+00
-6.000E+06
-1.200E+07
-1.800E+07
-2.400E+07
MAXIMUM
-5723797.
EG 1, EL 206, IPT 12 (-7048517.)
MINIMUM
-2.213E+07
EG 1, EL 869, IPT 11 (-2.193E+07)
CONSISTENT
CONTACT
FORCE
TIME 6.000
6606880.
7000000.
5500000.
4000000.
2500000.
1000000.
SIGMA-P1
RST CALC
TIME 6.000
2800000.
2200000.
1600000.
1000000.
400000.
MAXIMUM
485692.
EG 1, EL 169, IPT 21 (-141857.)
MINIMUM
-1.800E+07
EG 1, EL 208, IPT 11 (-1.697E+07)

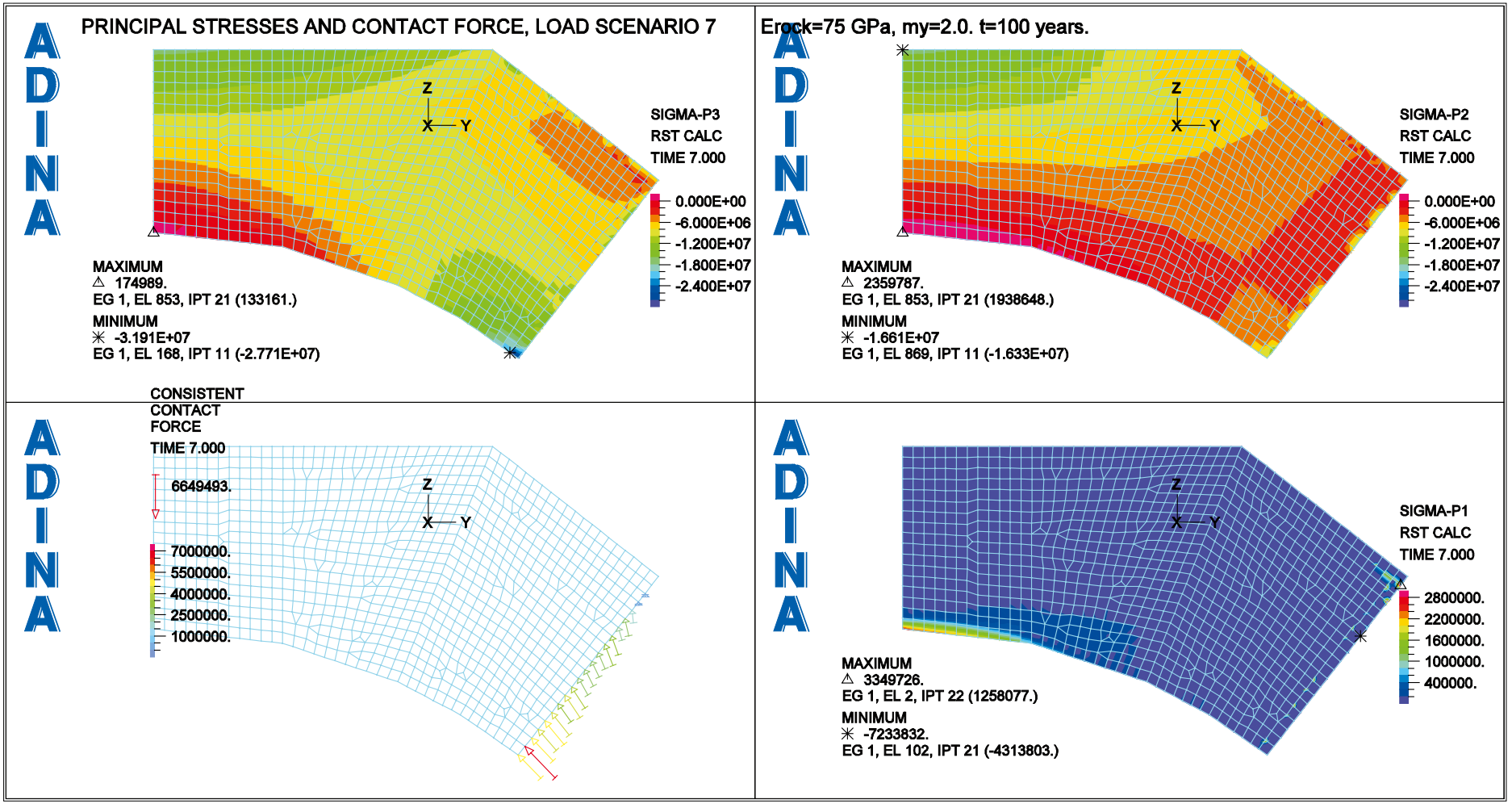
PRINCIPAL STRESSES AND CONTACT FORCE, LOAD SCENARIO 7
ADINA
Z
X
Y
SIGMA-P3
RST CALC
TIME 7.000
0.000E+00
-6.000E+06
-1.200E+07
-1.800E+07
-2.400E+07
MAXIMUM
△ 174989.
EG 1, EL 853, IPT 21 (133161.)
MINIMUM
✳ -3.191E+07
EG 1, EL 168, IPT 11 (-2.771E+07)
Erock=75 GPa, my=2.0. t=100 years.
ADINA
Z
X
Y
SIGMA-P2
RST CALC
TIME 7.000
0.000E+00
-6.000E+06
-1.200E+07
-1.800E+07
-2.400E+07
MAXIMUM
△ 2359787.
EG 1, EL 853, IPT 21 (1938648.)
MINIMUM
✳ -1.661E+07
EG 1, EL 869, IPT 11 (-1.633E+07)
ADINA
CONSISTENT
CONTACT
FORCE
TIME 7.000
6649493.
7000000.
5500000.
4000000.
2500000.
1000000.
Z
X
Y
ADINA
Z
X
Y
SIGMA-P1
RST CALC
TIME 7.000
2800000.
2200000.
1600000.
1000000.
400000.
MAXIMUM
△ 3349726.
EG 1, EL 2, IPT 22 (1258077.)
MINIMUM
✳ -7233832.
EG 1, EL 102, IPT 21 (-4313803.)

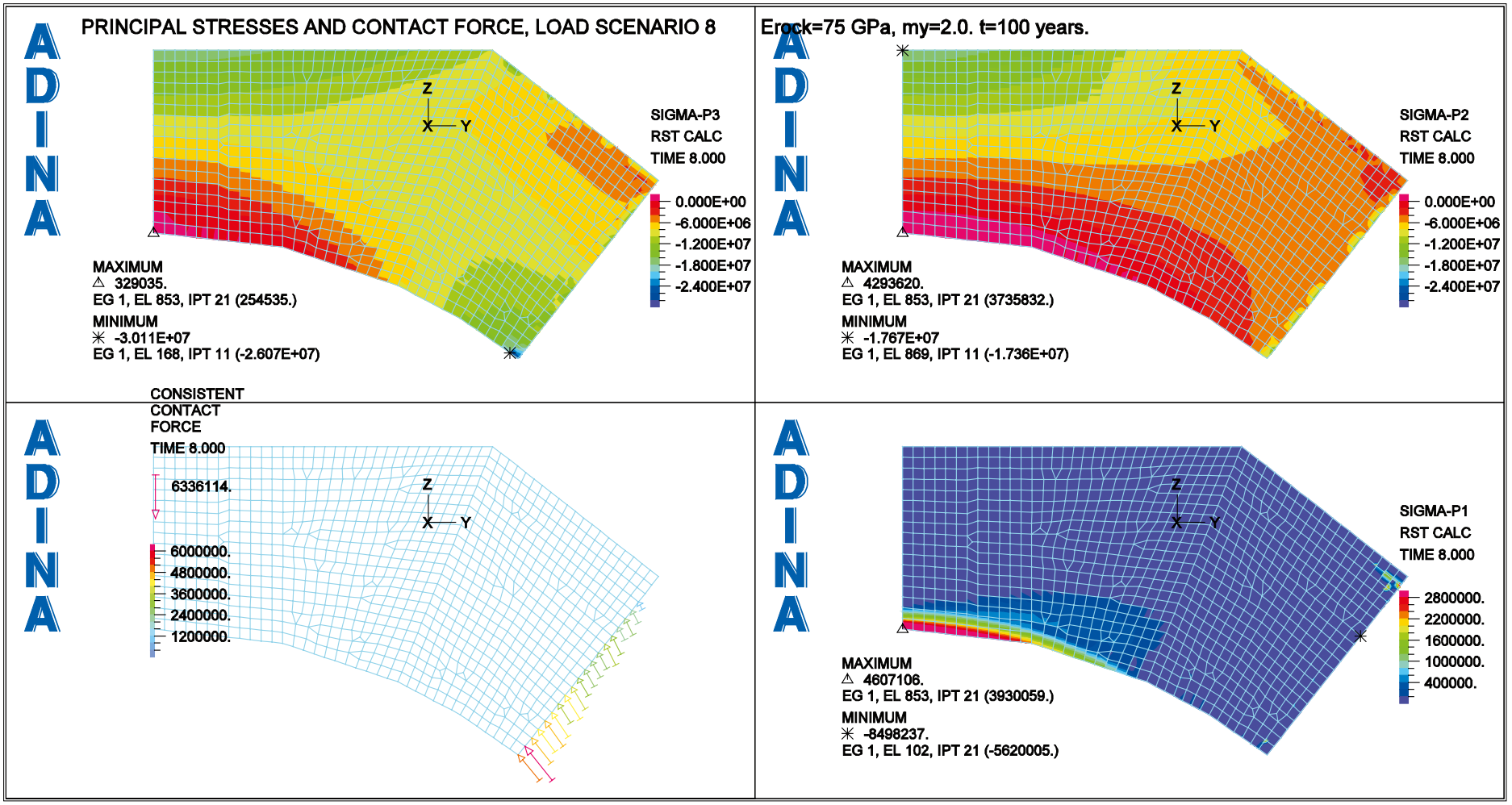
PRINCIPAL STRESSES AND CONTACT FORCE, LOAD SCENARIO 8
ADINA
Z
X
Y
SIGMA-P3
RST CALC
TIME 8.000
0.000E+00
-6.000E+06
-1.200E+07
-1.800E+07
-2.400E+07
MAXIMUM
329035.
EG 1, EL 853, IPT 21 (254535.)
MINIMUM
-3.011E+07
EG 1, EL 168, IPT 11 (-2.607E+07)
Erock=75 GPa, my=2.0. t=100 years.
ADINA
Z
X
Y
SIGMA-P2
RST CALC
TIME 8.000
0.000E+00
-6.000E+06
-1.200E+07
-1.800E+07
-2.400E+07
MAXIMUM
4293620.
EG 1, EL 853, IPT 21 (3735832.)
MINIMUM
-1.767E+07
EG 1, EL 869, IPT 11 (-1.736E+07)
ADINA
CONSISTENT
CONTACT
FORCE
TIME 8.000
6336114.
6000000.
4800000.
3600000.
2400000.
1200000.
Z
X
Y
ADINA
Z
X
Y
SIGMA-P1
RST CALC
TIME 8.000
2800000.
2200000.
1600000.
1000000.
400000.
MAXIMUM
4607106.
EG 1, EL 853, IPT 21 (3930059.)
MINIMUM
-8498237.
EG 1, EL 102, IPT 21 (-5620005.)

Appendix F

Stresses in mid section and contact with rock

F.1 Orientation

This appendix summarise the stresses obtained in the mid section of the plug and the traction stresses between plug and concrete. Since cracking occurs for some load combinations modified calculations are made in which the influence of cracking is approximately taken into account. Section F.2 show the procedure used for the calculations and Section F.3 explain what results are presented in Section F.4 to F.9.

F.2 Calculation procedure

Based on the σ_y stresses, i.e. stresses acting perpendicular to the rotational axis, in the plug mid section it is possible to integrate the normal force N and the moment M acting on the cross section. Knowing this the stress in an arbitrary point may be determined using Navier's formula

$$\sigma = \frac{N}{A} + \frac{M}{I} z \qquad \text{(Eq. F-1)}$$

where A is the cross sectional area, I is the moment of inertia and z is the distance from the centre of gravity to the point studied.

In Sections F.4 to F.9 the stresses σ_y obtained in the analyses for the uncracked cross section are compared with that estimated using Equation F-1 and it can be concluded that they agree well. However, for a cracked cross section the stress distribution will differ and the procedure used to determine this is illustrated in Figure F-1.

Knowing the external forces acting on the cross section, the eccentricity e can be determined as

$$e = \frac{M}{N} \qquad \text{(Eq. F-2)}$$

The height of the compressive zone x and finally the maximum stress σ_y can then be determined as

$$x = 3\left(\frac{h}{2} - e\right) \qquad \text{(Eq. F-3)}$$

$$\sigma_c = \frac{2N}{bx} \qquad \text{(Eq. F-4)}$$

where h and b is the height and width of the cross section, respectively. The stresses are assumed to be zero at a level of and below that of the compressive zone.

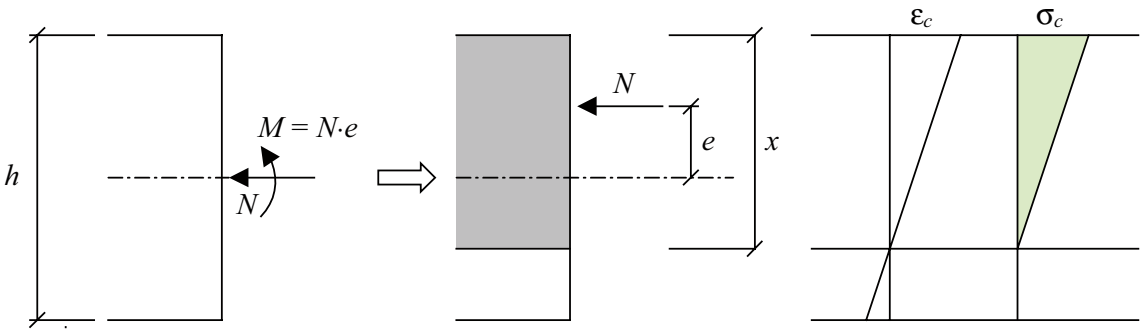

Figure F-1. *Equilibrium conditions for concrete cross section subjected to moment M and normal force N, assuming a fully linear behaviour.*

F.3 Results presented

In Sections F.4 to F.9 stresses obtained in the plug for material load combination 1.1–8.1 to 1.8–6.8, respectively, are shown. All results presented follow the same concept:

1) Stresses σ_y (perpendicular to rotational axis) for load combinations 1.Y–8.Y. [2]
2) Stresses σ_y for load combination 4.Y (worst case) compared with a sectional analysis using Equations F-1 to F-4.
3) Normal traction stresses (acting perpendicular to rock) between plug and rock.
4) Tangential traction stresses (acting parallel to rock; i.e. stresses due to friction) between plug and rock.

In some load combinations, i.e. combinations 4.2, 4.4 and 4.6, the eccentricity $e > h / 2$, which means that force equilibrium is not possible. This imply that the plug does not fulfil the bearing capacity required but is really an effect of unnecessary conservative load values obtained when the concrete cracking is not sufficiently taken into account in the finite element analyses. This is further investigated and discussed in Appendix G where a comparison to the σ_y stresses acquired for load combination 4.2 is made using a modified FE model, that approximately considerate the effect of concrete cracking.

The integrated normal force N, moment M and eccentricity e is, together with the height of the compressive zone x and compressive stress σ_y for a cracked section, presented in Table F-1 and Table F-2 for all load combinations.

From Table F-1 it can be seen that there is no compressive zone for load combinations 4.2, 4.4 and 4.6. Based on the normal force N and the moment M it is not possible to find force equilibrium in the mid cross section. Similar behaviour is obtained for load combinations 3.2, 3.4 and 3.6, though here equilibrium is possible. However, the worst cases, i.e. load combinations 3.2 and 4.2, are further studied in Appendix G and it is there shown that it is still possible to find equilibrium when using a modified, more realistic model.

Table F-1. Summary of normal force N, moment M, eccentricity e used to determine the height of the compressive zone x and the compressive stress σ_y for a cracked section according to Equations F-1 to F-4. Presented results are for load scenarios 1–4.

Load scenarios	Load combination	E_r [GPa]	μ [–]	N [MN]	M [MNm]	e [m]	x [1)] [m]	σ_y [1)] [MPa]
1	1.1	25	0.3	–25.0	–0.7	0.03	1.70	–
	1.2	25	2.0	–25.6	–1.0	0.04	1.70	–
	1.3	50	0.3	–30.3	0.3	–0.01	1.70	–
	1.4	50	2.0	–30.6	–0.1	0.00	1.70	–
	1.5	75	0.3	–32.8	0.7	–0.02	1.70	–
	1.6	75	2.0	–32.9	0.3	–0.01	1.70	–
2	2.1	25	0.3	–19.9	–3.6	0.18	1.70	–
	2.2	25	2.0	–20.3	–4.1	0.20	1.70	–
	2.3	50	0.3	–24.7	–2.8	0.11	1.70	–
	2.4	50	2.0	–24.8	–3.3	0.13	1.70	–
	2.5	75	0.3	–26.9	–2.4	0.09	1.70	–
	2.6	75	2.0	–26.8	–2.9	0.11	1.70	–
3	3.1	25	0.3	–8.5	–4.7	0.55	0.90	–18.9
	3.2	25	2.0	–7.1	–5.5	0.78	0.21 [3)]	–66.6 [3)]
	3.3	50	0.3	–8.6	–4.1	0.48	1.11	–15.6
	3.4	50	2.0	–7.1	–5.0	0.70	0.44 [3)]	–32.4 [3)]
	3.5	75	0.3	–8.7	–3.9	0.45	1.19	–14.6
	3.6	75	2.0	–7.1	–4.8	0.67	0.53 [3)]	–27.0 [3)]
4	4.1	25	0.3	–8.4	–5.2	0.62	0.70	–23.9

[2] Y indicate the material combination in use, ranging from 1 to 6, according to Table 3-4.

Load scenarios	Load combination	E_r [GPa]	μ [–]	N [MN]	M [MNm]	e [m]	x [1)] [m]	σ_y [1)] [MPa]
	4.2	25	2.0	–6.6	–6.2	0.93	– [2)]	– [2)]
	4.3	50	0.3	–8.4	–4.8	0.57	0.85	–19.7
	4.4	50	2.0	–6.6	–5.7	0.87	– [2)]	– [2)]
	4.5	75	0.3	–8.4	–4.6	0.55	0.91	–18.5
	4.6	75	2.0	–6.6	–5.5	0.84	– [2)]	– [2)]

1) If the compressive zone is x = 1.70 m the entire cross section is compressed and the linear finite element analyses carried out are valid. For these cases no compressive stress σ_y is given since they are already listed in Table 4-1.

2) The eccentricity e is larger than the available cross section h/2, and hence, the required normal force N is located outside the cross section; i.e. an impossible solution indicating inadequate capacity of the plug. This is further studied in Appendix G.

3) The eccentricity e is large compared to the available cross section h/2, and hence, the height of the compressive zone x becomes small and the compressive stresses σ_c large. This is further studied in Appendix G.

Table F-2. Summary of normal force N, moment M, eccentricity e used to determine the height of the compressive zone x and the compressive stress σ_y for a cracked section according to Equations F-1 to F-4. Presented results are for load scenarios 5–8.

Load scenarios	Load combination	E_r [GPa]	μ [–]	N [MN]	M [MNm]	e [m]	x [1)] [m]	σ_y [1)] [MPa]
5	5.1	25.0	0.3	–26.8	0.4	–0.01	1.70	–
	5.2		2.0	–27.5	–0.3	0.01	1.70	–
	5.3	50.0	0.3	–31.5	1.3	–0.04	1.70	–
	5.4		2.0	–32.2	0.7	–0.02	1.70	–
	5.5	75.0	0.3	–33.7	1.7	–0.05	1.70	–
	5.6		2.0	–34.3	1.1	–0.03	1.70	–
6	6.1	25.0	0.3	–21.7	–3.0	0.14	1.70	–
	6.2		2.0	–22.1	–3.5	0.16	1.70	–
	6.3	50.0	0.3	–25.7	–2.2	0.09	1.70	–
	6.4		2.0	–26.1	–2.7	0.10	1.70	–
	6.5	75.0	0.3	–27.6	–1.9	0.07	1.70	–
	6.6		2.0	–28.0	–2.3	0.08	1.70	–
7	7.1	25.0	0.3	–15.4	–3.8	0.25	1.70	–
	7.2		2.0	–12.9	–5.1	0.39	1.37	–18.9
	7.3	50.0	0.3	–15.4	–3.3	0.21	1.70	–
	7.4		2.0	–12.9	–4.4	0.35	1.51	–17.0
	7.5	75.0	0.3	–15.4	–3.0	0.20	1.70	–
	7.6		2.0	–12.8	–4.2	0.32	1.58	–16.3
8	8.1	25.0	0.3	–16.0	–4.0	0.25	1.70	–
	8.2		2.0	–12.7	–5.7	0.45	1.21	–21.0
	8.3	50.0	0.3	–16.1	–3.5	0.22	1.70	–
	8.4		2.0	–12.6	–5.1	0.40	1.35	–18.7
	8.5	75.0	0.3	–16.1	–3.3	0.21	1.70	–
	8.6		2.0	–12.6	–4.8	0.38	1.40	–17.9

1) If the compressive zone is 1.70 m the entire cross section is compressed and the linear finite element analyses carried out are valid. For these cases no compressive stress σ_y is given since they are already listed in Table 4-2.

F.4 Load combinations 1.1 to 8.1

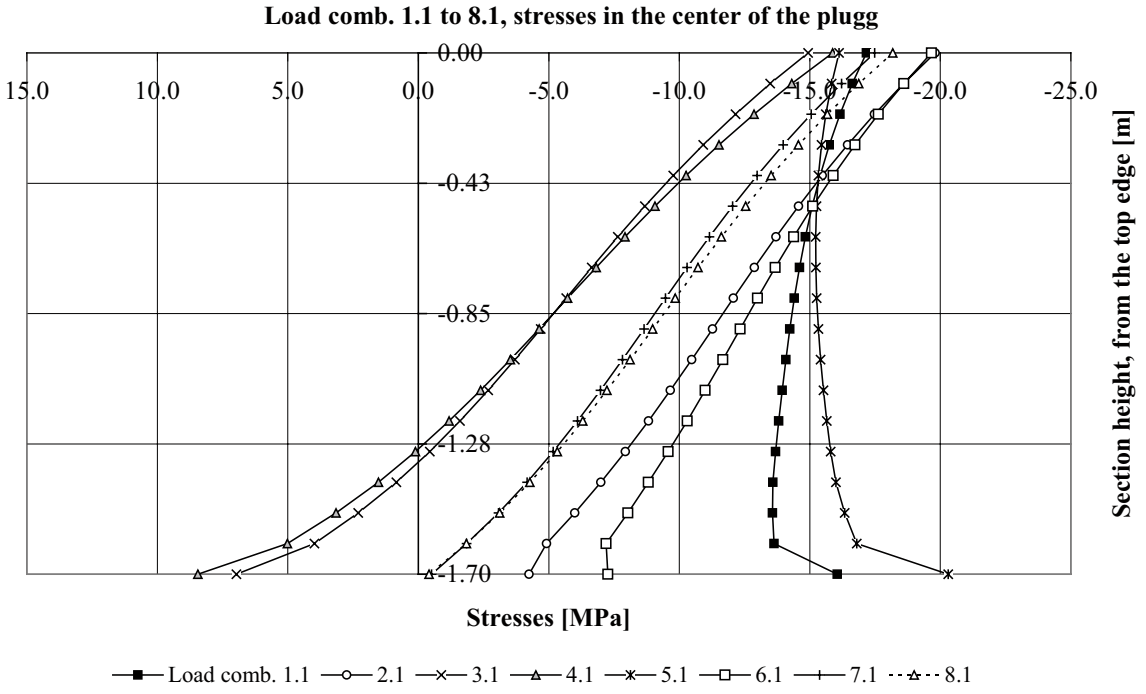

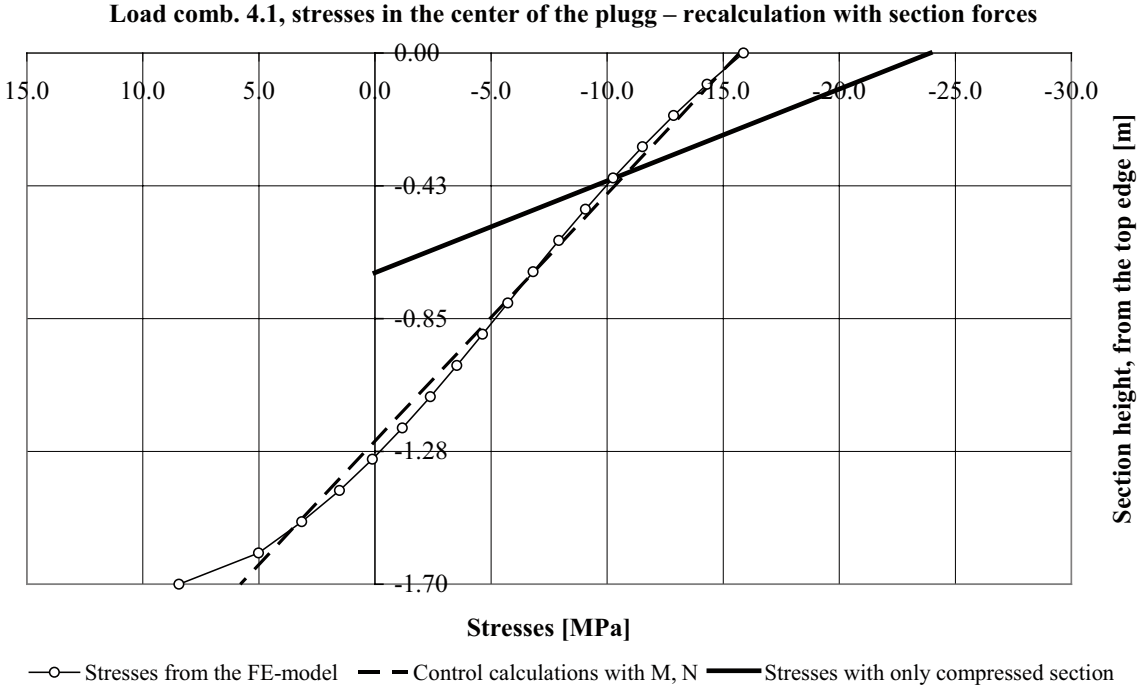

Figure F-2. *Stresses σ_y for load combinations 1.1–8.1 and stresses σ_y for load combination 4.1 (worst case) compared with a sectional analysis using Equations (F-1) to (F-4).*

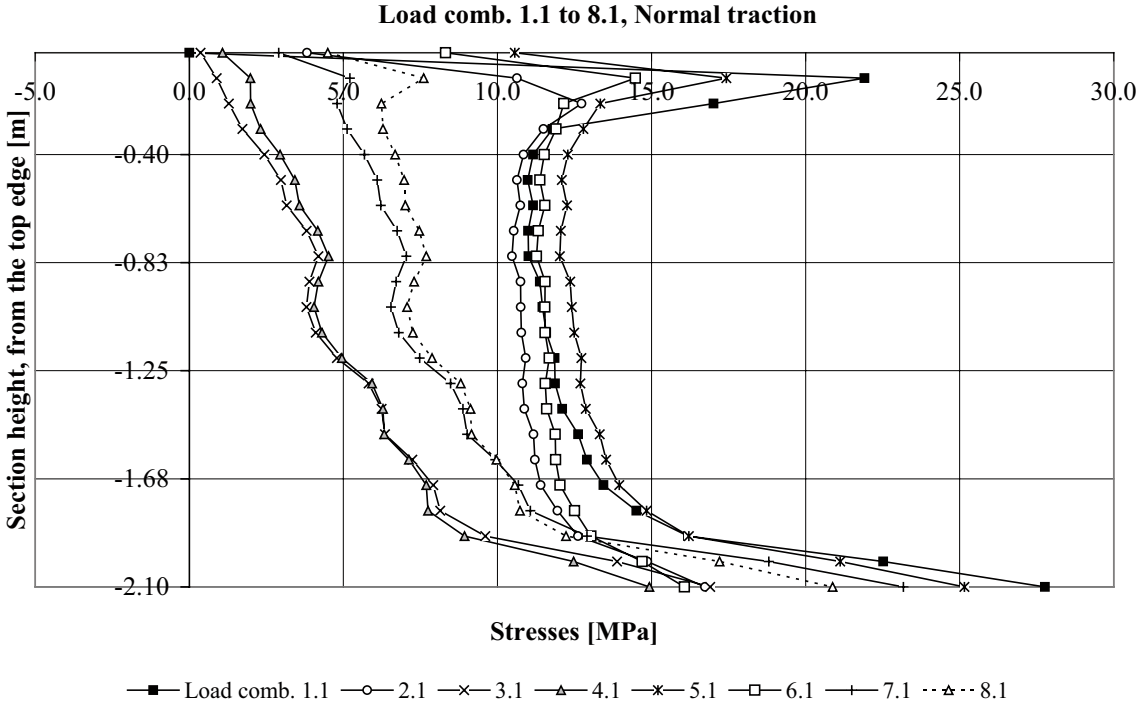

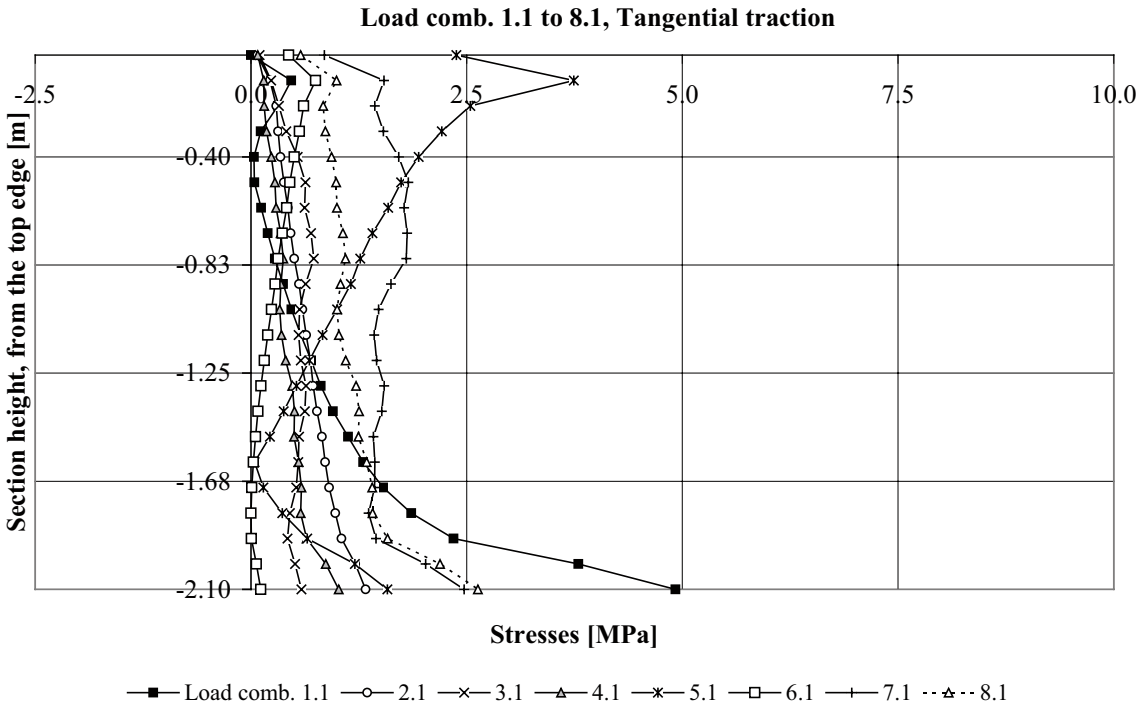

Figure F-3. *Normal and traction stresses between plug and rock for load combinations 1.1–8.1.*

F.5 Load combinations 1.2 to 8.2

The eccentricity e, according to Equation F-2, is larger than $h/2$ which means that the height of the compressive zone x in Equation F-3 becomes negative. Hence, no force equilibrium is possible for load combination 4.2 using the given values on the normal force N and the moment M. This is further discussed in Appendix G.

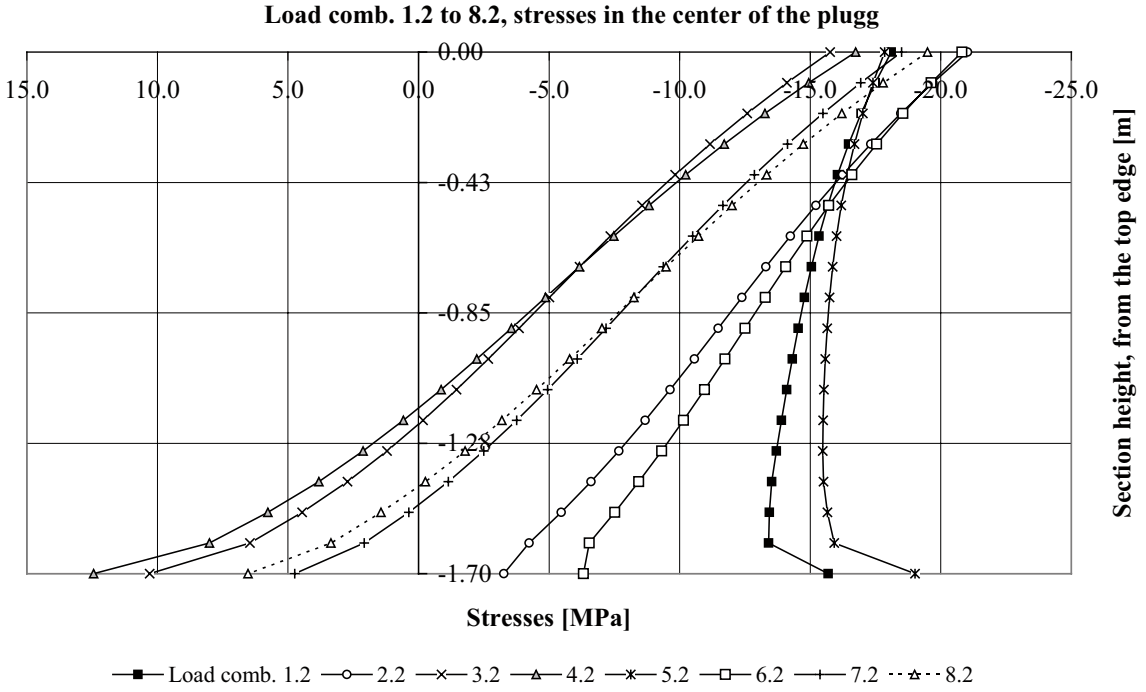

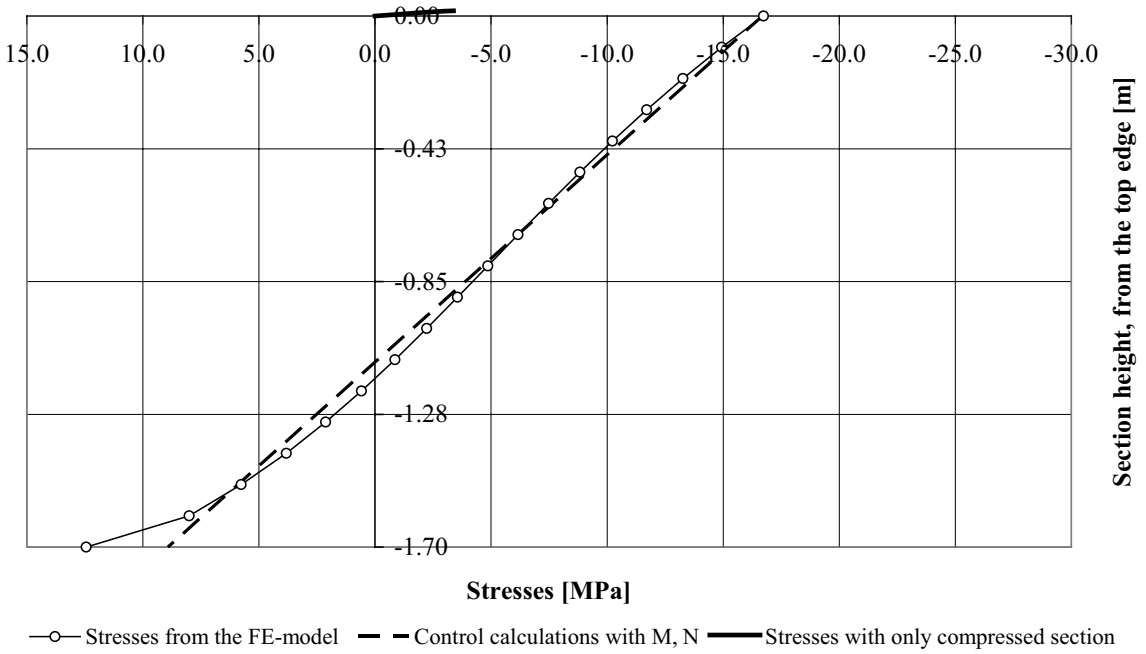

Figure F-4. *Stresses σ_y for load combinations 1.2–8.2 and stresses σ_y for load combination 4.2 (worst case) compared with a sectional analysis using Equations (F-1) to (F-4).*

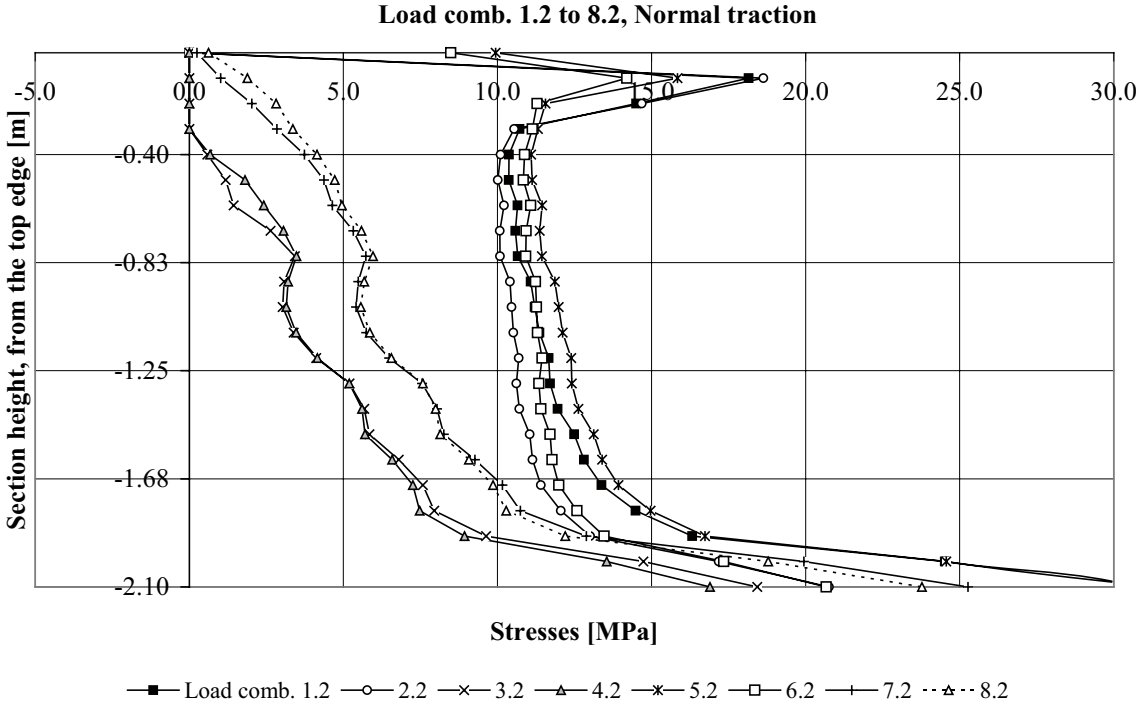

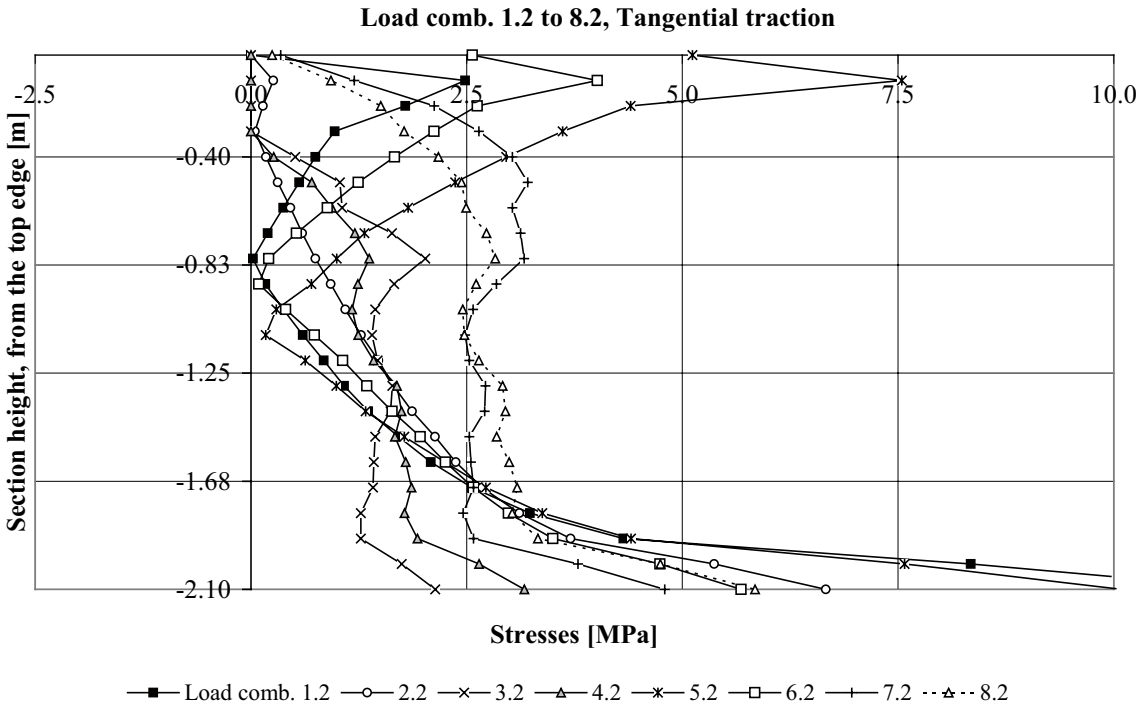

Figure F-5. *Normal and traction stresses between plug and rock for load combinations 1.2–8.2.*

F.6 Load combinations 1.3 to 8.3

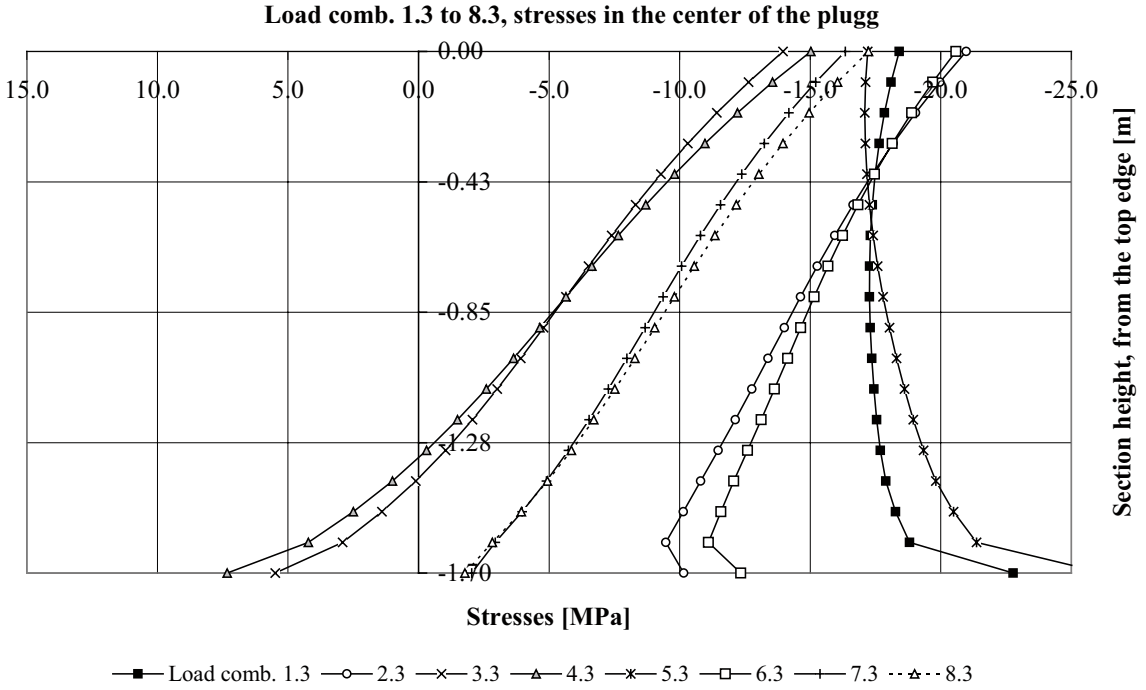

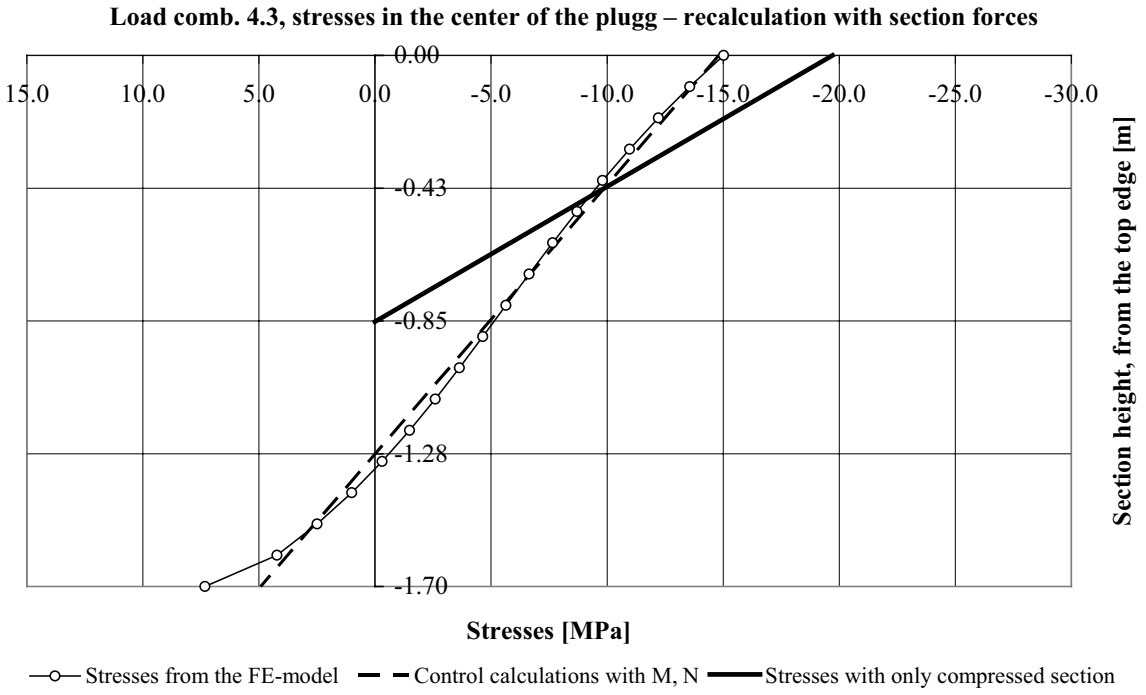

Figure F-6. *Stresses σ_y for load combinations 1.3–8.3 and stresses σ_y for load combination 4.3 (worst case) compared with a sectional analysis using Equations (F-1) to (F-4).*

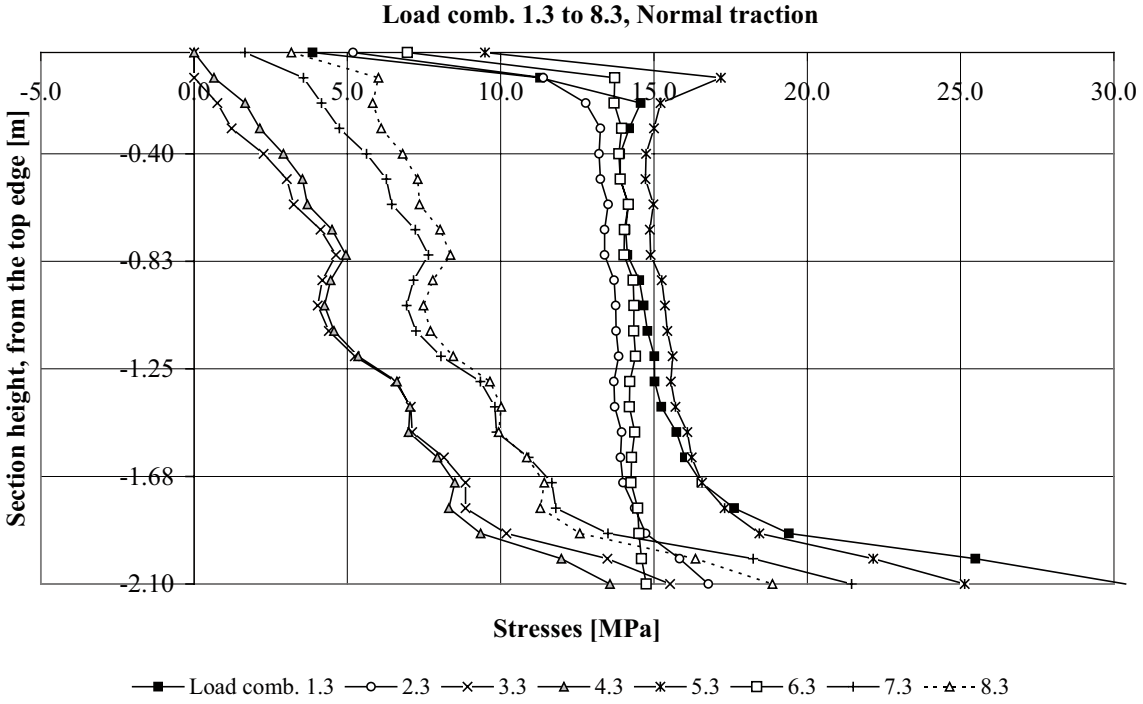

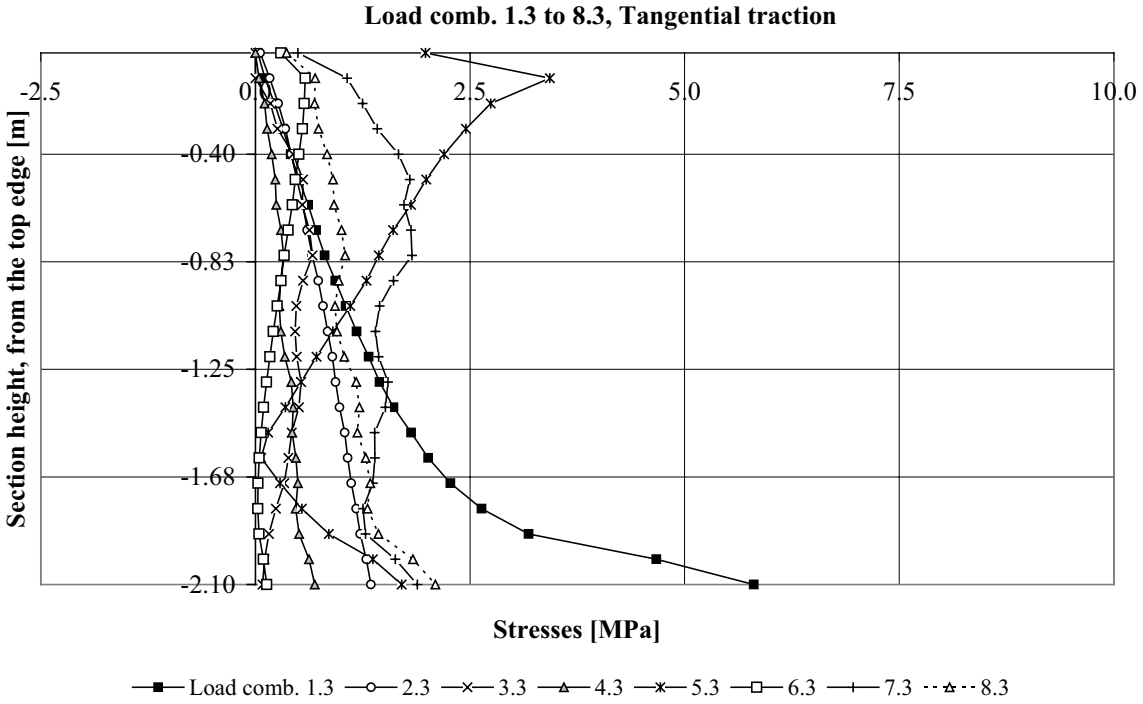

Figure F-7. *Normal and traction stresses between plug and rock for load combinations 1.3–8.3.*

F.7 Load combinations 1.4 to 8.4

The eccentricity e, according to Equation F-2, is larger than $h/2$ which means that the height of the compressive zone x in Equation F-3 becomes negative. Hence, no force equilibrium is possible for load combination 4.4 using the given values on the normal force N and the moment M. This is further discussed in Appendix G.

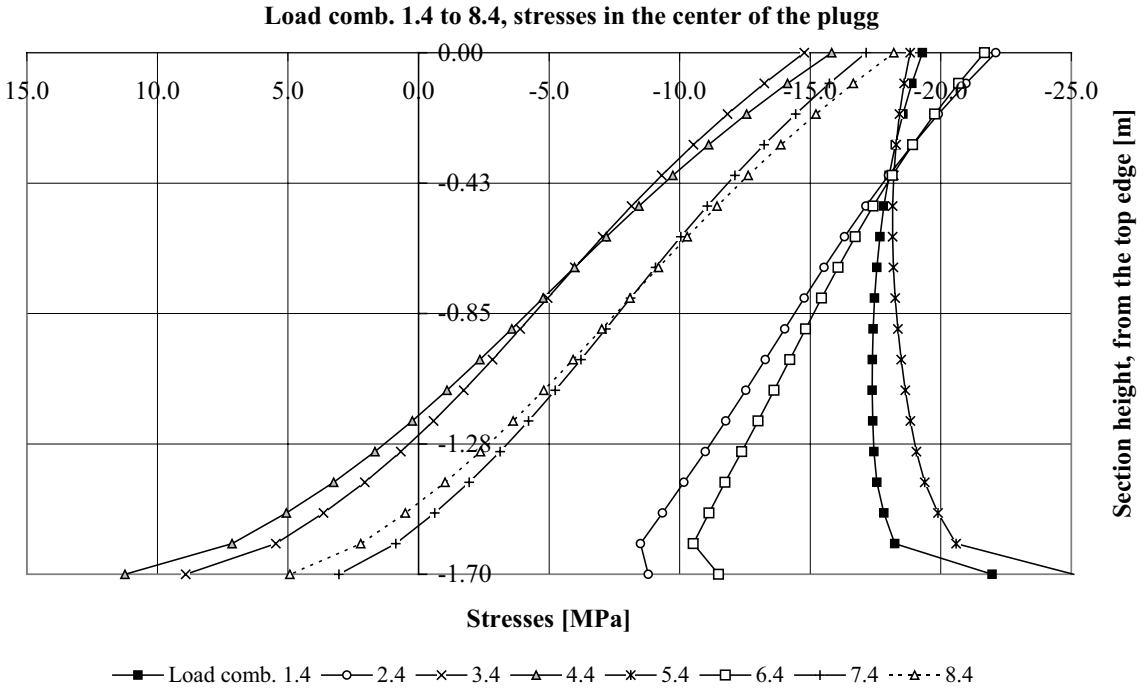

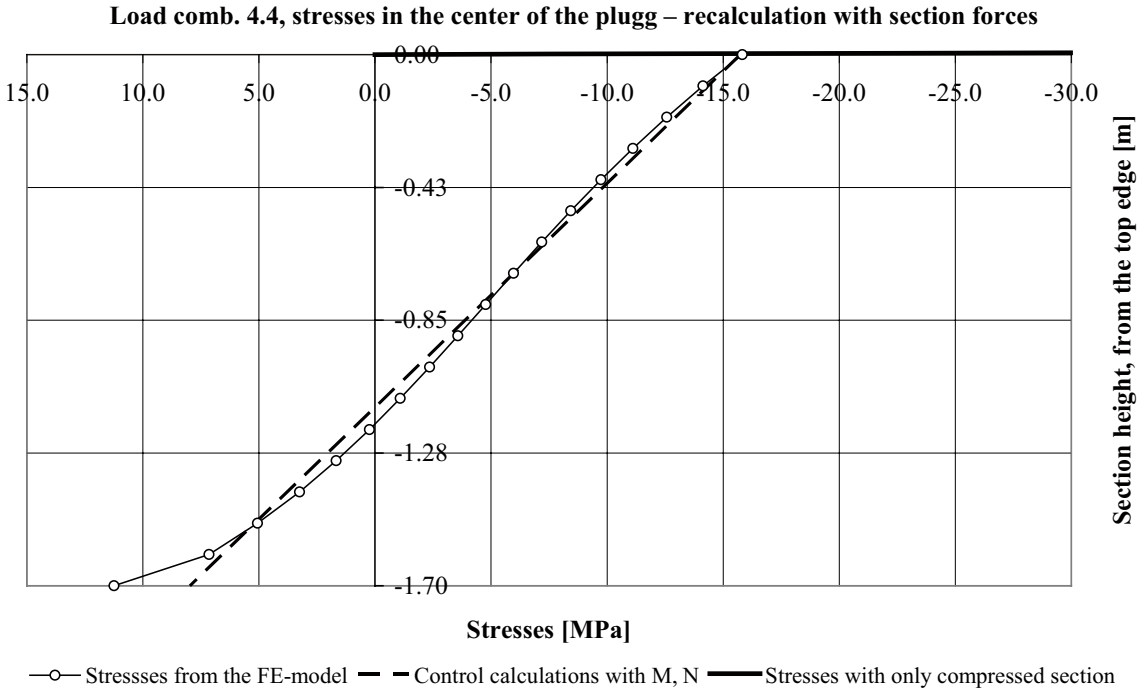

Figure F-8. *Stresses σ_y for load combinations 1.4–8.4 and stresses σ_y for load combination 4.4 (worst case) compared with a sectional analysis using Equations (F-1) to (F-4).*

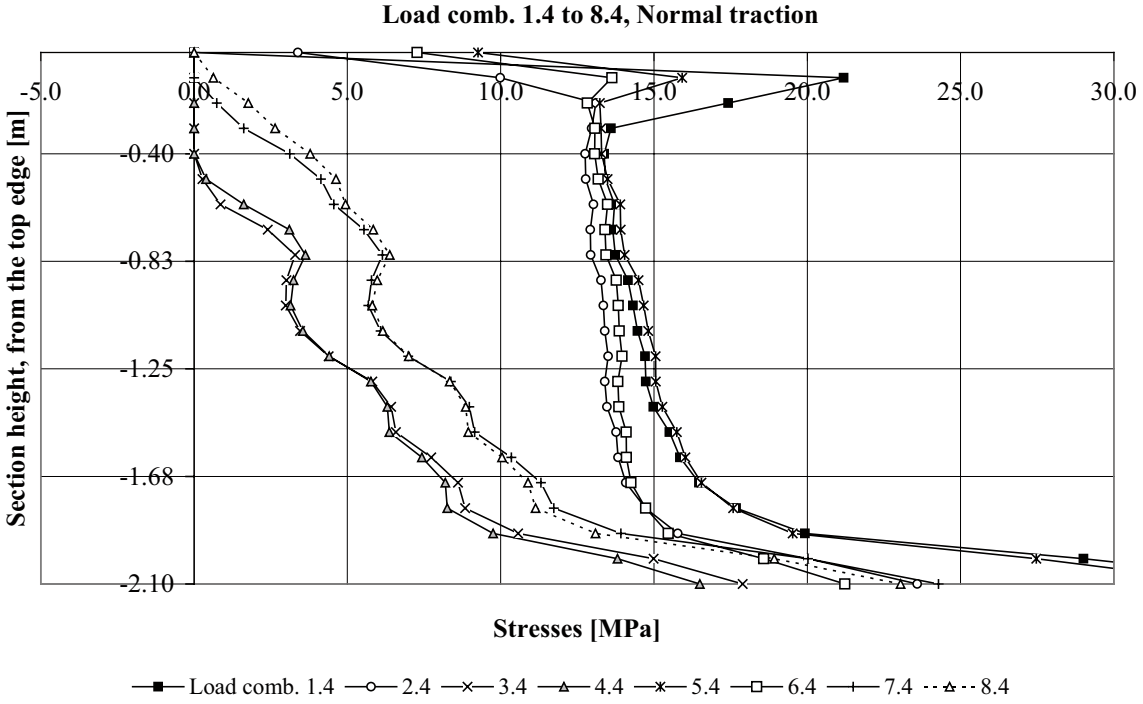

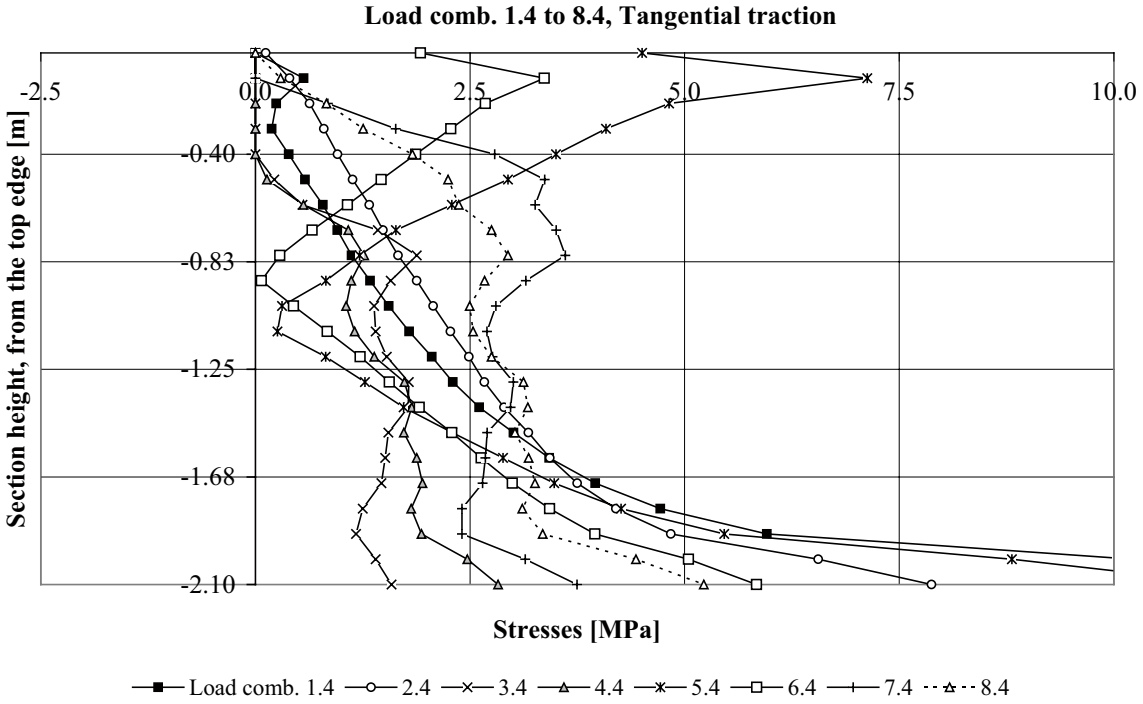

Figure F-9. *Normal and traction stresses between plug and rock for load combinations 1.4–8.4.*

F.8 Load combinations 1.5 to 8.5

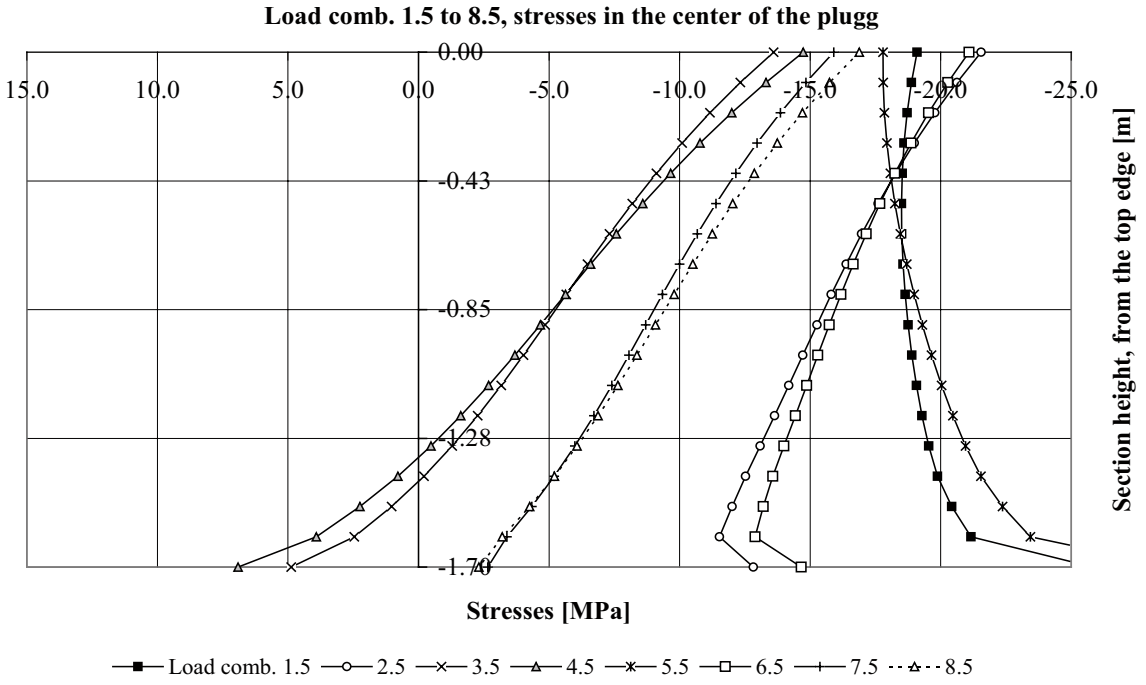

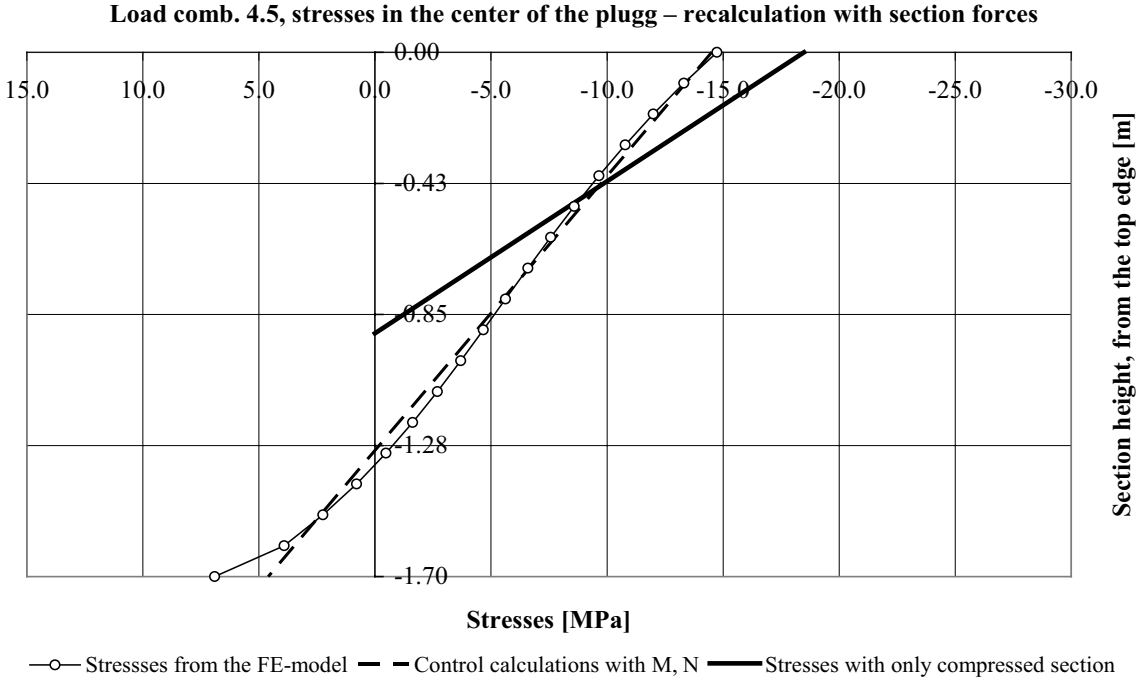

Figure F-10. *Stresses σ_y for load combinations 1.5–8.5 and stresses σ_y for load combination 4.5 (worst case) compared with a sectional analysis using Equations (F-1) to (F-4).*

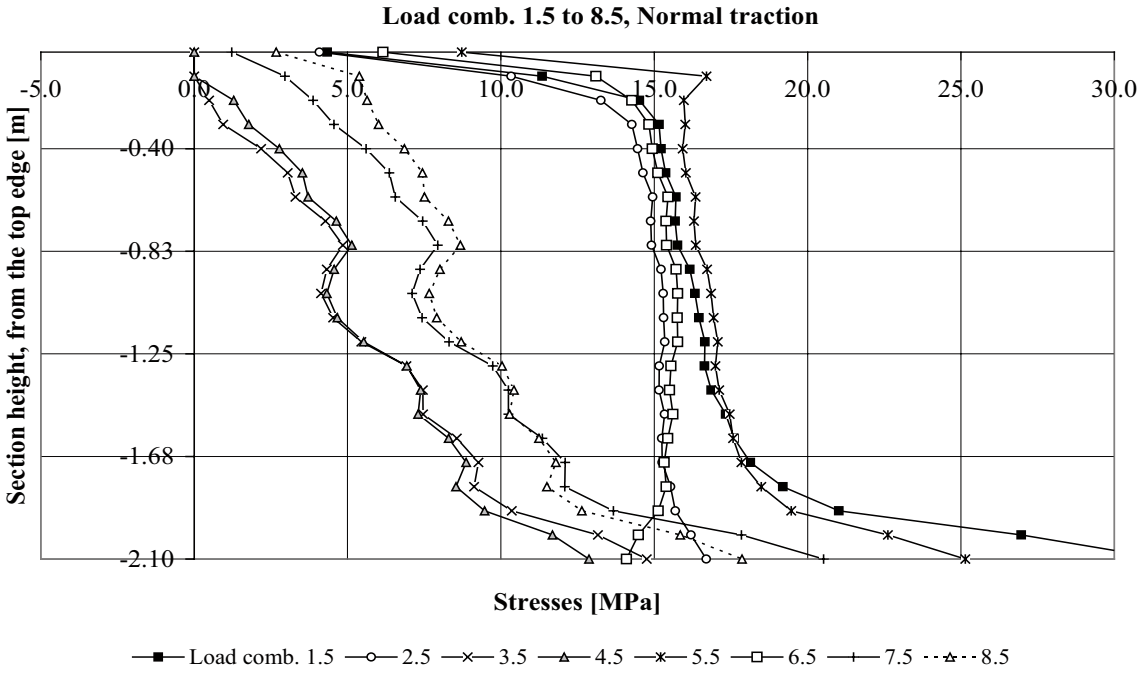

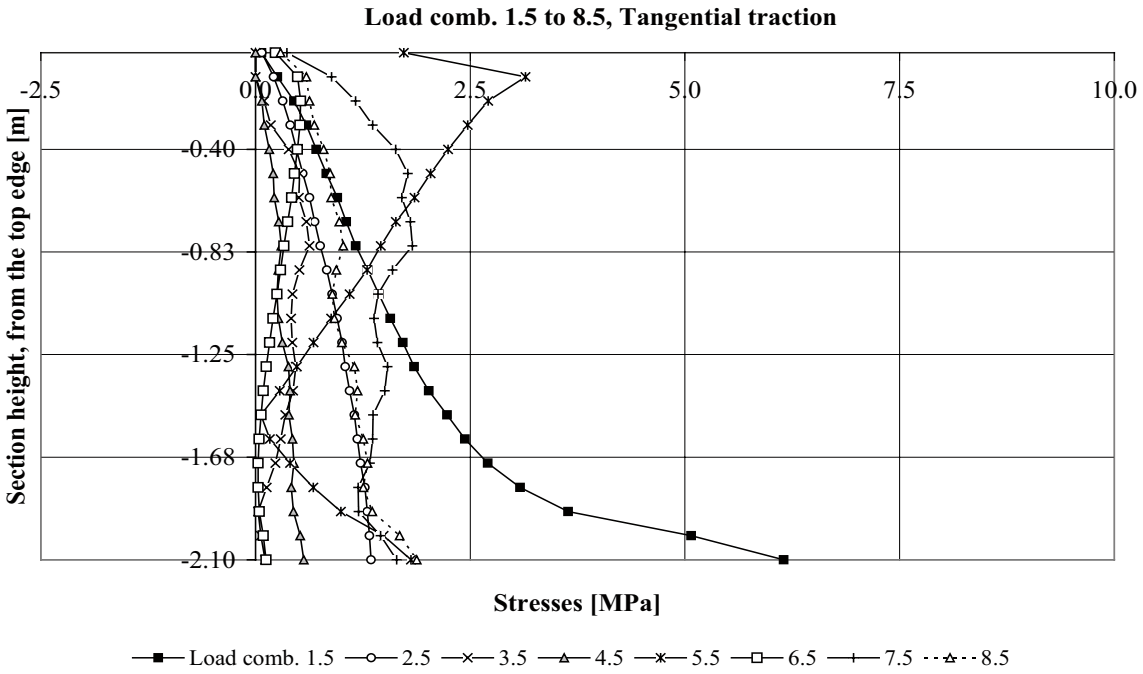

Figure F-11. *Normal and traction stresses between plug and rock for load combinations 1.5–8.5.*

F.9 Load combinations 1.6 to 8.6

The eccentricity e, according to Equation F-2, is larger than $h/2$ which means that the height of the compressive zone x in Equation F-3 becomes negative. Hence, no force equilibrium is possible for load combination 4.6 using the given values on the normal force N and the moment M. This is further discussed in Appendix G.

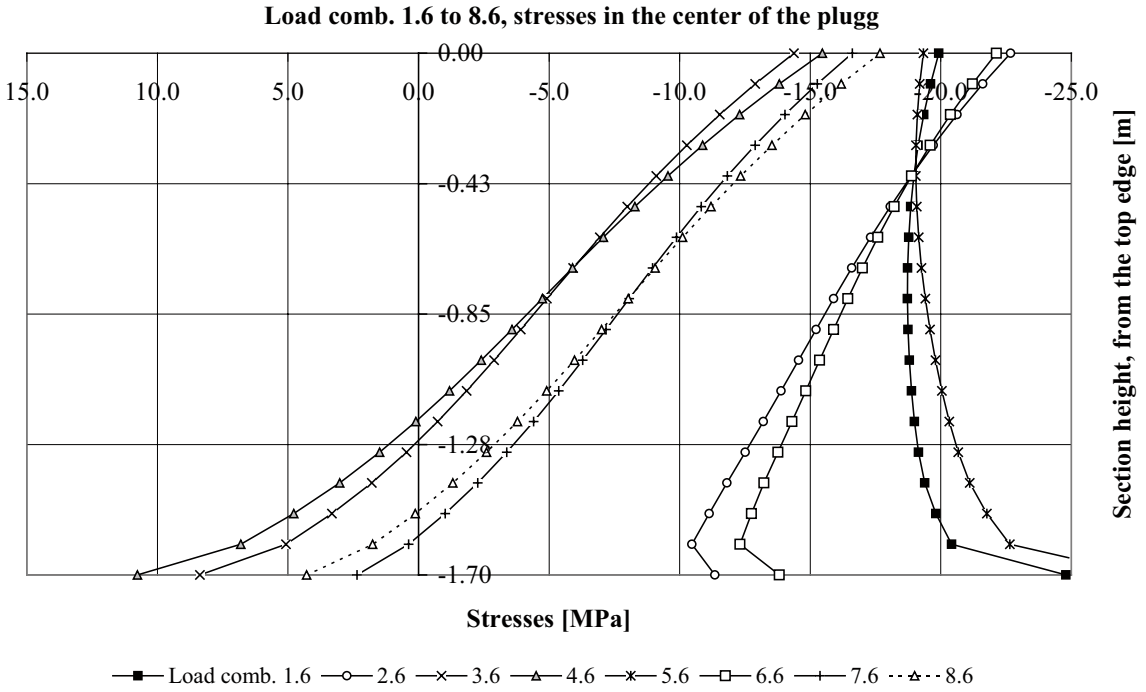

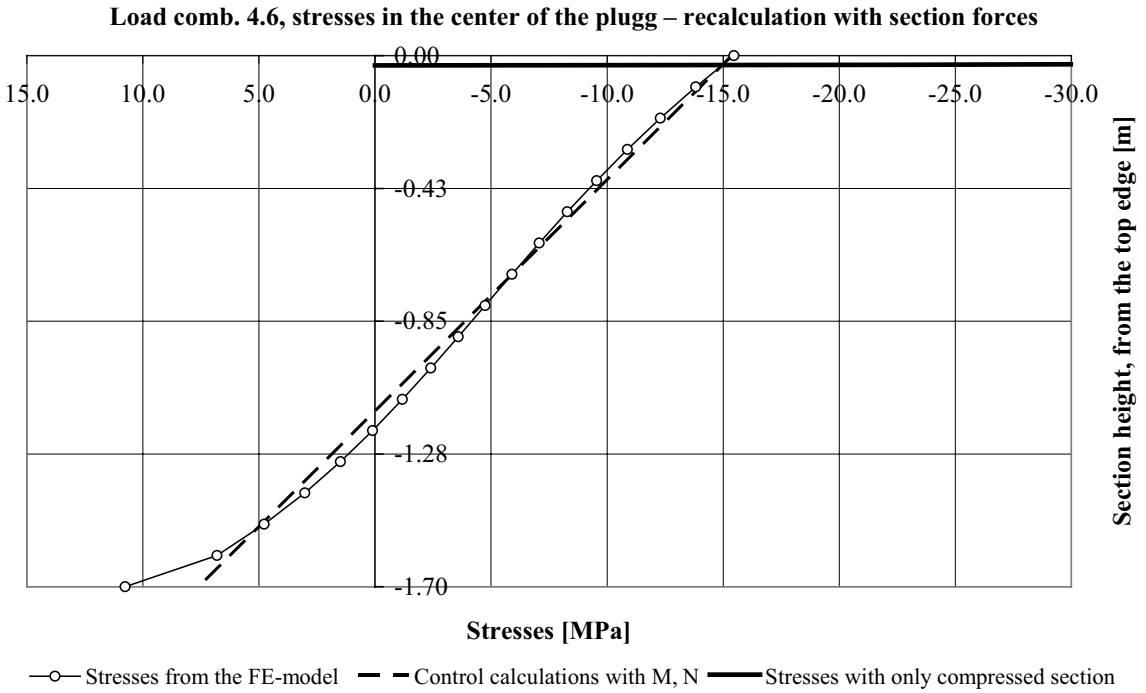

Figure F-12. *Stresses σ_y for load combinations 1.6–8.6 and stresses σ_y for load combination 4.6 (worst case) compared with a sectional analysis using Equations (F-1) to (F-4).*

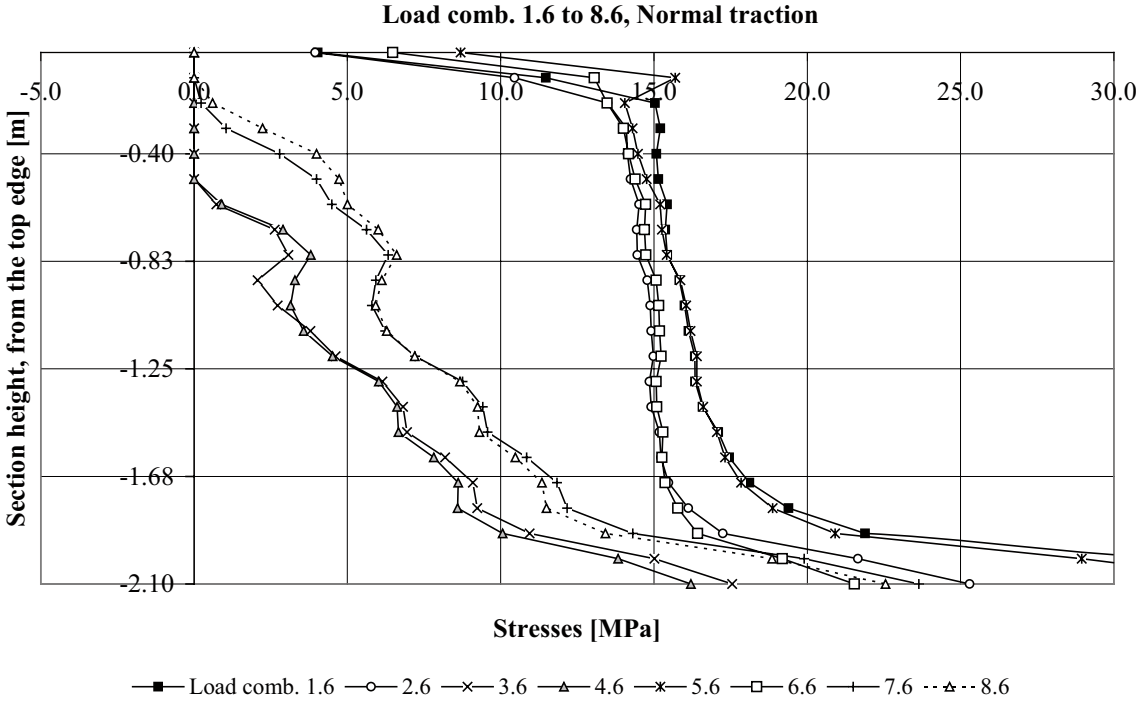

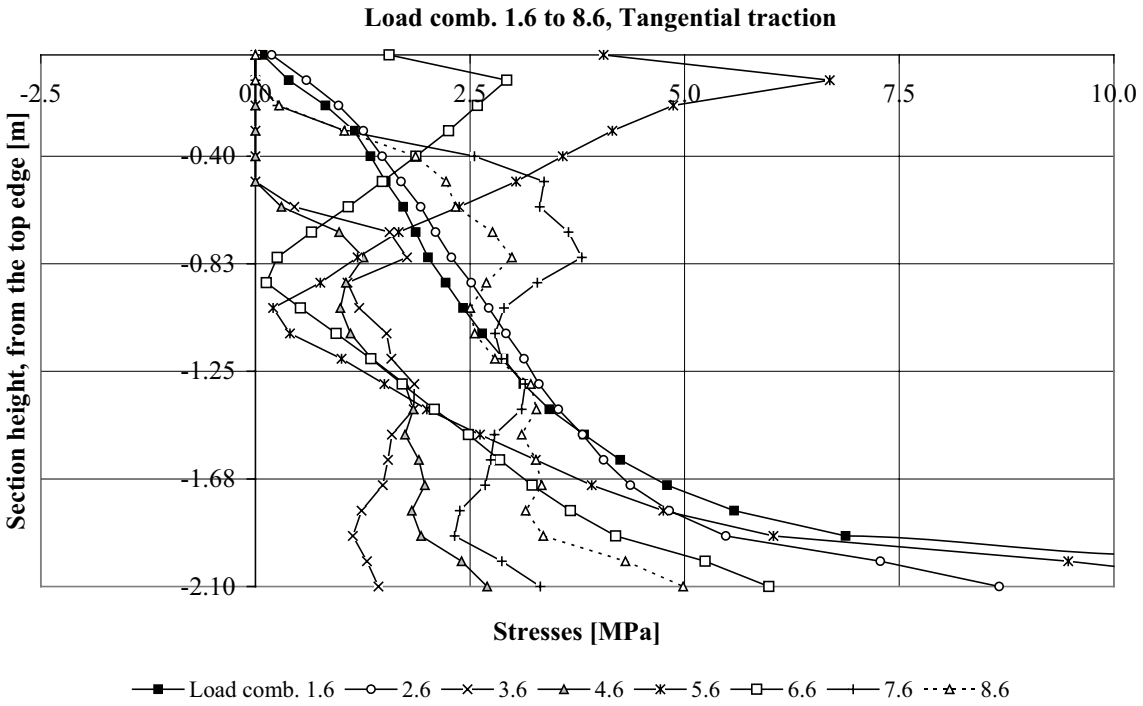

Figure F-13. *Normal and traction stresses between plug and rock for load combinations 1.6–8.6.*

Appendix G

Modified FE model – cracked concrete removed

G.1 Orientation

In Section 4.2.2.2 it is concluded that the concrete plug will crack due to the tensile stresses obtained when subjected to external and internal loads. However, the structural analyses presented in this report use a linear elastic material assumption; i.e. no cracking of the concrete is considered in the analyses and if this requirement is not fulfilled the concrete plug will crack and the results acquired from the analyses have to be properly modified to describe the correct structural behaviour of the plug.

This has also been approximately done in Appendix F, using force equilibrium to determine the σ_y stresses in the plug mid section. There is also a need, though, to verify these calculations and examining whether the changes thus obtained cause stress distributions in other parts of the plug than in the analysed section. Therefore, a modified finite element model, in which the cracked part of the plug is removed, is analysed; i.e. the cracked part of the plug is approximately excluded from the model the stresses are recalculated in the new model, thus compensating for the changed static. Due to this approximate approach it is also still possible to make use of linear elastic material properties for the concrete.

G.2 Initial analysis and general expectations

The response in the initial analysis is expected to differ compared to the result from the modified model. Nevertheless, it is still possible to determine the structural behavior in the most critical sections (i.e. middle of the plug) based on the results obtained in such a linear analysis.

It is also expected, that the cracking will produce changes in the stresses obtained in other parts of the concrete plug and this appendix present a method with which it is possible to approximately investigate what differences may occur.

G.3 Studied model

The load combinations 3.1 and 4.1 are chosen to investigate the plausibility of the method used. The load combinations 3.2 and 4.2 are then further examined since they, according to Table 4-1 and Table 4-2, produce highest tensile stresses, and hence are deemed to represent the most critical cases.

The plug mid section is chosen since the tension on the underside here is high see Figure G-1. The stresses are integrated into a moment/axial force for a typical section. A new section height is calculated through excluding the tensile part from the section, as described in Section F.2, which results in an increased compressive stress on the top side.

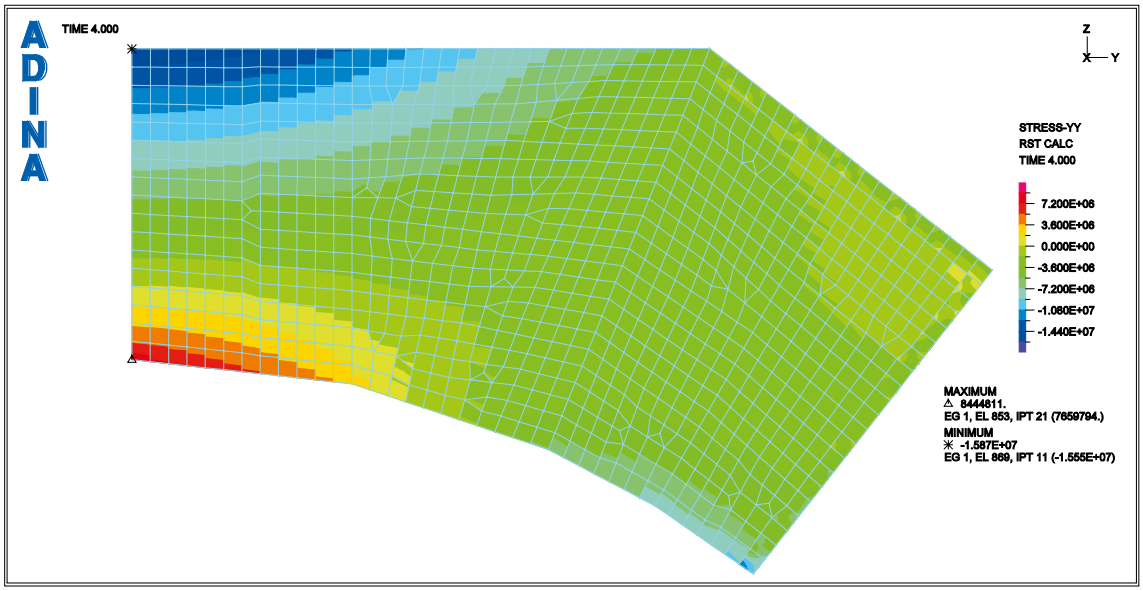

Figure G-1. *Stresses σ_y in plug for load combination 4.1. Studied section is marked.*

G.4 Simplified calculations

The moment M and axial force N are first integrated from the σ_y stresses and are then used to determine a modified stress distribution, assuming a cracked section, in accordance with Equations F-2 to F-4, see Figure G-2. Here it is found that the compressive zone is determined to $x = 0.70$ m and the maximal compressive stress to $\sigma_y = -23.9$ MPa. The latter may be compared with $\sigma_y = -15.7$ MPa obtained in the uncracked section for the same sectional forces.

The stress distribution from ADINA, the stresses from the integrated axial force and moment and the stresses from the excluded tensioned part are compared in Figure G-3 (also shown in Section F.4). From this it can be seen that the use of Navier's formula in Equation F-1 produce good agreement with the results from the finite element analyses. It is also clear that a cracked section produce a considerable smaller compressive zone, and conclusively, also higher compressive stresses.

A simplified section recalculation as this is valid only for the middle section. The result is generally on the safe side since the changed stiffness and static conditions would have positive effect on this particular section. The redistribution of the stresses in the rest of the plug, however, is further checked in Section G.5.

G.5 Model with removed tensioned zone

G.5.1 Basis for the new model

A new model is created, based on the distribution of the tensile stress and the height of the recalculated middle section in Figure G-2 and Figure G-3. The underside of the plug close to the mid section is affected by cracking and is removed as schematically shown in Figure G-4 and Figure G-5, using a somewhat smooth surface.

Since the stress distribution is different for the different load cases, it is assumed that each reduced model is valid only for a certain load combination. Resulting stresses from the modified model is shown in Section G.5.2

Node	distanse top edge [m]	σ YY [MPa]		N [MN]		N.x [MNm]
LOAD COMB. 4.1						
783	0.00	-15.87		-0.79		-0.675
782	-0.10	-14.31		-1.43		-1.073
781	-0.20	-12.86		-1.29		-0.836
780	-0.30	-11.52		-1.15		-0.634
779	-0.40	-10.26		-1.03		-0.462
778	-0.50	-9.07		-0.91		-0.317
777	-0.60	-7.92		-0.79		-0.198
776	-0.70	-6.81		-0.68		-0.102
775	-0.80	-5.72		-0.57		-0.029
774	-0.90	-4.63		-0.46		0.023
773	-1.00	-3.53		-0.35		0.053
772	-1.10	-2.38		-0.24		0.060
771	-1.20	-1.18		-0.12		0.041
770	-1.30	0.11		0.01		-0.005
769	-1.40	1.53		0.15		-0.084
768	-1.50	3.15		0.32		-0.205
767	-1.60	5.02		0.50		-0.376
766	-1.70	8.44		0.42		-0.359

N=	-8.41	MN	M=	-5.178 MNm
	-8410	kN		-5178 kNm

	distance top edge [m]	σ YY=N/A + M/W [MPa]
control		
top	0.000	-15.70
bott	-1.700	5.80

excentricity, top edge: e'=h/2-M/N=		0.23	[m]
compr. zone height: x=3*(h/2-M/N)=		0.70	[m]
recalculated stress, compression only			
top	0.000	-23.92	[MPa]
	-0.703	0.00	[MPa]

Figure G-2. *Determination of moment M and axial force F from stresses σ_y in load combination 4.1. Compressive zone x and stress σ_y for a cracked section is determined.*

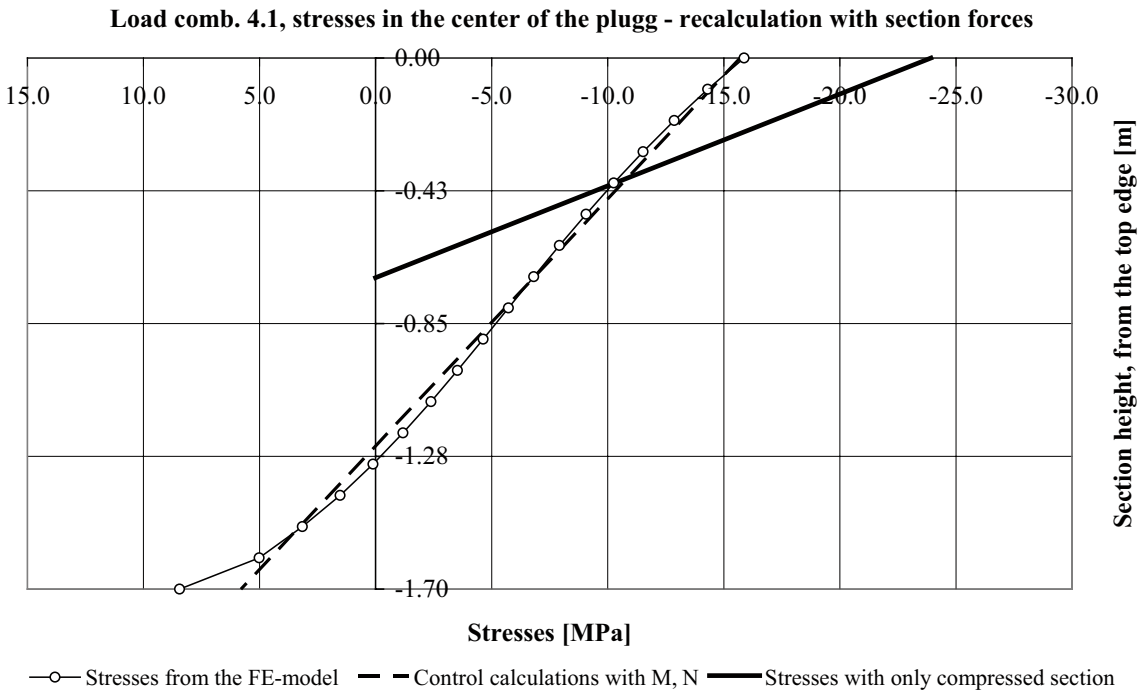

Figure G-3. *Stress distribution in plug mid section for load combination 4.1 from ADINA and values calculated in Figure G-2.*

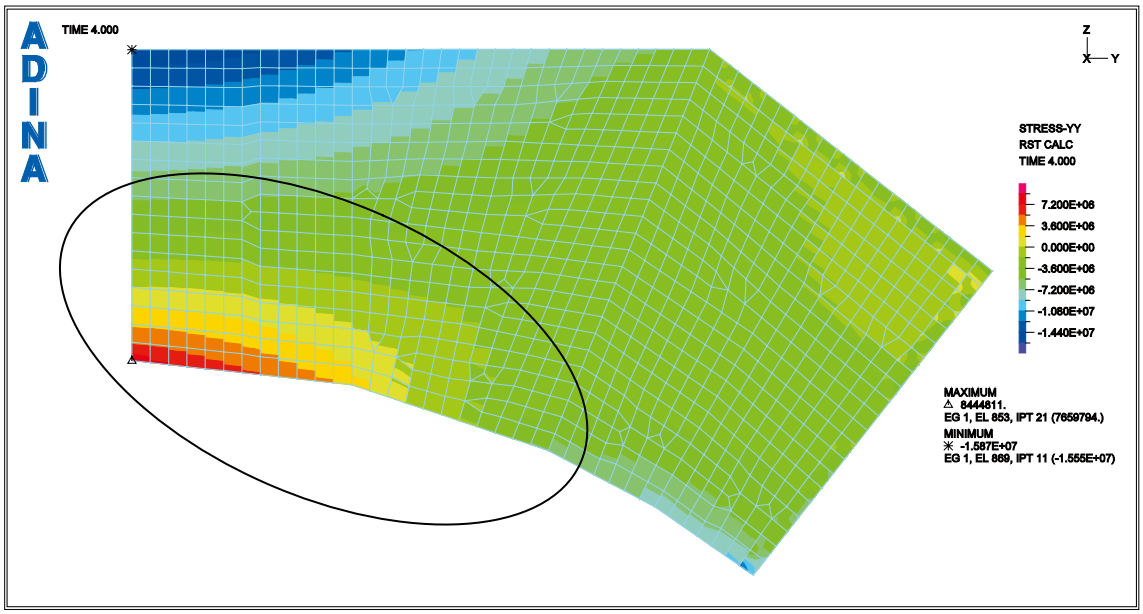

Figure G-4. *Stresses σ_y in plug for load combination 4.1. Concrete affected by tensile stresses that cause cracking and that will be removed is marked.*

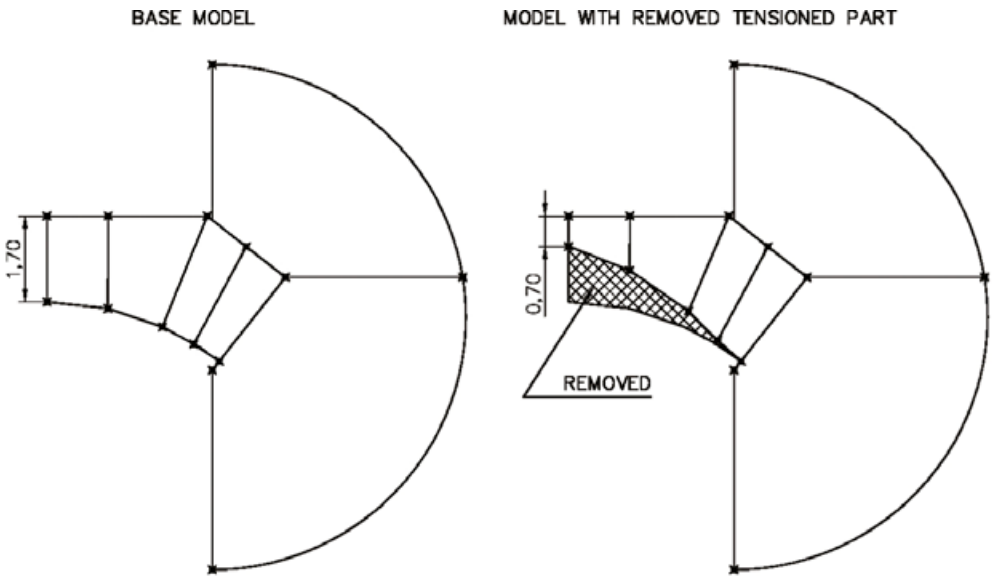

Figure G-5. *Schematic illustration of concrete zone considered to be affected by cracking and hence removed from the modified model. In the figure x = 0.70 m.*

G.5.2 Results from the modified model

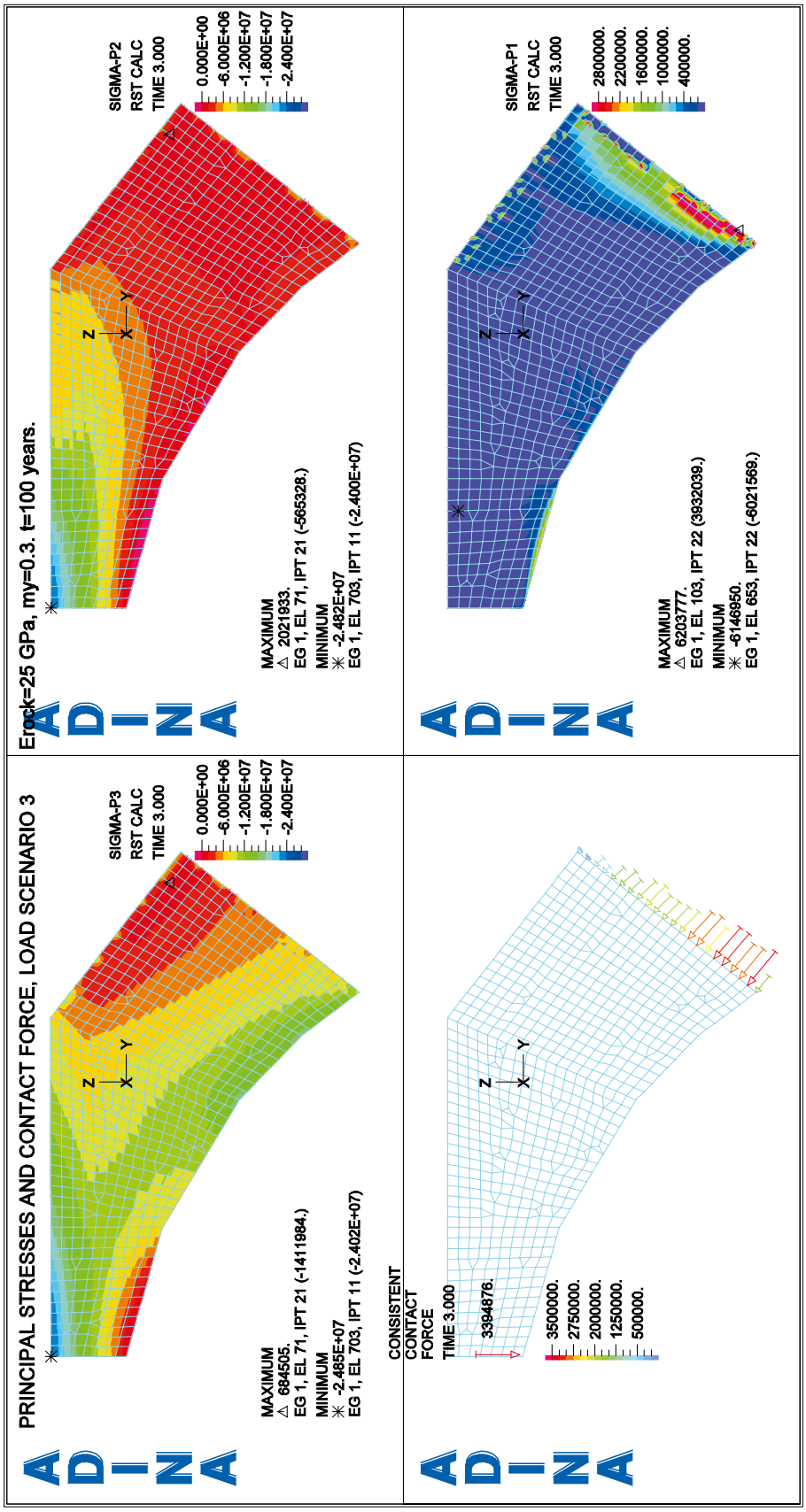

Figure G-6. *Resulting stresses for the modified model, when cracked concrete has been removed, for load combination 3.1. Compressive zone x = 0.70 m.*

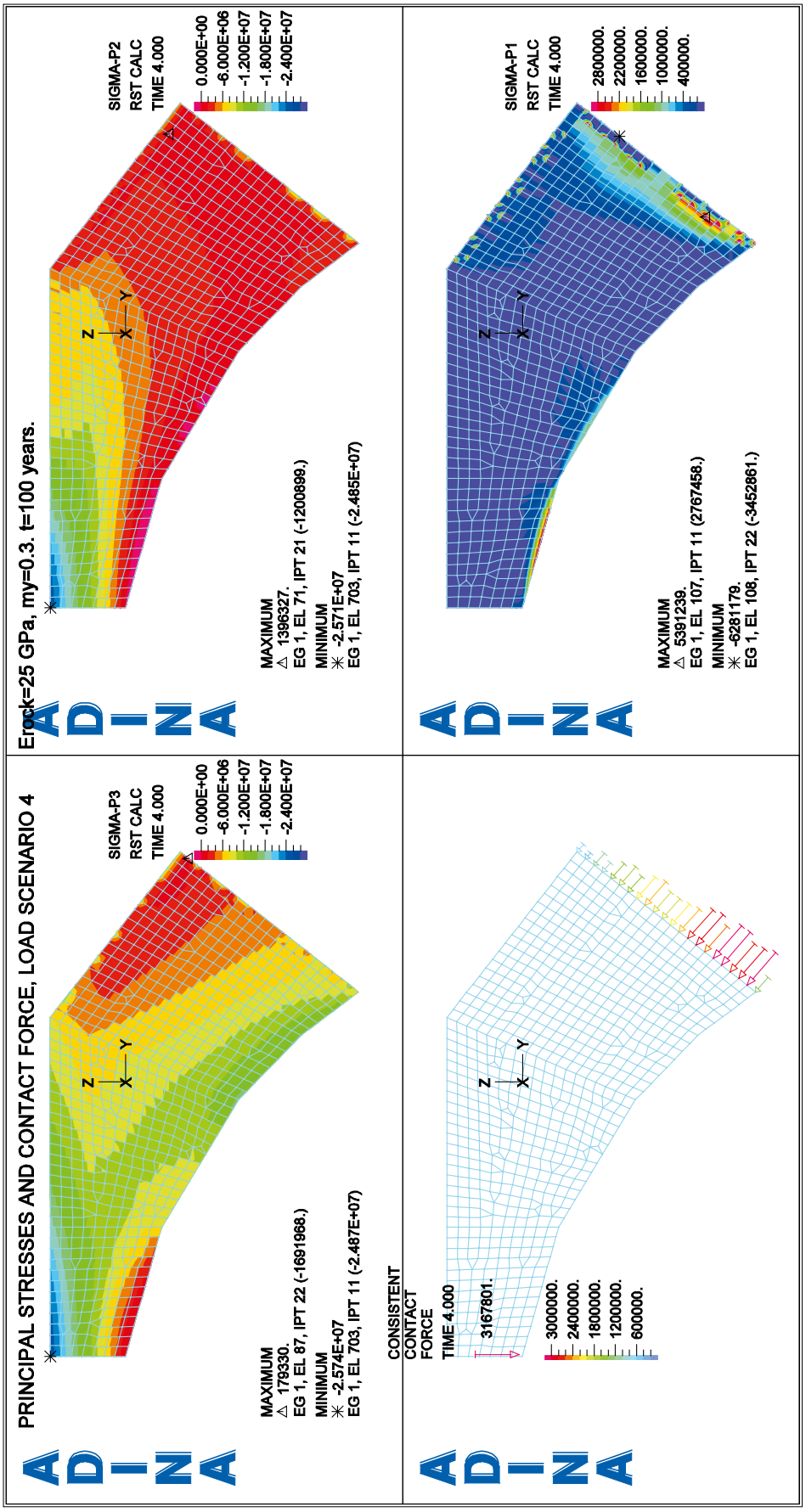

Figure G-7. *Resulting stresses for the modified model, when cracked concrete has been removed, for load combination 4.1. Compressive zone x = 0.70 m.*

Node	distanse top edge [m]	σ YY [MPa]		N [MN]		N.x [MNm]
LOAD COMB. 3.1						
667	0.00	-24.85		-1.24		-0.435
666	-0.10	-20.85		-2.09		-0.521
665	-0.20	-17.34		-1.73		-0.260
664	-0.30	-14.20		-1.42		-0.071
663	-0.40	-11.05		-1.10		0.055
662	-0.50	-7.92		-0.79		0.119
661	-0.60	-4.55		-0.46		0.114
660	-0.70	-0.71		-0.04		0.012
			N=	-8.87	MN	M= -0.987 MNm
				-8869	kN	-987 kNm

control	distance top edge [m]	σ YY=N/A + M/W [MPa]
top	0.000	-24.76
bott	-0.700	-0.58

Node	distanse top edge [m]	σ YY [MPa]		N [MN]		N.x [MNm]
LOAD COMB. 4.1						
667	0.00	-25.73		-1.29		-0.450
666	-0.10	-21.57		-2.16		-0.539
665	-0.20	-17.90		-1.79		-0.269
664	-0.30	-14.61		-1.46		-0.073
663	-0.40	-11.29		-1.13		0.056
662	-0.50	-7.99		-0.80		0.120
661	-0.60	-4.45		-0.44		0.111
660	-0.70	-0.28		-0.01		0.005
			N=	-9.08	MN	M= -1.039 MNm
				-9080	kN	-1039 kNm

control	distance top edge [m]	σ YY=N/A + M/W [MPa]
top	0.000	-25.69
bott	-0.700	-0.25

Figure G-8. *Determination of moment M and axial force N from stresses σ_y in load combination 3.1 and 4.1 obtained in the modified (i.e. reduced) model. Compressive zone x and stress σ_y for a cracked section is determined. The moment are expressed related to the system line of the modified mid cross section.*

LOAD COMB. 3.1				
667	0.00	-24.85	-1.24	-1.056
666	-0.10	-20.85	-2.09	-1.564
665	-0.20	-17.34	-1.73	-1.127
664	-0.30	-14.20	-1.42	-0.781
663	-0.40	-11.05	-1.10	-0.497
662	-0.50	-7.92	-0.79	-0.277
661	-0.60	-4.55	-0.46	-0.114
660	-0.70	-0.71	-0.04	-0.005

		N=	-8.87	MN
			-8869	kN
		M=	-5.421	MNm
			-5421	kNm

LOAD COMB. 4.1				
667	0.00	-25.73	-1.29	-1.094
666	-0.10	-21.57	-2.16	-1.618
665	-0.20	-17.90	-1.79	-1.164
664	-0.30	-14.61	-1.46	-0.803
663	-0.40	-11.29	-1.13	-0.508
662	-0.50	-7.99	-0.80	-0.280
661	-0.60	-4.45	-0.44	-0.111
660	-0.70	-0.28	-0.01	-0.002

		N=	-9.08	MN
			-9080	kN
		M=	-5.579	MNm
			-5579	kNm

Figure G-9. *Determination of moment M and axial force N from stresses σ_y in load combination 3.1 and 4.1 obtained in the modified (i.e. reduced) model. Compressive zone x and stress σ_y for a cracked section is determined. The moment are expressed related to the system line of the original (i.e. not reduced) mid cross section.*

G.5.3 Comment on the results

A comparison of the resulting stress distribution shows that the stresses remain similar in regions away from the critical section in the middle of the concrete plug, see Figure G-10. Hence, it is appropriate to use the original model together with the simplified method presented in Sections F.2 and G.4 to determine the maximum stresses in the cracked region to describe an accurate stress distribution in the mid section of the concrete plug.

The difference in the stress distribution that occur is somewhat expected. The new maximal compression stress in the middle section is somewhat higher than the one predicted in the simplified calculation but at the same time the compression force has also increased. The latter can be interpreted as that new geometry and stiffness conditions have been modified into a more inclined system lines.

The tensile stresses appearing in the plug parts closer to the surrounding rock are further discussed in Section G.7.

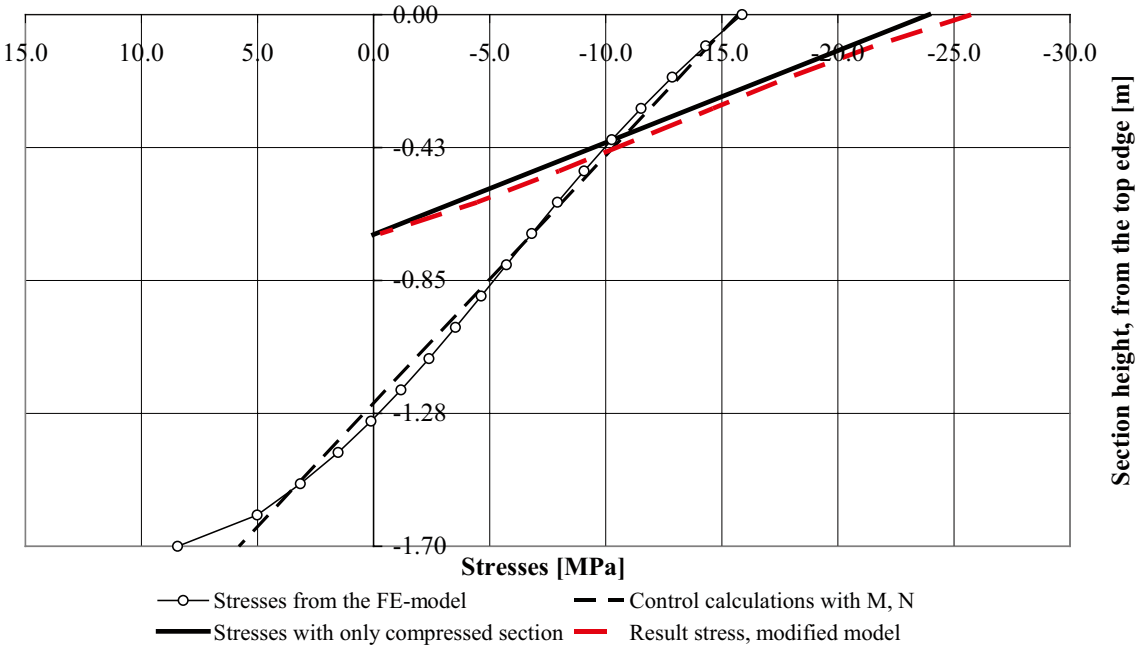

Figure G-10. *Comparison of stress distribution in plug mid section for load combination 4.1 from ADINA and values calculated using simplified method.*

G.6 Analysis for combinations 3.2 and 4.2

G.6.1 Results for the reduced model

The new model is created, based on the distribution of the principal tensile stress but the height of the recalculated middle section cannot be used directly. Even though the stresses compared to load combinations 3.1 and 4.1 are rather similar, the recalculation gives an eccentricity outside the section, see Figure G-11 and comment in Section F.3.

Nevertheless, it can be shown that with the help of the redistribution of stiffness and the change of the static system lines, the compressed concrete can carry the applied loads. The analyses are made iteratively, leading to a mid section height of x = 0.5 m, see Figure G-12 and Figure G-13.

Node	distanse top edge [m]	σ YY [MPa]		N [MN]		N.x [MNm]
LOAD COMB. 3.2						
783	0.00	-15.76		-0.79		-0.670
782	-0.10	-14.11		-1.41		-1.058
781	-0.20	-12.58		-1.26		-0.818
780	-0.30	-11.16		-1.12		-0.614
779	-0.40	-9.83		-0.98		-0.442
778	-0.50	-8.56		-0.86		-0.300
777	-0.60	-7.35		-0.73		-0.184
776	-0.70	-6.17		-0.62		-0.093
775	-0.80	-5.01		-0.50		-0.025
774	-0.90	-3.85		-0.38		0.019
773	-1.00	-2.67		-0.27		0.040
772	-1.10	-1.45		-0.15		0.036
771	-1.20	-0.17		-0.02		0.006
770	-1.30	1.21		0.12		-0.054
769	-1.40	2.72		0.27		-0.150
768	-1.50	4.46		0.45		-0.290
767	-1.60	6.45		0.65		-0.484
766	-1.70	10.29		0.51		-0.437
			N=	-7.08	MN	M= -5.517 MNm
				-7081	kN	-5517 kNm
LOAD COMB. 4.2						
783	0.00	-16.74		-0.84		-0.711
782	-0.10	-14.94		-1.49		-1.120
781	-0.20	-13.27		-1.33		-0.862
780	-0.30	-11.71		-1.17		-0.644
779	-0.40	-10.23		-1.02		-0.460
778	-0.50	-8.83		-0.88		-0.309
777	-0.60	-7.48		-0.75		-0.187
776	-0.70	-6.16		-0.62		-0.092
775	-0.80	-4.86		-0.49		-0.024
774	-0.90	-3.56		-0.36		0.018
773	-1.00	-2.23		-0.22		0.033
772	-1.10	-0.86		-0.09		0.022
771	-1.20	0.58		0.06		-0.020
770	-1.30	2.12		0.21		-0.096
769	-1.40	3.82		0.38		-0.210
768	-1.50	5.77		0.58		-0.375
767	-1.60	8.00		0.80		-0.600
766	-1.70	12.44		0.62		-0.529
			N=	-6.60	MN	M= -6.168 MNm
				-6597	kN	-6168 kNm

control	distance top edge [m]	σ YY=N/A + M/W [MPa]
top	0.000	-15.62
bott	-1.700	7.29

control	distance top edge [m]	σ YY=N/A + M/W [MPa]
top	0.000	-16.69
bott	-1.700	8.92

excentricity, top edge: e'=h/2-M/N= -0.08 [m]
compr. zone height: x=3*(h/2-M/N)= -0.25 [m]

recalculated stress, compression only

top	0.000	0.00	[MPa]
	0.255	-51.80	[MPa]

Figure G-11. *Determination of moment M and axial force N from stresses σ_y in load combination 3.2 and 4.2. Compressive zone x and stress σ_y for a cracked section is determined.*

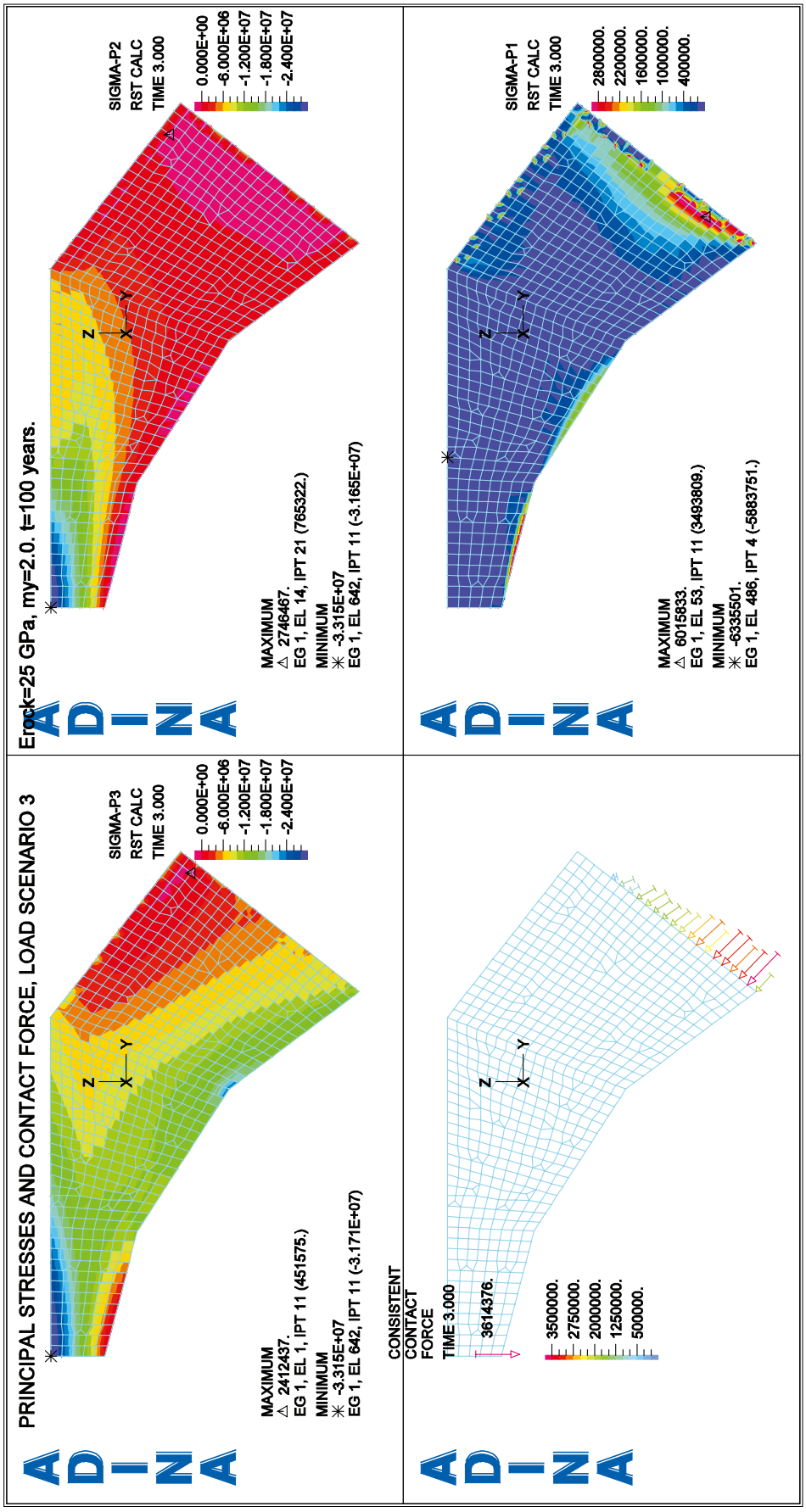

Figure G-12. *Resulting stresses for the modified model, when cracked concrete has been removed, for load combination 3.2. Compressive zone x = 0.50 m.*

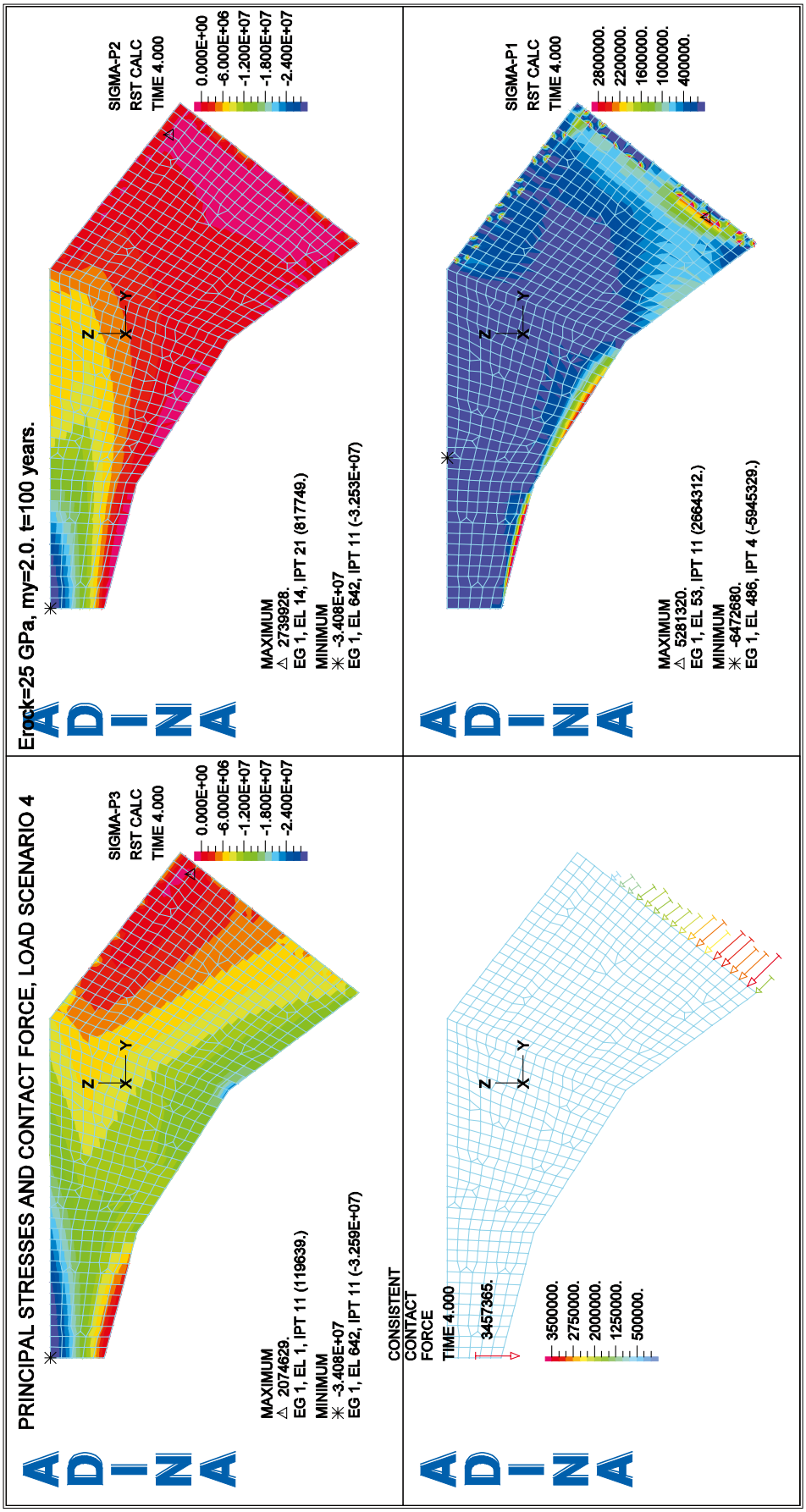

Figure G-13. *Resulting stresses for the modified model, when cracked concrete has been removed, for load combination 4.2. Compressive zone x = 0.50 m.*

Node	distanse top edge [m]	σ YY [MPa]		N [MN]		N.x [MNm]
LOADCOMB. 3.2						
637	0.00	-33.15		-1.66		-0.414
636	-0.10	-26.10		-2.61		-0.391
635	-0.20	-19.89		-1.99		-0.099
634	-0.30	-14.04		-1.40		0.070
633	-0.40	-7.99		-0.80		0.120
632	-0.50	-1.20		-0.06		0.015
			N=	-8.52	MN	M= -0.700 MNm
				-8518	kN	-700 kNm

control	distance top edge [m]	σ YY=N/A + M/W [MPa]
top	0.000	-33.84
bott	-0.500	-0.23

Node	distanse top edge [m]	σ YY [MPa]		N [MN]		N.x [MNm]
LOADCOMB. 4.2						
637	0.00	-34.08		-1.70		-0.426
636	-0.10	-26.77		-2.68		-0.402
635	-0.20	-20.31		-2.03		-0.102
634	-0.30	-14.21		-1.42		0.071
633	-0.40	-7.90		-0.79		0.118
632	-0.50	-0.67		-0.03		0.008
			N=	-8.66	MN	M= -0.731 MNm
				-8655	kN	-731 kNm

control	distance top edge [m]	σ YY=N/A + M/W [MPa]
top	0.000	-34.86
bott	-0.500	0.24

Figure G-14. *Determination of moment M and axial force N from stresses σ_y in load combination 3.2 and 4.2 obtained in the modified (i.e. reduced) model. Compressive zone x and stress σ_y for a cracked section is determined. The moment are expressed related to the system line of the modified mid cross section.*

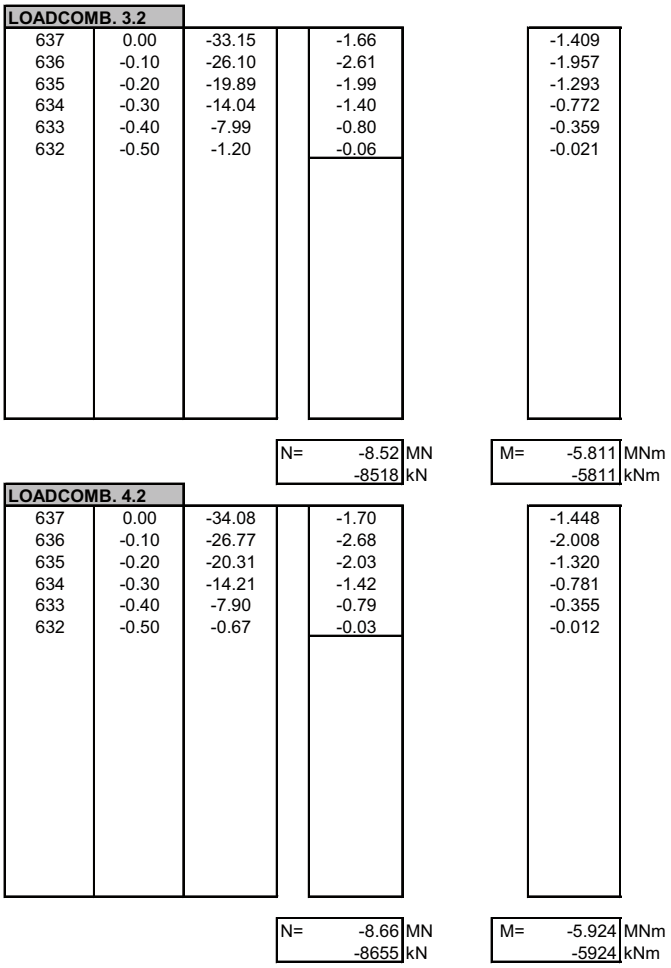

Figure G-15. *Determination of moment M and axial force N from stresses σ_y in load combination 3.2 and 4.2 obtained in the modified (i.e. reduced) model. Compressive zone x and stress σ_y for a cracked section is determined. The moment are expressed related to the system line of the original (i.e. not reduced) mid cross section.*

G.6.2 Comment on the results

The results of the modified model confirm those made for load combinations 3.1 and 4.1 in Section G.5.2. The compression force increases with the same margin, and at the same time the moment in the section is also reduced.

The tensile stresses appearing in the plug parts closer to the surrounding rock are further discussed in Section G.7.

G.7 Tensile stresses near the support line

In Figure G-16 to Figure G-17 and Figure G-18 to Figure G-19 the principal stresses in the concrete plug is shown for load combination 3.2 and 4.2, respectively.

From Figure G-16 and Figure G-18 it is found that there is a limited portion of the underside of the plug in the region where a reduction of the cross section has been made that cracks will appear. However, the approximation made is deemed to be good enough and the error obtained has negligible effect on the stresses in the plug mid section.

It is also shown that there will form cracks in a region close to the rock surface. However, as shown in Figure G-17 and Figure G-19, these cracks are directed perpendicular to the rock surface, and will therefore not affect the water tightness of the plug. Consequently, the appearances of these cracks are not deemed to be critical.

The appearances of such cracks are likely due to the restrain obtained due to the combination of concrete shrinkage and frictional forces between plug and rock. When a lower frictional coefficient is used the tensile stresses obtained in this region decrease, even though they do not fully disappear. In reality, though, there will presumable form only one or two such cracks since the tensile stresses acting on the concrete will decrease once the first crack appear.

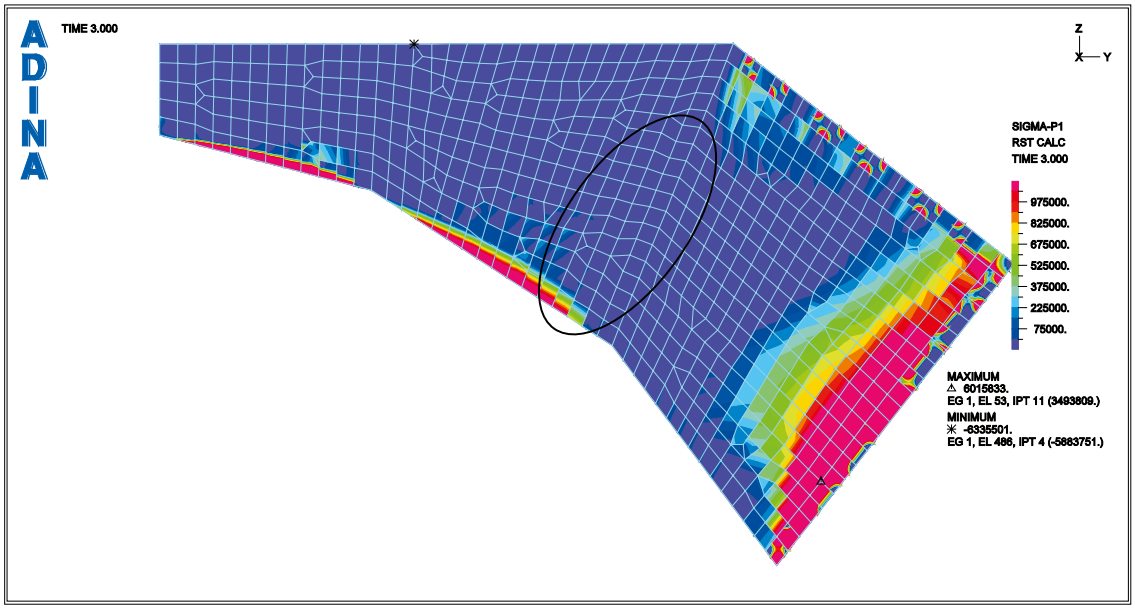

Figure G-16. *Principal stress σ_1 (maximal stress) in concrete plug when subjected to load combination 3.2 showing stresses ranging from 0 (purple) to 1 MPa (pink). Marked region is shown in Figure G-17. Compressive zone x = 0.50 m.*

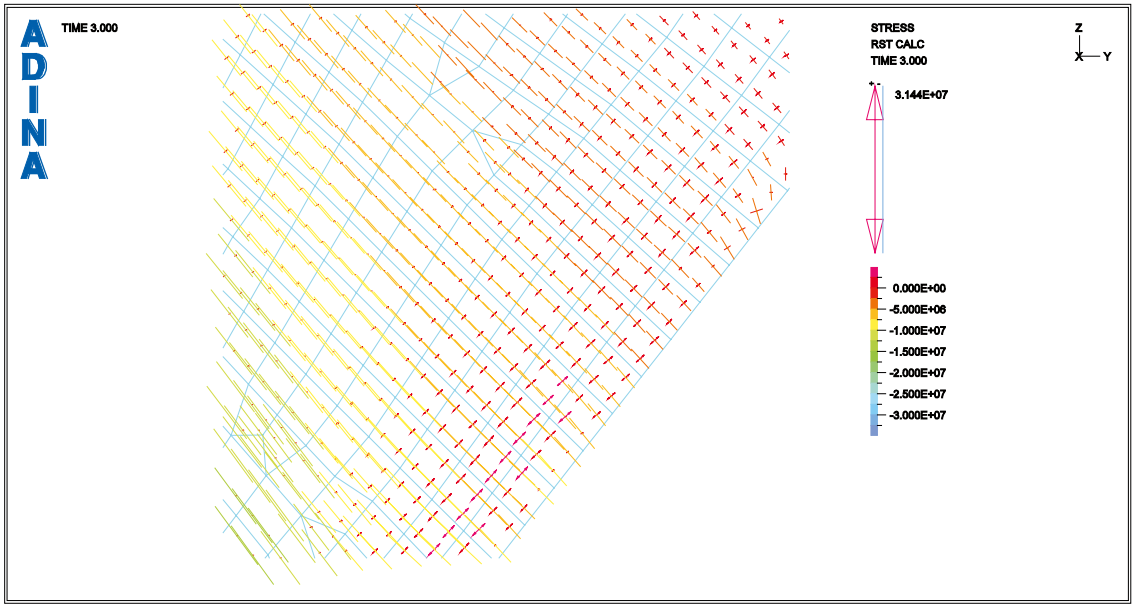

Figure G-17. *Vector plot of principal stresses σ_1 for load combination 3.2 in region marked in Figure G-16. The directions of the tensile stresses indicate the crack direction to be perpendicular to the rock surface.*

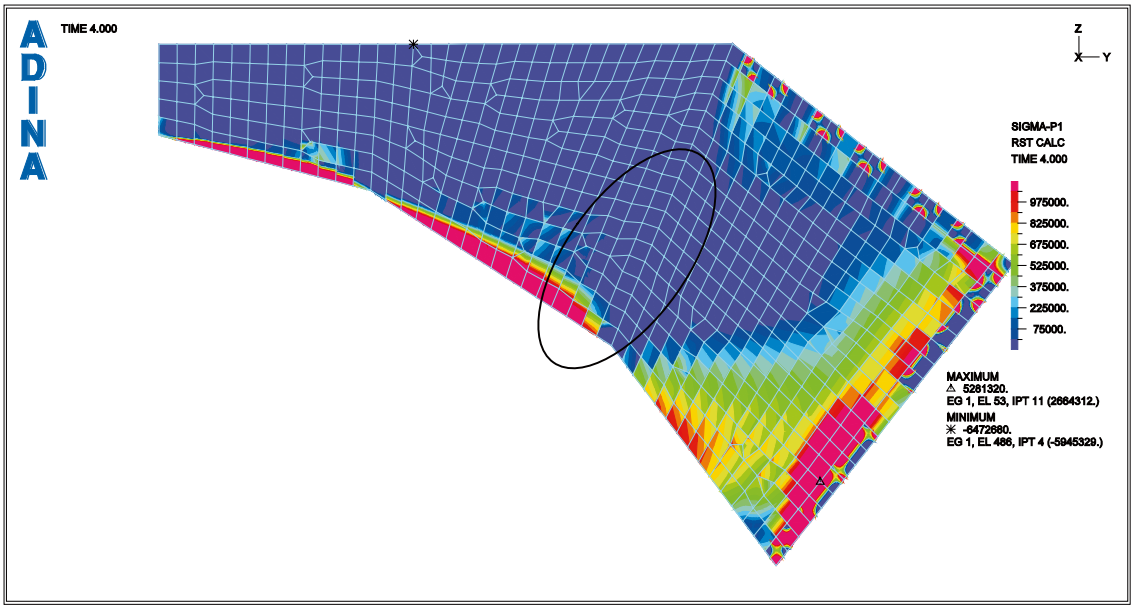

Figure G-18. *Principal stress σ_1 (maximal stress) in concrete plug when subjected to load combination 4.2 showing stresses ranging from 0 (purple) to 1 MPa (pink). Marked region is shown in Figure G-19. Compressive zone x = 0.50 m.*

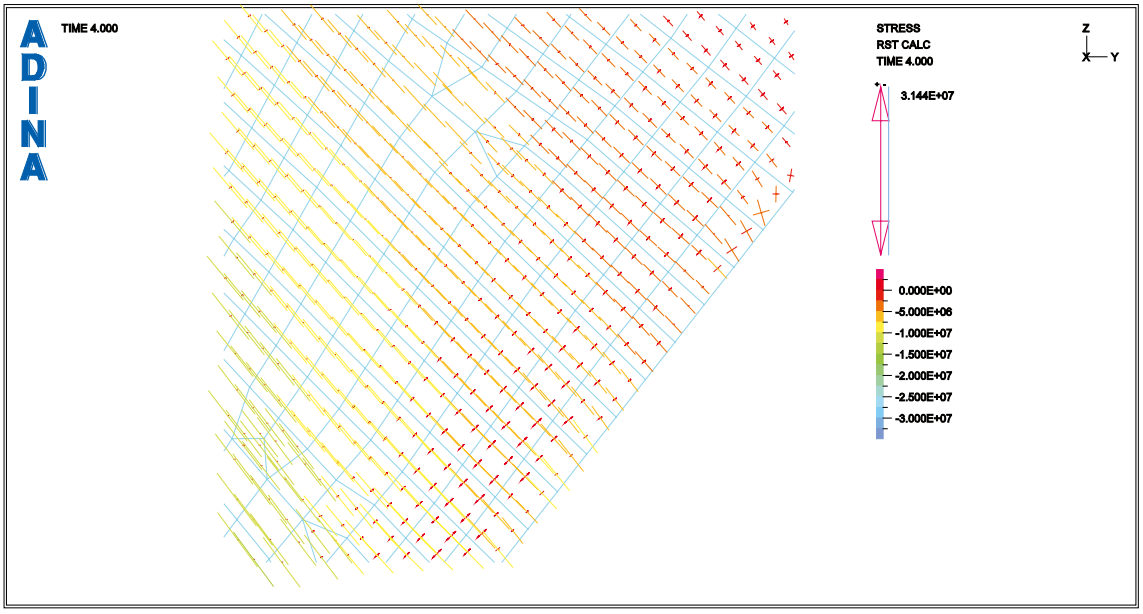

Figure G-19. *Vector plot of principal stresses σ_1 for load combination 4.2 in region marked in Figure G-18. The directions of the tensile stresses indicate the crack direction to be perpendicular to the rock surface.*

G.8 Hoop-stresses

The out-of-plane stresses, i.e. hoop-stresses σ_x, obtained are shown in Figure G-20 and Figure G-21. This can be compared with the principal stresses shown in Figure G-13 and hence be used to get an idea of what part of the load is carried in the plane and out-of-plane, respectively.

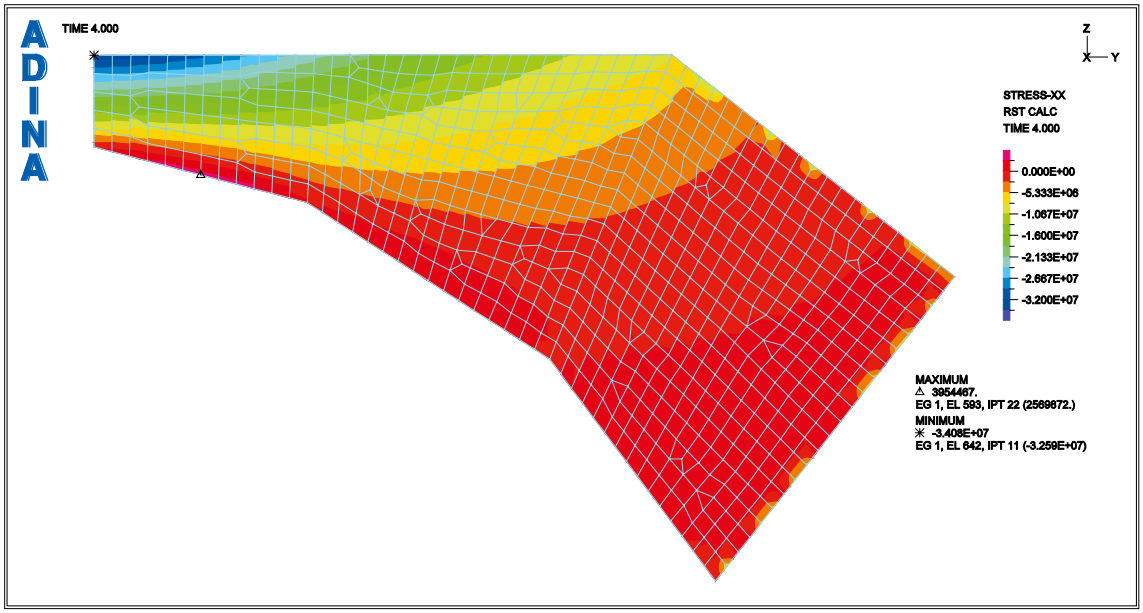

Figure G-20. *Out of plane hoop-stresses σ_x in concrete plug when subjected to load combination 4.2 showing stresses ranging from –30 MPa (purple) to 0 MPa (pink). Compressive zone x = 0.50 m.*

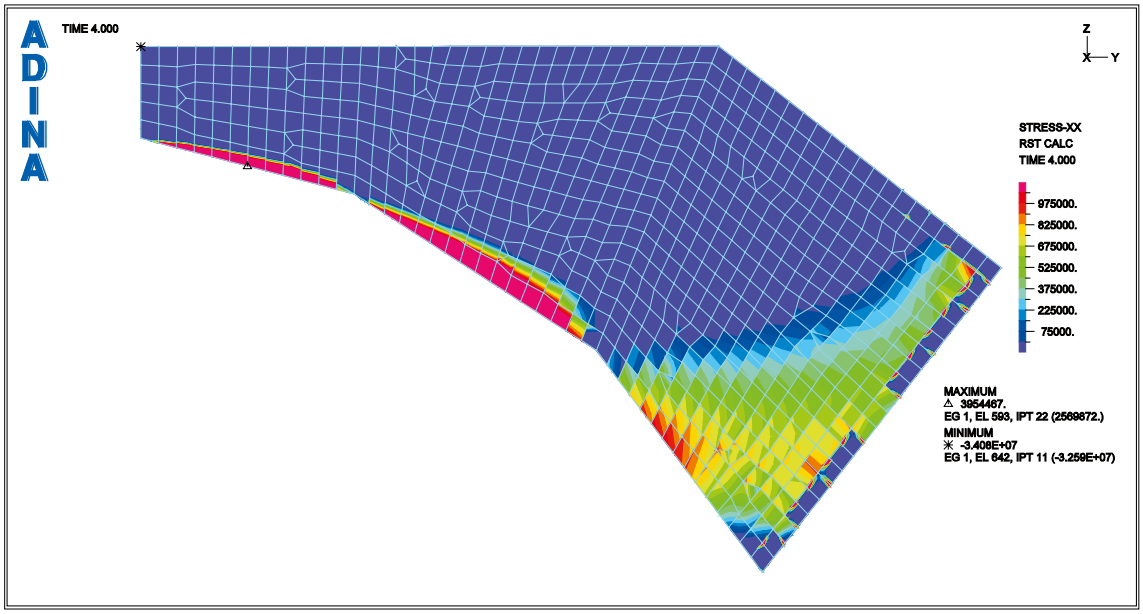

Figure G-21. *Out of plane hoop-stresses σ_x in concrete plug when subjected to load combination 4.2 showing stresses ranging from 0 (purple) to 1 MPa (pink). Compressive zone x = 0.50 m.*

Appendix H

Verification of FE model

The verification of the FE model is done with an analytical solution for a circular plate. The plate is assumed to be fully uncracked and subjected to an evenly distributed pressure of 2 MPa only. The results obtained are used to verify the use of the finite element model. The plug part connecting to the rock is not compared in this verification. The assumption here is that the relatively flat part of the centre line of the plug can be seen as a circular plate, with full restrain at the outer ring, see Figure H-2.

The choice for outer boundaries cannot be pinpointed directly, as the centre line of the flat part is somewhat shorter than the loaded vertical surface. A compromising assumption is made, that both lengths are evaluated and the results be seen as a lower and upper boundaries for the control. The calculation procedure for the circular plates uses the annotations given in Figure H-2.

In the case that we have assumed as valid, fully restrained plate, formulas according to Figure H-3.

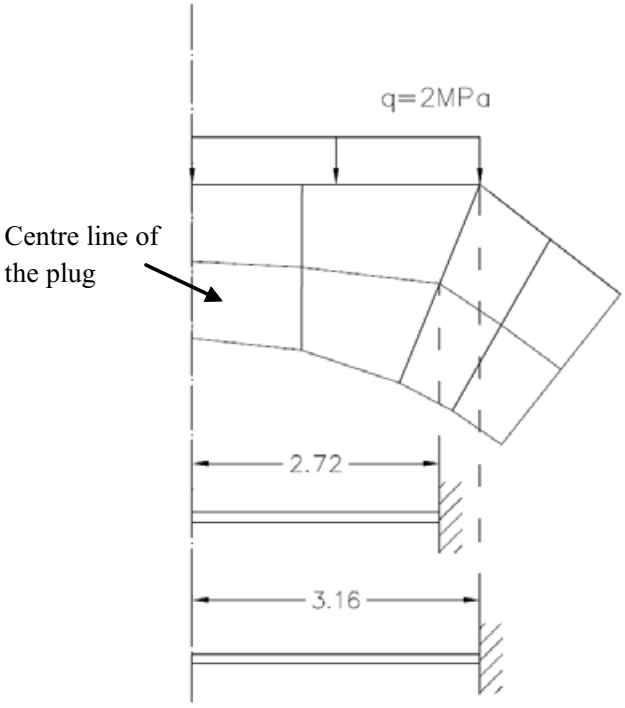

Figure H-1. *Centre line of the plug and assumed radium for the circular plate.*

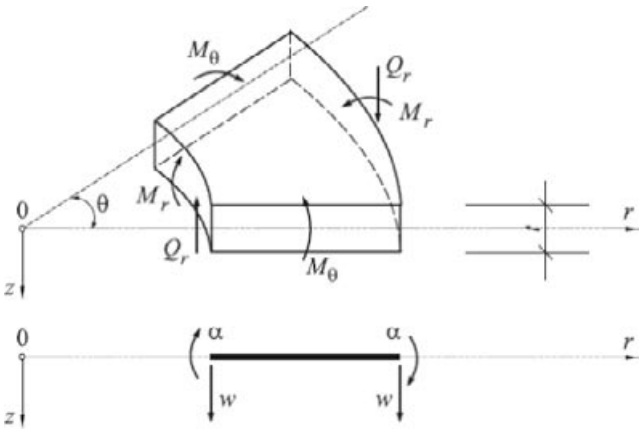

Figure H-2. *Annotation for the circular plate calculation.*

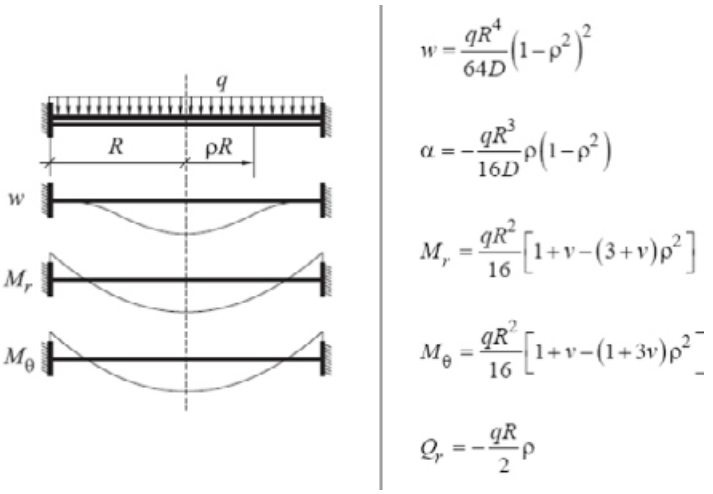

Figure H-3. *Formulas used in the verification.*

The horizontal force in the plate will be estimated from the inclination angle at the support.

Material properties: $E_c := 27.6GPa$ $\upsilon := 0.27$

Load: $q := 2MPa$

Moment calculation with L=2,72 m:

Moment calculation with L=2,72 m:

$R_{plate} := 2.72m$

Moment in the centre of the plug: $\rho := 0$

$$M_r := \frac{q \cdot R_{plate}^2}{16} \cdot \left[1 + \upsilon - (3 + \upsilon) \cdot \rho^2\right] \qquad M_r = 1.174 \cdot \frac{MN \cdot m}{m}$$

Reactions at the support line: $\rho := 1$

$$M_r := \frac{q \cdot R_{plate}^2}{q \cdot R16} \cdot \left[1 + \upsilon - (3 + \upsilon) \cdot \rho^2\right] \qquad M_r = -1.85 \cdot \frac{MN \cdot m}{m}$$

$$Q_r := -\frac{plate}{q \cdot R2} \cdot \rho \qquad Q_r = -2.72 \cdot \frac{MN}{m}$$

Estimation of the axial force in the plate:

angle at the support: $\alpha := 52deg$

$$Q_r = -2.72 \cdot \frac{MN}{m}$$

$$N := \frac{Q_r}{\tan(\alpha)} = -2.125 \cdot \frac{MN}{m}$$ (N is the horisontal force in the plate)

Moment calculation with L=3,16 m:

$R_{plate} := 3.16m$

Moment in the centre of the plug: $\rho := 0$

$$M_r := \frac{q \cdot R_{plate}^2}{16} \cdot \left[1 + \upsilon - (3 + \upsilon) \cdot \rho^2\right] \qquad M_r = 1.585 \cdot \frac{MN \cdot m}{m}$$

Reactions at the support line: $\rho := 1$

$$M_r := \frac{q \cdot R_{plate}^2}{16} \cdot \left[1 + \upsilon - (3 + \upsilon) \cdot \rho^2\right] \qquad M_r = -2.496 \cdot \frac{MN \cdot m}{m}$$

$$Q_r := -\frac{q \cdot R_{plate}}{2} \cdot \rho \qquad Q_r = -3.16 \cdot \frac{MN}{m}$$

Estimation of the axial force in the plate:

angle at the support: $\alpha := 52deg$

$$Q_r = -3.16 \cdot \frac{MN}{m}$$

$$N := \frac{Q_r}{\tan(\alpha)} = -2.469 \cdot \frac{MN}{m}$$ (N is the horisontal force in the plate)

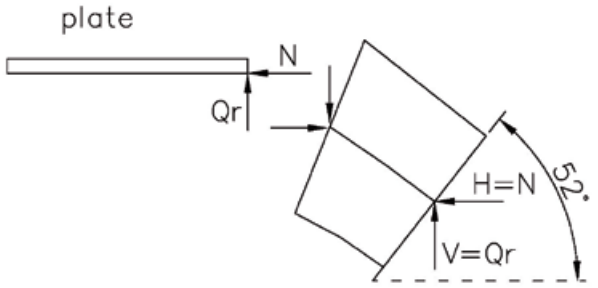

Figure H-4. *Geometrical prerequisites in the plate for determination of the normal force N in the centre of the plate.*

The results of the analytical solution are as follows (M, N – centre of the plate):

R=2.72 m (lower boundary): M = 1.17 MNm N= –2.13 MN

R=3.16 m (upper boundary): M = –1.59 MNmN= –2.45 MN

The analytical solution is compared to the 2D axis-symmetrical model used in the report. The axis-symmetrical model is also adjusted so that it has the same assumptions as the analytical solution:

- full restrain on the support boundary,
- evenly distributed load of 2 MPa on the vertical part only.

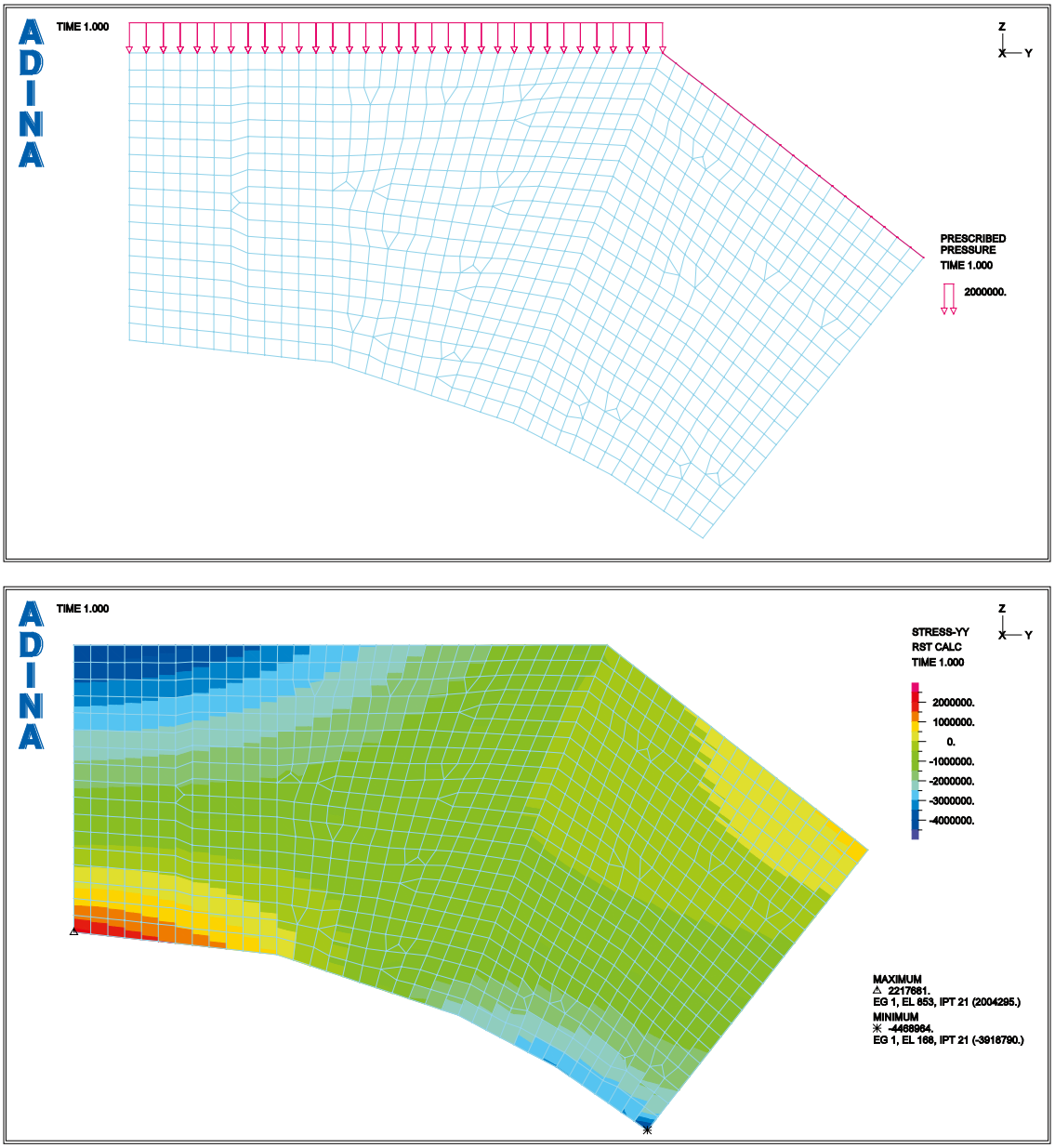

Figure H-5. *Loading and stress plots for 2D axis-symmetrical model.*

The moment and normal section forces are then calculated as previously done in Chapter Appendix F.

Node	distanse top edge [m]	σ YY [MPa]		N [MN]		N.x [MNm]
LOADCASE 1						
783	0.00	-4.45		-0.22		-0.189
782	-0.10	-4.00		-0.40		-0.300
781	-0.20	-3.60		-0.36		-0.234
780	-0.30	-3.22		-0.32		-0.177
779	-0.40	-2.87		-0.29		-0.129
778	-0.50	-2.55		-0.25		-0.089
777	-0.60	-2.24		-0.22		-0.056
776	-0.70	-1.94		-0.19		-0.029
775	-0.80	-1.65		-0.16		-0.008
774	-0.90	-1.36		-0.14		0.007
773	-1.00	-1.06		-0.11		0.016
772	-1.10	-0.75		-0.08		0.019
771	-1.20	-0.43		-0.04		0.015
770	-1.30	-0.08		-0.01		0.004
769	-1.40	0.31		0.03		-0.017
768	-1.50	0.76		0.08		-0.049
767	-1.60	1.28		0.13		-0.096
766	-1.70	2.22		0.11		-0.094

N=	-2.45	MN
	-2451	kN

M=	-1.408	MNm
	-1408	kNm

control	distance top edge [m]	σ YY=N/A + M/W [MPa]
top	0.000	-4.36
bott	-1.700	1.48

Stresses in the center of the plugg - recalculation with section forces

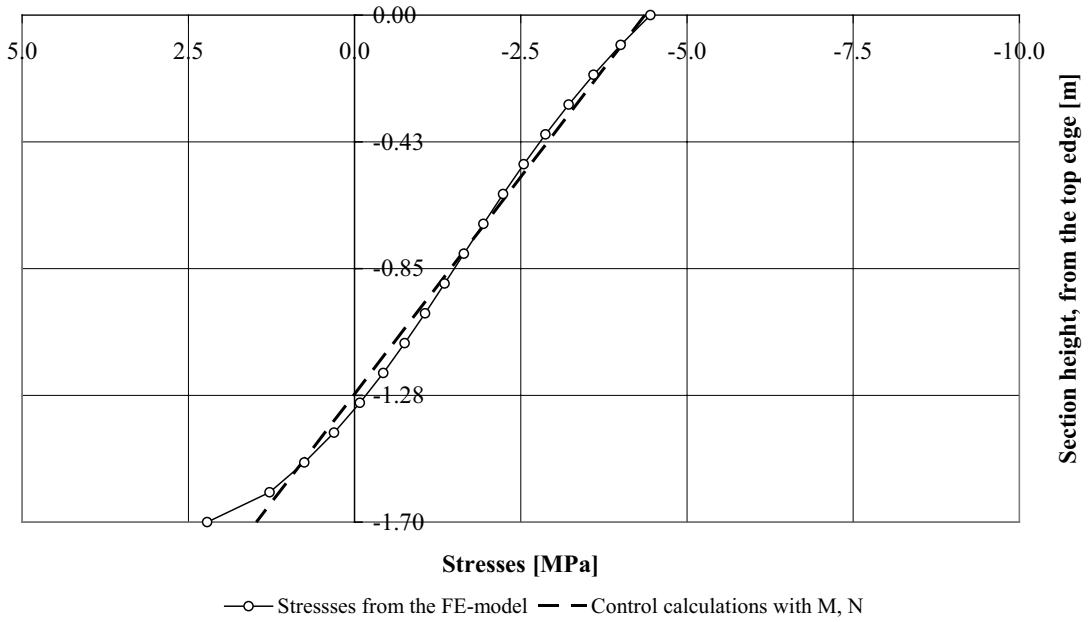

The results of the beam model are as follows (M, N, centre of the plug):

M = 1.41 MNm N= –2.45 MN

It is rather clear that the two models still have differences – in terms of boundary conditions, geometry etc. Nevertheless, the comparison does show that the results from the 2D axis-symmetrical model fit well in the upper and lower boundary presented by the analytical solution.

Appendix I

Input data to ADINA

I.1 Geometry elements

The model geometry is imported from a DXF-file (not presented in the report) and the numbering of points, lines and surfaces is automatically obtained in the import process.

In Figure I-1 to Figure I-3 the different geometry elements are presented, and are referred to often in the input text files presented in I.2.

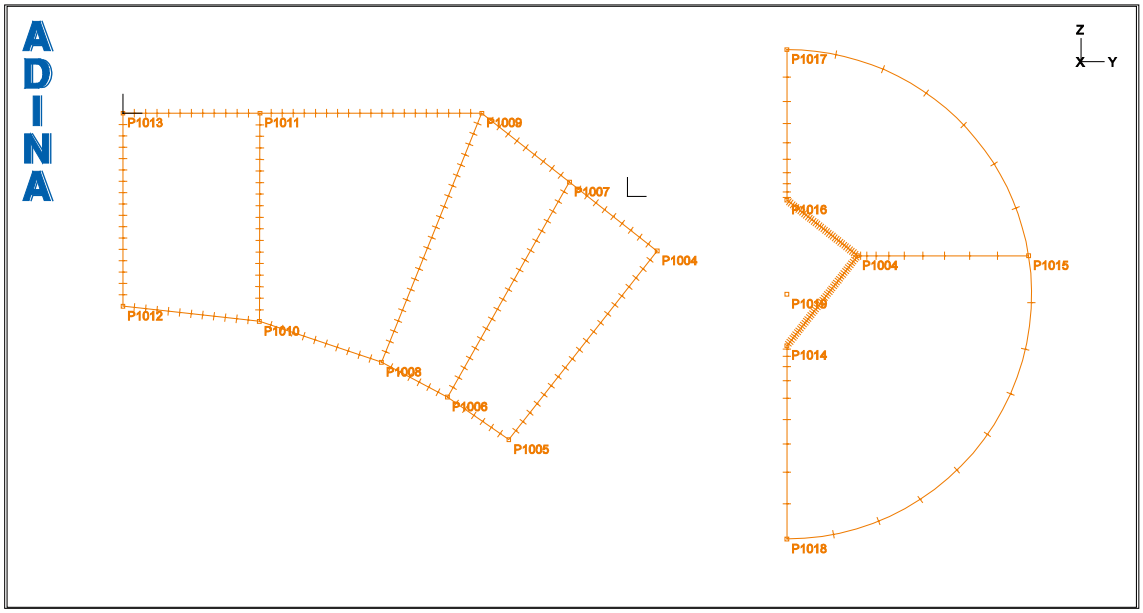

Figure I-1. *Point numbering.*

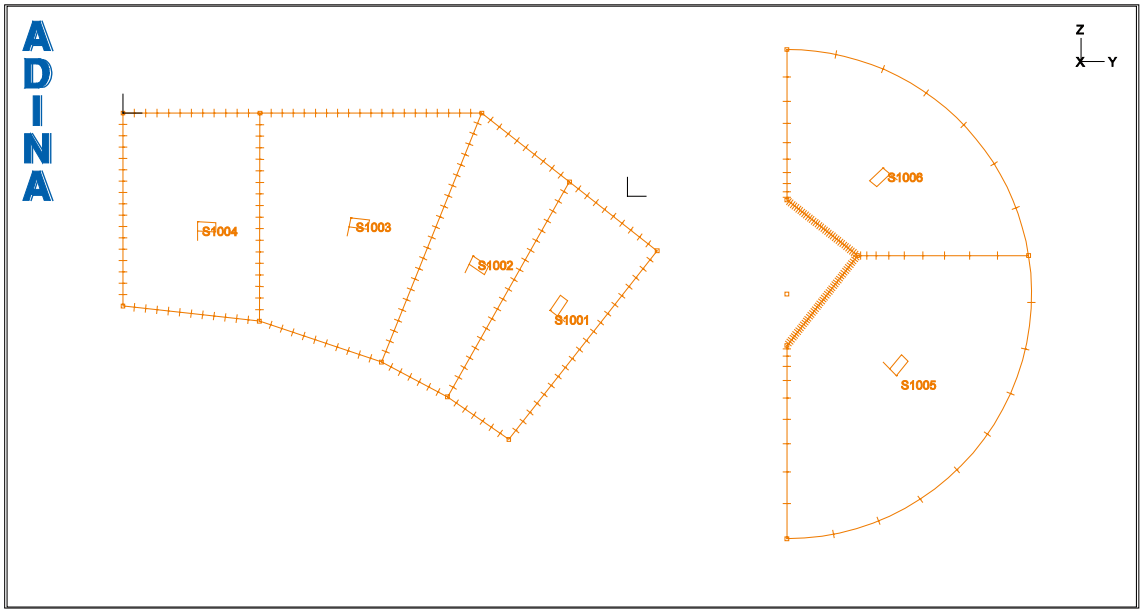

Figure I-2. *Line numbering.*

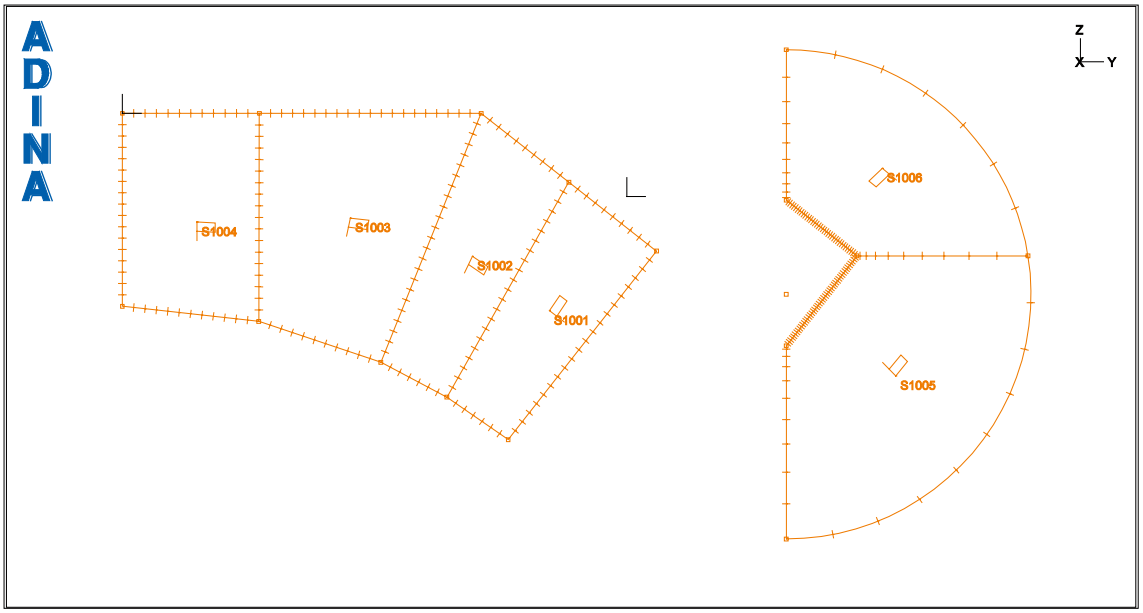

Figure I-3. *Surface numbering.*

I.2 Text input files

I.2.1 Indata_structural

```
indata_structural.in                                                    2008-12-11

CONTROL UNDO=-1 AUTOMREBUILD=NO
FILEECHO OPTION=FILE F=loggfil.ut
FILELOG OPTION=FILE F=loggfil.ut

******** geometry and elements

READ F='modell/geometry.in'

SUBDIVIDE MODEL MODE=LENGTH SIZE=0.100000000000000 NDIV=1 PROGRESS=GEOMETRIC MINCUR=1

SUBDIVIDE LINE NAME=1000 MODE=LENGTH SIZE=1.0
@CLEAR
1023
1022
@

SUBDIVIDE LINE NAME=1000 MODE=DIVISIONS NDIV=10 RATIO=10 PROGRESS=ARITHMETIC
@CLEAR
1018
1019
1020
@

SUBDIVIDE LINE NAME=1000 MODE=LENGTH SIZE=0.05
@CLEAR
1017
1021
@


READ F='modell/material.in'

READ F='modell/contact_2.in'

READ F='modell/shell_elements.in'

READ F='modell/boundary.in'



KINEMATICS DISPLACE=LARGE STRAINS=SMALL UL-FORMU=DEFAULT PRESSURE=NO,
     INCOMPAT=AUTOMATIC RIGIDLIN=NO
*

MASTER ANALYSIS=STATIC MODEX=EXECUTE TSTART=0.00000000000000 IDOF=0,
     OVALIZAT=NONE FLUIDPOT=AUTOMATIC CYCLICPA=1 IPOSIT=STOP,
     REACTION=YES INITIALS=NO FSINTERA=NO IRINT=DEFAULT CMASS=NO,
     SHELLNDO=AUTOMATIC AUTOMATI=OFF SOLVER=SPARSE,
     CONTACT-=CONSTRAINT-FUNCTION TRELEASE=0.00000000000000,
     RESTART-=NO FRACTURE=NO LOAD-CAS=YES LOAD-PEN=NO MAXSOLME=0,
     MTOTM=2 RECL=3000 SINGULAR=YES STIFFNES=0.000100000000000000,
     MAP-OUTP=NONE MAP-FORM=NO NODAL-DE='' POROUS-C=NO ADAPTIVE=0,
     ZOOM-LAB=1 AXIS-CYC=0 PERIODIC=NO VECTOR-S=GEOMETRY EPSI-FIR=NO,
     STABILIZ=YES STABFACT=1.00000000000000E-10 RESULTS=PORTHOLE,
     FEFCORR=NO BOLTSTEP=1 EXTEND-S=YES CONVERT-=NO DEGEN=YES,
     TMC-MODE=NO ENSIGHT-=NO



READ F='laster.in'
```

I.2.2 Geometry

```
geometry.in                                                                    2008-12-11

*120 00930 - Concrete plug


**********
COORDINATE POINTS SYSTEM=0
1000    -5      0       -5

LINE EXTRUDED NAME=1000 POINT=1000 DX=0.25 SYSTEM=0 PCOINCID=YES PTOLERAN=1.0E-05

SURFACE EXTRUDED NAME=1000 LINE=1000 DZ=0.25 SYSTEM=0 PCOINCID=YES PTOLERAN=1.0E-05 NDIV=1
OPTION=VECTOR

LOADDXF 'modell/geometri/2D.dxf' GCT=0.001


LINE ARC NAME=1022 MODE=1 P1=1018 P2=1015 CENTER=1019 PCOINCID=YES,
     PTOLERAN=1.00000000000000E-05 MODIFY-L=YES DELETE-P=YES

LINE ARC NAME=1023 MODE=1 P1=1015 P2=1017 CENTER=1019 PCOINCID=YES,
     PTOLERAN=1.00000000000000E-05 MODIFY-L=YES DELETE-P=YES


SURFACE PATCH NAME=1005 EDGE1=1017 EDGE2=1020 EDGE3=1022 EDGE4=1018

SURFACE PATCH NAME=1006 EDGE1=1018 EDGE2=1023 EDGE3=1019 EDGE4=1021
```

I.2.3 Boundary

```
boundary.in                                                    2008-12-11

*120 00930 - Concrete plug

FIXBOUNDARY SURFACES FIXITY=ALL
@CLEAR
@

FIXBOUNDARY POINTS FIXITY=ALL
@CLEAR
@

FIXITY NAME=SYMM
@CLEAR
 'Y-TRANSLATION'
 'X-ROTATION'
 'OVALIZATION'
@

FIXITY NAME=SLIPP
@CLEAR
 'Z-TRANSLATION'
 'X-ROTATION'
 'OVALIZATION'
@
*

FIXBOUNDARY LINES FIXITY=ALL
@CLEAR
*1017  'SLIPP'
*1015  'SYMM'
1023 'ALL'
1022 'ALL'
@
```

I.2.4 Material

```
material.in                                                                    2008-12-11

*120 00930 - Concrete plug


**betong**
MATERIAL ELASTIC NAME=1 E=26.7E+9 NU=0.27 DENSITY=2400 ALPHA=1e-5

**berg**
MATERIAL ELASTIC NAME=2 E=50E+9 NU=0.2 DENSITY=2400 ALPHA=1e-15

*Materialparametrarna för berget uppdateras för varje model
*i laster.in
*
*
*
```

I.2.5 Contact

```
contact_2.in                                                                    2008-12-11

*120 00930 - Concrete plug

CONTACT-CONT NSUPPRES=10 SEGMENT-=YES POSTIMPA=NO,
     CONTACT-=CONSTRAINT-FUNCTION XCONT-AL=KINEMATIC-CONSTRAINT,
     RT-SUBD=MAGNITUDE CSTYPE=NEW RT-ALGOR=CURRENT DISPLACE=LARGE,
     FRICTION=CURRENT DAMPING=NO DAMP-NOR=0.00000000000000,
     DAMP-TAN=0.00000000000000 TENSION-=YES
*
CGROUP CONTACT2 NAME=1 SUBTYPE=DEFAULT FORCES=YES TRACTION=YES,
     NODETONO=NO FRICTION=0.00000000000000 EPSN=1.00000000000000E-12,
     EPST=0.00000000000000 DIRECTIO=NORMAL CONTINUO=YES,
     INITIAL-=ALLOWED PENETRAT=ONE DEPTH=0.00000000000000,
     OFFSET=0.00000000000000 OFFSET-T=CONSTANT CORNER-C=NO,
     TBIRTH=0.00000000000000 TDEATH=0.00000000000000 TIED=NO,
     TIED-OFF=0.00000000000000 HHATIMC=0.00000000000000,
     FCTMC=0.500000000000000 FTTMC=0.500000000000000 RIGID-TA=NO,
     NORMAL-S=1.00000000000000E+11 TANGENTI=0.00000000000000,
     PTOLERAN=1.00000000000000E-08 RESIDUAL=0.00100000000000000,
     LIMIT-FO=1.00000000000000 ITERATIO=2 TIME-PEN=0.00000000000000,
     CONSISTE=DEFAULT USER-FRI=NO DESCRIPT='NONE',
     CFACTOR1=0.00000000000000 CS-EXTEN=0.00100000000000000,
     ALGORITH=DEFAULT RTP-CHEC=NO RTP-MAX=0.00100000000000000,
     XDAMP=NO XNDAMP=0.100000000000000 DISPLACE=DEFAULT FRIC-DEL=NO,
     GAP-VALU=0.00000000000000 EKTMC=0.00000000000000


CONTACTSURFA NAME=1 PRINT=DEFAULT SAVE=DEFAULT SOLID=NO BODY=0,
     ORIENTAT=INPUT SENSE=1 MARQUEEB=0 DESCRIPT='NONE'
@CLEAR
1017 -1 0
@


CONTACTSURFA NAME=2 PRINT=DEFAULT SAVE=DEFAULT SOLID=NO BODY=0,
     ORIENTAT=AUTOMATIC MARQUEEB=0 DESCRIPT='NONE'
@CLEAR
1004 -1 0
@

CONTACTSURFA NAME=11 PRINT=DEFAULT SAVE=DEFAULT SOLID=NO BODY=0,
     ORIENTAT=INPUT SENSE=1 MARQUEEB=0 DESCRIPT='NONE'
@CLEAR
1021 1 0
@


CONTACTSURFA NAME=12 PRINT=DEFAULT SAVE=DEFAULT SOLID=NO BODY=0,
     ORIENTAT=AUTOMATIC MARQUEEB=0 DESCRIPT='NONE'
@CLEAR
1010 -1 0
1007 -1 0
@


CONTACTPAIR NAME=1 TARGET=1 CONTACTO=2 FRICTION=0.000000000000000,
     TBIRTH=0.00000000000000 TDEATH=0.00000000000000,
     HHATTMC=0.00000000000000 FCTMC=0.00000000000000,
     FTTMC=0.00000000000000 NX=0 NY=0 NZ=0 OFFSETCO=BOTH,
     EKTMC=0.00000000000000

CONTACTPAIR NAME=2 TARGET=11 CONTACTO=12 FRICTION=0.000000000000000,
     TBIRTH=0.00000000000000 TDEATH=0.00000000000000,
     HHATTMC=0.00000000000000 FCTMC=0.00000000000000,
     FTTMC=0.00000000000000 NX=0 NY=0 NZ=0 OFFSETCO=BOTH,
     EKTMC=0.00000000000000

*CSURFACE NAME=1 NODES=3 NCOINCID=SURFACE,
*      NCTOLERA=1.00000000000000E-05 SUBSTRUC=0 GROUP=1
```

I.2.6 Elements

shell_elements.in 2008-12-11

```
*120 00930 - Concrete plug
*
EGROUP TWODSOLID NAME=1 SUBTYPE=AXISYMMETRIC MATERIAL=1
*
GSURFACE NODES=4 NCOINCID=BOUNDARIES NCTOLERA=1.000000000000000E-05 GROUP=1
@CLEAR
1001
1002
1003
1004
@

EGROUP TWODSOLID NAME=2 SUBTYPE=AXISYMMETRIC MATERIAL=2
*
GSURFACE NODES=4 NCOINCID=GROUP NCTOLERA=1.000000000000000E-05 GROUP=2
@CLEAR
1006
1005
@
```

I.2.7 Loads

```
laster.in                                                              2008-11-24


LOAD PRESSURE NAME=1 MAGNITUD=-6e6
LOAD PRESSURE NAME=2 MAGNITUD=-4e6
LOAD PRESSURE NAME=3 MAGNITUD=4e6
*
LOAD TEMPERATURE NAME=1 MAGNITUD=10.00000000000000
LOAD TEMPERATURE NAME=2 MAGNITUD=-10.00000000000000


LOAD-CASE NAME=1
*
LOAD-CASE NAME=2
*
LOAD-CASE NAME=3
*
LOAD-CASE NAME=4
*
LOAD-CASE NAME=5
*
LOAD-CASE NAME=6
*
LOAD-CASE NAME=7
*
LOAD-CASE NAME=8

APPLY-LOAD BODY=0 LCASE=2
@CLEAR
1  'PRESSURE' 1  'LINE' 1016 0 1
2  'PRESSURE' 1  'LINE' 1013 0 1

3  'PRESSURE' 1  'LINE' 1016 0 2
4  'PRESSURE' 1  'LINE' 1013 0 2

5  'PRESSURE' 1  'LINE' 1016 0 3
6  'PRESSURE' 1  'LINE' 1013 0 3

7  'PRESSURE' 1  'LINE' 1016 0 4
8  'PRESSURE' 1  'LINE' 1013 0 4



11 'PRESSURE' 1  'LINE' 1016 0 5
12 'PRESSURE' 2  'LINE' 1007 0 5
13 'PRESSURE' 2  'LINE' 1010 0 5
14 'PRESSURE' 1  'LINE' 1013 0 5

15 'PRESSURE' 1  'LINE' 1016 0 6
16 'PRESSURE' 2  'LINE' 1007 0 6
17 'PRESSURE' 2  'LINE' 1010 0 6
18 'PRESSURE' 1  'LINE' 1013 0 6

19 'PRESSURE' 1  'LINE' 1016 0 7
20 'PRESSURE' 2  'LINE' 1007 0 7
21 'PRESSURE' 2  'LINE' 1010 0 7
22 'PRESSURE' 1  'LINE' 1013 0 7

23 'PRESSURE' 1  'LINE' 1016 0 8
24 'PRESSURE' 2  'LINE' 1007 0 8
25 'PRESSURE' 2  'LINE' 1010 0 8
26 'PRESSURE' 1  'LINE' 1013 0 8


********  analysis


***************
*
* Lastfall 1-8
*
***************

DELETE THERMAL-MAPP


THERMAL-MAPP FILENAME='thermal_map.map' EXTERNAL=ALL TIME=0.00000000000000

*****************************

MATERIAL ELASTIC NAME=2 E=25E+9 NU=0.2 DENSITY=2400 ALPHA=7e-6
CONTACTPAIR NAME=1 TARGET=1 CONTACTO=2 FRICTION=0.3
CONTACTPAIR NAME=2 TARGET=11 CONTACTO=12 FRICTION=0.3

ADINA OPTIMIZE=SOLVER FILE='dat/modell_E25_mu03.dat' FIXBOUND=YES MID=NO OVERWRIT=YES


                                                                       1
```

```
*

MATERIAL ELASTIC NAME=2 E=25E+9 NU=0.2 DENSITY=2400 ALPHA=7e-6
CONTACTPAIR NAME=1 TARGET=1 CONTACTO=2 FRICTION=2.0
CONTACTPAIR NAME=2 TARGET=11 CONTACTO=12 FRICTION=2.0

ADINA OPTIMIZE=SOLVER FILE='dat/modell_E25_mu20.dat' FIXBOUND=YES MID=NO OVERWRIT=YES

*****************************

MATERIAL ELASTIC NAME=2 E=50E+9 NU=0.2 DENSITY=2400 ALPHA=7e-6
CONTACTPAIR NAME=1 TARGET=1 CONTACTO=2 FRICTION=0.3
CONTACTPAIR NAME=2 TARGET=11 CONTACTO=12 FRICTION=0.3

ADINA OPTIMIZE=SOLVER FILE='dat/modell_E50_mu03.dat' FIXBOUND=YES MID=NO OVERWRIT=YES

*

MATERIAL ELASTIC NAME=2 E=50E+9 NU=0.2 DENSITY=2400 ALPHA=7e-6
CONTACTPAIR NAME=1 TARGET=1 CONTACTO=2 FRICTION=2.0
CONTACTPAIR NAME=2 TARGET=11 CONTACTO=12 FRICTION=2.0

ADINA OPTIMIZE=SOLVER FILE='dat/modell_E50_mu20.dat' FIXBOUND=YES MID=NO OVERWRIT=YES

*****************************

MATERIAL ELASTIC NAME=2 E=75E+9 NU=0.2 DENSITY=2400 ALPHA=7e-6
CONTACTPAIR NAME=1 TARGET=1 CONTACTO=2 FRICTION=0.3
CONTACTPAIR NAME=2 TARGET=11 CONTACTO=12 FRICTION=0.3

ADINA OPTIMIZE=SOLVER FILE='dat/modell_E75_mu03.dat' FIXBOUND=YES MID=NO OVERWRIT=YES

*

MATERIAL ELASTIC NAME=2 E=75E+9 NU=0.2 DENSITY=2400 ALPHA=7e-6
CONTACTPAIR NAME=1 TARGET=1 CONTACTO=2 FRICTION=2.0
CONTACTPAIR NAME=2 TARGET=11 CONTACTO=12 FRICTION=2.0

ADINA OPTIMIZE=SOLVER FILE='dat/modell_E75_mu20.dat' FIXBOUND=YES MID=NO OVERWRIT=YES

*****************************
```

I.2.8 Indata_thermal

```
indata_thermal.in                                                    2008-12-11

CONTROL UNDO=-1 AUTOMREBUILD=NO
FILEECHO OPTION=FILE F=loggfil.ut
FILELOG OPTION=FILE F=loggfil.ut

******** geometry and elements

READ F='model1/geometry.in'

SUBDIVIDE MODEL MODE=LENGTH SIZE=0.100000000000000 NDIV=1 PROGRESS=GEOMETRIC MINCUR=1

SUBDIVIDE LINE NAME=1000 MODE=LENGTH SIZE=1.0
@CLEAR
1023
1022
@

SUBDIVIDE LINE NAME=1000 MODE=DIVISIONS NDIV=10 RATIO=10 PROGRESS=ARITHMETIC
@CLEAR
1018
1019
1020
@

SUBDIVIDE LINE NAME=1000 MODE=LENGTH SIZE=0.05
@CLEAR
1017
1021
@


LOAD TEMPERATURE NAME=1 MAGNITUD=1.0000000000000
*
TIMEFUNCTION NAME=2

@CLEAR
0       10
1       28
2       28
3       -12
4       -12
5       28
6       28
7       -12
8       -12

@

TIMEFUNCTION NAME=3

@CLEAR
0       10
1       28
2       3
3       -12
4       -19
5       28
6       3
7       -12
8       -19


@

TIMEFUNCTION NAME=4

@CLEAR
0       0
1       25
2       25
3       7
4       7
5       25
6       25
7       7
8       7

@


TIMESTEP NAME=DEFAULT
@CLEAR
8       1
@


                                        1
```

```
APPLY-LOAD BODY=0
@CLEAR
1  'TEMPERATURE' 1  'LINE' 1016 0 2 0.00000000000000  'TOP' 0 0
2  'TEMPERATURE' 1  'LINE' 1013 0 2 0.00000000000000  'TOP' 0 0
3  'TEMPERATURE' 1  'LINE' 1010 0 2 0.00000000000000  'TOP' 0 0
4  'TEMPERATURE' 1  'LINE' 1004 0 2 0.00000000000000  'TOP' 0 0
5  'TEMPERATURE' 1  'LINE' 1014 0 3 0.00000000000000  'TOP' 0 0
6  'TEMPERATURE' 1  'LINE' 1011 0 3 0.00000000000000  'TOP' 0 0
7  'TEMPERATURE' 1  'LINE' 1008 0 3 0.00000000000000  'TOP' 0 0
8  'TEMPERATURE' 1  'LINE' 1005 0 3 0.00000000000000  'TOP' 0 0
9  'TEMPERATURE' 1  'LINE' 1007 0 2 0.00000000000000  'TOP' 0 0
10  'TEMPERATURE' 1  'SURFACE' 1005 0 4 0.00000000000000  'TOP' 0 0
11  'TEMPERATURE' 1  'SURFACE' 1006 0 4 0.00000000000000  'TOP' 0 0
@
*
MATERIAL ISOTROPIC NAME=1 K=1.28000000000000 C=1.98e,
     JOULE-HE=NO ELECTRIC=0.00000000000000 MDESCRIP='NONE'
*
EGROUP TWODCONDUCTION NAME=1 SUBTYPE=AXISYMMETRIC MATERIAL=1,
     INT=DEFAULT DEGEN=NO DESCRIPT='NONE' THICKNES=1.00000000000000

GSURFACE NODES=4 PATTERN=AUTOMATIC NCOINCID=BOUNDARIES NCEDGE=1234,
     NCVERTEX=1234 NCTOLERA=1.000000000000000E-05 SUBSTRUC=0 GROUP=1,
     PREFSHAP=AUTOMATIC MESHING=MAPPED SMOOTHIN=NO DEGENERA=NO,
     COLLAPSE=NO MIDNODES=CURVED METHOD=ADVFRONT FLIP=NO
@CLEAR
1001
1002
1003
1004
@

EGROUP TWODCONDUCTION NAME=2 SUBTYPE=AXISYMMETRIC MATERIAL=1,
     INT=DEFAULT DEGEN=NO DESCRIPT='NONE' THICKNES=1.00000000000000

GSURFACE NODES=4 PATTERN=AUTOMATIC NCOINCID=GROUP NCEDGE=1234,
     NCVERTEX=1234 NCTOLERA=1.000000000000000E-05 SUBSTRUC=0 GROUP=2,
     PREFSHAP=AUTOMATIC MESHING=MAPPED SMOOTHIN=NO DEGENERA=NO,
     COLLAPSE=NO MIDNODES=CURVED METHOD=ADVFRONT FLIP=NO
@CLEAR
1005
1006
@

MASTER ANALYSIS=STEADY-STATE MODEX=EXECUTE TSTART=0.00000000000000,
     AUTOMATI=OFF IRINT=DEFAULT MAP-OUTP=YES MAP-FORM=NO,
     SOLVER=SPARSE MAXSOLME=0 MTOTM=2 RECL=3000 TMC-ITER=DEFAULT,
     RESULTS=PORTHOLE

ADINA-T OPTIMIZE=SOLVER FILE='thermal_map.dat' FIXBOUND=YES MID=NO OVERWRIT=YES
```